COO-3077-153

Courant Mathematics and
Computing Laboratory

U. S. Department of Energy

Lectures on Combustion Theory

Edited by
Samuel Z. Burstein, Peter D. Lax,
and Gary A. Sod

Research and Development Report
Prepared under Contract EY-76-C-02-3077
with the Office of Energy Research

Mathematics and Computing
September 1978

New York University

DISTRIBUTION OF THIS DOCUMENT IS UNLIMITED

MASTER

DISCLAIMER

This report was prepared as an account of work sponsored by an agency of the United States Government. Neither the United States Government nor any agency Thereof, nor any of their employees, makes any warranty, express or implied, or assumes any legal liability or responsibility for the accuracy, completeness, or usefulness of any information, apparatus, product, or process disclosed, or represents that its use would not infringe privately owned rights. Reference herein to any specific commercial product, process, or service by trade name, trademark, manufacturer, or otherwise does not necessarily constitute or imply its endorsement, recommendation, or favoring by the United States Government or any agency thereof. The views and opinions of authors expressed herein do not necessarily state or reflect those of the United States Government or any agency thereof.

DISCLAIMER

Portions of this document may be illegible in electronic image products. Images are produced from the best available original document.

UNCLASSIFIED

Courant Mathematics and Computing Laboratory

New York University

NOTICE

This report was prepared as an account of work sponsored by the United States Government. Neither the United States nor the United States Department of Energy, nor any of their employees, nor any of their contractors, subcontractors, or their employees, makes any warranty, express or implied, or assumes any legal liability or responsibility for the accuracy, completeness or usefulness of any information, apparatus, product or process disclosed, or represents that its use would not infringe privately owned rights.

Mathematics and Computing

C00-3077-153

Lectures given in a Seminar held during Spring semester 1977 at the Courant Institute

Edited by

Samuel Z. Burstein, Peter D. Lax, and Gary A. Sod

September 1978

U. S. Department of Energy

Contract EY-76-C-02-3077

UNCLASSIFIED

DISTRIBUTION OF THIS DOCUMENT IS UNLIMITED

THIS PAGE

WAS INTENTIONALLY

LEFT BLANK

Table of Contents

THIS PAGE

WAS INTENTIONALLY

LEFT BLANK

Introduction

This volume contains the elaborations of lectures at a seminar held at the Courant Institute in the spring of 1977 on the mathematical aspects of combustion. The purpose of the seminar was to put the achievements and problems of combustion theory into sharp focus and to bring them to the attention of the mathematical community, in the hope that, just as in the past, mathematical methods will shed light on these theories, and that mathematical ideas will lead to new and efficient computational procedures.

The first half of the semester was devoted to subjects that were reasonably well understood as mathematics; the speakers were mathematicians. After the spring recess the seminar was devoted to subjects not yet mathematically digested; among the speakers there were engineers, chemists, and physicists with sympathy in their hearts for mathematics.

The first part starts with a paper by Peter D. Lax which is a review of those numerical methods in fluid dynamics that are especially promising for reacting flows. This is followed by a report prepared by K. O. Friedrichs for the Navy in 1946, edited and presented by Gary A. Sod. The third paper by Peter D. Lax is a brief introduction to chemical kinetics, followed by papers by Alexandre Chorin, of the University of California at Berkeley, on reactive flows, by Gary A. Sod on a first step to modeling flows in an engine, and by Samuel Z. Burstein on combustion instability.

The second part consists of two papers by William Sirignano of Princeton University on flame spread and reactive flows in a one-dimensional engine, followed by three papers by Irvin Glassman of Princeton University on the burning rate of single coal particles, on hydrocarbon oxidation in a flow reactor, and on flame spreading.

We did not include in this collection an interesting lecture by Louis Howard of M.I.T. on his work with Nancy Kopell on reaction diffusion equations, the content of which is contained in these two papers:

> N. Kopell and L.N. Howard, "Plane Wave Solutions to Reaction-Diffusion Equations," Studies in Appl. Math., 52, 291 (1973).
>
> L.N. Howard and N. Kopell, "Slowly Varying Waves and Shock Structures in Reaction-Diffusion Equations," Studies in Appl. Math., 56, 95 (1977).

Another interesting lecture not included was by James Muckerman of the Brookhaven National Laboratory of the Department of Energy on the calculation of bimolecular rate constants based on the three papers:

> J. Muckerman and M.D. Faist, "Rate Constants from Monte Carlo Quasiclassical Trajectory Calculations: The Use of Important Samplings," to appear.
>
> P.A. Whitlock, J. Muckerman, and E.R. Fisher, "Theoretical Investigation of the Energetics and Dynamics of Reactions of O(d) with H_2," submitted to J. Chem. Phys.
>
> _____, "Theoretical Investigation of the Energetics and Dynamics of Reactions of O(3p d) with H_2 and C(d) with H_2," RIES Technical Report, Wayne State University, Detroit, Michigan (1976).

We heartily thank all of the speakers for their participation. Our thanks are due to Academic Press, Cambridge University Press, Gordon and Breach Science Publishers, and Pergamon Press for permission granted to reprint the articles of Professors Chorin, Glassman, Sirignano, and Sod.

Samuel Z. Burstein, Peter D. Lax, Gary A. Sod

Courant Institute, July 1978

The Numerical Solution of the Equations of Fluid Dynamics

Peter D. Lax

Courant Institute of Mathematical Sciences
New York University

1. Introduction

The theory of Chapman and Juguet for detonations and deflagrations describes reacting flows in the limit as the reaction rate goes to ∞, viscosity, diffusivity and heat conduction go to 0. In this theory the transition from burnt to unburnt gas takes place instantaneously over an infinitely thin reaction zone. In many problems of combustion one is interested in a finer resolution of the reaction zone; this is possible only by solving flow equations which contain an adequate description of all relevant chemical and physical processes: the rates at which the reactions proceed, the conversion of chemical energy to heat, the conduction of heat, the diffusion of the various species, and the effect of viscous forces. In the traditional engineering literature such problems are treated analytically, at the cost of drastic simplification which still retain shreds of the physico-chemical processes responsible for the phenomenon under investiga-

tion. This is the only avenue open, unless, as F.A. Williams remarks in his treatise on combustion theory, "one is willing to expend the labor required to obtain complete numerical solutions". With the advent of modern computers and modern numerical methods for calculating fluid flows, scientists are willing — and able — to expend such labor, although the complete modelling of a combustion problem, tracing dozens of intermediary products participating in the reaction, is beyond the scope of present day numerical methods. Much current research is directed at adopting existing methods for calculating fluid flows to the calculation of reacting flows. Many of these existing methods employ stabilizing devices, of which artificial viscosity is the most prevalent, that cause only marginal and acceptable numerical inaccuracies for non-reacting flows but would distort essential features of reacting flows such as flame velocity that depend on a balance between transport, heat conduction, and energy production. A. Chorin has made the important observation that among the many available methods the one developed by Glimm, [9], is the freest of artificial encumbrances. In Section 6 of this lecture we describe how and why Glimm's method works for nonreacting flows; the adoption to reacting flows is described in a subsequent lecture by Chorin.

Another phenomenon of numerical schemes which are of higher than minimal order of accuracy is oscillatory behavior near a discontinuity, which results in an overshooting of peak values. This is present in Lax-Wendroff type difference schemes, and also in spectral schemes, on account of the Gibbs phenomenon. In

ordinary fluid dynamics such an overshoot, when not excessive, is merely an aesthetic blemish; in reacting flows, where the rate of chemical reaction is so sensitive to temperature, an overshoot would prematurely trigger off ignition and would falsify the time history of burning. One cure for overshooting in LW or other types of higher order schemes lies in hybridization combined with artificial compression, as developed by A. Harten, [15]. The case for spectral methods lies in applying some summation method.

2. The equations of fluid dynamics

A conservation law asserts that the change in the amount of a substance contained in any portion of space is due to the flux of that substance across the boundary of the portion of space under consideration. Let's denote the density of the substance by u, its flux by f, and the portion of space under consideration by G. Then the conservation law says that

$$\int_G u\,dx\Big|_s^t + \int_s^t \int_{\partial G} f\cdot\nu \; dS\,dt = 0 \,, \tag{2.1}$$

where ν denotes the outward normal to the boundary ∂G of G. Using the divergence theorem the boundary integral term can be written as

$$\int_s^t \int_G \operatorname{div} f \; dx\,dt \,.$$

Letting s tend to t and G shrink to a point we deduce that at every point where u and f are differentiable, the differential conservation law

(2.2) $$U_t + \text{div } f = 0$$

is satisfied.

The rest of this section is devoted to a brief discussion of the classical conservation laws of mass, momentum and energy in fluid dynamics. We shall show how various transport mechanisms can be expressed by a suitable choice of flux.

We shall use the notation

ρ = mass density

M = momentum density

E = energy density

Momentum and energy densities can be expressed as follows:

(2.3) $$M = \rho V , \quad E = \rho e + \frac{1}{2} \rho V^2$$

where

V = flow velocity

e = internal energy per unit mass

Since the fluid is streaming past G with velocity V, mass is convected out of G at the rate

$$\int_{\partial G} \rho V \cdot \nu \, dS .$$

The mass flux due to this convection is

$(2.4)_{conv}$ $$f_{\text{mass conv}} = \rho V = M .$$

An additional flux of mass is due to <u>diffusion</u>; this is proportional to the negative gradient of mass density:

$(2.4)_{diff}$ $$f_{mass\ diff} = -D \text{ grad } \rho \ ;$$

D is called the coefficient of diffusion.

Momentum flux is the sum of two kinds of term, each representing two distinct transport mechanisms: convection, and impulse of forces exerted by the fluid. The convective term is entirely analogous to $(2.4)_{conv}$ and is of the form

$(2.5)_{conv}$ $$f^i_{mom\ conv} = M^i V$$

where the superscript i refers to the i^{th} Cartesian component, $i = 1,2,3$. To derive the impulsive terms, denote by F the force per unit area exerted by the fluid across a surface element through a point x and with outward normal ν. It is a basic law of continuum mechanics that F has the form

(2.6) $$F = P\nu \ ,$$

where P, called the pressure tensor, is a symmetric matrix function of x. The impulse of the force F of form (2.6) changes the momentum of the fluid contained in G at the rate

$$-\int_{\partial G} P\nu \, dS \ .$$

The rate at which momentum in the i^{th} coordinate direction changes is thus

$$-\int_{\partial G} P^i \cdot \nu \ dS$$

where P^i is the i^{th} row of P. This shows that

$(2.7)_P$ $$f^i_{\text{momentum } P} = P^i \ .$$

For a nonviscous fluid the pressure tensor is scalar, i.e. the identity multiplied by the scalar pressure p:

(2.8) $$P = pI \ .$$

In this case the flux of the momentum in the i^{th} direction is

$(2.7)_p$ $f^i_{\text{momentum } p} = pe^i$, e^i = unit vector in i^{th} direction .

For viscous fluids the scalar pressure tensor has to be augmented by a matrix which for incompressible fluids takes the simple form

(2.9) $$P_{visc} = \frac{\mu}{2}\left(\frac{\partial V^i}{\partial x_j} + \frac{\partial V^j}{\partial x_i}\right) \ ;$$

μ is called the coefficient of viscosity. The flux of momentum in the i^{th} direction due to viscous forces can be obtained by setting (2.9) into $(2.7)_P$:

$(2.7)_{visc}$ $$f^i_{\text{momentum visc}} = \frac{\mu}{2}[\text{grad } V^i + V_{x_i}] \ .$$

Energy flux is the sum of three terms; the first represents the effect of convection and has the value

$(2.10)_{conv}$ $$f_{\text{energy conv}} = EV \ .$$

The work done by a force of form (2.6) changes the energy contained in G at the rate

$$-\int_{\partial G} V\cdot F dS = -\int_{\partial G} V\cdot P\nu dS \ .$$

Since P is a symmetric matrix, the right side can be written as

$$-\int \nu \cdot PV dS \ ;$$

this shows that the energy flux due to work done by the pressure tensor is

$(2.10)_P$ $$f_{\text{energy } P} = PV \ .$$

If P is scalar, we have from (2.8) that

$(2.10)_p$ $$f_{\text{energy } p} = pV \ .$$

If viscosity plays a significant role, then $(2.10)_p$ has to be augmented by $(2.10)_P$, with P given by (2.9).

There is a third mechanism for transferring energy in and out of G: heat conduction. Newton's law states that the energy flux due to heat conduction is proportional to the negative temperature gradient:

$(2.10)_h$ $$f_{\text{energy heat}} = -c \ \text{grad} \ T \ ,$$

c is called the coefficient of heat conduction.

Flux across boundaries is not the only transfer mechanism; an additional change in the amount of a given substance can be caused by the continued creation or annihilation of substances due to sources or sinks distributed throughout space. Denote the rate of generation of substance by S; S is called the source strength (when S is negative, it measures the sink strength). The total amount created in a domain G during the time interval (s,t) is

$$\int_s^t \int_G S\,dx\,dt \ ,$$

and this has to equal the left side of (2.1); thus we obtain the equation:

$$\int_G u\,dx\Big|_s^t + \int_s^t \int_{\partial G} f\cdot\nu\,dS\,dt = \int_s^t \int_G S\,dx\,dt \ . \tag{2.11}$$

From this we can derive as before the analogue of the differential form (2.2), which for equation (2.11) is

$$u_t + \operatorname{div} f = S \ . \tag{2.12}$$

There are many processes in which source terms play an important role, par excellence chemically reacting flows; the chemical reaction is a source of mass for the products of the reaction, and a sink for the reactants. If the reaction is exothermic it is a source of heat energy, if endothermic a sink of energy. These source strengths will be denoted as follows:

$$S_{\text{mass } i} = r_i \ ,$$

where i labels the species participating in the chemical reaction and r_i, called a reaction rate, is the rate at which the density of the species i is changing as a result of the chemical reaction. The reaction rates r_i at x depend on the densities of the species participating in the reaction at x. The strength of the heat source is denoted by

$$S_{\text{energy}} = q \ ,$$

where q is the rate of energy release during the reaction; q is a function of the densities of the reactants.

Another energy transfer mechanism that is described in terms of sources and sinks is radiation; this mechanism becomes important at high temperatures.

The foregoing discussion shows that the conservation laws of fluid dynamics may contain a variety of fluxes and source terms. In Section 4 we shall show how the method of fractional steps can be used to disentangle the various transfer mechanisms from each other in the construction of approximate numerical solutions.

3. Theory of shock waves

It follows from the discussion in Section 2 that if diffusion, viscosity, heat conduction and chemical reactions are neglected, the laws of conservation of mass, momentum and energy are

$$\rho_t + \operatorname{div} M = 0 ,$$

$$M^i_t + \operatorname{div} (M^i V) + p_{x_i} = 0 , \tag{3.1}$$

$$E_t + \operatorname{div} (EV + pV) = 0 .$$

To make this system self-contained we have to adjoin relations (2.3):

$$M = \rho V , \quad E = \rho e + \frac{1}{2} \rho V^2 , \tag{3.2}$$

and the equation of state, which relates three thermodynamic variables, say e, p, ρ:

(3.3) $$p = p(e,\rho) \ .$$

The simplest equation of state is the classical polytropic relation

(3.3)' $$p = (\gamma-1)e\rho \ , \quad \gamma = \text{const.}$$

The system of conservation laws (3.1) supplemented by (3.2) and (3.3) is of the general form

(3.4) $$u_t^k + \text{div } f^k = 0 \ , \quad k = 1,\ldots,N \ ,$$

where each f^k is a function of the densities themselves:

(3.5) $$f^k = f^k(u^1,\ldots,u^N) \ .$$

To simplify the discussion we turn now to one-dimensional flows; a brief discussion of the two-dimensional case will be given at the end. Dropping dependence on y and z in (3.4) leaves

(3.6) $$u_t^k + f_x^k = 0 \ .$$

To analyze solutions of such a system we carry out the differentiation with respect to x in (3.6); we get a first order system which in matrix notation can be written as

(3.7) $$u_t + A(u)u_x = 0$$

where $u = (u^1,\ldots,u^N)^t$ and A is the matrix gradient of $f = (f^1,\ldots,f^N)^t$ with respect to u:

(3.8) $$A = (a_{kj}) \ , \quad a_{kj} = \frac{\partial f^k}{\partial u_j} \ .$$

This is a system of quasilinear equations; it is well known that

in order for the initial value problem to be properly posed, (3.7) has to be hyperbolic, i.e. the matrix A has to have* real eigenvalues $a^1, \ldots, a^N$, themselves functions of U. The eigenvalues have a very interesting physical interpretation: they are the local velocities with which sharp signals propagate in the medium described by equations (3.7). These are called the characteristic velocities of the equation (3.7).

The one-dimensional version of the system (3.1), (3.2), (3.3) is hyperbolic in this sense, provided that pressure is an increasing function of ρ at constant entropy. Since $\frac{d}{d\rho} e \Big|_{\text{entropy=const}} = \frac{p}{\rho v}$, when p is given as function of ρ and e its derivative with respect to ρ at constant entropy is given by

$$\frac{dp}{d\rho}\Big|_{\text{entropy=const}} = \frac{\partial p}{\partial \rho} + \frac{p}{\rho^2} \frac{\partial p}{\partial e} . \tag{3.9}$$

The increasing character is expressed by setting

$$\frac{dp}{d\rho}\Big|_{\text{entropy=const}} = c^2 . \tag{3.10}$$

The quantity c is called sound speed. In the polytropic case (3.3) we have

$$c^2 = \frac{\gamma p}{\rho} . \tag{3.10}'$$

The characteristic velocities for the equation of gas dynamics are

* If the eigenvalues are distinct, this condition suffices, in case of a multiple eigenvalue additional conditions have to be imposed.

(3.11) $\qquad V-c\ ,\quad C\ ,\quad V+c\ .$

According to the general theory of nonlinear hyperbolic equations of form (3.7), we may prescribe the initial values $u(x,0)$ arbitrarily; the corresponding solution U at the point x,t is uniquely determined by the initial data, in fact by the initial data on a finite interval, called the domain of dependence of the point (x,t) ; the domain of dependence is the smallest interval containing the intersection of all characteristic curves through x, t with the initial line t = 0; a characteristic curve is one which propagates with one of the characteristic velocities, i.e. satisfies one of the differential equations

(3.12) $$\frac{dx}{dt} = a^k(u)\ ,\quad u = u(x,t)\ ,\quad k = 1,\ldots,N\ .$$

In general solutions of a nonlinear hyperbolic equation develop singularities after a certain time has elapsed. The source of this breakdown is easiest seen for a single conservation law:

(3.13) $$u_t + f(u)_x = 0\ ,$$

which can be written as

(3.14) $$u_t + a(u)u_x = 0\ ,\quad a = \frac{df}{du}\ .$$

The left side of (3.14) can be interpreted as the derivative of u in the characteristic direction:

(3.15) $$\frac{du}{dt} = 0\ ,\quad \text{where}\quad \frac{dx}{dt} = a(u)\ .$$

This equation says that u is constant along the characteristic

curve, but then the speed $a(u)$ is constant along the characteristic curve, and so it follows that the characteristic curve is a straight line. Now let x_1 and x_2 denote any two points on the initial line $t = 0$, $u(x,0)$ the prescribed initial function. The speeds of the characteristic lines issuing from these points are $a_1 = a(u(x_1))$ and $a_2 = a(u(x_2))$; if these two lines are on collision course, then at the point (x,t) of their intersection $u(x,t)$ has to be equal to both u_1 and u_2, which shows that no solution can exist beyond that time, at least not a continuous one.

What does exist beyond that time? Experiments disclose the appearance of <u>discontinuous solutions</u>. In what follows we outline briefly the theory of these. For a mathematical definition of discontinuous solutions we have to go back to the physical definition of a conservation law: we say that u is a solution of the system of conservation laws (3.4) if the integral relations (2.1) are satisfied for all domains D and all times t and s. An entirely equivalent formulation is to require that the equations (3.4) be satisfied in the sense of <u>distribution theory</u>; that is, if we multiply (4.4) by any smooth test function $w(x,t)$ that vanishes for $|x|$ large, and if we integrate by parts, the resulting integral relation

$$(3.16)\qquad \iint (w_t u^k + \operatorname{grad} u \cdot f^k)\,dx\,dt - \int w(x,T)u^k(x,T)\,dx + \int w(x,0)u^k(x,0)\,dx = 0$$

holds for $k = 1,\ldots,N$.

Suppose that u is a piecewise smooth function in regions separated by smooth surfaces. It is not hard to show that u satisfies (3.4) in the distribution sense (3.16) iff

i) u satisfies equation (3.4) pointwise in each smooth region,

ii) across each surface of discontinuity the jump relations

$$s[u] = [f]\cdot\nu \tag{3.17}$$

hold, where [ ] denotes the jump of the quantity in brackets across the surface of discontinuity, ν the direction in which the surface propagates, and s the speed with which it propagates. These relations, called the Rankine-Hugoniot conditions and abbreviated as R-H, are easily derived from (3.16), or from the more physical equation (3.1).

In case of one space dimension the jump relations take the form

$$s[u^k] = [f^k] , \quad k = 1,\ldots,N , \tag{3.18}$$

where s is the speed with which the discontinuity propagates from left to right.

For small discontinuities the jump relation has a simple consequence. Using relation (3.8) we can write

$$[f] = \overline{A}[u] ,$$

where $\overline{A}$ is very close to $A(u) = \text{grad}_u f$. Substituting the above into (4.18) gives

(3.18)' $$s[u] = \bar{A}[u] ,$$

which shows that for [u] small, s is very close to an eigenvalue of A. Since these are the propagation velocities we conclude that small discontinuities propagate with velocities very close to the velocities of sharp signals — a most plausible result.

For a good theory of discontinuous solutions two things must be shown:

a) that every initial value problem has a solution in the sense of (4.16) which exists for all times $t > 0$.

b) that this solution is unique.

It turns out that b) is false! The following example shows it so for the single conservation law

(3.19) $$u_t + (\tfrac{1}{2} u^2)_x = 0 .$$

Define the function u_1 by

$(3.20)_1$ $$u_1(x,t) = \begin{cases} 0 & \text{for } x/2 < 1/2 \\ 1 & \text{for } 1/2 < x/t \end{cases} .$$

Since a constant satisfies equation (3.19), we see that u_1 consists of two solutions fitted together along the line $x/t = 1/2$. The speed of propagation of this line is chosen as $s = 1/2$, so that the R-H relation (3.18), for $[u_1] = 1-0 = 1$, $[f] = 1/2 - 0 = 1/2$, is satisfied. Thus u_1 is a solution of (3.19) in the distribution sense. Next we define

$$(3.20)_2 \qquad u_2(x,t) = \begin{cases} 0 & \text{for } x/t < 1/4 \\ 1/2 & \text{for } 1/4 < x/t < 3/4 \\ 1 & \text{for } 3/4 < x/t \ . \end{cases}$$

Here three constant states $u = 0, 1/2, 1$ are fitted together along two lines, whose propagation speed is chosen as $s = 1/4$ and $s = 3/4$ so that the R-H relation (3.18) is satisfied at both discontinuities; thus u_2 satisfies (3.19) in the distribution sense. Finally we define

$$(3.20)_3 \qquad u_3(x,t) = \begin{cases} 0 & \text{for } x/t < 0 \\ x/t & \text{for } 0 < x/t < 1 \\ 1 & \text{for } 1 < x/t \ . \end{cases}$$

Here the two constant states $u = 0$ and $u = 1$ are joined continuously by the function x/t; this function satisfies equation (3.19) pointwise.

The three functions u_1, u_2, u_3 have the same initial value: $u = 0$ for $x < 0$, $u = 1$ for $1 < x$. Clearly many more are possible. We abstract from these examples a principle that eliminates all but one of these solutions.

Let u_ℓ and u_r be two constants denoting the state on the left and on the right of a discontinuity. Let

$$(3.21) \qquad s = \frac{f_\ell - f_r}{u_\ell - u_r} \ ,$$

where

$$f_r = f(u_r) , \quad f_\ell = f(u_\ell) ;$$

then

$$u(x,t) = \begin{cases} u_\ell & \text{for } x/t < s \\ u_r & \text{for } s < x/t \end{cases} \tag{3.22}$$

is a discontinuous solution of (3.13) in the integral sense. We say that this discontinuity can be split if there is a value of v between u_ℓ and u_r such that

$$s_\ell = \frac{f_\ell - f(v)}{u_\ell - v} , \quad s_r = \frac{f(v) - f_r}{v - u_r} \tag{3.23}$$

satisfy

$$s_\ell < s_r . \tag{3.24}$$

In this case the split solution

$$u_{split}(x,t) = \begin{cases} u_\ell & \text{for } x/t < s_\ell \\ v & \text{for } s_\ell < x/t < s_r \\ u_r & \text{for } s_r < x/t \end{cases}$$

also satisfies the integral form of the conservation law (3.13), and has the same initial value as the solution u defined by (3.22 We call a discontinuity that can be split unstable. Solutions with unstable discontinuities are rejected as physically not realizable. Stability is opposite of instability:

A discontinuity (u_ℓ, u_r) is called stable if it cannot be split, i.e. if for all v between u_ℓ and u_r

(3.25) $$s_\ell \geq s_r \ .$$

Using the definitions (3.21) of s and (3.23) of s_ℓ, s_r we can write

$$s = \frac{u_\ell - v}{u_\ell - u_r} s_\ell + \frac{v - u_r}{u_\ell - u_r} s_r \ .$$

Since v lies between u_ℓ and u_r, this shows that s is a convex combination of s_ℓ and s_r; so it follows from (3.25) that

(3.25)' $$s_\ell \geq s \geq s_r \ .$$

Again using (3.21), (3.23) we can write this as

(3.25)" $$\frac{f_\ell - f(v)}{u_\ell - v} \geq \frac{f_\ell - f_r}{u_\ell - u_r} \geq \frac{f(v) - f_r}{v - u_r} \ .$$

Letting v tend to u_ℓ or u_r respectively, and recalling that df/du = a(u), we deduce that

(3.26) $$a_\ell \geq s \geq a_r \ .$$

This expresses the fact that sound waves originating on either side of the discontinuity propagate <u>toward</u> the discontinuity. The theoretical significance of this condition emerges if we look upon a discontinuous solution as a solution of a mixed initial-boundary value problem, the discontinuity serving as an internal boundary. Condition (3.26) guarantees that every characteristic drawn <u>backward</u> from either side of the discontinuity reaches the initial line. This shows that the initial data determine uniquely the solution on either side of the discontinuity; the R-H

condition (3.21) then serves as an ordinary differential equation for the determination of the line of discontinuity $x = x(t)$, with $s = dx/dt$. We shall call (3.26) the characteristic condition.

If $f(u)$ has no inflection points, then (3.26) implies (3.25). Suppose, e.g., that $f_{uu} > 0$; then $f' = a$ is an increasing function of u, so (3.26) implies that $u_\ell > u_r$. Since difference quotient also are increasing functions of their arguments, (3.25)" follows. When f has inflection points, the stability condition (3.25) is a genuine additional restriction.

It can be shown that every initial value problem for a single conservation law (3.13) has a unique solution in the integral sense (3.16) that exists for all time $t > 0$ and all whose discontinuities are stable in the sense of (3.25). In Section 7 we shall prove the uniqueness of such a solution, and construct solutions with piecewise constant initial data.

We turn now from single conservation laws to systems. Here we have not one but N signal speeds $a^1(u), \ldots, a^N(u)$. We claim that the appropriate extension of the characteristic condition (3.26) to this case is:

There exists an index k, $1 \leq k \leq N$, such that

$$(3.27)_1 \qquad a^k(u_\ell) > s > a^k(u_r)$$

while

$$(3.27)_2 \qquad a^{k-1}(u_\ell) < s < a^{k+1}(u_r) \ .$$

A discontinuity satisfying this condition is called a k-shock. The left half of the two inequalities says that exactly N-k+1

characteristic curves impinging on the discontinuity from the left; the right half of the inequalities say that exactly k impinge from the right. So altogether the total number of characteristics that impinge on the discontinuity from either side is N+1. Each of these characteristics carries one piece of information; these N+1 data, combined with the N-1 relations that can be obtained from the N R-H conditions (3.18) by eliminating s, are needed to determine, iteratively, the 2N components of u_ℓ and u_r.

We proceed now to show that solutions whose discontinuities violate the characteristic conditions (3.27) can be split into rarefaction waves, and thus are in this sense unstable. Therefore such solutions are rejected as not realizable physically.

The conservation laws (3.6) in both differential and integral form are invariant under a uniform stretching of both the x and t variables; it follows that (3.6) has so-called centered solutions, i.e. solutions that depend on x/t alone. We shall describe now these solutions; there are two kinds: shocks and rarefaction waves. A shock is of the form

$$u(x,t) = \begin{cases} u_\ell & \text{for } x/t < s \\ u_r & \text{for } s < x/t \end{cases} \tag{3.28}$$

where the states u_ℓ and u_r satisfy the R-H conditions (3.18). We ask: given u_ℓ, describe the set of states u_r that can be connected to u_ℓ through a single shock. This is easily answered if we are looking for weak shocks, i.e. states u_r close to u_ℓ. We claim that they form N one-parameter families $u_r = u(\varepsilon)$; we take now the jump relation (3.18):

$$s[u - u_\ell] = f(u) - f(u_\ell)$$

and differentiate twice, with respect to ε. Denoting $d/d\varepsilon$ by $'$ and recalling (3.8):

$$\text{grad}_u f = A$$

we get

$$(3.29)_1 \qquad s'[u] + su' = Au' ,$$

$$(3.29)_2 \qquad s''[u] + 2s'u' + su'' = Au'' + A'u' .$$

Setting $\varepsilon = 0$ in $(3.29)_1$ we get

$$su' = Au'$$

which shows that $s(0)$ is one of the eigenvalues of $A = A(u_\ell)$, $u'(0)$ the corresponding eigenvector $r = r(u_\ell)$. Setting $\varepsilon = 0$ in $(3.29)_2$ and setting $u' = r$, $s = a$ we get

$$(3.30) \qquad 2s'r + au'' = Au'' + A'r .$$

Now take the eigenvalue relation

$$ar = Ar , \quad u = u(\varepsilon) ,$$

and differentiate at $\varepsilon = 0$:

$$(3.31) \qquad a'r + ar' = Ar' + A'r .$$

Subtracting this from (3.30) gives

$$(2s' - a')r + a(u'' - r') = A(u'' - r') .$$

Multiplying this with the left eigenvector ℓ of A gives

$$2s' = a' \tag{3.32}$$

Now

$$a' = u' \cdot \text{grad}_u a = r \cdot \text{grad}_u a \ .$$

Let's assume that $r \cdot \text{grad}_u a \neq 0$, then

$$r \cdot \text{grad}_u a = 1 \tag{3.33}$$

can be achieved by normalizing r. It follows from (3.32), (3.33) and $u' = r$ that

$$1 = a' = \frac{1}{2} s' \ . \tag{3.34}$$

Note that when r is normalized by (3.33), the parameter ε needs rescaling in order to have $u' = r$. It is easy to see that, for ε small enough, the characteristic condition (3.27) is satisfied iff ε is negative.

Since a is any one of N eigenvalues, we see that N one-parameter families u_r can be connected to u_ℓ by a single shock; exactly one half of each family satisfies condition (3.27).

We turn now to rarefaction waves; differentiable solutions of (3.7) of form

$$u(x,t) = w(p) \ , \quad p = x/t \ . \tag{3.35}$$

Substituting this into (3.7) we get

$$-pw' + Aw' = 0 \ ,$$

which is solved by

(3.36) $$w' = cr(w) , \quad p = a(w) .$$

Differentiating the second relation with respect to p and using the first we get

(3.37) $$1 = \text{grad}_u a \cdot w = c \ \text{grad}_u a \cdot r .$$

In view of the normalization (3.33), c = 1. To obtain w(p) we solve the ODE (3.36), with initial value

$$w(p_o) = u_\ell , \quad p_o = a(u_\ell) .$$

Now let ε be a small positive quantity. We define the centered rarefaction wave as the composite

(3.38) $$u(x,t) = \begin{cases} u_\ell & \text{for} \quad x/t \leq p_o \\ w(x/t) & \text{for} \quad p_o < x/t < p_o+\varepsilon \\ w(p_o+\varepsilon) & \text{for} \quad p_o+\varepsilon \leq x/t . \end{cases}$$

The state $u_r = w(p_o+\varepsilon)$ is connected to u_ℓ through a rarefaction wave; since a is one of N possible eigenvalues, we have N halves of one-parameter families of states u_r that can be connected to u_ℓ by a single rarefaction wave.

Note that the two halves of the one-parameter families to which u_ℓ can be connected through either a shock or a rarefaction wave can be fitted together differentiably to form N complete one-parameter families $u_{r,k}(\varepsilon)$, k = 1,...,N. Given now any state u_o, it can be connected to a one-parameter family of states $u_1(\varepsilon_1)$ through a wave pertaining to the lowest speed a_1; u_1 in turn can

be connected to a one-parameter family of states $u_2(\varepsilon_1, \varepsilon_2)$ through a wave pertaining to the second wave speed a_2, etc. Continuing in this fashion we see that by going through all available waves we can connect any state u_o to an N parameter family of states $u_N = u_N(\varepsilon_1, \ldots, \varepsilon_N) = u_N(\varepsilon)$. We have shown earlier that $\frac{du}{d\varepsilon_k} = r_k$; since the right eigenvectors r_k are linearly independent it follows that for ε small the family $u_N(\varepsilon)$ simply covers a full neighborhood of u_o. Thus we have shown:

Suppose condition (3.33) holds; then given any two states u_o and u_n sufficiently close, there exists a solution $u(x,t)$ of (3.6) with initial values

$$u(x,0) = \begin{cases} u_o & \text{for } x < 0 \\ u_N & \text{for } 0 < x \,. \end{cases} \tag{3.39}$$

This solution is centered, i.e. a function of x/t, and consists of N+1 constant states separated by shocks or centered rarefaction waves:

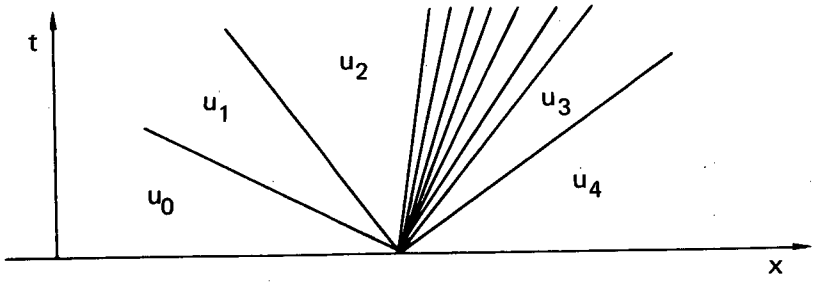

Figure 3.1

An initial value problem of form (3.39), with initial data consisting of two constant states, is called a Riemann initial value problem.

Condition (3.33) is a kind of a convexity condition; there are some important cases where it fails to hold, e.g. for so-called contact discontinuities $r \cdot \text{grad}_u a \equiv 0$; in this case the concept of shock and rarefaction wave coalesce and the result still holds.

For what systems does the above result hold in the large? that is, if we do not restrict the parameters ε to be small, how large a neighborhood of u_o is covered by $u(\varepsilon)$, and is the covering simple? if not, the initial value problem (3.39) has several solutions and we need some criterion in addition to (3.27) to identify the physically realizable solutions.

Bethe and Weyl have shown, see [1] and [34], that if p is a convex function of ρ^{-1} at constant entropy, then the initial value problem (3.39) has only one solution. Wendroff, [33], has investigated the situation when this convexity condition is violated.

In an interesting sequence of papers [24], Liu has analyzed the Riemann initial value problem when (3.33) is violated; he has derived an analogue of condition (3.25) for systems, and has applied it to the equations of gas dynamics.

4. The method of fractional steps

We are interested in approximating solutions of evolution equations of the schematic form

$$u_t = L(u) \tag{4.1}$$

by employing approximate solution operators $S_h(L)$ which, when

applied to the initial value $u_o = u(0)$ of a solution u of (4.1) furnishes an approximation to the value of the solution u at h:

$$S_h(L)(u_o) = u(h) + \text{error} \ . \tag{4.2}$$

Here h is a small quantity; to approximate u(t), t not small, the operator S_h is applied repeatedly:

$$S_h^N(L)(u_o) = u(t) + \text{error} \ , \quad t = Nh \ . \tag{4.2}_N$$

The approximating operator $S_h(L)$ is constructed so that the error in (4.2) is small; this implies that the error in $(4.2)_N$ is also if, and only if, the scheme is stable in the sense that $S_h^N(L)$ does not magnify. If this condition is fulfilled, then the error in $(4.2)_N$ is, roughly, N times the error in (4.2). This shows that we must choose S_h so that the error in (4.2) is $O(h^2)$.

The error in (4.2) can be appraised by Taylor's theorem:

$$u(h) = u(0) + hu_t(0) + O(h^2) = u_o + hL(u_o) + O(h^2) \ .$$

This shows that in order to make the error in (4.2), $O(h^2)$, $S_h(L)$ must satisfy

$$S_h(L) = I + hL + O(h^2) \ . \tag{4.3}$$

In many problems, par excellence in fluid dynamics the operator L is the sum of several operators L_i, each describing a different physical mechanism:

$$L = \sum L_i \ . \tag{4.4}$$

The method of fractional steps constructs an approximate solution

operator for (4.1) as the product of approximate solution operators $S_h(L_i)$ of the partial equations

$$(4.5)_i \qquad u_t = L_i(u) .$$

Each $S_h(L_i)$ satisfies

$$(4.6)_i \qquad S_h(L_i) = I + hL_i + O(h^2) .$$

We set

$$(4.7) \qquad S_h(L) = \prod S_h(L_i) .$$

It is easy to show that if each L_i satisfies $(4.6)_i$ then $S_h(L)$ defined by (4.7) satisfies (4.3), with $L = \sum L_i$.

The method of fractional steps has several distinct advantages:

i) Each equation $(4.5)_i$ usually has its own special feature (symmetry, invariance, etc.) which can be exploited to construct an efficient scheme $S_h(L_i)$.

ii) If each scheme $S_h(L_i)$ is stable in the sense that it does not increase some norm, such as the L_2 norm, common to all equations $(4.5)_i$, then likewise the product (4.7) does not increase that norm and so is automatically stable. Even if each $S_h(L_i)$ increase norm slightly

$$\|S_h(L_i)\| \leq 1 + O(h) ,$$

it only causes a similar slight norm increase by $S_h(L)$. Thus instead of having to check the stability of a complicated composite

scheme it suffices to check the stability of each of its factors.

iii) Programming convenience: one can write a program for implementing a scheme of form (4.5) which consists of n distinct packages strung together in series, each package solves an equation of form $(4.6)_i$. If one wants to incorporate an improved method for solving the i^{th} equation, only one of the packages has to be rewritten.

iv) Yet another advantage is described in Section 5.

Relation (4.3) says that applying the approximation scheme once leads to an error of size $O(h^2)$. Repeating the approximation N times, where $Nh = T$ = final time results in cumulative error of size $NO(h^2) = O(h)$, provided that the scheme is stable. To bring the error down to acceptable size may require making h so small that the time required to perform $N = T/h$ steps is unacceptable. In this case it is possible to reduce the number of steps required by employing a scheme that is accurate to second order, i.e. that approximates u(h) with an error $O(h^3)$. We explain how to do this in case the operator L is linear; we allow L to depend on t.

We start with Taylor's theorem to second order:

$$u(h) = u(0) + hu_t(0) + \frac{h^2}{2} u_{tt}(0) + O(h^3)$$

The first derivative of u is given by (4.1); the second can be obtained by differentiating (4.1) with respect to t:

$$u_{tt} = Lu_t + L_t u = (L^2 + L_t)u \ .$$

Substituting into the Taylor approximation gives

$$(4.8) \qquad u(h) = u(0) + hL(0)u(0) + \frac{h^2}{2}\,[L^2(0) + L_t(0)]u(0) + O(h^3) \ .$$

This shows that for second order accuracy we must have

$$(4.9) \qquad S_h(L) = I + hL(0) + \frac{h^2}{2}\,[L^2(0) + L_t(0)] + O(h^3) \ .$$

The reader may easily convince himself, in the simple case when all L_i are independent of t, that even if each S_i is a second order approximation to $(4.5)_i$:

$$(4.10) \qquad S_h(L_i) = I + hL_i(0) + \frac{h^2}{2}\,L_i^2(0) \ ,$$

the product (4.7) is still only a first order approximation to (4.1), unless all the L_i commute (which they don't in general). Gilbert Strang, [32], has devised a variant of the method which does not suffer from this restriction; we shall describe it for two terms, i.e. when L is of the form

$$(4.11) \qquad L = A + B \ .$$

Theorem (Strang): Suppose $S_h(A)$ and $S_h(B)$ are second order approximations to

$$u_t = Au \quad \text{and} \quad u_t = Bu \ ,$$

respectively. Then

$$(4.12) \qquad S_h(L) = S_{h/2}(B(0))S_h(A(0))\,S_{h/2}(B\,(\tfrac{h}{2}))$$

is a second order approximation to solutions of (4.1).

The proof is a simple matter of algebra: By (4.9) we have, modulo terms $O(h^3)$:

$$S_{h/2}(B(0)) = I + \frac{h}{2} B(0) + \frac{h^2}{8} [B^2 + B_t] ,$$

$$S_h(A(0)) = I + hA(0) + \frac{h^2}{2} [A^2 + A_t] ,$$

$$S_{h/2}(B(\tfrac{h}{2})) = I + \frac{h}{2} B(\tfrac{h}{2}) + \frac{h^2}{8} [B^2 + B_t]$$

$$= I + \frac{h}{2} B(0) + \frac{h^2}{8} [B^2 + 3B_t] .$$

The triple product (4.12) is, mod $O(h^3)$,

$$I + h[A(0) + B(0)] + \frac{h^2}{2} [A^2 + A_t + \frac{2}{4} B^2 + B_t + \frac{B^2}{2} + BA + AB] ,$$

and this by (4.11) is indeed equal to

$$I + hL(0) + \frac{h^2}{2} [L^2 + L_t] .$$

We turn now to nonlinear equations of the form (2.12), where the flux f is the sum of fluxes f_j:

$$u_t + \sum_j \operatorname{div} f_j = S . \tag{4.13}$$

The analogue of the method of fractional steps constructs approximations to solutions of (4.13) as a product of operators approximating solutions of the partial equations

$$u_t + \operatorname{div} f_j = 0 \tag{4.14}_i$$

and

$$u_t = S . \tag{4.15}$$

In practice the equations $(4.14)_i$ are often further decomposed as

$$u_t + \partial_x f^1 + \partial_y f^2 + \partial_z f^3 = 0$$

and their solutions approximated by products of operators approximating solutions of the partial equations

$$(4.16) \qquad u_t + \partial_x f^1 = 0 , \quad u_t + \partial_y f^2 = 0 , \quad u_t + \partial_z f^3 = 0 .$$

If (4.13) stands for the equations of fluid dynamics, then the partial equations $(4.14)_i$ might stand for equations of fluid dynamics in which the only transport mechanisms are convection and those are due to scalar pressure, or might describe fluid flow governed by diffusion, viscosity and heat conduction; (4.15) describes the chemical reaction. Since these partial systems evolve on different time scales, the way they are mixed together is crucial to the success of the fractional step method. The method of fractional steps has been developed by Godunov, [11], Marchuk [25] and Yanenko [35]; it is an outgrowth of the alternating direction method of Peaceman, Ratchford and Douglas, [28].

5. Difference approximation of conservation laws

We start with one dimensional conservation laws:

$$(5.1) \qquad u_t + f_x = 0 .$$

We divide x-space into cells I_k of length δ,

$$(5.2) \qquad I_k = ((k - 1/2)\delta, (k + 1/2)\delta) .$$

We denote by v_k^n an approximation to the average density of u over the cell I_k at time step n, and by $g_{k+1/2}^{n+1/2}$ an approximation to the

average flux f between time step n and n+1/2 at the boundary between I_k and I_{k+1}. The approximation to (5.1) then is

$$v_k^{n+1} - v_k^n + \frac{\tau}{\delta}\left(g_{k+1/2}^{n+1/2} - g_{k-1/2}^{n+1/2}\right) = 0 \tag{5.3}$$

where τ is the time step from n to n+1. Since the flux f is a function of the density u, we take the approximate flux $g_{k+1/2}^{n+1/2}$ to be a function of the approximate densities at a finite number of points near the point k+1/2 and time n+1/2:

$$g_{k+1/2}^{n+1/2} = g(v_{k-r+1}^n, \ldots, v_{k+r}^n, v_{k-r+1}^{n+1}, \ldots, v_{k+r}^{n+1}) \ . \tag{5.4}$$

We require g to be <u>consistent</u> with f, in the sense that

$$g(u, \ldots, u) = f(u) \ . \tag{5.5}$$

It is convenient to regard v as being defined for all x, t:

$$v(x,t) = v_k^n \quad \text{for} \quad x \text{ in } I_k \ , \quad t_n < t < t_n + \delta \ .$$

We show now that the consistency condition (5.5) guarantees that if a sequence of solutions of (5.3) with initial values $u_o(x)$ tends as $\delta, \tau \to 0$ boundedly and almost everywhere to some function u(x,t), then this limit u is a solution of the integral form (4.16) of the conservation law with initial value $u_o(x)$. For let w(x,t) be any smooth test function which is zero for x, t large; multiply (5.3) by $\delta w(k\delta, t_n)$, sum over k and n and sum by parts; we get

$$\sum\left(\frac{w_k^{n-1} - w_k^n}{\tau} v_n^k + \frac{(w_k^n - w_{k+1}^n)}{\delta} g_{k+1/2}^{n+1/2}\right)\delta\tau = \delta \sum w_k^o v_k^o \ . \tag{5.6}$$

If v_n^k tends to u boundedly and a.e., then $g_{k+1/2}^{n+1/2}$, defined by (5.4) and satisfying (5.5), tends to f(u), boundedly and a.e., and (5.6) tends to

$$-\iint (w_t v + w_x f)dxdt - \int w(x,0)u_o(x)dx = 0 .$$

This is precisely relation (3.16).

Here are some examples of approximations to flux functions:

i) $$g_{k+1/2}^{n+1/2} = \frac{f(u_k^n) + f(u_{k+1}^n)}{2} ,$$

ii) $$g_{k+1/2}^{n+1/2} = f\left(\frac{u_k^n + u_{k+1}^n}{2}\right) ,$$

iii) $$g_{k+1/2}^{n+1/2} = \frac{f(u_k^{n+1}) + f(u_k^n)}{2} ,$$

iv) $$g_{k+1/2}^{n+1/2} = \frac{f(u_k^n) + f(u_{k+1}^n)}{2} - \frac{\tau}{2\delta} A\left(\frac{u_k^n + u_{k+1}^n}{2}\right)(f(u_{k+1}^n) - f(u_k^n))$$

The following observations are obvious but useful.

a) If g is consistent with f, and if h is a function of v_j^n that vanishes when all its arguments are equal, then g+h too is consistent with f. For example we can augment the approximate flux function in i) to

v) $$g_{k+1/2}^{n+1/2} = \frac{f(u_k^n) + f(u_{k+1}^n)}{2} + c(u_k^n - u_{k+1}^n) ,$$

another consistent flux approximation.

b) Suppose the flux f is the sum of several fluxes $f_1 + f_2 + \ldots = f$, and suppose we treat these fluxes by the method of fractional steps explained in Section 4. If at each step we employ

a flux approximation consistent with the partial flux f_i, then the overall scheme will be consistent with the total flux f. This applies in particular to the important case when the number of space variables is greater than 1, and the flux has an x and a y component.

c) The flux approximation has to be so chosen that the scheme (5.3) is stable. Our examples i) and ii) are unstable, iii) is stable, iv) is stable if δ/τ exceeds the signal speeds, and v) is stable if c is large enough and δ/τ is small enough.

6. The methods of Godunov and Glimm

These methods were devised for conservation laws in one space variable:

$$u_t + f_x = 0 \ . \tag{6.1}$$

As in Section 5 we divide the x-axis into cells I_k, each of length δ, centered at $x = k\delta$, see (5.2). Given any initial data $u_o(x)$ we can project it onto the space of functions which are constant on each I_k by setting

$$v^o(x) = v_k^o = \frac{1}{\delta}\int_{I_k} u_o(x)dx \ , \quad x \text{ in } I_k \ . \tag{6.2}$$

We define the functions $v_{k+1/2}(x,t)$ as the solution of equation (6.1) with the following initial values:

$$v_{k+1/2}(x,0) = \begin{cases} v_k^o & \text{for } x < (k+1/2)\delta \\ v_{k+1}^o & \text{for } (k+1/2)\delta < x \end{cases} \tag{6.3}$$

This is a Riemann initial value problem of form (3.39); its solution consists of N+1 states separated by N waves centered at $x = (k+1/2)\delta$, $t = 0$. Each wave travels with a speed that equals or is bounded by one of the signal speeds a. Denote the maximum signal speed by $|a|_{max}$; it follows then that the centered waves issuing from two adjacent centers $(k-1/2)\delta$ and $(k+1/2)\delta$ don't intersect each other as long as

$$t \leq \frac{\delta}{2|a|_{max}} \quad . \tag{6.4}$$

So during the time interval (6.4) the solutions $v_{k+1/2}$ with initial values (6.3) can be fitted together to form a single exact solution $v(x,t)$ of (6.1) with initial value v^0 given by (6.2). This solution consists of constant states separated by centered waves, see Fig. 6.1.

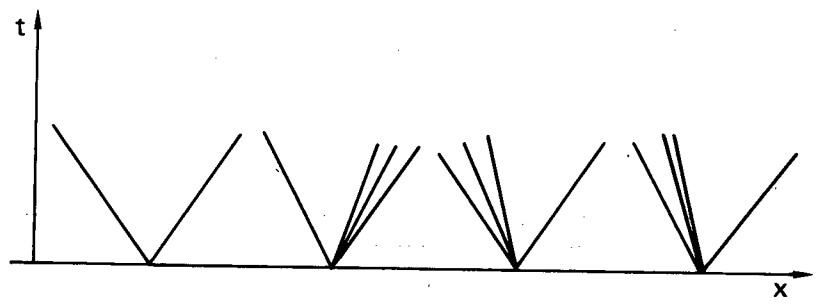

Figure 6.1

After time (6.4) the waves issuing from adjacent centers start to interact; in a numerical method developed in the fifties [11], Godunov replaces $v(k,\tau)$ at $\tau = \delta/2|a|_{max}$ by its piecewise constant projection defined by (6.2). Note that the integration indicated by (6.2) need not be carried out explicitly; for $v(x,t)$ is an exact solution of (6.1), so the integral form of (6.1) gives

$$\int_{I_k} v(x,\tau)dx = \int_{I_k} v(x,0)dx + \int_0^\tau f(v((k-1/2)\delta,t))dt - \int_0^\tau f(v((k+1/2)\delta,t))dt \quad .$$

This can be rewritten as

$$v_k^1 = v_k^o + \frac{\tau}{\delta}\,(g_{k+1/2}^{1/2} - g_{k-1/2}^{1/2}) \tag{6.5}$$

where

$$g_{k+1/2}^{1/2} = f(v_{k+1/2}((k+1/2)\delta,t)) \ , \tag{6.6}$$

since $v_{k+1/2}(x,t)$, being centered at $(k+1/2)\delta$, is independent of t.

Once v^1 has been determined as a piecewise constant function, the basic step is repeated; this is done as many times as necessary to reach the times T at which the phenomena under investigation are taking place. We denote by $t_1,\ldots,t_M$ the intermediate times at which the projections (6.2) take place.

Note that if $v_k^o = v_{k+1}^o$, then $v_{k+1/2}(x,t) \equiv v_k^o$; by (6.6) we have then $g_{k+1/2}^{1/2} = f(v_k^o)$; this proves that the approximate flux (6.6) employed in Godunov's scheme is consistent with the exact flux f.

Glimm's method resembles Godunov's inasmuch as the approximations $v(x,t)$ employed are piecewise constant functions of x at the selected times $t_1,t_2,\ldots$, and are exact solutions in the strips $t_{n-1} < t < t_n$, and are discontinuous across $t = t_n$. However Glimm defined v differently at time t_n; instead of (6.2) Glimm sets

$$v(x,t_n+0) = v(k\delta+\alpha^n\delta, t_n-0) \ , \quad x \in I_k \ , \tag{6.7}$$

where $v(x,t_n \pm 0)$ denotes the limiting values of v as $t \to t_n$ from below and above t_n respectively, and $\{\alpha^n\}$ is a sequence of random variables chosen from a sample uniformly distributed in $(-\frac{1}{2}, \frac{1}{2})$.

Glimm shows that for almost all choices of $\{\alpha^n\}$, $v = v(x,t,\alpha)$ converges to an exact solution as $\delta \to 0$. Here is a slightly modified form of his argument.

Let $w(x,t)$ be a smooth test function, $= 0$ for $|x|$ large. Multiply $v_t + f(v)_x = 0$ by w, and integrate by parts in the strip $t_{n-1} \leq t \leq t_n$; we get

$$\int_{-\infty}^{\infty} [w(x,t_n)v(x,t_n-0) - w(x,t_{n-1})v(x,t_{n-1}+0)]dx$$
$$- \int_{t_{n-1}}^{t_n} \int_{-\infty}^{\infty} [w_t v + w_x f(v)]dxdt = 0 .$$

Sum over $0 \leq n \leq M$; denoting $t_M = T$ we get

$$(6.8) \quad \int_0^T \int_{-\infty}^{\infty} [w_t v + w_x f(v)]dxdt$$
$$- \int_{-\infty}^{\infty} w(x,T)v(x,T)dx + \int_{-\infty}^{\infty} w(x,0)v(x,0)dx = r$$

where

$$(6.9) \quad r = \sum_1^M r_n$$

with

$$(6.10) \quad r_n = \int_{-\infty}^{\infty} w(x,t_n)[v(x,t_n-0) - v(x,t_n+0)]dx .$$

Lemma 6.1: Denote by η an upper bound for the total variation of $v(x,t)$ as function of x. Then

(6.11) $$|r_n| \leq \text{const } \delta\eta |w|_{max} .$$

Proof: Denote the variation of $v(x, t_{n-1}+0)$ over the union of I_k and I_{k+1} by $\eta_{k+1/2}$. Since v is constant over each I_k,

(6.12) $$\sum \eta_{k+1/2} \leq \eta .$$

Glimm shows that for x in I_k

(6.13) $$|v(x, t_n-0) - v(x, t_n+0)| \leq \text{const } (\eta_{k-1/2} + \eta_{k+1/2}) ,$$

for detailed proof we refer to [9]; here we merely observe that if $\eta_{k+1/2}$ and $\eta_{k-1/2}$ are both zero, then $v(x, t_{n-1}+0)$ has the same value in all three intervals I_{k-1}, I_k, I_{k+1}, so that $v(x,t)$ is constant in I_k for $t_{n-1} < t < t_{n+1}$, and therefore $v(x, t_n-0)$ $= v(x, t_n+0)$ in I_k. Thus if the right side of (6.13) is zero, so is the left side; while this does not prove inequality (6.13), it makes it plausible.

We multiply (6.13) by $w(x, t_n)$ and integrate over I_k; since the length of I_k is δ we obtain

(6.14) $$\int_{I_k} |w(x, t_n)||v(x, t_n-0) - v(x, t_n+0)| dx$$
$$\leq \text{const } \delta(\eta_{k-1/2} + \eta_{k+1/2}) |w|_{max} .$$

Comparing (6.10) and (6.11) we conclude that

$$|r_n| \leq \text{const } \delta |w|_{max}^2 \sum \eta_{k+1/2} \leq 2 \text{ const } \delta\eta |w|_{max} ,$$

where in the last step we used (6.12). This proves (6.11).

The approximate solution $v(x,t)$ depends on the sequence of random variables α. Next we show

Lemma 6.2:

$$\left| \int r_n d\alpha^n \right| \leq \text{const } \delta^2 \eta |w_x|_{\max} . \tag{6.15}$$

Proof: The function $v(x,t_n-0)$ does not depend on α^n, and $v(x,t_n+0)$ depends on α^n through formula (6.7). So integrating (6.10) gives

$$\int r_n d\alpha^n = \sum_k \int_{I_k} w(x,t_n)[v(x,t_n-0) - \bar{v}_k(t_n)]dx , \tag{6.16}$$

where

$$\bar{v}_k(t_n) = \frac{1}{\delta}\int_{I_k} v(x,t_n-0)dx .$$

Since $\bar{v}_k$ is the mean value of v over I_k, the integral of $[v - \bar{v}_k]$ over I_k is 0; therefore we deduce from (6.16) that

$$\int r_n d\alpha^n = \sum_k \int_{I_k} [w(x,t_n) - w(k\delta,t_n)][v(x,t_n-0) - \bar{v}_k(t_n)]dx \tag{6.17}$$

It follows from (6.13) that for x in I_k

$$|v(x,t_n-0) - \bar{v}_k(t_n)| \leq \text{const } (\eta_{k-1/2} + \eta_{k+1/2}) ; \tag{6.18}$$

furthermore,

$$|w(x,t_n) - w(k\delta,t_n)| \leq \delta |w_x|_{\max} \tag{6.19}$$

for all x in I_k. Using (6.19) and (6.18) to estimate the integrand shows

$$\int_{I_k} [w(x,t_n) - w(k\delta,t_n)][v(x,t_n-0) - \overline{v}_k(t_n)]dx$$

$$\leq \text{const } (\eta_{k-1/2} + \eta_{k+1/2})\delta^2 |w_x|_{max} .$$

Summing over all k we deduce from (6.17), using (6.12), that (6.15) holds.

Lemma 6.3: For $m \neq n$,

$$\int r_m r_n d\alpha \leq \text{const } \delta^3 \eta^2 |w|_{max} |w_x|_{max} , \tag{6.20}$$

where $d\alpha = d\alpha^1 d\alpha^2 \ldots d\alpha^M$.

Proof: Suppose $m < n$; then r_m is independent of α^n; so we get, using (6.11) and (6.15) that

$$\left| \int r_m r_n d\alpha^n \right| = \left| r_m \int r_n d\alpha^n \right| \leq \text{const } \delta\eta |w|_{max} \delta^2 \eta |w_x|_{max} .$$

Integrating with respect to the rest of the α^j yields inequality (6.20).

We are now ready for the main estimate; using (6.11) and (6.20) we get

$$\int r^2 d\alpha = \int (\sum_1^M r_n)^2 d\alpha = \int \sum r_m r_n d\alpha \tag{6.21}$$

$$= \sum_1^M \int r_n^2 d\alpha + \sum_{n \neq m} \int r_n r_m d\alpha$$

$$\leq \text{const } M\delta^2 \eta^2 |w|_{max}^2 + \text{const } M^2 \delta^3 \eta^2 |w|_{max} |w_x|_{max} .$$

M is the number of time steps, δ the size of the space step. Since the size of the time step, subject to inequality (6.4), is taken

to be as large as possible, i.e. $\delta/2|a|_{max}$, we have

$$T = t_M = \sum_1^M t_n - t_{n-1} \geq M\delta/2|a|_{max} .$$

Setting this into (6.21) we obtain the estimate

$$\int r^2 d\alpha \leq C\delta \tag{6.22}$$

where

$$C = \text{const } \eta^2 |w|_{max} |a|_{max} T\{ |w|_{max} + T|a|_{max} |w_x|_{max}\} . \tag{6.23}$$

In [9] Glimm estimates for all t the total variation of the approximate solutions v for all choices of α in terms of u total variation of the initial data. This gives an estimate for η valid for all α.

The quantity r, defined by (6.8), is the amount by which the approximation v fails to satisfy the integral form (4.16) of the conservation law. We call r the residual, with respect to the test function w.

Given any ε, it follows from (6.23) that

$$|r| < \varepsilon$$

except possibly for an α-set of measure $\leq C\delta\varepsilon^{-2}$. Given N conservation laws and K test functions $w_1, \ldots, w_K$, all residuals are $< \varepsilon$ except possibly on a set which is the union of the exceptional sets for each individual w and each conservation, and which may therefore have as large a measure as $CKN\delta\varepsilon^{-2}$; this estimate is unduly pessimistic, allowing for no overlap among the exceptional sets.

What are the implications for realistic values of the parameters? Let's take the case that the total variation of the initial data is 1; then we cannot expect a better estimate for η than $\eta = 1$. Let's take a test function w with $|w|_{max} = |w_x|_{max} = 1$. Suppose the maximum sound speed $|a|_{max} = 1$, and let's take as final time $T = 1$. A realistic value for the constant in inequality (6.18) is 1. Setting all these numbers into (6.23) gives $C = 2$, so we conclude, for a single conservation law and test function, that

$$|r| < \varepsilon$$

except possibly on a set of α of measure $2\delta\varepsilon^{-2}$. It is not unreasonable to want to make $\varepsilon = 10^{-2}$, and ordinary prudence requires making the measure of the exceptional set less than 10^{-2}. To satisfy this we must have

$$2\delta\ 10^{2} < 10^{-2}\ ,$$

i.e. the spatial step size δ must be less than 5×10^{-5}! This is a very fine grid, hardly called for to achieve a resolution which, with $|w|_{max} = |w_x|_{max} = 1$, is of the order of unity.

It is illuminating to examine how Glimm's scheme treats a particularly simple Riemann initial value problem

$$u(x,0) = \begin{cases} u_\ell & \text{for } x < 0 \\ u_r & \text{for } 0 < x\ , \end{cases}$$

where u_ℓ and u_r are so chosen that the exact solution consists of a single shock wave propagating with speed s:

$$u(x,t) = \begin{cases} u_\ell & \text{for } x < st \\ u_r & \text{for } st < x \,. \end{cases} \tag{6.24}$$

For this calculation it is convenient to take $I_k = (k\delta,(k+1)\delta)$; with this choice Glimm's scheme reads

$$v(x,t+0) = v(k\delta + \beta^n\delta, t_n - 0) \tag{6.25}$$

where $\beta^n = \alpha^n + 1/2$, $n = 1,2,\ldots$. Note that the β's are uniformly distributed in $(0,1)$.

Since $v(x,t-0)$ is the exact solution (6.24), we get from (6.25) that

$$v(x,\ +0) = \begin{cases} u_\ell & \text{for } x < J_1\delta \\ u_r & \text{for } J_1\delta < x \end{cases}$$

where

$$J_1 = \begin{cases} 1 & \text{if } \delta\beta^1 < s\tau \\ 0 & \text{if } \delta\beta^1 > s\tau \,. \end{cases}$$

Repeating this M times we get

$$v(x,M\tau) = \begin{cases} u_\ell & \text{for } x < J_M\delta \\ u_r & \text{for } J_M\delta < x \end{cases} \tag{6.26}$$

where

$$J_M = \text{no. of } \beta^j < s\tau/\delta \,, \quad j \leq M \,. \tag{6.27}$$

The location of the shock in the approximate solution at time $T = M\tau$ is

$$(6.28) \qquad J_N\delta = \frac{J_M}{M} N\delta = \frac{J_M}{M} T \frac{\delta}{\tau} .$$

As $M \to \infty$, J_M/M defined by (6.27) tends to $s\tau/\delta$, so the shock location tends to $\frac{s\tau}{\delta} T \frac{\delta}{\tau} = sT$, the exact location of the shock at time T. A simple calculation shows that the expected deviation of J_M/M from its expected value $s\tau/\delta = \kappa$ is $c/\sqrt{M}$, where $c = \sqrt{\kappa(1-\kappa)}/\sqrt{2\pi}$. So using (6.28) and $T = M\tau$ we see that the expected deviation of the calculated value of the shock position from the true one is

$$c(T/\tau)^{1/2}\delta .$$

Let's take $T = 1$, $\delta/\tau = 1$, $s = 1/2$; then $\kappa = 1/2$. To make the expected deviation $< \varepsilon$, we must have

$$\delta < 8\pi\varepsilon^2 .$$

For $\varepsilon = 10^{-2}$ this means $\delta < 2.5 \times 10^{-3}$. This is not too bad but gets worse as T increases.

Note that the accuracy of Glimm's scheme applied to the special Riemann problem above can be increased appreciably by taking the sequence β^n not at random but as uniformly distributed as possible. From the point of view of equidistribution an attractive choice is $\beta^n = n\theta \pmod 1$, where θ is an algebraic number, say $\sqrt{2}$. The error in shock position when applied to the special Riemann problem above is $O(\frac{\log N}{N})$. The use of such sequences in Monte Carlo calculations has been suggested by R.D. Richtmyer in the early 50's, and in connection with Glimm's scheme by the author, [21]. Chorin has successfully introduced other types of well distributed sequences.

Recently Tai Ping Liu succeeded in showing the convergence of Glimm's scheme to a solution for equidistributed sequences when the initial data are arbitrary. The time rate of convergence is an open problem; its determination will have to be, most likely, a combination of theory and numerical experimentation.

Godunov has successfully applied his method to systems of conservation laws in several space variables by using the method of fractional steps. Glimm's method has been applied by Chorin in several space variables, again using the method of fractional steps. No analytical results are available in this case.
A. Harten has observed that when Glimm's method is used in fractional steps to calculate the propagation of a contact discontinuity in two dimensions, the resulting one dimensional problems are resolved in terms of shocks. This introduces a certain amount of excess entropy production.

7. Entropy and viscosity

In Section 3 we saw that several solutions in the integral sense of a system of nonlinear conservation laws could have the same initial values. Since the initial configuration ought to determine the flow in the future, only one of these several solutions can occur in nature, and all others have to be excluded on the basis of some physical or mathematical principle. In Section 3 we have formulated two such principles:

i) stability, ii) the characteristic condition.

In this section we formulate two further principles, and show that, in sufficiently simple cases, all four are equivalent.

We start with the following question: if u is a smooth solution of the system of conservation laws (3.6):

$$u_t + f(u)_x = 0 , \tag{7.1}$$

does u satisfy some other conservation law that is not merely a linear combination of the equations (7.1). To answer this we write (3.7) in the differential form (3.7):

$$u_t + A(u)u_x = 0 , \quad A = \text{grad } f . \tag{7.2}$$

Let $U = U(u)$ be some function of u; multiplying (7.2) grad U $= (U_{u^1}, \ldots, U_{u^N})$ we get

$$U_t + \text{grad } UA\, u_x = 0 . \tag{7.3}$$

If there is a function F(u) such that

$$\text{grad } UA = \text{grad } F \tag{7.4}$$

then (7.3) can be written as a conservation law:

$$U_t + F_x = 0 . \tag{7.5}$$

Since in our derivation we used the differential form (7.2) of the equation, we cannot conclude that a solution of (7.1) in the integral sense satisfies (7.5) in the integral sense; in fact, as we shall see, the opposite of this is true.

We remark that (7.4) is a system of N linear differential equations for the two functions U and F. For $N \leq 2$ there are plenty of solutions; for $N > 2$ there are none in general, except in special cases. For example, Godunov has observed that when A is

symmetric, i.e.

$$\frac{\partial f^i}{\partial u^j} = \frac{f^j}{\partial u^i} \tag{7.6}$$

then

$$U = \sum u^{j^2} \quad \text{and} \quad F = \sum u^j f^j - g \tag{7.7}$$

satisfies (7.4), where g is defined by

$$\frac{\partial g}{\partial u^j} = f^j , \quad j = 1,\ldots,n ; \tag{7.8}$$

note that (7.6) is the compatibility relation for (7.8). The equations of gas dynamics, discussed in Section 3, have an extra conservation law, where U is entropy S. Generalizing this case we define U to be an entropy function for the system (7.1) if equation (7.4) can be satisfied, and if U is a convex function of u. Note that U in (7.7) is a convex function; so is -S in gas dynamics.

According to the laws of thermodynamics, entropy is a non-decreasing function along a particle path; we shall deduce a similar property of the generalized entropy functions defined above. We look at solutions of (7.1) which are limits of viscous equations. We envisage here an artificial viscosity, of the form

$$u_t + f_x = \lambda u_{xx} , \quad \lambda > 0 . \tag{7.9}$$

Suppose that as $\lambda \to 0$, solutions $u(\lambda)$ of (7.9) tend boundedly, a.e. to a limit u. Then $u_t(\lambda)$ tends to u_t, $f(u(\lambda))_x$ to $f(u)_x$ and the right side of (7.9) tends to 0 in the sense of distributions; therefore u satisfies in the distribution sense

$$u_t + f_x(u) = 0 .$$

Let's rewrite (7.9) in nonconservation form:

$$u_t + Au_x = \lambda u_{xx} \cdot \tag{7.9)'}$$

Suppose U is an entropy function; then multiplying (7.9)' by grad U we get, using (7.4),

$$U_t + F_x = \lambda \text{ grad } U \cdot u_{xx} \cdot \tag{7.10}$$

Using the chain rule we get, differentiating $U_x = \text{grad } U \cdot u_x$, that

$$U_{xx} = \text{grad } U \cdot u_{xx} + u_x^T U_{uu} u_x \cdot \tag{7.11}$$

Since U is an entropy function, it is convex, i.e. the matrix of its second derivatives is positive definite:

$$U_{uu} > 0 \cdot \tag{7.12}$$

We deduce from (7.11) and (7.12) that

$$\text{grad } U \cdot u_{xx} \leq U_{xx} \cdot$$

Substituting this into (7.10) we get

$$U_t + F_x \leq \lambda U_{xx} \cdot \tag{7.13}$$

Suppose that $u(\lambda)$ is a sequence of solutions of (7.9) that tends as $\lambda \to 0$ boundedly and a.e. to a limit u. Then $U(\lambda) = U(u(\lambda))$ and $F(\lambda) = F(u(\lambda))$ tend to U and F in the sense of distributions, while the right side of (7.13) tends to zero in the sense of distributions. So we have proved the

Viscosity Theorem: Let U be an entropy function for the system (7.1). Let u be a limit, boundedly, a.e., of a sequence $u(\lambda)$ of

solutions of the viscous equations (7.9). Then u satisfies the conservation laws (7.1), and the inequality

$$U(u)_t + F(u)_x \leq 0 \ . \tag{7.14}$$

Suppose u is a piecewise smooth solution with discontinuities; then $U_t + F_x = 0$ in the smooth regions, while on a discontinuity $x = x(t)$

$$U_t + F_x = \delta(x - x(t))\{s[U_\ell - U_r] - [F_\ell - F_r]\} \ . \tag{7.15}$$

We draw two conclusions from this:

$$s[U_\ell - U_r] - [F_\ell - F_r] \leq 0 \ . \tag{7.15}'$$

Denote by $\overline{U}(t)$ the total entropy at time t:

$$\overline{U}(t) = \int U(x,t)dx \ ; \tag{7.16}$$

then

$$\frac{d\overline{U}}{dt} = \int U_t dx = \sum s[U_\ell - U_r] - [F_\ell - F_r] \ . \tag{7.16}'$$

This shows that the left side of (7.15)' is the rate at which entropy is diminished at the discontinuity. (7.14) and (7.15)' are called entropy conditions.

The viscosity theorem characterizes solutions of (7.1) that are limits of viscous solutions without carrying out the limiting procedure; the characterization is in terms of entropy. We connect now this entropy condition to the stability condition stated in Section 3:

Entropy Theorem: Let u be a piecewise continuous solution of a single conservation law that satisfies the entropy inequality (7.15)' for all entropy functions. Then the discontinuities of u are stable in the sense of condition (3.25).

Proof, due to Hopf [16] and Kruzkov, [19]:

Let (u_ℓ, u_r) be a discontinuity of u, say $u_\ell < u_r$; let v be any value between the two:

$$u_\ell < v < u_r .$$

We define U by

$$U(u) = \begin{cases} 0 & \text{for } u < v \\ u-v & \text{for } v < u . \end{cases}$$

Note that U is a convex function. Set U into the differential equation (7.4); we get

$$F_u(u) = \begin{cases} 0 & \text{for } u < v \\ a(u) & \text{for } v < u . \end{cases}$$

Integrating gives

$$F(u) = \begin{cases} 0 & \text{for } u < v \\ f(u) - f(v) & \text{for } v < u \end{cases}$$

With this choice of U and F we have

$$U_\ell - U_r = v - u_r , \quad F_\ell - F_r = fv - f_r .$$

Set this, together with definition (3.21) of s, into (7.15)'; after a little rearrangement we get

$$(7.17) \qquad f(v) \geq \frac{u_r - v}{u_r - u_\ell} f_\ell + \frac{v - u_\ell}{u_r - u_\ell} f_r ,$$

which is equivalent with condition (3.25) when $u_\ell < u_r$. The case $u_\ell > u_r$ can be reduced to the previous case by using the conservation law, entropy and stability condition satisfied by -u.

If we combine the viscosity and entropy theorems, we deduce that the following statements about discontinuous solutions of single conservation laws are equivalent:

(I) u is the limit of solutions of the viscous equation (7.9).

(II) u satisfies the entropy condition (7.14) for every entropy function.

(III) The discontinuities of u are stable in the sense of (3.25).

A direct derivation of (III) from (I) is contained in [18].

As remarked in Section 3 for convex f (III) is equivalent with

(IV) The discontinuities of u satisfy the characteristic condition (3.26).

Next we show that discontinuous solutions that satisfy the stability condition are uniquely determined by their initial data. The proof is based on the

Contraction Theorem (Keyfitz, [18]): Let u and v both be solutions of

$$u_t + f_x = 0$$

and suppose that both satisfy the stability condition (3.25); then

$$(7.18) \qquad |u(t) - v(t)| = \int_{-\infty}^{\infty} |u(x,t) - v(x,t)|dt$$

is a decreasing function of t.

Proof: We write

$$(7.19) \qquad |u-v| = \sum \varepsilon_n \int_{I_n} (u-v)dx$$

where the intervals I_n are chosen so that (u-v) is of sign ε_n over I_n. Denote the endpoints of I_n as $[a_n, b_n]$; of course $b_n = a_{n+1}$. Since u and v depend on t, so do $a_n(t)$ and $b_n(t)$; we assume the dependence is differentiable. Differentiate (7.19):

$$(7.20) \qquad \frac{d}{dt}|u-v| = \sum \varepsilon_n \left[\int_{I_n} (u_t - v_t)dx + (u-v)\frac{dx}{dt}\Big|_{a_n}^{b_n} \right] .$$

Replacing u_t by $-f(u)_x$, v_t by $-f(v)$, and carrying out the integration we get

$$(7.20)' \qquad \frac{d}{dt}|u-v| = \sum \varepsilon_n \Big[f(v) - f(u) + (u-v)s \Big]_{a_n}^{b_n}$$

where s abbreviates dx/dt, $x = a_n$ or b_n.

If a_n or b_n is a point of continuity for both u and v, then u = v there and so the contribution to the right side of (7.20)' is zero. Suppose on the contrary that, say, b_n is a discontinuity of u but not for v, with say

$$(7.21) \qquad u_\ell = u(b_n - 0) \leq v(b_n) \leq u(b_n + 0) = u_r .$$

In this case u-v < 0 in I_n so $\varepsilon_n = -1$. Using the definition (3.21)

of s and the abbreviations

$$f_r = f(u_r) , \quad f_\ell = f(u_\ell) , \quad f = f(v)$$

we can write the corresponding term on the right of (7.20)' as

$$(7.22) \qquad - \left[f - f_\ell + (u_\ell - v) \frac{f_\ell - f_r}{u_\ell - u_r} \right] .$$

According to condition (3.25)'

$$\frac{f_\ell - f}{u_\ell - v} \geq \frac{f - f_r}{v - u_r} .$$

This and (7.21) readily imply that (7.22) is nonpositive.

Condition (3.25) is invariant when u is replaced by -u, f(u) by -f(-u), v by -v, f by -f; this proves that when the inequality in (7.21) is reversed, the contribution to the right side of (7.20)' is still nonpositive. Similarly, condition (3.25) is invariant when x is replaced by -x and f by -f; this proves that the contributions to the right side of (7.20)' at the lower endpoints are likewise nonpositive. Finally, since u and v enter the inequality symmetrically, contributions to the right side of (7.20)' at discontinuities of v are likewise nonpositive, as long as these are distinct from the discontinuities of u. If the discontinuities of u and v intersect only at discrete times, we conclude from (7.20) that $|u-v|$ is a nonincreasing function of t; the exceptional case can be reduced to this by changing slightly the initial data of one of the functions. This completes the proof of the contraction theorem.

It follows that if u = v at time t = 0, then u = v for all t; this proves the

Uniqueness Theorem: Two solutions of a single conservation law both of which satisfy the stability condition and which are equal at t = 0 are equal at all times t > 0.

We turn now to the question of existence of stable solutions with prescribed initial values; we content ourselves with Riemann initial values, consisting of two constant states

$$u(x,0) = \begin{cases} w & \text{for } x < 0 \\ z & \text{for } 0 < x \,. \end{cases} \tag{7.23}$$

We have remarked earlier that for $u_\ell < u_r$ (3.25)" is equivalent with (7.17); the geometric interpretation of this is that f lies above the secant in the interval (u_ℓ, u_r). When $u_\ell > u_r$, condition (3.25) demands that f lie below the secant in (u_r, u_ℓ).

To solve the initial value problem in the case, say, w < z we construct the convex envelope g of f between z and w defined as the largest convex function g which is $\leq$ f, see Fig. 7.1, where g appears as a dotted line. Denote by $w = u_0 < u_1 < \ldots < u_k = z$ the

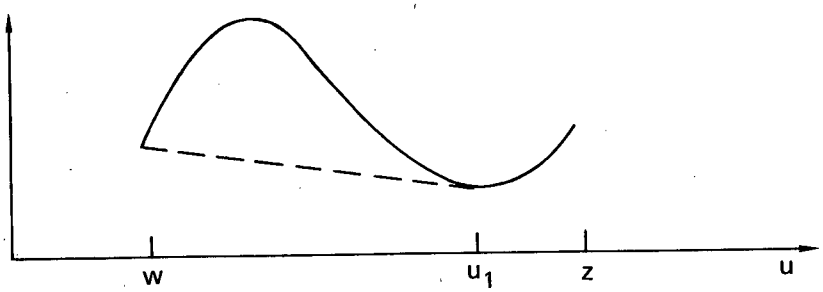

Figure 7.1

endpoints of intervals where g = f. Then the solution of the

initial value problem consists of k+1 constant states connected by k waves; if g = f in (u_j, u_{j+1}), u_j and u_{j+1} are connected through a centered rarefaction wave; if g < f there, the wave connecting them is a straight shock. In the case depicted in Fig. 7.1, k = 2:

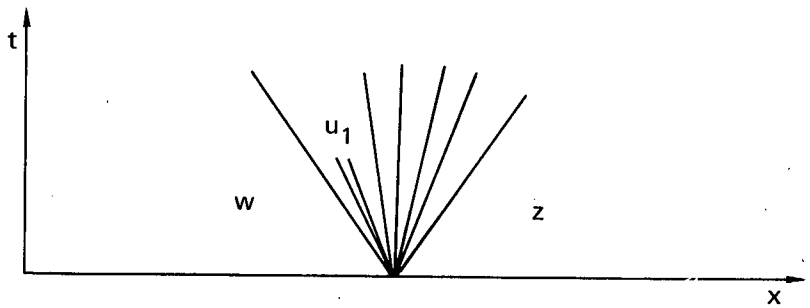

Figure 7.2

Clearly $u_\ell < u_r$ for each shock, and f lies above the secant g in (u_ℓ, u_r).

We note the following general properties of solutions:

i) If f has ℓ inflection points $k \leq \ell+1$.

ii) If k = 2, then the shock is sonic on one side but not, in general, on the other.

The occurrence of shocks which are sonic on one side when f has inflection points is analogous to detonation waves satisfying the Chapman-Juguet condition.

We turn now to systems, for which we have already defined the entropy concept and have proved the viscosity theorem. Next we state a local version of the

Entropy Theorem: Let u be a piecewise continuous solution of a system of conservation laws that has an entropy function U. Suppose further that the jumps of u across discontinuities are

small. Then the discontinuities of u are stable iff the entropy condition (7.15)' is satisfied.

Sketch of proof: It was shown in Section 3 that the states u_r that satisfy the R-H conditions form N one parameter families $u_r(\varepsilon)$; the states that satisfy the stability condition (3.25) make up half of this family, corresponding to $\varepsilon < 0$ under the normalizations (3.33) and $u'(0) = r$.

Abbreviate the left side of (7.15)' by R:

$$R = s[U_\ell - U_r] - [F_\ell - F_r] . \tag{7.24}$$

Obviously $R(0) = 0$; we show now that also $R'(0) = 0$. For differentiating (7.24) we get

$$R'(0) = -sU'(0) + F'(0) .$$

Multiply (7.4) by $u'(0)$; using the fact that $u'(0) = r$ and therefore $Au'(0) = ar$ we get

$$aU'(0) = F'(0) .$$

Since $a(0) = s(0)$, we deduce from the last two relations that $R'(0) = 0$.

A straightforward but slightly tedious calculation shows that $R''(0) = 0$ and

$$R'''(0) = \frac{1}{2} r^T U_{uur} .$$

Since the entropy U is assumed to be a convex function of u, it follows that $R'''(0) > 0$. This shows that for ε small enough, $R(\varepsilon) < 0$ iff $\varepsilon < 0$. This proves that for small discontinuities the stability and entropy conditions are equivalent, as asserted.

Notice that if $R''(0)$ were $\neq 0$ then $R(\varepsilon)$ has the same sign for all ε small, regardless of the sign of ε. Therefore if we assume the truth of the entropy theorem, it follows without any tedious calculation that R, the rate of entropy production, is at most cubic in the shock strength ε.

The contraction theorem is most likely not valid for systems. A uniqueness theorem for a special class of systems of 2 conservation laws has been given by Oleinik in [27]; a more general uniqueness theorem, using entropy, has been given by Diperna, [7].

We close this section by remarking that the circle of ideas described in this section remains an active area of research. The concepts of entropy and stability are central in describing solutions that are limits of solutions of equations with viscosity, real or artificial. The characteristic condition, always necessary, is not always sufficient and has to be supplemented by the first two.

Bibliography

[1] Bethe, H., The theory of shock waves for an arbitrary equation of state, OSRD, Div. B, Report No. 545, 1942.

[2] Boris, J.P. and Book, D.L., "Flux-Corrected Transport. I. SHASTA, A Fluid Transport Algorithm that Works", J. Comp. Phys., 11, 1973, 38-69.

[3] Chorin, A.J., "Random Choice Solution of Hyperbolic Systems", J. Comp. Phys., 22, 1976, 517-533.

[4] Courant, R. and Friedrichs, K.O., Supersonic Flow and Shock Waves, 1948, Wiley-Interscience, New York, reprinted by Springer Verlag.

[5] Dafermos, C.M., "Structure of solutions of the Riemann problem for hyperbolic systems of conservation laws", Arch. Rat. Mech. Anal., 53, No. 3, 1974, 203-217.

[6] Diperna, R.J., "Existence in the large for quasilinear hyperbolic conservation laws", Arch. Rat. Mech. Anal., 52, 1973, 244-257.

[7] Diperna, R.J., "Uniqueness of solutions of quasilinear hyperbolic conservation laws", to appear.

[8] Douglis, A., "The continuous dependence of generalized solutions of nonlinear partial differential equations upon initial data", Comm. Pure Appl. Math., 14, 1961, 267-284.

[9] Glimm, J., "Solutions in the large for nonlinear hyperbolic systems of equations", Comm. Pure Appl. Math., 18, 1965, 697-715.

[10] Glimm, J. and Lax, P.D., "Decay of solutions of systems of nonlinear hyperbolic conservation laws", Mem. Amer. Math. Soc., 101 (1970).

[11] Godunov, S.K. and Bagrynovskii, Y., "Difference Schemes for Many Dimensional Problems, D.A.N. 115, 1957, 431.

[12] Godunov, S.K., "On the uniqueness of solutions of the equations of hydrodynamics", Mat. Sb. 40, 1956, 467-478.

[13] Greenberg, J., "Estimates for fully developed shock solutions", Indiana Univ. Math. J., 22, 1973, 989-1003.

[14] Harlow, F., "The particle-in-cell method for fluid dynamics", Methods of Comp. Phys., Vol. 3, B. Alder, ed., Acad. Press, New York, 1964, 319-343.

[15] Harten, A., "The Artificial Compression Method for Computing Shocks and Contact Discontinuities", Comm. Pure Appl. Math., XXX, 1977, 611-638.

[16] Hopf, E., "The partial differential equation $u_t + uu_x = \mu u_{xx}$", Comm. Pure Appl. Math., 3, 1950, 201-230.

[17] Hopf, E., "On the right weak solution of the Cauchy problem for a quasilinear equation of first order", J. Math. Mech., 19, 1969, 483-487.

[18] Keyfitz, B., (Quinn), "Solutions with shocks; an example of an L_1 contractive semigroup", Comm. Pure Appl. Math., 24, 1971, 125-132.

[19] Krushkov, N., "Results on the character of continuity of solutions of parabolic equations and some of their applications", Math. Zametky, 6, 1969, 97-108.

[20] Lax, P.D., "Weak solutions of nonlinear hyperbolic equations and their numerical computation", Comm. Pure Appl. Math., 7, 1954, 159-193.

[21] _____, "Shock waves and entropy", Proc. Symp. Univ. Wisc., 1971, E.H. Zarantonell, ed., 603-634.

[22] _____, "Hyperbolic systems of conservation laws and the mathematical theory of shock waves", 1972, SIAM, Phil., Pa.

[23] Lax, P.D. and Wendroff, C., "Difference schemes for hyperbolic equations with high order of accuracy", Comm. Pure Appl. Math., 17, 1964, 381-394.

[24] Liu, Tai-Ping, "The entropy condition and the admissibility of shock", Math. Anal. and Appl., 53, 1976, 78-88.

_____, "Solutions in the large for the equations of nonisentropic gas dynamics", Indiana Univ. Math. J., 26, 1977, 147-177.

[25] MacCormack, R.W., "Numerical solution of the interaction of a shock wave with a laminar boundary layer", Lecture Notes on Physics, No. 8, Springer Verlag, Berlin, 1971.

[26] Nishida, T. and Smoller, J.A., "Solutions in the large for some nonlinear hyperbolic conservation laws", Comm. Pure Appl. Math., 26, 1973, 183-200.

[27] Oleinik, O.A., "On the uniqueness of the generalized solution of Cauchy's problem for a nonlinear system of equations occurring in mechanics", Uspehi Mat. Nauk, 73, 1957, 169-176.

[28] Peaceman, D.W. and Rachford, H.H. Jr., "The Numerical Solution of Parabolic and Elliptic Equations, Journ. Soc. Ind. Appl. Math., III, 1955, 28-42.

[29] Richtmyer, R.D. and Morton, W., "Difference Methods for Initial Value Problems", Interscience, New York, 1967.

[30] Serrin, J., "Mathematical Principles of Classical Fluid Mechanics", Handbuch der Physik, Vol. 8, 1959, 125-263.

[31] Smoller, J., "A uniqueness theorem for Riemann problems", Arch. Rat. Mech. Anal., 33, 1969, 110-115.

[32] Strang, G., "Accurate Partial Difference Methods", Num. Math., 6, 1964, 37-46.

[33] Wendroff, B., "The Riemann problem for materials with non-convex equations of state II; general flow", J. Math. Anal. Appl., 38, 1972, 640-658.

[34] Weyl, H., "Shock waves in arbitrary fluids, Comm. Pure Appl. Math., 2, 1948, 103-122.

[35] Yanenko, N.N., "The method of fractional steps; the solution of problems in mathematical physics in several variables". English translation, New York, Springer-Verlag, 1971.

ON THE MATHEMATICAL THEORY OF DEFLAGRATIONS AND DETONATIONS

K. O. Friedrichs

Courant Institute of Mathematical Sciences
New York University
New York, New York 10012

While the propagation of a shock wave is completely determined by the conservation laws, the boundary conditions of the problem, and the additional condition that the entropy increase in the process, the same is not true for the propagation of a detonation wave and of the flame front in an ordinary combustion process. More conditions must be added to the conservation laws in order to provide sufficient data for the unique determination of the propagation process. For detonations this necessity was recognized by Chapman and Jouguet when they introduced their famous hypothesis. For combustion processes this necessity was more or less tacitly assumed by Jouguet and others when they attacked the calculation of the flame speed by taking heat conduction into account without even trying to determine the flame speed from the conservation laws and boundary conditions alone.

It is natural to expect that the needed additional conditions could be derived from an investigation of the internal mechanism of the combustion or detonation process. Thus v. Neumann [1] has arrived at a justification of the Chapman-Jouguet hypothesis for detonations by taking into account that the chemical reaction takes place over a zone of finite width; his arguments are based on the assumption that a detonation is initiated by a shock. For combus-

tion processes, which do not involve shocks, no unique determination can be achieved without taking heat conduction into account.

It is the intention of the present paper to offer a unified and more complete discussion of the question of determinacy for detonations and deflagrations[1]. In order to be able to point out the contrast between these two kinds of processes we shall treat both of them on the basis of the same assumptions: We shall take viscosity and heat conduction into account and assume a finite rate of chemical reaction. (Accordingly, we shall not postulate that a detonation process begins with a shock.) From the discussion of the internal mechanism of the detonation and deflagration process on this basis we shall obtain the desired additional conditions which make unique determination of the whole process possible by excluding certain detonation or deflagration processes which would be compatible with the conservation laws. In particular we shall find as a result that a detonation begins with a shock and that the Chapman-Jouguet hypothesis furnishes the correct additional condition provided that for a given value of the reaction rate the viscosity and the heat conductivity are sufficiently small. If, on the other hand, the reaction rate is very high, for given viscosity and heat conductivity, the detonation no longer begins with a shock; and if the reaction rate is excessively high, the Chapman-

[1] We propose to use the term deflagration for those combustion processes which take place in a very narrow zone of constant width and which therefore in good approximation can be described by a discontinuity. For detonation and deflagration processes we shall employ the common name "reaction process".

Jouguet hypothesis is no longer correct; (see Appendix II). The additional condition for deflagrations is such that it prescribes the flame speed dependent on heat conduction and reaction rate.

To fix the ideas we have considered the problem of determining the flow under the following circumstances: In an infinite tube a piston moves in a prescribed manner beginning at an initial time at an initial cross-section. At the same time a reaction process begins at the piston and travels into the quiet unburnt gas. This problem includes the important case that the tube is closed at the initial cross-section; for, this case results when the piston remains at its original place. The case of an open end results when the piston is withdrawn with sufficiently large speed. Also the case is included that in a doubly infinite tube containing combustible and non-combustible gas, not separated by a piston, a reaction begins at the interface. One needs only force the piston to move in the same manner in which the initial cross-section would move anyhow if there were no piston.

Before describing the results in greater detail we formulate the basic assumption underlying our investigations, viz. that the reaction process in question may approximately be considered as a sharp discontinuity. More precisely the assumption is that the "reaction zone," across which chemical composition, pressure, temperature, and velocity change is very narrow and of nearly constant width; (see Appendix I). By this we mean, firstly, that the space rates of change of the pertinent quantities over a section in the field of flow outside of the reaction zone are negligibly small when compared to the rates of change of the same

quantities inside the reaction zone and, secondly, that the time rate of change of the width of the reaction zone is small when compared with the average speed with which the gases cross the reaction zone. This assumption appears to be justified only if the coefficients of viscosity and heat conduction are sufficiently small and the rate of reaction is sufficiently large. (We leave aside the question whether or not under these circumstances the assumption is always justified.) The pertinent quantities on both sides of the "reaction front" are then connected by the same well-known laws of conservation of mass, momentum, and energy that hold for the quantities at both sides of a discontinuity surface.

Next we give a brief account of the indeterminacies that one encounters when one tries to determine a flow involving a reaction discontinuity solely by using the conservation laws and the boundary conditions. To this end it is necessary to distinguish various types of reaction processes. Among the detonations there is, as is well known, a particular one, the "Chapman-Jouguet" detonation, which is singled out from others by the property that the flow of the burnt gas is sonic when observed from the reaction front. We have termed "strong" or "weak" a detonation if it involves a pressure rise greater or less than for a Chapman-Jouguet detonation.[1] Similarly, we have termed "strong" or "weak" a deflagration if it involves a pressure drop greater or less than for a Chapman-Jouguet deflagration, which again is characterized by the condition that the flow burnt gas is sonic when observed from the reaction

[1] For the following see [2].

front. A constant volume detonation is the limiting case of a weak one, producing the least pressure rise (and the least temperature rise) among all detonations for the same explosive; a constant pressure deflagration is also the limiting case of a weak one, producing the least drop in density (and the greatest temperature rise) among all deflagrations.

We now consider the flow of gas in a half-finite tube resulting, as indicated before, when a reaction front starts to move from the finite end of the tube into the unburnt gas under the influence of a piston which moves in a prescribed manner. We then ask for the gas motions which are compatible with the conservation laws and the piston motion. Mathematically speaking, we ask for the solutions of the flow differential equations compatible with the transition conditions at the discontinuity front and with the boundary condition, which expresses that the gas adjacent to the piston has the same velocity as the piston. This problem will be referred to as the "external flow problem." The answer, explained in detail in [2] is this:[1] Suppose the reaction process is a detonation; if then the piston moves in the same direction as the reaction front, and if the velocity u_p of the piston exceeds the gas velocity u_D which would be produced by a Chapman-Jouguet detonation, then there is just one flow involving a strong detonation in which the burnt gas has the prescribed

[1] It should be emphasized that the theory as considered in this report, based on the assumption that the reaction front be a sharp discontinuity, does not offer any possibility of predicting whether a detonation or a deflagration will occur in a given situation (except that under certain circumstances deflagration flow is not possible).

piston velocity. If, however, the piston velocity u_P is less than u_D, adjustment of the velocity of the burnt gas to the piston velocity can always be achieved by a Chapman-Jouguet detonation followed by an appropriate rarefaction wave, but it can also be achieved by a set of weak detonations followed either by a shock or a rarefaction wave. Thus, in case $u_P < u_D$, the solution of the mathematical problem is not unique; there is a one-parametric set of solutions.

For deflagration processes the degree of indeterminacy is still higher. To any piston velocity u_P one has still the choice of a flame velocity arbitrary within certain limits[1] and can achieve adjustment of the gas velocity to the piston velocity by sending ahead of the flame a shock of appropriate strength. Again, there is a one-parametric set of solutions as long as the deflagration remains weak. If the resulting deflagrations become strong ones, the possibilities of adjustment become still greater and the set of solutions is two-parametric.

To express these determinacy statements in a simple form we introduce as "degree of under-determinacy" of the external flow problem the number t of conditions that must be imposed on the data of the flow problem in order to make the solution unique. Summarizing we then have:

[1] The limiting case is the one in which the flame together with the pre-compression shock are just equivalent to a detonation.

Strong detonations	$t = 0$,
Weak detonations	$t = 1$,
Weak deflagrations	$t = 1$,
Strong deflagrations	$t = 2$.

Chapman-Jouguet detonations and deflagrations are here classed with strong detonations or weak deflagrations respectively.

These peculiar under-determinacies are a consequence of Jouguet's important rule (cf. [2]); concerning the properties of the gas flow observed from the reaction front:

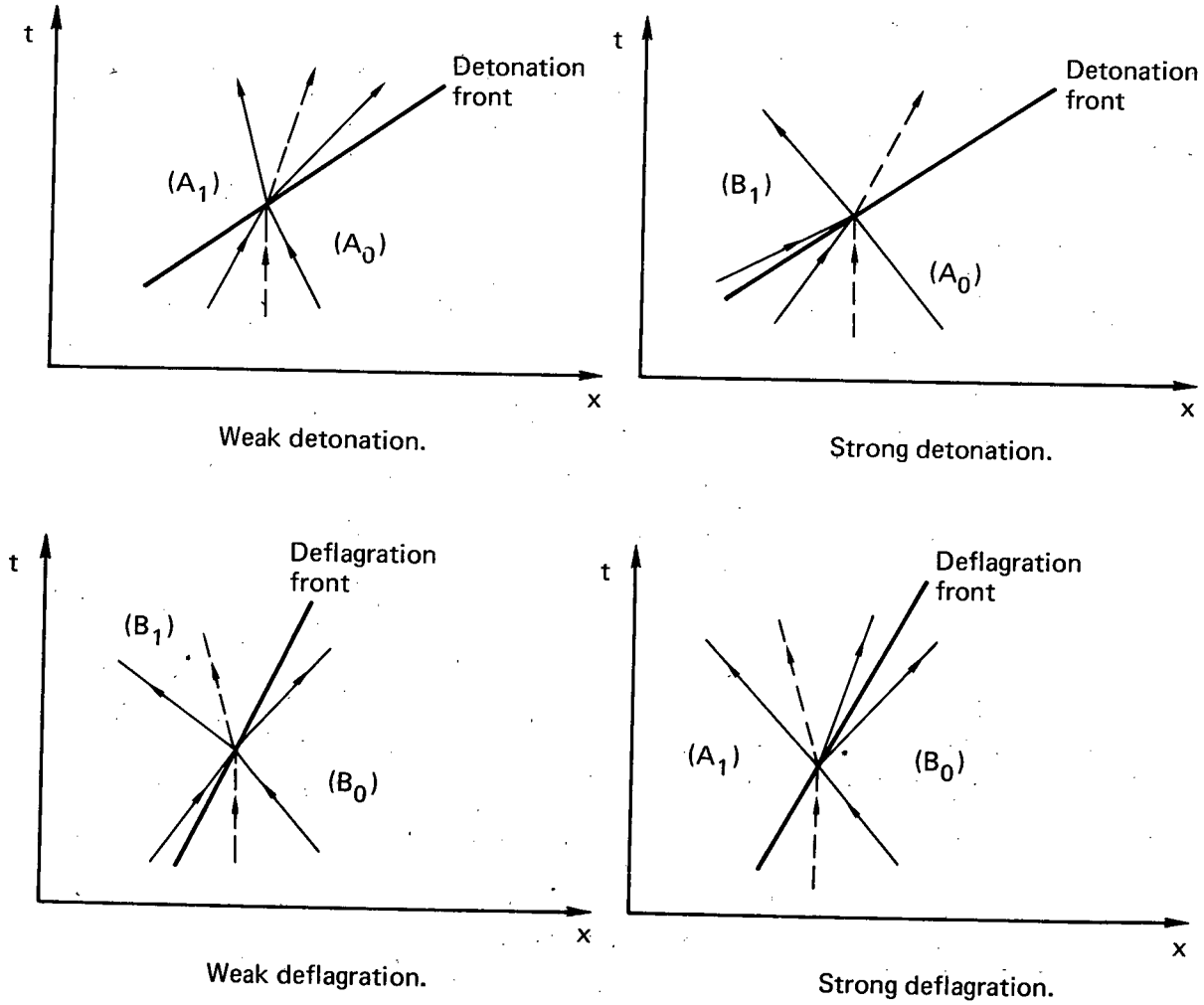

Particle paths and sound paths ↗ at detonation or deflagration fronts.

Figure 1

The flow ahead of a detonation front is supersonic, and subsonic ahead of a deflagration front. The flow is subsonic behind a strong detonation and a weak deflagration front, supersonic behind a weak detonation and a strong deflagration front. The flow is here always understood relative to the reaction front.

We now proceed to discuss the chief aim of the present paper, namely to decide which of the flow processes, still permitted by the conservation laws, are excluded through the action of viscosity, heat conduction, and chemical reaction. To this end we shall take into account that the reaction zone has a finite extension. We then shall set up the differential equations governing the transition across such a reaction zone and investigate under which circumstances these differential equations possess solutions satisfying the boundary conditions imposed at the two ends of the reaction zone. These boundary conditions consist in prescribing the chemical composition, pressure, temperature, and velocity of the gases at both ends of the reaction zone in such a way that the laws of conservation of mass, momentum, and energy are satisfied by these quantities. The differential equations in the interior of the reaction zone express the same conservation laws, but take into account chemical reaction, viscosity, and heat conduction.

Investigations of this kind for shocks not involving a chemical reaction have been made in detail by various authors[1]. The result was that a transition between the given quantities at both sides of the zone is always possible provided that the

[1] See e.g. Becker [3] and Weyl [4].

direction of the flow corresponds to increasing entropy. Our investigation will show that the same is true for strong detonations and for Chapman-Jouguet detonations. For other modes of reaction, however, the situation is completely different. Here are the results of our analysis:

Unless the rate of reaction is excessively high, weak detonations, though compatible with the conservation laws, are impossible. The condition that the detonation be strong or of the Chapman-Jouguet type is, therefore, the desired additional condition mentioned in the beginning. Consequently, a flow involving a detonation is uniquely determined. For, if the piston velocity is high, $u_P > u_D$, there is a unique solution involving a strong detonation, as mentioned before; for lesser piston velocity, however, $u_P \leq u_D$, there is now only one possible flow left in which the velocity of the burned gas equals the piston velocity, and that is the flow involving a Chapman-Jouguet detonation. In particular we see that for a tube with a closed end, $u_P = 0$, or open end, $u_P << 0$, a Chapman-Jouguet detonation is the only possible one. Thus the occurrence of this particular detonation is here deduced and no additional hypothesis is required.

If, however, the reaction rate is excessively high, the analysis yields the result that the Chapman-Jouguet detonation is impossible. Instead, a particular weak detonation is possible which travels with a well-determined velocity (depending on pressure and temperature in the unburnt gas, reaction rate, viscosity, and heat conductivity). If the piston velocity is large enough, adjustment still requires a strong detonation. For lesser

piston velocities, for example for closed or open ends, adjustment is effected by the particular weak detonation followed by an appropriate shock or an appropriate rarefaction wave.

As to deflagrations the results of the analysis are that strong deflagrations are impossible altogether.[1] A weak deflagration is possible only with a well-determined speed. We distinguish the "flame velocity," i.e. the velocity of the reaction front relative to the tube, from the "burning speed," i.e. the speed of the reaction front relative to the unburnt gas ahead of it. While the flame velocity depends on the boundary conditions of the problem as a whole, the burning speed depends only on pressure and temperature in the unburnt gas, and also on reaction rate, heat conductivity and viscosity. That the burning speed has this particular value is the desired additional condition for deflagrations. As stated before, for a burning speed arbitrary within certain limits, a deflagration flow can be found which is adapted to the piston motion. A further limitation is imposed by excluding strong deflagrations. Thus we see: Within certain limits for the data of the problem there exists a uniquely determined flow involving a deflagration and adapted to the piston motion.

We call attention to a number of detailed investigations of the transition process in reaction zones. Detonation transitions

[1] This result could also be established by v. Neumann's argument ignoring viscosity and heat conduction and taking only the finite rate of chemical reaction into account.

have been determined in detail by Eyring and his collaborators[1]. Deflagration flame speeds have been calculated by Jouguet and others[2], on the basis of various assumptions about the details of the transition process. The aim of the present report is different: it is not intended to give new methods for calculating such transition processes. The intention is solely to decide the question of determinacy by investigating such transition processes systematically on the basis of the existing theory.

1. The internal mechanism of the reaction process.

We assume the process to be strictly one-dimensional[3] and observe the process from a frame moving with instantaneous flame or detonation speed. We assume that the flow so observed is steady at the time considered in the neighborhood of the reaction zone[4].

---

[1] See [5] for an excessively high reaction rate, [6] for actual reaction rates. The latter paper contains a great number of detailed investigations concerning detonations primarily of solid explosives.

[2] Cf. Lewis and v. Elbe [7], Jost [8], Semenov [9], further [10] and [11]; the latter report gives a survey of earlier work.

[3] This assumption is no serious restriction for the discussion of the internal mechanism since the flow in the neighborhood of a point of a reaction front may be considered one-dimensional to the same degree of accuracy as the assumption is valid that the reaction front is a sharp discontinuity.
The assumption of the one-dimensional character of the flow is, however, a serious restriction for the external flow problem since this assumption is known to be never quite satisfied for combustion waves.

[4] The assumption of "local steadiness" does by no means imply that we consider only reaction processes that proceed with constant velocity into the unburnt gas. See the discussion in the Appendix.

This is in agreement with our basic assumption (p. 3) that the reaction zone is very narrow and of nearly constant width. Consequently, all quantities depend only on an abscissa x, and not on the time. At each place x, there is a mixture of burnt and unburnt gas; we denote by ε the fraction of mass of burnt gas in the mixture. We denote pressure and specific volume by p and τ and introduce the "reduced temperature" $\theta = p\tau$, a quantity which has the dimension of velocity squared. We assume burnt and unburnt gas to be ideal. Accordingly, θ is proportional to the temperature[1]. The internal energy e per unit mass of the burnt and of the unburnt gas is assumed to be a function of θ only, (actually e depends also somewhat on the pressure p, see also footnote[1]: denoting by g the energy of formation per unit mass (at absolute zero temperature), we introduce the total energy per unit mass

$$E = e + g \ .$$

Burnt and unburnt gas are distinguished by the superscripts (1) and (0). The total energy per unit mass of the mixture is then

$$E^{(\varepsilon)}(\theta) = (1-\varepsilon)E^{(0)}(\theta) + \varepsilon E^{(1)}(\theta) \ .$$

On the energy functions $E(\theta)$ we require that

$$\frac{\partial E^{(\varepsilon)}}{\partial \varepsilon} < 0$$

or

$$E^{(0)}(\theta) > E^{(1)}(\theta) \ .$$

[1] The absolute temperature is given by $R\theta/M$ where R is the gas constant and M the molecular weight. We disregard the dependence of the molecular weight on the mixture ratio ε.

This condition implies that the "liberated energy"

$$E^{(o)}(0) - E^{(1)}(0)$$

is positive. (It is convenient to make this assumption although most of our conclusions hold without it.) Our requirement is satisfied if burnt and unburnt gas are "polytropic"; i.e. if the energies are given by

$$E^{(0)}(\theta) = \frac{\theta}{\gamma_o - 1} + g_o \ , \qquad E^{(1)}(\theta) = \frac{\theta}{\gamma_1 - 1} + g_1$$

with constant γ_o, γ_1, g_o, g_1, provided that the temperature is below a certain limit[1].

By v we denote the velocity of the steady gas flow and by $m = \tau^{-1} v$ the "mass flux" of mixture through a unit cross-section per unit time. By S we denote the mass of burnt gas created per unit mass of unburnt gas per unit time. We assume that the "reaction rate," S, depends on θ and p, (cf. footnote 1), and that S vanishes below a certain "safety temperature":

$$S = 0 \quad \text{for} \quad \theta \leq \theta_S \ .$$ [2]

---

[1] This limit corresponds to $\theta \leq \dfrac{(\gamma_o - 1)(\gamma_1 - 1)}{\gamma_o - \gamma_1} (g_o - g_1)$. If one assumes $\gamma_o = 1.4$, $\gamma_1 \sim 1.2$, the molecular weight $M_o = M_1 \sim 30$, and the "liberated energy" $g_o - g_1 \sim .7$ kcal/gr, then the limit is about 3200°K. This case is, however, unrealistic since for such temperatures the value of γ for combustible gases will hardly ever be as high as 1.4.

[2] The latter assumption is made only to achieve mathematical simplicity. In recent papers [6], [10], [11], the reaction rate is assumed to be of the form

(footnote continued)

The transition between the two states on both sides of the reaction front is effected by the action of viscosity and heat conduction[1]. We introduce corresponding coefficients μ and λ such that

$$-\mu \frac{dy}{dx} \quad \text{and} \quad -\lambda \frac{d\theta}{dx}$$

are the viscous pressure and heat per unit mass conducted through a unit cross-section per unit time[2]. These coefficients depend on p, τ, and ε; but we need pay only little attention to this dependence of our general discussion.

We now formulate the laws governing the process. The continuity equation simply assumes the form

(footnote continued)

$$S = S_\infty e^{-A/\theta}$$

where A, proportional to the activation energy, is so large that S is negligible when θ assumes values corresponding to a temperature of 300°K. The reduced safety temperature θ_s has no precise significance (as the ignition temperature has in the older literature); it is simply a value below which S can be set equal to zero for all practical purposes. The maximal reaction rate, S_∞, may depend on P.

[1] We ignore diffusion and radiation. Diffusion should not be neglected in the actual calculation of flame speeds according to [11]. We felt that for the sake of simplicity we could disregard diffusion since the additional terms due to it would not seem to entail any essential change in the general results.

One might object to using the notions viscosity, heat conduction, and diffusion if the width of the transition zone is extremely small. It seems likely, though, that nevertheless our results remain correct in qualitative respects, in particular as far as determinacy is concerned.

[2] The customary coefficients of viscosity and heat conduction are, in our notation, $3/4\mu$ and λ/R, R being the gas constant such that $R\theta$ is the temperature.

(0) $$m = \text{const.}$$

The law of conservation of momentum is

(1)' $$-\mu \frac{dv}{dx} + p + mv = P = \text{const.}$$

Conservation of energy[1] is expressed by

(2)' $$-\lambda \frac{d\theta}{dx} + m[E^{(\varepsilon)}(\theta) + \frac{1}{2} v^2] + v[p - \mu \frac{dv}{dx}] = mQ = \text{const.}$$

The balance between burnt and unburnt gas is given by

(3)' $$-v \frac{d\varepsilon}{dx} + (1-\varepsilon)S(\theta) = 0 ,$$

assuming a first order reaction from a unimolecular mechanism[2].

The problem is to investigate possible solutions of these differential equations if the values of the quantities v, p, τ, and ε are given at the end points of the reaction zone. We modify this problem by prescribing the same values of these quantities at $x = \infty$ and $x = -\infty$. That it is justified with good approximation to substitute the modified problem for the original one follows

---

[1] If we were to consider diffusion we would introduce a coefficient δ such that $-\delta\, d\varepsilon/dx$ is the fraction of mass of burnt gas diffusing through a cross-section per unit time. Then we would have to add the term $\tau d(\delta\, d\varepsilon/dx)dx$ to equation (3)' and $-\delta d[E^{(\varepsilon)}(\theta) + \frac{1}{2} v^2]/dx$ to equation (2)' in order to express the diffusion of energy. The resulting modified equation (2)' would differ somewhat from those in the literature (see [11] where only the diffusion of the energy of formation is taken into account.

[2] If a different mechanism of reaction were assumed leading to terms $(1-\varepsilon)^2 S$ or $(1-\varepsilon)(1+n\varepsilon)S$, cf. [10] and [11], no change in the general conclusions would result.

from our basic assumption (p. 3) that the width of the reaction zone is very narrow. More specifically, the assumption was that the rate of change of the pertinent quantities outside the reaction zone is negligibly small as compared to the rates of change of these quantities inside the reaction zone. Consequently, these quantities appear to be nearly constant at the ends of the reaction zone over a region whose extension is large compared with the width of the reaction zone. It is then natural to assume that the process inside the reaction zone can very well be approximated by a process that extends over the whole field from $x = -\infty$ to $x = +\infty$ and in which the pertinent quantities assume at $\pm\infty$ those values that are prescribed for the proper process at the ends of the finite reaction zone.[1]

Accordingly we ask for solutions of the equations (1)', (2)', and (3)' which are defined for $-\infty < x < \infty$ and which approach finite limit values (with $\tau \neq 0$) as $x \to \pm\infty$; then the derivatives approach zero as seen from (1)', (2)', and (3)'. Solutions which behave in that way at $x = \infty$ or $x = -\infty$ will be called "regular"

---

[1] This procedure, typical for the treatment of "boundary layer phenomena" is always employed for differential equations in which the terms of highest order are multiplied by small factors. (In our case these factors are μ, λ, and S_∞^{-1}.)

No accuracy would be gained by trying to discuss the solutions for a finite range $x_o \leq x \leq x_1$; for, the conservation laws $(1)'_\infty$ and $(2)'_\infty$ would not be accurately valid unless accidentally

$$\frac{dt}{dx} = \frac{d\theta}{dx} = \frac{d\varepsilon}{dx} = 0 \quad \text{at} \quad x = x_o \quad \text{and} \quad x = x_1 .$$

For the infinite range it follows from regularity (see Section 2) that these derivatives vanish at the end points.

there. The limit values for $x \to -\infty$ are denoted by p_o, τ_o, θ_o, and ε_o; those for $x \to \infty$ by p_1, τ_1, θ_1, and ε_1. The boundary conditions then consist in prescribing these values; in particular we prescribe

$$\varepsilon_o = 0 , \quad \varepsilon_1 = 1 ,$$

expressing that the gas consists of unburnt gas at $x = -\infty$ and of completely burnt gas at $x = +\infty$. From relation (3)' we then deduce that the flux m is positive:

$$m = m \int_{-\infty}^{\infty} d\varepsilon = \int_{-\infty}^{\infty} (\tau-1)(1-\varepsilon)S(\theta)dx > 0 .$$

From this fact it follows that the reaction begins in the unburnt gas at $x = -\infty$ and ends in the burnt gas at $x = \infty$.

The values p_o, τ_o, θ_o, v_o, and p_1, τ_1, θ_1, v_1 for unburnt and burnt gas are those that are prescribed at both sides of the discontinuity front. These quantities are not prescribed arbitrarily, they are to satisfy the conservation laws: (0) and

$$(1)'_\infty \qquad p_o + mv_o = p_1 + mv_1 = P ,$$

$$(2)'_\infty \qquad E_o + \theta_o + \frac{1}{2} v_o^2 = E_1 + \theta_1 + \frac{1}{2} v_1^2 = Q ,$$

through which at the same time the values of the constants P and Q are determined. Here we have set

$$E^{(o)}(\theta_o) = E_o \quad \text{and} \quad E^{(1)}(\theta_1) = E_1 .$$

The conservation laws follow immediately for any regular solution from the differential equations (1)' and (2)', since these

equations reduce to $(1)'_\infty$ and $(2)'_\infty$ for $x = \infty$ and $x = -\infty$.

A further assumption which we impose on our boundary values is

$$\theta_o < \theta_s < \theta_1 ,$$

expressing that no reaction can take place in the unburnt gas at its initial temperature, and that reaction would take place at the final temperature if unburnt gas were still left.[1]

For the following arguments it is convenient to eliminate v and p by

$$v = m\tau \quad \text{and} \quad p = \tau^{-1}\theta ,$$

and to consider τ, θ and ε as the only dependent variables; the equations then become

$$(1) \qquad -\mu m \frac{d\tau}{dx} + \tau^{-1}\theta + m^2\tau = P ,$$

$$(2) \qquad -\lambda \frac{d\theta}{dx} + m[E^{(\varepsilon)}(\theta) - \frac{1}{2} m^2\tau^2 + P\tau] = mQ ,$$

$$(3) \qquad -m \frac{d\varepsilon}{dx} + \tau^{-1}(1-\varepsilon)S(\theta) = 0 .$$

The constant coefficients m, P, Q, and the boundary values τ_o, τ_1, θ_o, θ_1, $\varepsilon_o = 0$, and $\varepsilon_1 = 1$ are subject to the conservation laws

$$(1)_o \qquad \tau_o^{-1}\theta_o + m^2\tau_o = \tau_1^{-1}\theta_1 + m^2\tau_1 = P ,$$

$$(2)_o \qquad E_o + \theta_o + \frac{1}{2} m^2\tau_o^2 = E_1 + \theta_1 + \frac{1}{2} m^2\tau_1^2 = Q .$$

---

[1] Relation $\theta_o > \theta_s$ would imply $S > 0$ for $\theta = \theta_o$ and would hence not be compatible with equation $(3)'$ for a regular solution.

We now consider the system of differential equations (1), (2), (3) and ask whether or not it possesses regular solutions assuming the prescribed boundary values.

2. Regularity and determinacy.

We shall introduce as "degree of regularity" for each endpoint a number r such that the manifold of solutions of the differential equations (1), (2), (3) which are regular at that endpoint and assume the prescribed boundary values there depends on r parameters.

Let us first consider the endpoint $x = \infty$. To determine the degree of regularity r_1 at the end $x = \infty$ we shall introduce characteristic exponents, α, by the following formal procedure. We expand the differential equations (1), (2), (3) with respect to powers of $\tau-\tau_1$, $\theta-\theta_1$, and $\varepsilon-\varepsilon_1 = \varepsilon-1$. The terms of order zero vanish by definition of P and Q. The terms of first order constitute a system of linear differential equations with constant coefficients, the "linearized" differential equations for $x = \infty$. Upon inserting into these equations multiples of an exponential function $e^{\alpha x}$ for $\tau-\tau_1$, $\theta-\theta_1$, and $\varepsilon-1$, we obtain three linear equations for the three coefficients whose determinant is a cubic equation for α. The three roots of this cubic equation are the three characteristic exponents. We anticipate the fact, shown later on, that for our equations these characteristic exponents are always real. Suppose we have r_1 negative and $3-r_1$ positive characteristic exponents, then r_1 is the degree of regularity. This fact is implied by the well-known theory of singular points of ordinary differential

equations. The behavior of the r_1 parametric set of regular solutions can be characterized by the regular solutions of the linearized equations; the latter are a linear combination of exponential functions $e^{\alpha x}$ if the characteristic roots are different; otherwise terms like $xe^{\alpha x}$ or $x^2e^{\alpha x}$ enter. In case one characteristic exponent is zero, one cannot say off-hand what the degree of regularity is; a special consideration is needed.

The linearized equations at $x = \infty$ for the quantities $\tau-\tau_1$, $\theta-\theta_1$, $\varepsilon-1$ are immediately found to be

$$(1)^+ \qquad m\mu_1 \frac{d(\tau-\tau_1)}{dx} + \tau_1^{-2}\theta_1(\tau-\tau_1) - m^2(\tau-\tau_1) - \tau_1^{-1}(\theta-\theta_1) = 0 ,$$

$$(2)^+ \qquad \lambda_1 \frac{d(\theta-\theta_1)}{dx} - m\left\{\frac{\theta-\theta_1}{\gamma_1-1} - \Delta E_1(\varepsilon-1) - \tau_1^{-1}\theta_1(\tau-\tau_1)\right\} = 0 ,$$

$$(3)^+ \qquad m \frac{d(\varepsilon-1)}{dx} + \tau_1^{-1}S_1(\varepsilon-1) = 0 ,$$

where we have set $\frac{1}{\gamma-1} = \frac{\partial E^{(\varepsilon)}(\theta)}{\partial\theta}$, $\Delta E = E^{(o)} - E^{(1)}$, and the subscript (1) indicates that these quantities and also μ, λ, and S are to be taken for $\theta = \theta_1$, $\tau = \tau_1$, $\varepsilon = 1$.

For the characteristic exponent α one then obtains the equation

$$\begin{vmatrix} m\mu_1\alpha - m^2 + \tau_1^{-2}\theta_1 & -\tau_1^{-1} & 0 \\ -m\tau_1^{-1}\theta_1 & \lambda_1\alpha - \frac{m}{\gamma_1-1} & m\Delta E_1 \\ 0 & 0 & m\alpha + \tau_1^{-1}S_1 \end{vmatrix} = 0$$

or

$$(4) \qquad [m\tau_1\alpha + S_1][m\tau_1^2\lambda_1\mu_1\alpha^2 - (m^2\tau_1^2\lambda_1 - \theta_1\lambda_1 + m^2\tau_1^2 \frac{\mu_1}{\gamma_1 - 1})\alpha - \frac{m}{\gamma_1 - 1}(\gamma_1\theta_1 - m^2\tau_1^2)] = 0 .$$

The first bracket has evidently one negative root. As to the second bracket, which we write in the form $a\alpha^2 - b\alpha + c$ we observe that it has real roots since the discriminant

$$b^2 - 4ac = (m^2\tau_1^2\lambda_1 - \theta_1\lambda_1 + m^2\tau_1^2 \frac{\mu_1}{\gamma_1 - 1})^2 + 4 \frac{m^2\tau_1^2\lambda_1\mu_1}{\gamma_1 - 1}(\gamma_1\theta_1 - m^2\tau_1^2)$$

$$= (m^2\tau_1^2\lambda_1 - \theta_1\lambda_1 - m^2\tau_1^2 \frac{\mu_1}{\gamma_1 - 1})^2 + 4m^2\tau_1^2\lambda_1\mu_1\theta_1$$

is positive.

Since $a > 0$ we see that the second bracket has one positive and one negative root if $c < 0$. If $c = 0$, we have $b = b_o = (\gamma_1 - 1)\theta_1\lambda_1 + \frac{\gamma_1}{\gamma_1 - 1}\theta_1\mu_1 > 0$ and hence the bracket has one vanishing and one positive root. If $c > 0$ we have $b > b_o > 0$ and hence the bracket has two positive roots.

In case $c < 0$ we have $r_1 = 2$ and in case $c > 0$ we have $r_1 = 1$. A detailed investigation of the vector field corresponding to the differential equation would show that in case $c = 0$ a two parametric set of regular solutions exists; hence $r_2 = 2$ also in this case. Since the condition $c \gtrless 0$ is equivalent with $\gamma_1\theta_1 \gtrless m^2\tau_1^2$ we have to distinguish the following two cases

$$\text{Case } (A_1) \qquad m^2\tau_1^2 > \gamma_1\theta_1 ,$$

$$\text{Case } (B_1) \qquad m^2\tau_1^2 \leq \gamma_1\theta_1 .$$

The degree of regularity in these cases is:

$$\text{Case } (A_1) \qquad r_1 = 1 \ ,$$

$$\text{Case } (B_1) \qquad r_1 = 2 \ .$$

Employing the sound speed $c_1 = \sqrt{\gamma_1 \theta_1}$ for the burnt gas in state (1) we can write the condition for cases (A_1) and (B_1) in the form

$$\text{Case } (A_1) \qquad v_1 > c_1 \ ,$$

$$\text{Case } (B_1) \qquad v_1 \leq c_1 \ .$$

Thus the flow of the burnt gas in state (1) is supersonic in case (A_1) and subsonic or sonic in case (B_1).

For the state (o) at the end $x = -\infty$ we obtain a similar equation for α, the only difference being that $S = 0$ in state (o) since $\theta_o \leq \theta_S$ was assumed. The equation for α then becomes

$$(4)^- \qquad m\alpha\left[m\tau_o^2\lambda_o\mu_o\alpha^2 - (m^2\tau_o^2\lambda_o - \theta_o\lambda_o + m^2\tau_o^2\frac{\mu_o}{\gamma_o - 1})\alpha - \frac{m}{\gamma_o - 1}(\gamma_o\theta_o - m^2\tau_o^2)\right] = 0 \ ,$$

where λ_o, μ_o, γ_o refer to $\theta = \theta_o$, $\tau = \tau_o$, $\varepsilon = 0$. The first factor here has the root $\alpha = 0$. The bracket always has one positive root and in addition one positive, vanishing, or negative root depending on whether $\gamma_o\theta_o - m^2\tau_o^2 > 0$, $= 0$, or < 0.

To determine the degree of regularity r_o at the end $x = -\infty$ we first recall that $\theta_o < \theta_s$ was assumed. Hence for every regular solution assuming the prescribed boundary values at $x = -\infty$ we

have $\theta < \theta_s$ if x is sufficiently negative, for $-\infty < x \leq x_s$ say. By virtue of $S = 0$ for $\theta \leq \theta_s$ equation (3) entails $\varepsilon = 0$ for $-\infty < x \leq x_s$. The investigation of the manifold of solutions regular at $x = -\infty$ is thus reduced to the investigation of the regular solutions of equation (1) and (2) with $E^{(\varepsilon)}(\theta) = E^{(o)}(\theta)$. The characteristic exponents for this problem are the roots of the bracket in relation (4)$^-$. Hence we conclude: If both roots of the bracket are positive we have $r_o = 2$. The same is true if one of the roots is zero, as a detailed investigation of the vector field corresponding to the differential equation would show. If one of the roots is negative, however, the other one being positive, we have $r_1 = 1$. Accordingly, we distinguish the following two cases:

$$\text{Case } (A_o) \qquad m^2\tau_o^2 \geq \gamma_o\theta_o \,,$$

$$\text{Case } (B_o) \qquad m^2\tau_o^2 < \gamma_o\theta_o \,.$$

The degree of regularity is

$$r_o = 2 \qquad \text{in Case } (A_o) \,,$$

$$r_o = 1 \qquad \text{in Case } (B_o) \,.$$

Employing the sound speed c_o in the unburnt gas we write the condition for cases (A_o) and (B_o) in the form

$$\text{Case } (A_o) \qquad v_o \geq c_o \,,$$

$$\text{Case } (B_o) \qquad v_o < c_o \,.$$

Thus, the flow of the unburnt gas at $x = -\infty$ is supersonic or sonic there in case A_o, while it is subsonic in case B_o.

We see that four different cases are to be distinguished according to whether case A or case B obtains at $x = \infty$ or at $x = -\infty$. It is now very interesting that by virtue of Jouguet's rule (see [2], p. 215) these four cases just correspond to the four cases of strong and weak detonations and deflagrations; the Chapman-Jouguet detonation or deflagration, characterized by $v_1 = c_1$, is here classed with the strong detonations or weak deflagrations respectively.

We now shall determine in a formal way, simply by counting the number of parameters, the manifold of solutions which are regular at both endpoints. The set of solutions which are regular at $x = \infty$ is r_1-parametric. Among these solutions those are to be selected which are regular at $x = -\infty$. Since all solutions regular at $x = -\infty$ form a r_o-parametric set in the three-parametric set of all solutions, it is clear that the condition to be regular at $x = -\infty$ is expressed by $3-r_o$ relations. Thus $3-r_o$ conditions are imposed on the r_1 parameters characterizing the solutions regular at $x = \infty$. One of these parameters can always be chosen arbitrarily (within limits), since from every solution satisfying the boundary conditions one obtains a set of others by substituting $x + \text{const.}$ for x. Thus $3-r_o$ conditions are imposed on r_1-1 parameters. If $r_1-1 > 3-r_o$, an $(r_o + r_1 - 4)$-parametric set of solutions can be expected to exist. If $r_1-1 = 3-r_o$, one solution (or else a finite number of them) can be expected to exist. If $r_1-1 < 3-r_o$ more conditions are imposed than parameters are available. These conditions will be satisfied only if the coefficients entering the differential equations or the boundary values assume appropriate

values. In other words, $4 - r_o - r_1$ conditions are imposed on coefficients and boundary values. We term the number

$$s = 4 - r_o - r_1$$

the "degree of over-determinacy." From Jouguet's rule and the determination of the values of r_o and r_1 given before we find

Strong detonation,	Case (A_oB_1),	$s = 0$
Weak detonation,	Case (A_oA_1),	$s = 1$
Weak deflagration,	Case (B_oB_1),	$s = 1$
Strong deflagration,	Case (B_oA_1),	$s = 2$.

Upon comparing this table with the table for the degree of under-determinacy given in the Introduction (p. 7) we realize the fundamental fact that the degree of over-determinacy resulting from the internal mechanism of the reaction process equals the degree of under-determinacy of the external problem flow. The number of conditions needed to make the flow problem unique thus equals the number of conditions imposed by the mechanism of the reaction process.

This result may be interpreted as follows: All strong detonations are possible. Weak or Chapman-Jouguet detonations are only possible if one of the parameters of the process satisfies one condition. As such a parameter we may consider the flux m. As we shall see later, weak detonations exist just for such values of the flux that lead to Chapman-Jouguet detonations except for sufficiently high values of the reaction rate, for which a larger

value of the flux leads to a possible weak detonation. Weak deflagrations are also only possible if one of the parameters, the flux m say, satisfies one condition. As we shall see later, weak deflagrations exist indeed for only a particular value of the flux. Strong deflagrations should exist only if two conditions are satisfied by the parameters. As we shall see later, strong deflagrations do not exist at all.

It must be emphasized that these statements are so far derived in a purely formal manner. They are obtained by balancing the number of available parameters with the number of conditions imposed. A definite statement about the existence and uniqueness cannot be made on this basis. As a matter of fact these arguments are not sufficient to exclude weak detonations and strong deflagrations. More detailed considerations are needed for this purpose. In the following Sections (3 and 4) we shall first investigate certain limiting cases of weak deflagrations and strong detonations, and then proceed to discuss in Section 5 the problem of existence of solutions in general.

3. Weak deflagrations.

The degree of over-determinacy was found to be $s = 1$ for weak deflagrations. As indicated above, such deflagrations can therefore be expected to exist only if the coefficients of the differential equations satisfy one condition. This condition may be considered a condition for the constant m, the flux, or for the burning velocity $v_o = \tau_o m$. The question arises whether or not to given values of τ_o, θ_o, and given functions $S(\theta)$ and $E^{(\varepsilon)}(\theta)$ there

really is a value of the flux m for which the problem has a solution. We shall deal with this question in Section 5.

Here we shall consider only the limiting case of a constant pressure deflagration in which this question can easily be answered. This limit case results if either heat conductivity λ and viscosity μ approach zero, if the reaction rate S approaches zero[1], or if the pressure p_o increases indefinitely while the temperature θ_o remains fixed. This limit case, to which actual situations frequently come very near, has always been assumed for numerical determinations of the flame speed (see [10], [11]).

To describe the limiting "constant pressure problem" we first introduce dimensionless quantities

$$\tilde{m} = m\tau_o/\sqrt{\theta_o} ,$$

$$\tilde{\mu} = \mu S_\infty/p_o\tilde{m}^2 , \qquad \tilde{\lambda} = S_\infty/p_o\tilde{m}^2 ,$$

$$\tilde{P} = P/p_o , \qquad \tilde{Q} = Q/\theta_o ,$$

and introduce the new variables

$$\tilde{x} = xS_\infty/m\tau_o$$

$$\tilde{\tau} = \tau/\tau_o , \qquad \tilde{\theta} = \theta/\theta_o .$$

[1] For example by letting $S_\infty \to 0$, (cf. footnote on p. 13).

The objection may be raised that for small values of the reaction rate the basic assumption (pp. 3 and 12) cannot be satisfied. Nevertheless it is necessary to consider the limit $S \to 0$ for the discussion of the mathematical implications of the problem formulated in Section 1.

The equations (1), (2), (3) then become

$$-\tilde{\mu}\tilde{m}^2 d\tilde{\tau}/d\tilde{x} + \tilde{\theta}/\tilde{\tau} + \tilde{m}^2\tilde{\tau} = \tilde{P} ,$$

$$-\tilde{\lambda} d\tilde{\theta}/d\tilde{x} + E^{(\varepsilon)}(\theta_o\tilde{\theta})/\theta_o - \frac{1}{2}\tilde{m}^2\tilde{\tau}^2 + \tilde{P}\tilde{\tau} = \tilde{Q} ,$$

$$- d\varepsilon/d\tilde{x} + \tilde{\tau} - 1(1-\varepsilon)S(\theta_o\tilde{\theta})/\theta_o = 0 .$$

This system of differential equations depends on the parameters $\tilde{m}$, $\tilde{\lambda}$, $\tilde{\mu}$, $\tilde{P}$, $\tilde{Q}$, and θ_o. We obtain the limiting problem by considering a set of such systems for which $\tilde{m}$ approaches zero while the other parameters are kept fixed. In other words: The differential equations of the limiting problem are simply obtained by omitting the three terms involving the factor $\tilde{m}^2$.

The fact that $\tilde{\lambda}$ and $\tilde{\mu}$ are fixed while $\tilde{m}$ approaches zero evidently implies $\lambda S_\infty/p_o \to 0$ and $\mu S_\infty/p_o \to 0$. The limiting equations will therefore represent a good approximation if $\lambda S_\infty/p_o$, $\mu S_\infty/p_o$, and $\tilde{m}$ are small. In that case we can re-introduce the original quantities. Thus we obtain the equations of the constant pressure problem in the following form:

$$(\tilde{1}) \qquad p = P = p_o ,$$

$$(\tilde{2}) \qquad -\lambda \frac{d\theta}{dx} + m[E^{(\varepsilon)}(\theta) + \theta] = mQ ,$$

$$(\tilde{3}) \qquad -m \frac{d\varepsilon}{dx} + p\theta^{-1}(1-\varepsilon)S(\theta) = 0 ,$$

where we have eliminated τ from (2) and (3), using $(\tilde{1})$.

Relation $(\tilde{1})$ expresses the fact that under the conditions of the limiting problem the pressure does not vary across the flame front: we have constant pressure combustion. Further we see that

the term representing the kinetic energy has dropped out from (2).

The boundary conditions are $\theta = \theta_1$, $\varepsilon = 1$ at $x = \infty$, and $\varepsilon = 0$ at $x = -\infty$. The constant Q is given by $Q = E_1 + \theta_1$. The relation $E_o + \theta_o = Q$, which holds for regular solutions determines the value $\theta = \theta_o$ at $x = -\infty$.

To investigate possible solutions of this problem one may consider θ as independent variable running from θ_o to θ_1 and combine the equations to

$$(5) \qquad \frac{d\varepsilon}{d\theta} \frac{p\lambda}{m^2} \frac{S(\theta)}{\theta} \frac{1-\varepsilon}{E_1 + \theta_1 - E^{(\varepsilon)}(\theta) - \theta} .$$

It is immediately seen that this equation has a saddle-singularity at the point $\theta = \theta_1$, $\varepsilon = 1$. There is just one solution curve that enters this point from the region $\varepsilon < 1$, $\theta < \theta_1$. If this curve is followed backwards it will enter the axis $\varepsilon = 0$ at a point with $\theta > \theta_s$ provided $p_o\lambda/m^2$ is sufficiently large; if $p_o\lambda/m^2$ is sufficiently small the curve will enter the line $\theta = \theta_s$ at a point with $\varepsilon > 0$. It is thus clear that there is just one value of $p_o\lambda/m^2$ for which the curve enters the line $\theta = \theta_s$ with $\varepsilon = 0$. Since $d\varepsilon/d\theta = 0$ for $\theta \leq \theta_s$, the curve will enter the line $\theta = \theta_o$ also with the value $\varepsilon = 0$. That for this solution the quantity x approaches ∞ as $\theta \to \theta_1$ and $-\infty$ as $\theta \to \theta_o$ is immediately seen from (2) and (3).

Thus it is shown that in the limit, as the quantities $\lambda S_\infty/p_o$ and $\mu S_\infty/p_o$ approach zero, a deflagration process exists with a well-defined flux m and flame speed v_o. As will be shown later (at the end of Section 5), the same is true for small values

of these quantities, in other words, for sufficiently small values of $\lambda S_\infty/p_o$ and $\mu S_\infty/p_o$ a deflagration exists which is nearly a constant pressure combustion and which is characterized by a uniquely defined burning speed v_o.

Computations of the burning speed can be carried out by solving equations ($\tilde{2}$) and ($\tilde{3}$) or (5) through interactions, (see [9], and [10], in the latter report the term $d(\delta\, d\varepsilon/dx)dx$ was added to equation (3) in order to take diffusion into account); it was found in the quoted reports that for the actual situations considered the approximation involved in (2) and (3) was rather accurate since the omitted terms turned out to be very small for the calculated solution.

It is interesting that essentially only the combination $p\lambda/m^2$ or the dimensionless combination

$$(6) \qquad m^2\theta_o/p\lambda S_\infty = (v_o^2/\theta_o)/(\lambda S_\infty/p)$$

enters the constant pressure problem, as seen from equation (5). (More precisely, the problem depends only on the dimensionless quantity (6) in addition to the functions $S(\theta)/S_\infty$ and $E^{(\varepsilon)}(\theta)/\theta_o$; note $E_o + \theta_o = E_1 + \theta_1$.) The quantity (6) approaches a finite limit value as $\lambda S_\infty/p_o$ approaches zero. Therefore, for small values of $\lambda S_\infty/p_o$, the flux m is proportional to $\sqrt{p_o\lambda S_\infty/\theta_o}$ and the burning speed v_o to $\sqrt{\lambda S_\infty \theta_o/p_o}$. If in particular λ, S_∞, and the reduced initial temperature θ_o are kept fixed, the flux increases like $\sqrt{S_\infty/p_o}$ and the burning speed decreases like $\sqrt{S_\infty/p_o}$ as p_o increases. If S_∞ were independent of p or increased with p_o of less than first order, the latter result would mean that the

burning speed should decrease with increasing pressure. This does not seem to be confirmed experimentally[1]. It is thus indicated that S_∞ increases with p_o of higher than first order. What happens when p_o decreases cannot be derived by considering expression (6), since the approximation made is no longer valid if $p_o/\lambda S_\infty$ is small. Whether or not deflagrations are then possible will be discussed later on, in Section 5.

4. Strong detonations and Chapman-Jouguet detonations.

We next consider strong detonations, including Chapman-Jouguet detonation; according to Jouguet's rule they have it in common with weak deflagrations that the flow of the burnt gas is subsonic. The flow of the unburnt gas, however, is supersonic (or sonic). The degree of over-determinacy was found to be $s = 0$. Hence no conditions need be imposed on the data other than the inequality $m^2\tau_1^2 \leq \gamma_1\theta_1$, or $v_1 \leq c_1$. Whether or not it is true under this condition that a unique solution exists will be discussed in the next Section, 5.

In the present section we shall consider a limiting case obtained by letting $\mu S_\infty/p_o$ and $\lambda S_\infty/p_o$ approach zero. We imagine, in particular that viscosity μ and heat conductivity λ approach zero while S_∞ and p_o are kept fixed. This limiting problem presents an analogy to the limiting problem considered in Section 3; the limiting behavior of the present limiting problem is, however, quite different from that encountered in Section 3.

[1] See e.g. [8], p. 146, Table 27.

Consider a sequence of solutions. There are two possibilities: either the terms $\mu \frac{d\tau}{dx}$ and $\lambda \frac{d\theta}{dx}$ in equations (2) drop out in the limit, or $\frac{d\tau}{dx}$ and $\frac{d\theta}{dx}$ become infinite. For those values of x for which the first case occurs, the equations

$$(1)_\infty \qquad \tau^{-1}\theta + m^2\tau = P \ ,$$

$$(2)_\infty \qquad E^{(\varepsilon)}(\theta) - \frac{1}{2} m^2\tau^2 + P\tau = Q \ ,$$

$$(3) \qquad -m \frac{d\varepsilon}{dx} + \tau^{-1}(1-\varepsilon)S(\theta) = 0 \ ,$$

are satisfied in the limit. If the second case occurs at a place x, a discontinuity of τ and θ occurs in the limit while ε remains continuous. Such a discontinuity would simply be a shock not involving a reaction.

A more detailed investigation (see Section 5) of the limit process $\lambda S_\infty/p_o$, $\mu S_\infty/p_o \to 0$ will yield that a strong detonation can in the limit be described as a shock, not involving a reaction, immediately followed by a reaction process governed by equations $(1)_\infty$, $(2)_\infty$, (3). This confirms the accepted idea about a detonation process, which was formulated more specifically by G.I. Taylor and v. Neumann (see [1], e.g.).

The question arises whether to given values of τ_o, θ_o, τ_1, θ_1, and m with $\tau_o^{-1}c_o < m \leq \tau_1^{-1}c_1$ satisfying the conservation laws, a transition process exists which consists of a shock followed by a reaction. We assume that the temperature to which the shock raises the unburnt gas is above safety temperature. Otherwise the reaction process would simply be a deflagration process, which

cannot exist in the present limiting case[1]. Denoting the quantities past the shock front by an asterisk we require

$$\theta_o < \theta_s < \theta_* \ .$$

To find out whether the equations $(1)_\infty$, $(2)_\infty$, (3) possess a solution we determine τ and θ as functions of ε from $(1)_\infty$ and $(2)_\infty$, and insert in (3). This is possible if the Jacobian

$$J = \frac{dE^{(\varepsilon)}}{d\theta}\,(m^2 - \tau^{-2}\theta) - \tau^{-2}\theta$$

of $(1)_\infty$ and $(2)_\infty$ does not vanish. Introducing quantities $\gamma^{(\varepsilon)}$ and $c_{(\varepsilon)}$ by

$$dE^{(\varepsilon)}/d\theta = 1/(\gamma^{(\varepsilon)} - 1) \ ,$$

$$c^2_{(\varepsilon)} = \gamma^{(\varepsilon)}\theta \ ,$$

we find

$$J = (m^2 - \tau^{-2}c^2)/(\gamma - 1) \ ,$$

where τ, c, and γ depend on ε. Since the flow is subsonic in the state (*) past the shock we have $J_* < 0$. In the neighborhood of the state (*) we may therefore express τ and θ in terms of ε and the solution of the equation resulting from (3) is uniquely determined through the initial condition $\varepsilon = 0$ at $x = 0$, say, where we may place the shock front. The question then is whether on continuing the solution one would obtain a value for which J changes

[1] Expressing τ and θ through ε by $(1)_\infty$ and $(2)_\infty$, equation (3) becomes a differential equation for ε, which yields $d\varepsilon/dx = 0$ for $\varepsilon = 0$ since $S(\theta_o) = 0$ for $\theta_o \leq \theta_s$. The sole solution of this differential equation vanishing for $x = -\infty$ is therefore $\varepsilon = 0$.

sign. The final state is also subsonic, $J_1 < 0$, and the transitions from the state (*) to any of the intermediate states between (*) and (1) correspond, as regards the conservation laws, to a set of weak deflagrations. All the intermediate states are thus subsonic. Consequently, J remains negative throughout[1].

The differential equation for ε resulting from (3) possesses, therefore, a solution with $\varepsilon = 0$ for $x = 0$. Since for this solution, $d\varepsilon/dx \to 0$ as $\varepsilon \to 1$, the final state (1) is approached as $x \to \infty$. Thus it is seen that a limiting type detonation consisting of a shock followed by a reaction in possible for arbitrary values of the flux m, satisfying $\tau_o^{-1} c_o < m \leq \tau_1^{-1} c_1$. [2]

The reaction process in a strong (limit type) detonation following the shock has it in common with a weak deflagration that unburnt gas in a subsonic state is transformed into burnt gas in a subsonic state. The two processes differ, however, in other respects. The initial temperature in a deflagration is below safety temperature while the reaction in a detonation begins with a higher temperature. Also in a deflagration the rates of change $d\tau/dx$, $d\theta/dx$, $d\varepsilon/dx$ are zero initially while there is no such restriction for the reaction process following a shock; for small values of λ and μ the rates of change undergo such great changes

[1] Whether or not $\partial E^{(\varepsilon)}/\partial\varepsilon$ changes sign during this process is immaterial, cf. however, v. Neumann's report [1], in which transition process are discussed on the basis of equations $(1)_\infty$ and $(2)_\infty$.

[2] For numerical determination of such processes and various detailed discussions see the reports by Eyring and his collaborators, [5] (where an excessively high reaction rate was assumed) and [6]. (The case shown in Fig. 10a, p. 44 in [6] and labeled "steady deflagration" there is a "weak detonation" in our terminology.)

in the narrow shock zone that adjustment to any values of these rates at the beginning of the reaction zone is possible. It can thus be understood that for the reaction process in a detonation no definite value of the flux is required as for proper deflagrations.

5. Discussion of possible processes with the aid of the vector field.

It is very helpful for the further discussion to refer to the vector field in the $(\tau, \theta, \varepsilon)$-space generated by the differential equations (1), (2), and (3). It is convenient for our discussion to consider as positive the direction of decreasing x; when we speak of following a solution curve $\mathcal{K}$ we always imply that we travel in direction of decreasing x. All vectors of the field point to smaller values of ε except on the surfaces $\varepsilon = 1$ and in the region $\theta \leq \theta_s$, where they lie in the surfaces $\varepsilon = \text{const.}$ Every solution curve that hits the surface $\theta = \theta_s$ will stay on the plane $\varepsilon = \text{const.}$ from there on.

Further important properties of this vector field are these: $d\tau = 0$ on the cylinder $\theta + m^2\tau^2 = P\tau$ and $d\theta = 0$ on the surface $\mathcal{E}$ given by the equation

$$E^{(\varepsilon)}(\theta) = \frac{1}{2} m^2\tau^2 - P\tau + Q_o \ .$$

Points of intersections of the surface $\mathcal{E}$ with the cylinder $\theta + m^2\tau^2 = P\tau$ and the plane $\varepsilon = \text{const.}$ will be denoted by A_ε and B_ε. The conservation laws $(1)_\infty$ and $(2)_\infty$ are obviously satisfied at such points. Any two such points on the plane $\varepsilon = \text{const.}$ with

$\theta > 0$ and $\tau > 0$ evidently represent the two states on both sides of a possible shock transition in the gas mixture characterized by the values of ε considered. Therefore, one of these two points, A_ε, corresponds to a supersonic, the other, B_ε, to a subsonic flow. We assume the values of the constants P and Q such that the surface $\mathcal{E}$ intersects the initial plane $\varepsilon = 0$ at two points A_o and B_o with $\theta > 0$, $\tau > 0$. From the discussion on p. 33 it follows that for every $\varepsilon > 0$ two points of intersection A_ε and B_ε exist as long as A_ε or B_ε do not become sonic, or, what is equivalent, do not coalesce. We assume that this is not the case for $0 \leq \varepsilon < 1$; this assumption is primarily a condition on the flux m. We also assume that $\theta > 0$, $\tau > 0$ at these points for $0 \leq \varepsilon \leq 1$. We then have two curves $\mathcal{A}$ and $\mathcal{B}$ of points A_ε and B_ε along which θ and τ are continuous functions of the parameter ε. (The last assumption made here is somewhat stronger than necessary. For the discussion of weak deflagrations, for example, only the existence of the curve $\mathcal{B}$ is needed. Incidentally, the existence of the supersonic state A_ε with $\theta > 0$, $\tau > 0$ always implies the existence of the subsonic state B_ε, but the converse is not true.)

At the points A_ε, B_ε we have $d\tau = d\theta = 0$, $d\varepsilon/dx > 0$ except for $\varepsilon = 1$ or $\theta \leq \theta_s$; hence the field vector points in the negative ε-direction at these points. The projections of the field vectors on the planes $\varepsilon = \text{const.}$ have singularities at the points A_ε and B_ε. At a point A_ε the projected field has a nodal point and the solution curves of the projected field lead from the neighborhood of this point into it. At the point B_ε the projected field has a saddle-singularity; (see Figures 2 to 5). At the points A_ε

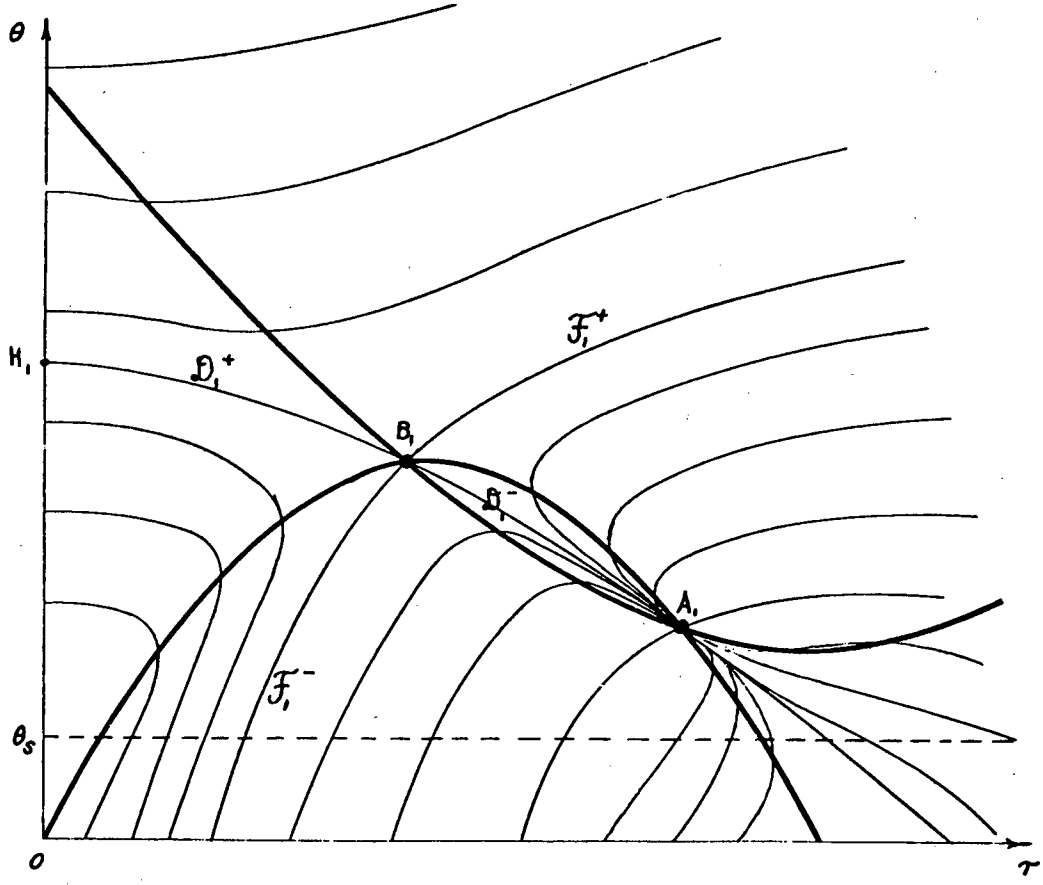

Figure 2

Detonation

(Integral curves of the projected vector field on the plane $\varepsilon = 1$ for a detonation)

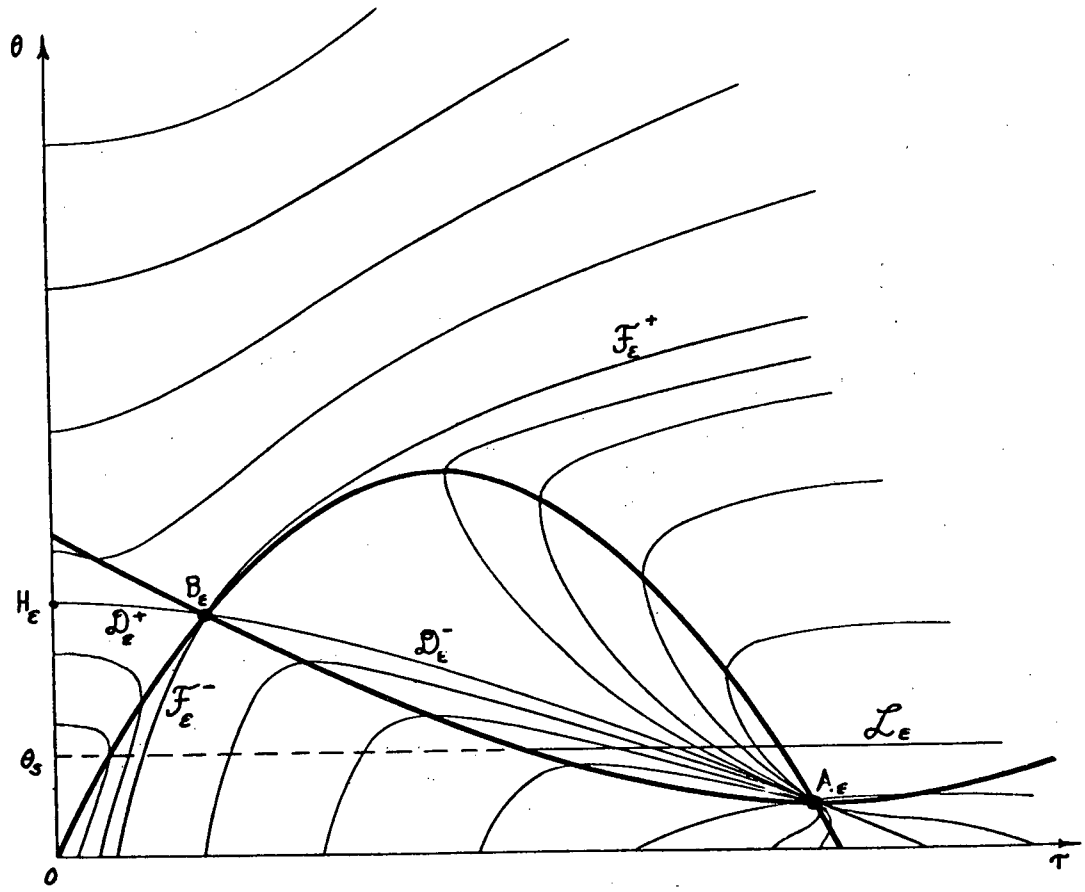

Figure 3

Detonation

(Integral curves of the projected vector field on the plane ε = const. for a detonation)

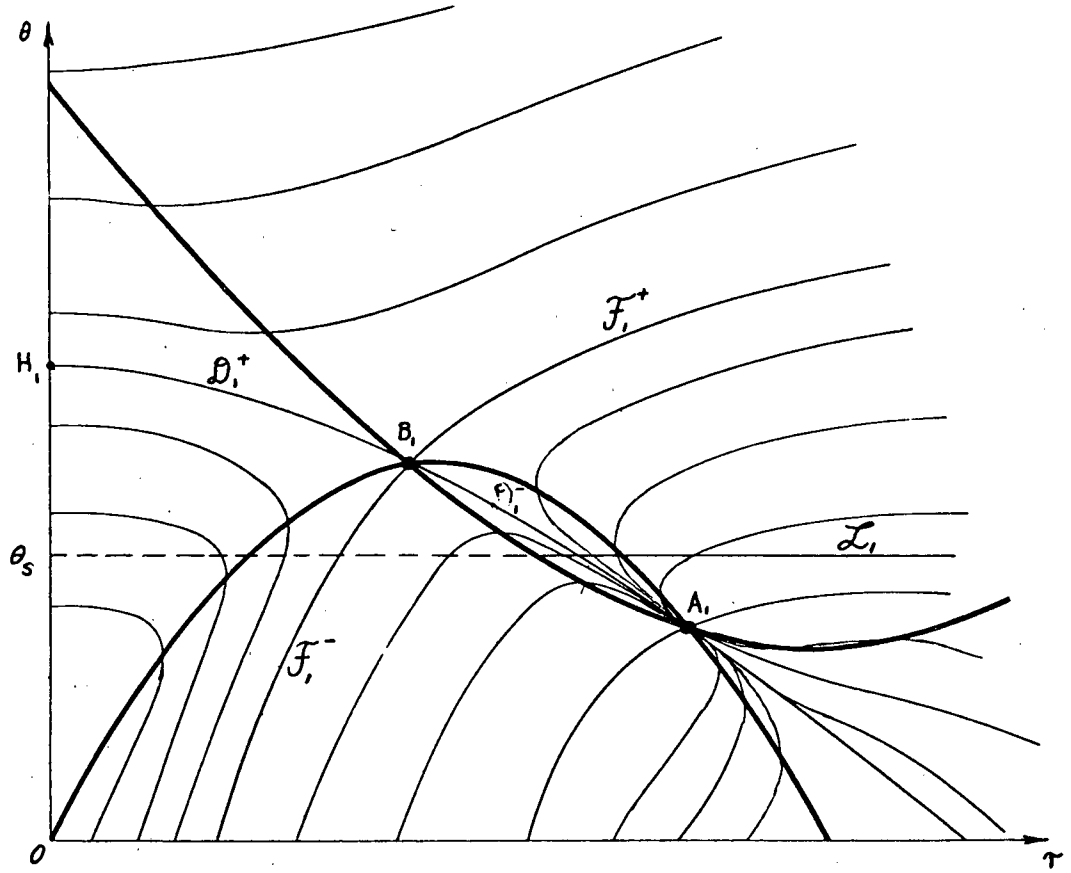

Figure 4

Deflagration

(Integral curves of the projected vector field on the plane $\varepsilon = 1$ for deflagration)

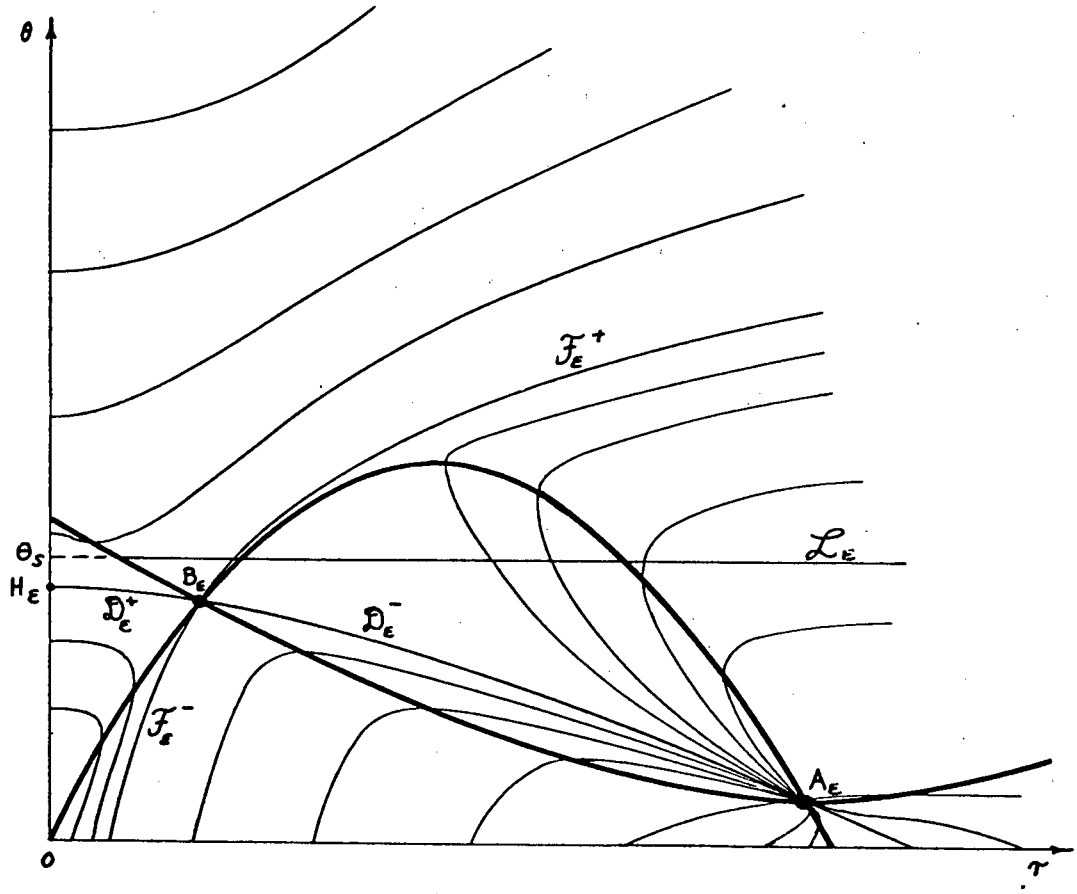

Figure 5

Deflagration

(Integral curves of the projected vector field on the plane ε = const. for a deflagration)

and B_ε on the surface $\varepsilon = 1$ and in the region $\theta \leq \theta_s$ the three-dimensional vector field has singularities.

If we are interested in a deflagration we must assume that $\theta < \theta_s$ for the initial point B_o, (see p. 31); if we are interested in a detonation we must assume, (see p. 33 and Figs. 2, 3), that $\theta > \theta_s$ at the point B_o, which in this case is connected with the initial point A_o through a curve representing a shock. We require somewhat more for detonations, viz. that $\theta > \theta_s$ on the whole line $\mathcal{B}$. We first investigate which <u>strong deflagrations</u> and <u>weak detonations</u> are possible. Both processes have it in common that the flow in the burnt gas is supersonic. The state (1) thus belongs to the case (A), and corresponds to a point A_1. As was shown earlier there exists in case (A_1) only a one-parametric set of solutions which are regular at $x = \infty$, and the values of the parameter may be chosen arbitrarily provided it is so chosen that ε decreases as x decreases. Thus there exists only one solution curve, $\mathcal{C}$, starting at A_1 which could represent one of the processes mentioned. If this solution curve $\mathcal{C}$ reaches the point B_o it represents a strong deflagration, if it reaches the point A_o it represents a weak detonation.

In the following we shall consider problems differing in the reaction rate S, all other parameters being unaltered; we may, for example, assume the factor S_∞ (cf. 1 on p. 13) to vary from 0 to ∞. The curves $\mathcal{A}$ and $\mathcal{B}$ are evidently independent of S; the curve $\mathcal{C}$, however, depends on S. If we want to emphasize this dependence we write $\mathcal{C}(S)$.

If the reaction rate S is very high compared with p_o/λ and p_o/μ, all vectors point nearly in negative ε-direction except near $\varepsilon = 1$ and $\theta \leq \theta_s$. In this case, therefore, any solution curve is approximately a straight line in the negative ε-direction until it meets the surface $\theta = \theta_s$. Therefore, the curve $\mathcal{C}$ that begins at the point A_1, i.e. at $\varepsilon = 1$, $\theta = \theta_1$, $\tau = \tau_1$, ends up on $\varepsilon = 0$ nearly with the values $\theta = \theta_1$, $\tau = \tau_1$, hence with nearly $\theta = \theta_1 > \theta_s$. Thus we see that $\mathcal{C}$ ends up on $\varepsilon = 0$ at a point with $\theta > \theta_s$ if S is sufficiently high. At such a point $d\varepsilon/dx > 0$ and hence there is no continuation of the curve on the plane $\varepsilon = 0$ and hence none of the desired initial states is reached.

Let us consider the opposite extreme that the reaction rate S is very small; then the direction of the field vector lies everywhere nearly in the plane ε = const. except near the curves $\mathcal{A}$ and $\mathcal{B}$. Consider any "cylindrical" neighborhood of the line $\mathcal{A}$ and exclude from it an arbitrarily small neighborhood of the point A_1. If S is small enough then clearly the vector field on the lateral surface of the "cylinder" points into its interior. The curve $\mathcal{C}$, beginning at A_1, can therefore never lead far away from the curve $\mathcal{A}$; for, as soon as moved away from $\mathcal{C}$, the rate of change $d\varepsilon/dx$ would become much smaller than $|d\tau/dx| + |d\theta/dx|$ and therefore the curve $\mathcal{C}$ would again be drawn nearer into the neighborhood of $\mathcal{A}$. Consequently, the curve $\mathcal{C}$ meets the surface $\theta = \theta_s$ not far from the intersection A^s of this surface with the curve $\mathcal{A}$, remains from there on the plane ε = const. and soon enters the point A_ε.

In general the course of the curve $\mathcal{C}$ can be delimited as follows: Let $(\tau_\varepsilon, \theta_\varepsilon)$ be the coordinates of the point A_ε. From the

assumption $\partial E^{(\varepsilon)}/\partial\varepsilon > 0$ made earlier (p. 23) it follows that τ_ε increases and θ_ε decreases with decreasing ε. [1] The statement then is that the curve $\mathcal{C}$ remains in the cell

$$\tau_1 \leq \tau \leq \tau_\varepsilon , \quad \theta_\varepsilon \leq \theta \leq \theta_1 , \quad 0 \leq \varepsilon \leq 1 .$$

This follows from the fact that the field vector at the boundary of this cell points into its interior except on $\varepsilon = 0$.

This statement implies that the curve $\mathcal{C}$ never ends up at the point B_0, since B_0 is evidently not contained in the cell just described. In other words, strong deflagrations are impossible.

Let us denote the points at which the curve $\mathcal{C}$ enters either the surface $\varepsilon = 0$ or the surface $\theta = \theta_s$ as "terminal points" $T_{\mathcal{C}}$. They form a "terminal line" $\mathcal{T}$ which connects the point $\tau = \tau_1$, $\theta = \theta_1$, $\varepsilon = 0$ (for finite S) with the point A^s (for $S = 0$).

The terminal point $T_{\mathcal{C}}$ depends continuously[2] on the reaction rate S. Therefore, if we let S vary from ∞ to 0, the terminal

---

[1] From (1) and (2) we have

$$\frac{d\theta_\varepsilon}{\gamma_\varepsilon - 1} + \frac{\partial E^{(\varepsilon)}}{\partial\varepsilon}\, d\varepsilon = -\tau_\varepsilon^{-1}\theta_\varepsilon d\tau_\varepsilon ,$$

$$d\theta_\varepsilon = -(m^2\tau_\varepsilon - \tau_\varepsilon^{-1}\theta_\varepsilon)d\tau_\varepsilon$$

where $P = \tau_\varepsilon^{-1}\theta_\varepsilon + m^2\tau_\varepsilon$ has been used. Eliminating $d\theta_\varepsilon$ one has

$$(\gamma_\varepsilon - 1)\,\frac{\partial E^{(\varepsilon)}}{\partial\varepsilon}\, d\varepsilon = (m^2\tau_\varepsilon - \gamma_\varepsilon\tau_\varepsilon^{-1}\theta_\varepsilon)d\tau_\varepsilon$$

whence the statement follows since the state A_ε is supersonic and hence $m^2\tau_\varepsilon^2 \geq \gamma_\varepsilon\theta_\varepsilon$.

[2] This follows immediately from $d\theta/dx \neq 0$ on $\theta = \theta_s$, $\varepsilon > 0$ and $d\varepsilon/dx \neq 0$ on $\varepsilon = 0$, $\theta > \theta_s$; the continuity at $\theta = \theta_s$, $\varepsilon = 0$ can be shown by a more refined consideration.

point will move continuously along the terminal line from the plane $\varepsilon = 0$ into the surface $\theta = \theta_s$. Consequently there is a particular value of S of S_∞ for which the terminal point lies on the intersection of the plane $\varepsilon = 0$ and the surface $\theta = \theta_s$. We then speak of the "extreme" situation and the "extreme" terminal point T^*. Otherwise, if the terminal point lies on the surface $\theta = \theta_s$ we speak of a "normal" situation, if it lies on $\varepsilon = 0$, of an "abnormal" one.

In the extreme situation a weak detonation exists; for, since $\theta = \theta_s$ at the extreme terminal point, the solution curve starting at this point remains on the surface $\varepsilon = 0$. That this solution curve ends up at A_o follows from the fact that the field has an attractive singularity at A_o and that the terminal point $T^* = (\tau^*, \theta^*)$ lies in the cell $\tau_1 \leq \tau^* \leq \tau_o$, $p_o \leq p^* \leq p_1$ and hence belongs to those points that are attracted by A_o. It is clear that a solution curve can reach A_o only if its terminal point lies on $\varepsilon = 0$ and $\theta = \theta_s$. Hence, a weak detonation exists only in the extreme situation, i.e. if the reaction rate S assumes a particular high value S^*.

The discussion of the terminal line $\mathfrak{T}$ will also be useful for the investigation of strong detonations. Before we enter the discussion of strong detonations and weak deflagrations we must investigate the possible continuations of solution curves after they have entered the region $\theta \leq \theta_s$.

In the region $\theta \leq \theta_s$ the actual vector field agrees with the projected vector field. Suppose the point $B_\varepsilon = (\tau_\varepsilon, \theta_\varepsilon, \varepsilon)$ on the curve $\mathfrak{B}$ lies below $\theta = \theta_s$, i.e. suppose $\theta_\varepsilon < \theta_s$. Then the vector

field has a saddle singularity at B_ε, (see p. 36). Consequently, two solution curves, $\mathcal{D}_\varepsilon^+$ and $\mathcal{D}_\varepsilon^-$, leave B_ε (see Fig. 3); and two solution curves, $\mathcal{F}_\varepsilon^+$ and $\mathcal{F}_\varepsilon^-$, enter B_ε; (the curves with $\theta > \theta_\varepsilon$ are $\mathcal{D}_\varepsilon^+$ and $\mathcal{E}_\varepsilon^-$, the one with $\theta < \theta_\varepsilon$ are $\mathcal{D}_\varepsilon^-$ and $\mathcal{F}_\varepsilon^-$). We see from the vector field (Fig. 3 and Fig. 5) that $\mathcal{E}_\varepsilon^-$ ends up at the point A_ε on $\mathcal{A}$.

A solution curve $\mathcal{S}$ can enter the region $\theta \leq \theta_s$ only at a point where $d\theta/dx \leq 0$, hence only on the section $\mathcal{L}$ of the surface $\theta = \theta_s$ cut out by the surface $\mathcal{E}$ (see p. 35). The intersection of $\mathcal{L}$ with a plane ε = const. will be denoted by $\mathcal{L}_\varepsilon$, (see Fig. 3 and Fig. 5). We consider the continuation of the solution curve $\mathcal{S}$ after its entry into $\theta \leq \theta_s$ on the segment $\mathcal{L}_\varepsilon$. There are two cases. Either, the point $B_\varepsilon = (\tau_\varepsilon, \theta_\varepsilon, \varepsilon)$ lies above the plane $\theta = \theta_s$, i.e. $\theta_\varepsilon > \theta_s$. Then the continuation of $\mathcal{S}$ from $\mathcal{L}_\varepsilon$ on, ends up in the point A_ε, as seen from the vector field (Fig. 3). Or, the point B_ε lies in the region $\theta \leq \theta_s$ (see Fig. 5). Then the curve $\mathcal{F}_\varepsilon^+$ entering B_ε with decreasing θ intersects the segment $\mathcal{L}_\varepsilon$ in a point G_ε. If $\mathcal{S}$ enters $\mathcal{L}_\varepsilon$ on one side of G_ε (on the side with larger τ), its continuation ends up at A_ε as before. If $\mathcal{S}$ enters $\mathcal{L}_\varepsilon$ on the other side its continuation ends up on $\tau = 0$ unless it has left the region $\theta \leq \theta_s$ before reaching $\tau = 0$. If $\mathcal{S}$ enters $\mathcal{L}_\varepsilon$ at G_ε the continuation of $\mathcal{S}$ leads along $\mathcal{F}_\varepsilon$ to B_ε and from there on $\mathcal{S}$ can be either continued along $\mathcal{D}_\varepsilon^-$ up to A_ε or along $\mathcal{D}_\varepsilon^+$ up to $\tau = 0$ unless $\mathcal{D}_\varepsilon^+$ leaves $\theta \leq \theta_s$ before reaching $\tau = 0$.

We now enter the discussion of <u>strong detonations</u>. Strong and Chapman-Jouguet detonations imply subsonic or sonic flow in

the burnt gas at $x = \infty$. Hence case (B_1) obtains, or the state (1) corresponds to a point B_1. Consequently, according to the statements made earlier, (see Section 3, p. 21) there is a two-parametric set of solutions regular at $x = \infty$. Hence there is a one-parametric set of solution curves $\mathcal{C}$ leaving the point B_1. We want to show that among the curves $\mathcal{C}$ there is a one $\mathcal{C}^*$, which ends up at A_0, and thus represents a strong (or Chapman-Jouguet) detonation.

The set of curves $\mathcal{C}$ is limited by two curves remaining on the plane $\varepsilon = 1$. One of these two curves, $\mathcal{C}_1^+$, leads to larger values of θ, and ends up on the plane $\tau = 0$ at a point H_1 (see Fig. 2). The other curve, $\mathcal{C}_1^-$, leads to smaller values of θ and ends up in the point A_1; it represents the possible shock transition from state A_1 to state B_1. The set of curves $\mathcal{C}$ may be characterized by a parameter β, which for $\beta = 0$ yields $\mathcal{C}_1^+$ and for $\beta = 1$ yields $\mathcal{C}_1^-$.

On the basis of the assumption made earlier (p. 41) that the curve $\mathcal{B}$ lies above the plane $\theta = \theta_s$ we see from the remarks made before that all curves $\mathcal{C}$ that enter the plane $\theta = \theta_s$ end up on $\mathcal{A}$; none therefore meet $\mathcal{B}$ below $\theta = \theta_s$ or end up on $\theta = 0$. Therefore the curves $\mathcal{C}$ end up either on $\tau = 0$, $\varepsilon = 0$, or on $\mathcal{A}$. The so defined end points will be called "ultimate" points and denoted by $U_{\mathcal{C}}(S)$ or $U_\beta(S)$.

We investigate whether or not the point U_β depends continuously on the parameter β. The continuity of U_β could be interrupted only in three cases. The first case would be that U_β were the ultimate point of a curve $\mathcal{C}$ which passes through a saddle singularity of the differential equation. This possibility is

excluded; for there is no saddle singularity except on $\varepsilon = 1$ since $\mathcal{B}$ was assumed to lie above $\theta = \theta_s$. The second case would be that $d\tau/dx = 0$ at a point U_β on $\tau = 0$; this is excluded for $\theta < 0$ as seen from the differential equation (1). The third case would be that $d\varepsilon/dx = 0$ at a point U_β on $\varepsilon = 0$. This case can arise at points on $\varepsilon = 0$ with $\theta = \theta_s$.

Let β_* be a value of β such that the coordinates ε and θ of U_β approach 0 and θ_s respectively as $\beta \uparrow \beta_*$ (i.e. β approaches β_* from below). A more detailed investigation would show that then $\mathcal{U}^* = \mathcal{U}_{\beta *}$ ends up at a point $U^* = U_{\beta_*}$ with $\varepsilon = 0$ and $\theta = \theta_s$.

If, for values of β somewhat greater than β_*, the curve $\mathcal{U}_\beta$ ends up on $\varepsilon = 0$ with $\theta > \theta_s$, the point U_β is continuous at β_*. If, however, such a curve $\mathcal{U}_\beta$ does not reach $\varepsilon = 0$ it will meet $\theta = \theta_s$ for a value $\varepsilon > 0$ and end up on it. Thus $U_\beta = A_\varepsilon$ for such values of β, and as $\beta \downarrow \beta^*$ (i.e. as β approaches β^* from above), $U_\beta \to A_o$. Thus U_β is not continuous at $\beta = \beta^*_*$.

These considerations make it evident that the ultimate points U_β vary continuously from the position $U_o = H_1$ on, until either β reaches a value β_* for which U^* is on $\varepsilon = 0$, $\theta = \theta_s$ or until for $\beta = 1$ a point U_1 on $\varepsilon = 0$ with $\theta > \theta_s$ is reached without passing through such a point U_*. We maintain that the latter possibility cannot arise in the normal situation $S < S^o$.

To this end we investigate the curves $\mathcal{U}$ for values of β slightly less than 1. They remain near the curve $\mathcal{U}_1^-$ until they come near to the point A_1; from then on they will remain near the curve $\mathcal{C}$, which leaves the point A_1. In the limit, $\beta \to 1$, we have a curve $\mathcal{U}$ which coincides with $\mathcal{U}_1^-$ up to the point A_1 and then

coincides with the curve $\mathcal{C}$. The ultimate point U_1, therefore, lies on $\varepsilon = 0$ with $\theta < \theta_s$ only if this is the case for the terminal point of $\mathcal{C}$, viz. in the "abnormal" situation. In the normal situation no terminal point on $\varepsilon = 0$ with $\theta > \theta_s$ exists. Consequently, in the normal situation there exists an ultimate point U_*, $\varepsilon = 0$ with $\theta = \theta_s$.

The curve $\mathcal{D} = \mathcal{D}_*$ whose ultimate point is U_* remains on the plane $\varepsilon = 0$ after having passed through U_*, and enters the point A_o. It is evident that the curve $\mathcal{D}_*$ represents a strong detonation. Thus we have established that <u>in normal situations a strong detonation is possible</u>. It is not so easily seen whether or not strong detonations are possible in the abnormal case since it is not obvious whether or not there are ultimate points on $\varepsilon = 0$ with $\theta = \theta_s$ from which the continuation leads into A_o.

Suppose the value of the reaction rate S is such that we are in a normal situation but near to the extreme situation. Then the ultimate point U^* is near to the terminal point $T_{\mathcal{C}}$ of the curve $\mathcal{C}$. Hence the curve $\mathcal{D}^*$ ending up at U^* will first lie near to the curve $\mathcal{D}_1^-$ leading from B_1 to A_1 and then near to the curve $\mathcal{C}$ leading from A_1 to $T_{\mathcal{C}}$. Thus we see: in the extreme case, in which the point $T_{\mathcal{D}}^*$ falls on $T_{\mathcal{C}}$, the strong detonation is represented by a curve consisting of the curve $\mathcal{D}_1^-$ in the plane $\varepsilon = 0$ from B_1 to A_1, then by $\mathcal{C}$ leading from A_1 to $T_{\mathcal{C}}$ and finally by a section leading from $T_{\mathcal{C}}$ to A_o. In other words: <u>in the extreme situation not only a weak detonation exists but also a strong detonation which consists of the weak detonation followed by a shock</u>. In a normal but nearly extreme situation the strong detonation will be

approximately a weak detonation followed by a shock. The extreme situation, however, will occur only for extremely high reaction rates.

Let us consider how a detonation looks in the limiting case when the reaction rate approaches zero; as far as the curves in the $(\tau,\theta,\varepsilon)$-space are concerned this is equivalent to assuming that λ and μ approach zero since $\lambda S_\infty/p_o$ and $\mu S_\infty/p_o$ are the essential dimensionless parameters. The field vectors in this case lie almost in the planes ε = const. except on the lines $\mathcal{A}$ and $\mathcal{B}$. As was stated earlier, the projection of the vector field in the planes ε = const. has a saddle singularity at the points B_ε. Hence there are two lines $\mathcal{D}_\varepsilon^+$ and $\mathcal{D}_\varepsilon^-$ depending on ε, which lead out of B_ε. For $\varepsilon = 1$ they coincide with $\mathcal{D}_1^+$ and $\mathcal{D}_1^-$. The curve $\mathcal{D}_\varepsilon^+$ leads to larger values of θ, while $\mathcal{D}_\varepsilon^-$ leads to smaller values of θ. In the limit $S \to 0$, or, in dimensionless form, $\mu S_\infty/p_o \to 0$ and $\lambda S_\infty/p_o \to 0$, the solution curves $\mathcal{C}$ leaving the point B_1 consist of sections of the curve $\mathcal{B}$ followed by the curves $\mathcal{E}_\varepsilon^+$ or $\mathcal{E}_\varepsilon^-$ until these meet the plane $\tau = 0$ or the line $\mathcal{A}$. From this remark it is clear that the ultimate points $U_\beta = U_\beta(0)$ on the plane $\varepsilon = 0$ consist of the curve $\mathcal{D}_o^+$ on $\varepsilon = 0$ from the point H_o on the plane $\tau = 0$ to the point B_o, then of the curve $\mathcal{D}_o^-$ up to the point A_o. It is clear from this description that the curve $\mathcal{D}^*(0)$ consists of the curve $\mathcal{B}$ from B_1 to B_o followed by $\mathcal{D}_o^-$ on $\varepsilon = 0$ up to A_o. In the limit case $\mu S/p_o \to 0$, $\lambda S/p_o \to 0$, therefore, the strong detonation consists of a shock followed by a reaction

process, as expected.[1]

Finally we are going to show that weak deflagrations exist unless the reaction rate exceeds a certain bound. To this end we should find out whether or not any of the curves $\mathcal{D}$ starting at the point B_1 can end up at the point B_o. The situation differs from that for detonations in that it must now be assumed that $\theta < \theta_s$ at B_o, (see p. 41 and Fig. 5). As a consequence the line $\mathcal{U}(S)$ of ultimate points $U_\beta(S)$ is modified for small values of S. For large values of S, the situation is as before. For $S = \infty$, the initial part of the ultimate line $\mathcal{U}(S)$ leads from the point H_1 on $\tau = 0$ straight over to the projection of H_1 on $\varepsilon = 0$. For large values of S, therefore, the ultimate line $\mathcal{U}(S)$ also begins at H_1 and leads on the plane $\tau = 0$ over to the plane $\varepsilon = 0$. From there on U leads on $\varepsilon = 0$ to the point $\mathcal{J}_\mathcal{C}$ if $\theta > \theta_s$ at A_1, or to a point U^* if $\theta < \theta_s$ at A_1.

For small values of S, however, the situation is quite different. We can no longer assert that the ultimate line leads over from H_1 on the plane $\tau = 0$ to the plane $\varepsilon = 0$. As a matter of fact, for small values of S the ultimate line stops on $\tau = 0$ at a point with $\varepsilon > 0$ and jumps discontinuously over to the line $\mathcal{A}$; the reason being that a curve $\mathcal{L}$ exists which enters the line below $\theta = \theta_s$; (this possibility was excluded for detonations, (see pp. 41,42). We first consider the case S = 0. In that case the curves $\mathcal{D}$ consist of sections of the curve $\mathcal{B}$ followed by sections

[1] If this picture of a detonation is accepted, then v. Neumann's result that no weak detonations exist is implied by the fact that the curve $\mathcal{B}$ connects the point B_o with B_1 and not with A_1.

of the curves $\mathcal{D}_\varepsilon^+$ or $\mathcal{E}_\varepsilon^-$ (see Fig. 4). Since the curve $\mathcal{B}$ now meets the plane $\theta = \theta_s$ before $\varepsilon = 0$ is reached it is clear that none of the curves $\mathcal{D}$ will reach the plane $\varepsilon = 0$.

The ultimate line $\mathcal{U}(0)$ in this case consists of the intersections of the lines $\mathcal{D}_\varepsilon^+$ with $\tau = 0$ from H_1 on up to a value $\varepsilon = \varepsilon_s$ for which $\mathcal{B}$ intersects $\theta = \theta_s$, from there on of the part of the curve $\mathcal{A}$ with $\varepsilon > \varepsilon_s$. The ultimate line thus suffers a discontinuity. Evidently we have $\varepsilon < \varepsilon_s$ on the line $\mathcal{U}(0)$. This confirms the statement that $\mathcal{U}(0)$ does not reach the plane $\varepsilon = 0$.

It is now clear that for sufficiently small values of S the ultimate line $\mathcal{U}(S)$ will also not reach the plane $\varepsilon = 0$. As for $S = 0$, the ultimate line will consist of one part on the plane $\tau = 0$ and another part which is a section of the curve $\mathcal{A}$. The values of the parameter β referring to these two parts are separated by a value $\hat{\beta}_o(S)$ such that the solution curve $\mathcal{D}_{\hat{\beta}_o}$ enters the point $G_{\hat{\varepsilon}}$ for a certain value $\hat{\varepsilon}(S)$ of ε and then enters the point $B_{\hat{\varepsilon}}$. (We recall that G_ε is the point at which the solution curve $\mathcal{F}_\varepsilon^+$ through B_ε intersects the plane $\theta = \theta_s$, see p. 40.) For sufficiently large values of S no such value $\hat{\varepsilon}$ of ε exists since then the ultimate line remains above $\theta = \theta_s$ until it ends at $\mathcal{T}_\mathcal{C}$ or U^*. Therefore, there is a largest value S^o of S for which a value $\hat{\varepsilon}$ exists. It is then seen that this value is $\hat{\varepsilon} = 0$. Consequently, there is a value β^o of β such that the curve $\mathcal{D}^o = \mathcal{D}_{\beta^o}$ for $S = S^o$ meets the plane $\varepsilon = 0$ at the point G_o and ends up at the point B_o. This curve $\mathcal{D}^o$ then represents a weak deflagration. Thus we have shown that <u>for every value of the flux</u> m <u>and for an appropriate reaction rate a weak deflagration exists</u>.

The argument presented holds just as well if the points A_1 and B_1 coalesce so that the flow corresponding to this point is sonic. Thus we see that for an appropriate reaction rate Chapman-Jouguet deflagrations are possible.

In the limiting case where m and S_∞ approach zero in such a way that $s = S_\infty/m^2$ approaches a finite value, a deflagration is always possible for an appropriate value of S_∞/m^2, as was shown in Section 3. In this limiting case $d\theta = 0$ and $d\varepsilon = 0$ for the vector field except on the plane $\theta = P\tau$, on which the vector field is given by $(\tilde{2})$, $(\tilde{3})$; (see p. 28). The points B_0 and B_1 lie on this plane $\theta = p\tau$. The line $\mathcal{L}_1^+$ is the line $\theta = \theta_1$ on $\varepsilon = 1$ with decreasing τ. The line $\mathcal{J}_0^+$ is the line $\theta = P\tau$ on $\varepsilon = 0$ with increasing τ. The point G_0 is then the intersection of $\theta = P\tau$ with $\theta = \theta_s$. As is easily seen there is only one line $\mathcal{L}$ on the plane $\theta = P\tau$ and this line meets the point G_0 only for a special value s_0 of $s = S/m^2$.

Suppose we let m increase holding the initial state (τ_0, θ_0) fixed. Let S(m) be the value of S for which a deflagration exists. We have not proved that S depends continuously on m, but we can be sure that a continuous curve of points (m,S) in a (m,S)-plane exists representing pairs of values of m and S for which deflagrations are possible. Eventually the flux m will reach a value m_C for which the points A_1 and B_1 coalesce and a Chapman-Jouguet situation arises. Let S_C be the corresponding value of the reaction rate S. Then we can at least say that for every value of the reaction rate $S \leq S_C$ deflagrations are possible with an appropriate value of the flux m.

APPENDIX I

On The Assumption About The Discontinuous Character Of The Reaction Process

The considerations of this report rest on the "basic" assumption (see p. 3) that the reaction process may be considered approximately a sharp discontinuity; more specifically, that, firstly, the rates of change of the pertinent quantities in the field of flow outside of the reaction zone are negligibly small when compared to the rates of change of the same quantities inside the reaction zone and, secondly, that the rate of change of the width of the reaction zone is small when compared with the average speed with which the gases cross the reaction zone. It was further assumed (p. 21) that the flow, when observed from a frame moving with the instantaneous velocity of the reaction front, is steady in the neighborhood of the reaction front at the time considered.

We first want to show that this latter assumption is consistent with the assumption of the discontinuous character of the reaction. Suppose we define the velocity $\dot{x}$ of a border of the reaction zone $u_t + \dot{x}u_x = 0$, and suppose we choose the velocity of our frame such that $x = 0$ at one point inside the reaction zone. Then the assumption that the rate of change of the width of the reaction zone is small compared with the average gas velocity in the zone can then be formulated as $|\dot{x}| << u$ everywhere in the zone. Consequently, $|u_t| << |uu_x|$ everywhere in the zone. The term u_t, can, therefore, be omitted from the differential equation which expresses the fact that the acceleration $u_t + uu_x$ equals the total

applied force per unit mass. For similar reasons one can omit the terms τ_t, θ_t, and ε_t from the differential equations expressing the balance of mass flow, energy, and chemical reaction. In other words, to the degree of accuracy implied by our basic assumption, the equations characterizing non-steady flow reduce to the equations (1)', (2)', (3)' in addition to m = const. Thus our assumption of "local steadiness" is in agreement with our "basic" assumption.

Secondly we want to mention that frequently reaction flow processes occur in which our basic assumption is not satisfied. Detonations, consisting of a chemical reaction process initiated by a shock, are frequently followed by rarefaction waves. It is clear that this rarefaction wave interferes with the reaction process, but the interference can be ignored if our basic assumption is satisfied and the changes which the rarefaction wave produces in a section of the width of the reaction zone are significant. If, however, the reaction zone is so wide that this interference can no longer be ignored, then pressure and temperature in the reaction zone are diminished and the strength of the initiating shock is reduced. In particular, the speed of the detonation wave is then less than that calculated without interference and could thus be less than that of a Chapman-Jouguet detonation. If the interaction is strong the detonation may eventually cease.

The occurrence of a lower detonation limit may be explained in this way, since the reaction rate is low, and hence the reaction zone is wide, if the concentration of the combustible component in the unburnt explosive mixture is low. (See Wendlandt [12].)

Spherical detonation waves maintaining the Chapman-Jouguet condition are possible inasmuch as the detonation process can be considered a discontinuity, as Taylor has shown [13]. The rarefaction wave following the detonation front begins, however, with an infinite rate of change of the significant quantities, (see [13]). Consequently, this rarefaction wave always interferes with the detonation wave noticeably and diminishes its strength and speed. It can thus be understood why the speed of spherical detonation waves is less than required by the Chapman-Jouguet hypothesis. Calculations of such spherical detonation waves with sub-Chapman-Jouguet speed were carried out by Eyring and his collaborators [5], [6].

The gradual building up of a detonation wave ignited at the closed end of a tube may also be explained as due to the interference of a rarefaction wave with the reaction process. The condition that the flow velocity vanish at the closed end requires that a simple rarefaction wave follow the detonation wave. This rarefaction wave, when it begins, involves an infinite drop of pressure, temperature and velocity; thus a noticeable interference is clearly indicated. (For numerical calculations of the gradual building up of a detonation see [6].)

As regards deflagration processes it would seem probable that combustion processes occur in which the width of the reaction zone widens noticeably. Otherwise it would seem impossible to explain how a flame could ever overtake a shock front preceding it. Such combustion processes would then be analogous to rarefaction waves

and not to shock discontinuities. No theoretical treatment of such processes seems to exist.

These remarks are intended to show that the frequently observed deviations from the predictions of the discontinuity theory are not due to the unsteadiness of the process as such but rather to the occurrence of a relatively wide reaction zone which permits the interference of the outside flow with the reaction process.

APPENDIX II

It was shown in the text that for an "excessively" high reaction rate $S = S(p,\theta)$ a weak detonation occurs instead of the Chapman-Jouguet detonation (see p. 44). It is of interest to know how high a reaction rate must be in order to be "excessive" in this sense. The excessive cases are separated from the regular ones by "maximal" cases in which a Chapman-Jouguet detonation is just possible, while such a detonation is impossible for a reaction rate higher than a maximal one. We shall present some such maximal reaction rates numerically. From these results it will appear that for maximal reaction rates the transition zone becomes extremely small, of the order of magnitude of one mean free path, if viscosity and heat conduction are those of air at $300^{\circ}K$ and atmospheric pressure. Under these circumstances the notions of viscosity and heat conduction in the transition zone become meaningless. If, however, viscosity and heat conduction are ten times as large as

for atmospheric air at $300^{\circ}K$, excessive reaction rates may well be possible. For example, S would then be excessive if it vanishes up to $900^{\circ}K$ and equals 16.10^{10} sec^{-1} or more for higher temperatures. The width of the transition zone would then be about ten times as long as a mean free path.

We assume that unburnt and burnt gas are polytropic with exponents $\gamma_o = 1.4$ and $\gamma_1 = 1.2$. For the mixture consisting of the fraction ε of burnt gas and $1-\varepsilon$ of unburnt gas we define γ by

$$\frac{1}{\gamma-1} = \frac{\varepsilon}{\gamma_o-1} + \frac{\varepsilon}{\gamma_1-1} .$$

Then we have for the energy per unit mass of the mixture the expression

$$E^{(\varepsilon)}(\theta) = \frac{\theta}{\gamma-1} + (1-\varepsilon)F ,$$

in which the liberated energy per unit mass F is assumed to be

$$F = 32.5\ \theta_o$$

which corresponds to a value 665 cal/gm if the initial temperature is $M_o\theta_o/R_o = 300^{\circ}K$ and the molecular weight of the unburnt gas is $M_o = 29$.

About the heat conductivity λ and viscosity μ we have made the assumption

$$\frac{\lambda}{\mu} = \frac{\gamma}{\gamma-1}$$

which was proposed by Becker [3]. We shall in particular consider as reference value for μ the value

$$\mu_o = 2.44 \cdot 10^{-4} \text{ gm/cm sec}$$

with $\gamma = \gamma_o = 1.4$, the corresponding value of λ is then

$$\lambda_o = 8.54 \cdot 10^{-4} \text{ gm/cm sec} .$$

We recall that the customary coefficients of viscosity and heat conductivity are $\frac{4}{3}\mu$, and $R\lambda$ in our notation; (see footnote 2 on p. 14).

The reaction rate S was assumed to be zero up to a safety temperature $\theta = \theta_s$; for $\theta > \theta_s$ we have assumed

$$\mu S = \text{const.} ;$$

thus, if μ is independent of temperature and pressure the same is then assumed of the reaction rate for $\theta > \theta_o$. This assumption is rather unrealistic because both the reaction rate and the viscosity will increase with the pressure; but this assumption should be sufficient to given information about the order of magnitude of maximal reaction rates. In Fig. 6 we have plotted such maximal reaction rates, or rather the values $\frac{\mu}{\mu_o} S$, in which μ_o is the reference viscosity given above. For a safety temperature of $900^{\circ}K$ or $\theta_s = 3\theta_o$, for example, we find as maximal value of the reaction rate $S = 16 \cdot 10^9 \frac{\mu_o}{\mu} \text{ sec}^{-1}$ for $\theta > \theta_s$. The velocity v_o with which the detonation wave travels into the unburnt gas at rest, solely determined by the Chapman-Jouguet condition, equals $v_o = 15 \cdot 7 \text{ m sec}^{-1}$. The width of the reaction zone is roughly given by

$$\delta = v_o S^{-1} .$$

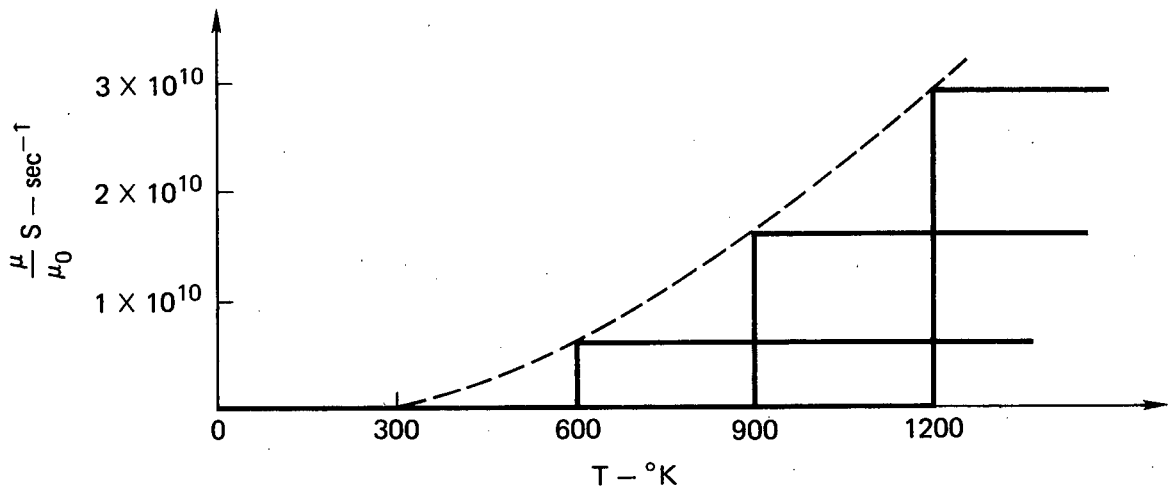

Fig. 6

Maximal reaction rates S as functions of the temperature T.

(If the reaction rate exceeds a maximal one, a Chapman-Jouguet detonation is not possible. μ/μ_o is the ratio of actual viscosity to that for atmospheric air at room temperature.)

In the case $\theta_s = 3\theta_o$, $S = 16 \cdot 10^9 \frac{\mu_o}{\mu}$ sec^{-1}, we therefore have

$$\delta = 98 \cdot 10^{-7} \frac{\mu}{\mu_o} \text{ cm} ,$$

a length which for $\mu = \mu_o$ would be about equal to one free mean path in air.

To determine maximal reaction rates we observe that the Chapman-Jouguet condition cannot be satisfied if it would lead to a situation called "abnormal" in Section 5, p. 39. In abnormal situations, the curve $\mathcal{C}$ starting at the point A_1, ends up on the plane $\varepsilon = 0$ with a value $\theta > \theta_s$.

A maximal situation, in which the Chapman-Jouguet condition can just be satisfied, therefore corresponds to what was called an "extreme" situation, in which the curve ends up on $\varepsilon = 0$ just with $\theta = \theta_s$. To obtain a maximal reaction rate we then proceed as follows. To a given initial state (τ_o, p_o, θ_o) corresponding to the point $_o$, we determine the end state (τ_1, p_1, θ_1) from the Chapman-Jouguet condition. The flux m is then also determined. We now assume any value for the reaction rate S, or rather for μS and determine the curve . The value of θ with which ends upon $\varepsilon = 0$ is then taken as safety temperature θ_s. We finally select those values for the reaction rate S for which the safety temperature turns out to be between $600^{\circ}K$ and $900^{\circ}K$.

The curve was characterized as the graph of that solution of the differential equation which leaves the point $_1$ with decreasing x. All other solution curves entering $_1$ lie on $\varepsilon = 1$. Consequently, can also be characterized as the only solution curve leaving the point $_1$ without $d\varepsilon = 0$. Hence ε can be introduced as parameter. The differential equations then become, after introducing $t = m^2\tau$:

$$(1-\varepsilon)\mu S \frac{dt}{d\varepsilon} = t(p+t-p_1-t_1) ,$$

$$(1-\varepsilon)\gamma\mu S \frac{dpt}{d\varepsilon} = t[pt - \frac{\gamma-1}{2} t^2 + (\gamma-1)tt_1$$

$$+ (\gamma-1)(1-\varepsilon)fp_1t_1 - p_1t_1 - \frac{\gamma-1}{2} t_1^2] .$$

The desired solution $t = t(\varepsilon)$, $p = p(\varepsilon)$ is then the one that assumes the values (t_1, p_1) for $\varepsilon = 1$ and permits expansion with

respect to powers of $(1-\varepsilon)$. It is easily obtained from this power series for small values of $(1-\varepsilon)$ and by finite differences for larger values of $1-\varepsilon$ up to $\varepsilon = 0$.

This is a reproduction of a NAVORD Report 79-46, dated June 25, 1946.

Bibliography

[1] von Neumann, J., "Progress Report on the theory of detonation waves." John von Neumann collected works, Vol. VI, edited by A.H. Taub, Macmillan Co., New York, N.Y. (1963).

[2] Courant, R. and Friedrichs, K.O., Supersonic Flow and Shock Waves, Interscience, New York (1948).

[3] Becker, R., "Stosswelle und Detonation." Zeitschrift fur Physic, Vol. 8, 1922.

[4] Weyl, E., "Shock waves in arbitrary fluids." Comm. Pure Appl. Math., 2, 103 (1949).

[5] Parlin, R.B., Duffy, G., Powell, R.E., and Eyring, H., "The Theory of Explosion Initiation." NDRC, Division 8, OSRD No. 2026, 1943. Confidential.

[6] Eyring, H., Powell, R.E., Duffy, G.H., and Parlin, R.B., "The Chemical Reaction in a Detonation Wave." NDRC, Division 8, OSRD No. 3796, 1944. Confidential.

[7] Lewis, E. and von Elbe, G., Combustion, Flames and Explosions of Gases. Cambridge University Press, Cambridge, 1938.

[8] Jost, Wilhelm, Explosions- und Verbrennungs- vorgänge in Gasen. Edwards Brothers, Ann Arbor, 1943.

[9] Semenov, N.N., "Thermal Theory of Combustion and Explosion." NACA, Technical Memorandum No. 1024, 1026.

[10] Boys, S.F. and Corner, J., "The Structure of the Reaction Zone in the Burning of a Colloidal Propellant." Ministry of Supply. A.C.1139, I.B.8, (WA-66-49). August, 1941. Secret.

[11] Corner, J., "Theories of Flame-Speeds in Gases." Armament Research Department. October 1943. Theoretical Research Report No. 1/43, (WA-1297-4). Secret.

[12] Wendlandt, Rudolph, "Die Detonationsgrenze in Explosiven Gasgemischen. Z. Phys. Chem., 1925, p. 227.

[13] Taylor, G.I., "Detonation Waves." Ministry of Supply. Explosives Res. Comm., R.C. 178, A.C. 639 (W-12-144), February 1941. Confidential.

Chemical Kinetics

Peter D. Lax

Courant Institute of Mathematical Sciences
New York University

The propagation of chemical reactions in combustion is governed by the rate at which energy is transported in and out of the reaction zone, and on the rate at which the chemical reactions proceed. In the simplest models the reaction is assumed to proceed at an exponential rate exp{kt}, k being a function of temperature, changing from 0 to some high value beyond the so-called ignition temperature. In reality chemical reactions are more complex, astonishingly complex; a good understanding of them is necessary to gauge the limitations of simple models and to develop more realistic ones. The purpose of this lecture is to present the elements of chemical kinetics. For a more thorough treatment we recommend a text on Physical Chemistry such as [5]; for the state of the art the Symposium Proceedings contained in [6] should be consulted.

A chemical reaction is the formation of one or several compounds, called <u>products</u> of the reaction, out of one or several compounds or elements called <u>reactants</u>. Household examples are

$$2H_2 + O_2 \rightarrow 2H_2O$$

or

$$H_2 + I_2 \rightarrow 2HI \ .$$

Generally, denoting reactants by M_j and products by N_j,

(1) $$\sum \mu_j M_j \rightarrow \sum \nu_j N_j \ .$$

The coefficients ν_j and μ_j, such as the factors 2 in the oxidation of hydrogen, are called stoichiometric coefficients.

The products of a chemical reaction are built out of the same ingredients as the reactants, i.e. the same nuclei and electrons, but their arrangement is different. The chemical reaction accomplishes the rearrangement as a continuous process starting with the reactants and ending up with the products. With each point in configuration space along this path of deformation one can associate a potential energy, also called energy of formation, defined as the energy needed to put the configuration together out of its widely separated ingredients.

The initial and final states consist of the reactants and products, respectively; these are stable elements and therefore are local minima for the potential energy function. This shows that along a path of deformation the potential energy passes through a peak. There are many possible paths of deformation; the actual reaction is channelled overwhelmingly along the path where the peak value of energy is a minimum. The difference between the minimum peak value and the initial energy is called the activation energy; it is the minimum energy required for the reaction to take place.

The above description of a chemical reaction as a rearrangement in one step is an oversimplification and describes only elementary reactions. Most reactions are complex, consisting of a network of elementary reactions; these elementary reactions lead to the creation, and eventual annihilation, of a large number of

intermediate products-atoms, free radical, activated states. This network of elementary reactions is called the reaction mechanism.

In order to analyze a chemical reaction, one has to perform three tasks:

a) Find all relevant reaction mechanisms.

b) Determine the rates at which the elementary reactions entering a mechanism proceed.

c) Determine the overall rate at which the reaction mechanism proceeds.

Typical reaction mechanisms may involve upward of 80 species; finding all the relevant ones is an art. We call the readers attention to the on-going controversy about the rate at which fluorocarbons released by spray cans are removed from the upper atmosphere; the controversy is about possible reaction mechanisms involving ozone and fluorocarbons. The most intriguing aspect of reaction mechanisms is catalysis, where the presence of a small amount of catalyst makes possible a reaction mechanism which proceeds extremely fast, at the end of which the catalyst is restored. We remark that since elementary reaction rates are rapidly varying functions of temperature, a reaction mechanism that is the relevant one, i.e. the fastest, at one temperature may be irrelevant at a higher temperature.

The determination of rates of elementary reactions is a collaborative effort between experimenters and theorists. We shall say a few words about the theory, a combination of statistical mechanics and quantum chemistry. As remarked earlier, an elementary reaction can take place only if energy, exceeding the

activation energy, is supplied. The source of that energy is the translational energy of sufficiently energetic molecules; upon collision translational energy is converted into internal energy. Assuming that particles are statistically independent of each other, the familiar Stosszahl Ansatz, the number of collisions will be proportional to the product of the concentration of reactions. Suppose the reaction is given by equation (1); let's denote the concentration of species M_j by $[M_j]$, of N_j by $[N_j]$, measured in moles/cm^3. Then the rate at which these concentrations change is

$$\frac{d}{dt}[M_j] = -\mu_j k_f \prod [M_j]^{\mu_j} ,$$

$$\frac{d}{dt}[N_j] = \nu_j k_f \prod [M_j]^{\mu_j} . \qquad (2)$$

This is called the law of mass action, and k_f is called the forward reaction rate. Many, theoretically all, reactions go both forward and backward; the forward reaction rate is denoted by k_f, the backward rate as k_b, and the reaction (1) is written as

$$\sum \mu_j M_j \underset{k_b}{\overset{k_f}{\rightleftarrows}} \sum \nu_j N_j .$$

Equilibrium is established at such concentrations where the forward and backward reaction rates are equal. Since the law of mass action for the backward reaction is

$$\frac{d}{dt}[M_j] = \mu_j k_b \prod [N_j]^{\nu_j} ,$$

$$\frac{d}{dt}[N_j] = -\nu_j k_b \prod [N_j]^{\nu_j} ,$$

at equilibrium

$$k_f \prod [M_j]^{\mu_j} = k_b \prod [N_j]^{\nu_j} .$$

These relations lead to an easy determination of the ratio k_f/k_b, and only one of the two rate constants k_f or k_b need to be measured.

As we shall show below, the reaction rate is an exponentially decreasing function of the activation energy. Since the activation energy for the backward reaction equals the activation energy of the forward reaction plus the energy released in the forward reaction, it follows that for reaction in which a great deal of energy is released, the backward reaction is negligibly slow.

Since the number of energetic particles whose collision leads to possible chemical reaction is a rapidly increasing function of temperature, so is the reaction rate. Arrhenius' law states that

$$k = Be^{-E/RT}$$

where E is the activation energy, R the gas constant and B a constant. A more elaborate statistical collision theory, taking internal degrees of freedom into account, gives

$$k = B(T)e^{-E/RT} ,$$

where B is a function of temperature, typically a power of T. Rates calculated this way are much higher than experimentally observed values. The reason is that not all collisions lead to a reaction, only those where the colliding molecules are properly oriented. This can be corrected empirically by cutting down k by a fudge factor called a steric factor. A more satisfactory calculation can

be based on a statistical theory involving reactants, products and the so-called activated complex, defined as the configuration at the min-max point along the optimal path deformating the reactants into products. Note that the activated complex is in equilibrium, although an unstable one. This method yields good results when the structure of the activated complex is well known; this is a task for quantum chemistry, which has been carried out only for the simplest molecules.

Once a reaction mechanism has been proposed and the rates of the elementary reactions occurring therein have been determined, the law of mass action tells the rate at which species are created or consumed in each elementary reaction. The rate of change of concentration of any specie is the sum of the rates of its creation minus the sum of the rates of its destruction. The resulting system of ODE's together with the specification of all initial concentrations, completely determine the time history of the reaction mechanism. In some simple cases solutions can be expressed in terms of special functions; but the only general way of solving systems of ODE's is by numerical methods.

Rates of elementary reactions within a single mechanism can, and typically do, differ by many orders of magnitude; this has the effect, called stiffness, that various components grow or decay at vastly different rates, which creates special difficulties in finding solutions numerically. We illustrate the difficulty on the simple linear equation

$$\frac{d}{dt} x = -kx , \quad x(0) = 1 ,$$

k large positive, whose exact solution is e^{-kt}. The crude forward scheme

$$\frac{x(t+\delta) - x(t)}{\delta} = -kx(t) ,$$

whose solution is

$$x(t+\delta) = (1 - k\delta)x(t) ,$$

leads to

$$x(n\delta) = (1 - k\delta)^n . \tag{3}$$

When k is large, say $\mathcal{O}(10^4)$, the solution (3) is exponentially unstable, unless $\delta < \frac{2}{k} = \mathcal{O}(10^{-4})$, a prohibitively small time step. A remedy is to use instead the <u>implicit backward</u> scheme

$$\frac{x(t+\delta) - x(t)}{\delta} = -kx(t+\delta) ,$$

whose solution is

$$x(t+\delta) = \frac{1}{1 + k\delta} x(t) ,$$

so that

$$x(n\delta) = (\frac{1}{1 + k\delta})^n .$$

This is stable and approximates well e^{-kt}, $t = n\delta$, regardless of the size of k.

We now try the implicit second order scheme

$$\frac{x(t+\delta) - x(t)}{\delta} = -k \frac{x(t) + x(t+\delta)}{2} ,$$

whose solution is

$$x(t+\delta) = \frac{1 - k\delta/2}{1 + k\delta/2} x(t) ,$$

so that

$$x(n\delta) = (\frac{1 - k\delta/2}{1 + k\delta/2})^n .$$

This is stable, i.e. uniformly bounded, for all k and δ, but for k large is not a good approximation to e^{-kt}, $t = n\delta$. What is true for this simple example is true for systems, and shows that to obtain accurate solutions of stiff systems one must use a specially designed numerical scheme. The most versatile and best known method is due to W. Gear, see [2]. Gear's method is available as a user-oriented packaged program, see [3].

At the end of this talk we will show how to exploit stiffness by making use of asymptotic methods.

We now give some examples:

(I) Reaction: $H_2 + I_2 \rightarrow 2HI$

Reaction mechanism

Elementary reactions	Rate constants
$I_2 \rightleftarrows 2I$	k_f, k_b
$I + H_2 \rightarrow HI + H$	k_2
$H + I_2 \rightarrow HI + I$	k_3
$H + I \rightarrow HI$	k_4

Differential equation:

$$\frac{d}{dt}[I_2] = -k_f[I_2] + k_b[I]^2 - k_3[H][I_2] ,$$

$$\frac{d}{dt}[H_2] = -k_2[I][H_2] ,$$

$$\frac{d}{dt}[H] = k_2[I][H_2] - k_3[H][I_2] ,$$

$$\frac{d}{dt}[I] = 2k_f[I_2] - 2k_b[I]^2 - k_2[I][H_2] + k_3[H][I_2] - k_4[H][I] .$$

(II) Reaction: $A \rightarrow B + C$

Reaction mechanism

Elementary reactions	Rate constants
(4) $A + A \rightleftarrows A^* + A$	k_f, k_b
(5) $A^* \rightarrow B + C$	s

A^* is a so-called activated molecule, formed by collision of energetic molecules A; the activated molecule A^* decays spontaneously into the fragments B and C.

Differential equations:

$$(6) \qquad \frac{d}{dt}[A] = -k_f[A]^2 + k_b[A][A^*] ,$$

$$(7) \qquad \frac{d}{dt}[A^*] = k_f[A]^2 - k_b[A][A^*] - s[A^*]$$

(III) Reaction: $2O_3 \rightarrow 3O_2$

Reaction mechanism

Elementary reactions	Rates
(8) $O_3 \rightleftarrows O_2 + O$	k_f, k_b
(9) $O + O_3 \rightarrow 2O_2$	s

Differential equations:

$$(10) \qquad \frac{d}{dt}[O_3] = -k_f[O_3] + k_b[O_2][O] - s[O][O_3] ,$$

$$(11) \qquad \frac{d}{dt}[O_2] = k_f[O_3] - k_b[O_2][O] + 2s[O][O_3] ,$$

$$(12) \qquad \frac{d}{dt}[O] = k_f[O_3] - k_b[O_2][O] - s[O][O_3] .$$

Examples (II) and (III) are stiff systems in the sense that in both systems the first reaction, (4) respectively (8), is much faster than the second, (5) and (9) respectively. Of course, since they are of modest size, there is no difficulty in solving these systems numerically; we shall show now how to exploit the stiffness to give an asymptotic analysis of the last stages of these reactions.

Assume in case (II) that k_f and k_b are very much larger than s; then the third term on the right in equation (7), $s[A^*]$, is very much smaller than the first two, $k_f[A]^2$ and $k_b[A][A^*]$. As a consequence the effect of the third term is negligible until the first two terms become very nearly equal. The points where the first two terms are equal:

$$k_f[A]^2 = k_b[A][A^*] \ , \tag{13}$$

are called equilibrium states for the reaction (4), for at such points the forward and backward reactions exactly cancel each other. Once a neighborhood of equilibrium is reached, the third term in (7) becomes important. We add (6) and (7) and obtain

$$\frac{d}{dt} m = -s[A^*] \tag{14}$$

where m denotes the sum

$$m = [A] + [A^*] \ . \tag{15}$$

Since equilibrium (13) holds approximately, we deduce that

$$k_f[A] \simeq k_b[A^*] \tag{16}$$

which implies that

(16)' $$[A^*] \simeq \frac{k_f}{k_f + k_b} m \ .$$

Substituting this into (14) we obtain an equation of simple exponential decay for m, giving

(17) $$m \simeq \text{const.} \exp\left(\frac{-sk_f t}{k_f + k_b}\right) \ .$$

Using (15) and (16) we deduce from (17) that

(17)' $$[A] \simeq \text{const} \exp\left(\frac{-sk_f}{k_f + k_b} t\right) \ .$$

We now turn to case (III); here too k_f and k_b are very much larger than s; here too this fact can be exploited to give an asymptotic analysis of the last stage of the reaction. As before, the third term in all three equations (10)-(12), $s[O][O_3]$, is small compared to the first and second terms, $k_f[O_3]$ and $k_b[O_2][O]$; therefore the effect of this third term is negligible until the first two terms become very nearly equal, i.e. until we come near equilibrium for reaction (8):

(18) $$k_f[O_3] = k_b[O_2][O] \ .$$

We also assume that ozone and oxygen atom concentrations are small compared to that of oxygen molecules. If so, we can calculate the value of $[O_2]$ since $3[O_3] + 2[O_2] + [O]$ is a constant in time. Denote this value of $[O_2]$ by Y; from (18),

(19) $$[O_3] \simeq KY[O] \ , \quad K = k_b/k_f \ .$$

To calculate the time histories of $[O_3]$ and $[O]$ add equations (10) and (12); we get

(20) $$\frac{d}{dt} m = -2s[O_3][O] ,$$

where

(21) $$m = [O_3] + [O] .$$

Using (19) and (21) we get

$$[O_3] \simeq \frac{KYm}{1+KY} , \quad [O] = \frac{m}{1+KY} .$$

Substituting this into (20) gives

$$\frac{d}{dt} m = - \frac{2KYs}{(1+KY)^2} m^2$$

whose solution is

(22) $$m(t) = \frac{1}{Ht + \text{const}} , \quad H = \frac{2KYs}{(1+KY)^2} .$$

We now turn to an asymptotic method developed by chemists, called the quasi-steady state approximation; it is applicable in situations where one of the components is very nearly in steady state, i.e. its concentration hardly changes with time. This is the case e.g. in (II), where the value of $[A^*]$ is determined mainly by the equilibrium of the reactions in (4); although A^* decays spontaneously, the rate of decay s is assumed to be small, so that equilibrium is reestablished. The method consists in assuming that exact steady state has been reached, i.e. that the time derivative of the component in question is zero. The resulting algebraic relation is used to eliminate one of the concentrations from the

system of differential equations; the remaining diminished system of ODE's is free of stiffness.

We now apply this method to system (II); setting $\frac{d}{dt}[A^*] = 0$ in (7) gives

$$k_f[A]^2 - k_b[A][A^*] - s[A^*] = 0 \,, \tag{23}$$

from which

$$[A^*] = \frac{k_f[A]^2}{k_b[A] + s} \simeq \frac{k_f}{k_b}[A] \,, \tag{24}$$

i.e. A and A^* are very nearly in equilibrium. Now add (23) to (6); we get using (24)

$$\frac{d}{dt}[A] = -s[A^*] = -\frac{sk_f}{k_b}[A] \,,$$

whose solution is

$$[A] = \text{const} \exp\left(-\frac{sk_f}{k_b}t\right) \,. \tag{25}$$

This result agrees with (17)' when k_b is very much larger than k_f, but disagrees otherwise. Which is correct? numerical integration of the system (6), (7) gives the nod to (17)'; this is not surprising since one can prove rigorously that (17)' is true. In their interesting article [1], "The Steady State Approximation: Fact or Fiction?", Farrow and Edelson analyse a reaction mechanism involving 81 elementary reactions; the ODE system describing the reaction is stiff. They solve this system by Gear's method; this solution differs significantly from previously obtained solutions using the steady state approximation. Since Gear's method is reliable, this shows that the steady state method is not. Nevertheless

we feel that there is need for asymptotic methods – provided that they are valid – such as the one described earlier, or the one expounded in [4] for studying inhomogeneous reactions, where concentrations are functions of space as well as of time. Combustion processes, such as in fuel injected internal combustion engines, are typically inhomogeneous; the detailed solution of complicated ODE's at many points in space would be prohibitively expensive.

The reaction mechanisms in combustion can be complicated indeed. In [6], Westbrook, Dryer et al. discuss the reaction of carbon monoxide and methane in the presence of vapor; the reaction mechanism they establish includes 20 chemical species and 56 reactions. For other examples we refer the reader to the literature of mechanisms for the burning of hydrocarbon fuels, see e.g. [7] and I. Glassman et al. herein.

Bibliography

[1] Farrow, L.A. and Edelson, D., "The Steady State Approximation: Fact or Fiction?", Int. J. of Chemical Kinetics, Vol. 6, 1974, pp. 787-800.

[2] Gear, C.W., "Numerical Initial Value Problems in Ordinary Differential Equations", Prentice Hall, Englewood Cliffs, N.J., 1971.

[3] Hindmarsh, A.C., "GEAR: Ordinary Differential Equation System Solver", Technical Report No. UCID 30001, Rev. 2, Lawrence Livermore Laboratory, 1972.

[4] Kreiss, H., Problems with different time scales for ordinary differential equations, Report No. 68, Uppsala Univ., Dept. of Computer Science, 1977.

[5] Moore, W.J., Physical Chemistry, 4th ed., Prentice Hall, Englewood Cliffs, N.J., 1972.

[6] Symposium on Reaction Mechanisms, Models, and Computers, J. Physical Chemistry, Vol. 81, No. 25, 1977, pp. 2309-2586.

[7] Combustion, Flames and Explosions of Gases, Lewis, Bernard and von Elbe, Guenther, Academic Press,

RANDOM CHOICE METHODS WITH APPLICATIONS TO REACTING GAS FLOW

Alexandre Joël Chorin*

Department of Mathematics and Lawrence Berkeley Laboratory
University of California
Berkeley, California 94720

Abstract

The random choice method is analyzed; appropriate boundary conditions are described, and applications to reacting gas flow in one dimension are carried out. These applications illustrate the advantages of the method.

Introduction

The random choice method for solving hyperbolic systems was introduced as a numerical tool in [2]. It grew from a constructive existence proof due to Glimm [5]. In this method, the solution of the equations is constructed as a superposition of locally exact elementary similarity solutions; the superposition is carried out through a sampling procedure. The computing effort per mesh point is relatively large, but the global efficiency is high when the solutions sought contain components of widely differing time scales. This efficiency is due to the fact that the appropriate interactions can be properly taken into account when the elementary similarity solutions are computed. The aim of the present lecture is to provide a further analysis of the method, and to illustrate its usefulness in the analysis of reacting gas flow. Examples are given of detonation and deflagration waves, with infinite and finite reaction rates.

We begin by describing the method briefly. Consider the hyperbolic system of equations

$$\underline{v}_t = (\underline{f}(\underline{v}))_x, \quad \underline{v}(x,0) \text{ given}, \tag{1}$$

when $\underline{v}$ is the solution vector, and subscripts denote differentiation. The time t is divided into intervals of length k. Let h be a spatial increment. The solution is to be evaluated at the points (ih,nk) and $((i+\frac{1}{2})h,(n+\frac{1}{2})k)$, $i = 0,\pm1,\pm2,\ldots$, $n = 1,2,\ldots$. Let $\underline{u}_i^n$ approximate $\underline{v}(ih,nk)$, and $\underline{u}_{i+1/2}^{n+1/2}$ approximate $\underline{v}((i+\frac{1}{2})h,(n+\frac{1}{2})k)$. The algorithm is defined if $\underline{u}_{i+1/2}^{n+1/2}$ can be found when $\underline{u}_i^n$, $\underline{u}_{i+1}^n$ are known. Consider the following Riemann problem:

$$\underline{v}_t = (f(\underline{v}))_x, \quad t > 0, \quad -\infty < x < +\infty,$$

$$\underline{v}(x,0) = \begin{cases} \underline{u}_{i+1}^n & \text{for } x \geq 0, \\ \underline{u}_i^n & \text{for } x < 0. \end{cases}$$

Let $\underline{w}(x,t)$ denote the solution of this problem. Let θ_i be a value of a random variable θ, $-\frac{1}{2} \leq \theta \leq \frac{1}{2}$. Let P_i be the point $(\theta_i h,\frac{k}{2})$, and let

$$\tilde{\underline{w}} = \underline{w}(P_i) = \underline{w}(\theta_i h,\tfrac{k}{2})$$

be the value of the solution $\underline{w}$ of the Riemann problem at P_i. We set

$$\underline{u}_{i+1/2}^{n+1/2} = \tilde{\underline{w}}.$$

In other words, at each time step, the solution is first approximated by a piecewise constant function; it is then advanced in time exactly, and new values on the mesh are obtained by sampling. The usefulness of the method depends on the possibility of solving Riemann problems efficiently.

Simple Examples and Partial Error Estimates

In order to explain the method further and analyze its limitations, we consider in this section simple examples of its use; the first one was already discussed in [7]. Consider the equation

$$v_t = v_x \tag{2}$$

in $-\infty < x < +\infty$, $t > 0$, with $v(x,0) = g(x)$ given. One can readily see that if a single θ is picked per half time step, Glimm's method reduces to

$$u^{n+1/2}_{i+1/2} = \begin{cases} u^n_{i+1} & \text{if} \quad \theta h \geq -k/2 \\ u^n_i & \text{if} \quad \theta h < -k/2 \ . \end{cases}$$

It follows that

$$u^n_i = v(ih+\eta, t) \ ,$$

where $\eta = \eta(t)$ is a random variable which depends on t alone; i.e., the computed solution equals the exact solution with a shift independent of x. The magnitude of η depends on the choices of θ. Consider the following strategies for picking θ:

i) θ is picked at random from the uniform distribution on $[-\frac{1}{2}, \frac{1}{2}]$;

ii) n is assumed known in advance; the interval $[-\frac{1}{2}, \frac{1}{2}]$ is divided into n subintervals of equal lengths and θ_i is picked in the middle of the i^{th} subinterval;

iii) (A compromise between i) and ii)): $[-\frac{1}{2}, \frac{1}{2}]$ is divided into m subintervals, $m << n$, and θ_1 is picked at random in the first subinterval, θ_2 in the second subinterval, θ_{m+1} in the first subinterval, etc.

A fourth strategy which relies on the well-equipartitioned sequences studied by Richtmyer and Ostrowski was suggested by Lax [6], but is not useful in the present context.

If strategy i) is used, we have

$$x+\eta = \text{displacement of the initial value}$$

$$= \sum_{i=1}^{2n} \eta_i \ ,$$

where

$$\eta_i = \begin{cases} \frac{h}{2} & \text{if} \quad h\theta_i < -k/2 \\ -\frac{h}{2} & \text{if} \quad h\theta_i \geq -k/2 \ . \end{cases}$$

The variance of η_i is readily evaluated:

$$\text{var}\ (\eta_i) = \frac{h^2}{4}\ (1-\frac{k}{h})(1+\frac{k}{h}) \ ;$$

the variance of η is thus

$$\frac{nh^2}{4}\ (1-\frac{k}{h})(1+\frac{k}{h}) \ ,$$

and the standard deviation of η, which measures its magnitude is $\frac{\sqrt{n}h}{2}\ \{(1-\frac{k}{h})(1+\frac{k}{h})\}^{1/2} = 0\ (\sqrt{n}h)$.

If the second strategy is used,

$$u_i^n = v(x+\eta, t) \ , \quad |\eta| \leq \frac{1}{2n} \ ,$$

if $n = O(h^{-1})$, $\eta = O(h)$. If the third strategy is used, and n is a multiple of m, $\eta = O(h\sqrt{n/m})$, since only in every m^{th} half step is the outcome of the sampling in doubt.

Assume v is of compact support. Following a suggestion by Lax, we define the resolution of the scheme by

$$Q^{-1} = \min_q \|u_i^n - v(ih+q, t)\|$$

where $\| \ \|$ denotes the maximum norm. The scheme has resolution of order m if $Q = O(h^{-m})$. The displacement d of the scheme is defined by

$$Q^{-1} = \|u_i^n - v(ih+d, t)\|$$

$$= \min_q \|u_i^n - v(ih+q, t)\| \ .$$

The method applied to the present problem has almost first order accuracy, almost first order displacement, but infinite resolution. There is no smoothing and no numerical diffusion or dispersion. For any k/h, the domain of dependence of a point is always a single point. The answers are always bounded. If the Courant condition $k/h \leq 1$ is violated, the equation being approximated is $v_t = (h/k)v_x$. Clearly, since these results are independent of k/h, they generalize to hyperbolic systems with constant coefficients.

Consider now the equation

$$v_t = a(x,t)v_x \ ,$$

in $-\infty < x < +\infty$, $t > 0$, $v(x,0) = g(x)$ given, and $a(x,t)$ a Lipschitz continuous function of both x and t. The method is not well suited to the solution of such an equation, both because the solution of the Riemann problem requires a possibly laborious integration of a characteristic equation, and because the errors will turn out to be large compared with those incurred in other available methods. The analysis is nevertheless illuminating.

Let C_{x_0} be the characteristic

$$\frac{dx}{dt} = -a(x,t) , \quad x(0) = x_0 .$$

For each i, we have

$$u_{i+1/2}^{n+1/2} = \begin{cases} u_i^n & \text{if } P = (\theta h, \frac{k}{2}) \text{ lies to the right of } C_{(1+\frac{1}{2})h} \\ u_{i+1}^n & \text{if } P \text{ lies to the left of } C_{(i+\frac{1}{2})h} . \end{cases}$$

As before

$$u_i^n = v(x+\eta, t) , \quad x = ih , \quad t = nk ;$$

where η is a random variable which now depends on both x and t.

If θ is picked at random from the uniform distribution on $[-\frac{1}{2}, \frac{1}{2}]$ (Strategy i)) we have as before $\eta = O(h\sqrt{n})$. Strategy ii) clearly yields an error O(1). Strategy iii) is more advantageous; the standard deviation of η is again bounded by $O(h\sqrt{n/m})$. However, the mean of η is no longer zero. Assume $k = O(h)$. Note that $a(x,t)$ may vary by $O(mh)$ before this change affects the values of η. Thus, $\overline{\eta}$ = mean of $\eta = O(mh)$, and $\eta = O(mh) + O(h\sqrt{n/m})$. If

$n = O(h^{-1})$ and $m = O(n^{1/3})$, then $\eta = O(h^{2/3})$. We have less than first order accuracy and more than first order displacement.

We now try to assess the relative displacement of two points. Let us assume that the first sampling strategy is used, i.e., θ is picked at each step from the uniform distribution on $[-\frac{1}{2}, \frac{1}{2}]$. Consider first the quantity

$$\Delta\eta(h,k) = (\eta(x,t+k) - \eta(x+h,t+k)) - (\eta(x,t) - \eta(x+h,t)) ,$$

i.e., the difference between the numerically induced translations experienced by two neighboring points during one time step. If $\Delta\eta(h,k) > 0$, information is lost: one value of $v(x,0)$ disappears. If $\Delta\eta(h,k) < 0$, a false constant state is created. $\Delta\eta(h,k)$ can take on the values $0, \pm h$. $\Delta\eta(h,k) \neq 0$ if $P = (\theta h, \frac{k}{2})$ falls to the left of the characteristic through one of the points (ih,nk), $((i+1)h,nk)$ and to the right of the other. This happens with probability $O(h)$, i.e., the variance of $\Delta\eta(h,k)$ is $O(h^3)$. Therefore, the variance of $\Delta\eta(h) = \eta(x,t) - \eta(x+h,t)$ is $nO(h^3) = O(h^2)$ if $n = O(h^{-1})$, and the standard deviation of $\Delta\eta(h)$ is $O(h)$, i.e., neighboring values in the range of v do not fly far apart. The same estimate holds for the other sampling strategies.

Consider now the relative displacement $\Delta\eta$ of two values far apart. Let $\eta_1 = \eta(x,t)$, $\eta_2 = \eta(x+X,t)$, and $\Delta\eta = \eta_2 - \eta_1$, and thus

$$u_i^n = v(x+\eta_1,t) = g(x_1) , \quad ih = x , \quad nk = t ,$$

$$u_{i+i_0}^n = v(x+X+\eta_2,t) = g(x_2) , \quad i_0 h = X ,$$

where $g(x) = v(x,0)$. Let C_{x_1} be the characteristic through $(x_1,0)$,

and similarly for C_{x_2}. x_2-x_1 has increased by $\pm h$ each time $P = (\theta h, \frac{k}{2})$ fell between the two characteristics. Assume the first sampling strategy is used. There are two sources of error which make $\Delta\eta \neq 0$. There is the standard deviation of the sum of the random variables which equal $\pm h$ when P is between the characteristics, and are zero otherwise, (this is clearly $O(h\sqrt{n})$), and there is the uncertainty in the slope of the characteristics due to the lateral displacement of the solution; this is again $O(h\sqrt{n})$ and induces an error $O(h^{3/2}n^{3/4}) = O((h\sqrt{n})^{3/2})$; if $n = O(h^{-1})$, this is $O(h^{3/4})$. Thus $\Delta\eta = O(h\sqrt{n})$, and the resolution is not of higher order than the accuracy. Similar results hold for the other sampling strategies.

We now turn to the nonlinear problem

$$\underline{v}_t = (f(\underline{v}))_x ,$$

where f is a function of v but not explicitly a function of x and t. The method of analysis we have used here is not applicable, since values of $\underline{v}$ are not merely propagated along characteristics. Furthermore, we have here no way of taking into account properly the fact that rarefaction or loss of information incurred in the numerical process correspond to genuine properties of the differential equations. All we can provide here is a heuristic analysis. Consider the third sampling strategy. Since the slope of the characteristic depends on the values of v and not on x, the values of v at neighborhing points remain attached to neighboring points, we expect the term $O(mh)$ in η to disappear, and have $\eta = O(h\sqrt{n/m})$.

Thus, the resolution should be at least $O(h\sqrt{n/m})$. Note that if $n = O(h^{-1})$ and $m = O(n)$, the random element in the method loses its significance.

In the case of a shock separating two constant states, one can readily see that $d = O(h\sqrt{n/m})$ but the resolution is infinite. One can trivially define resolution in a neighborhood. Thus, what we have is a rather awkward first order method, which resolves shocks very sharply. We also know that it keeps fluid interfaces perfectly sharp [2]. It is useful for the analysis of problems in cartesian coordinates in which the dynamics of the discontinuities are of paramount significance. We shall provide examples of such problems in later sections. Recent results (see, e.g., [8]) show that in such problems substantially higher accuracy cannot be achieved.

Boundary Conditions

The correct imposition of boundary conditions in our method requires careful thought, and was not adequately discussed in [2]. It is clear that even in the case of equation (2) the presence of a boundary can detract from both accuracy and resolution. The lateral displacement of the solution may make some function values disappear across the boundary and care must be taken to ensure the possibility of their retrieval. Additional storage across the boundary and careful accounting of the lateral displacement provide a remedy.

The following procedure has been introduced in [2] to reduce the lateral displacement of the solution (and thus reduce the loss

of information at walls), when the third sampling strategy is used. The goal is to obtain as fast as possible solution values on both sides of whatever wave pattern emerges in the solution of the Riemann problem, and thus rapidly offset a displacement to right by a displacement to the left (or vice versa). We pick an integer $m' < m$, and m and m' mutually prime, and n_0 integer, $n_0 < m$, and construct the sequence of integers

$$n_{i+1} = (n_i + m')(\text{mod } m) \quad . \tag{3}$$

The subintervals of $[-\frac{1}{2}, \frac{1}{2}]$ are then sampled in the order $n_0, n_1, n_2, \ldots$ rather than in the natural succession. One can further modify the sampling so that of two successive values of θ, one lies in $[-\frac{1}{2}, 0]$ and one in $[0, \frac{1}{2}]$. These procedures do not increase the error far from the wall, and are quite effective, although no analytical assessment of their efficiency is available.

Suppose we are solving the equations of gas dynamics (equations (4) below), and using the third sampling strategy, modified by (3) or not. Assume the velocity v is given at the boundary. One can find a state (i.e., a set of values for the gas variables) which has the given velocity and which can be connected to the state one mesh point into the fluid by a simple wave (see, e.g., [4]). This is equivalent to solving half a Riemann problem, and provides an appropriate solution field which can be sampled. The same result can be obtained by symmetry considerations. Consider a boundary point to the right on the region of flow; let the boundary conditions be imposed at a point $i_0 h$. A fake right state at $(i_0 + \frac{1}{2})h$ is created, with

$$\rho_{i_0+1/2} = \rho_{i_0-1/2} ,$$

$$v_{i_0+1/2} = 2V - v_{i_0-1/2} ,$$

$$p_{i_0+1/2} = p_{i_0-1/2} ,$$

where ρ, v, p are respectively the gas density, velocity and pressure, and V is the velocity of the wall. The constant state in the middle of the Riemann solution is the wall state, and it is sampled to the left of the slip line $\frac{dx}{dt} = V$.

This procedure contains a pitfall, not noticed in [2]; let θ be chosen in accordance with our usual sampling strategy; let θ_1, θ_2 be the values of θ at two successive time steps (θ_1 and θ_2 are not independent). θ_1', θ_2', the values used at the wall, differ from θ_1 and θ_2 since only part of the interval $[-\frac{1}{2}, \frac{1}{2}]$ is sampled (or else one does not remain to the left of the wall line $\frac{dx}{dt} = V$). θ_1' and θ_2' can presumably be obtained by a linear change of variables. Consider a specific part of the wave pattern at the wall. Since θ_1', θ_2' are not independent, the possibility exists that whenever θ_1' picks up the specific part we are considering, θ_2' is such that this information is lost to the wall. This possibility was not noticed in [2], and its removal by the methods whose description follows contributes to the sharpening of the results obtained in [2].

It is always consistent to pick θ_1', θ_2' by a linear change of variables from two values picked independently from the uniform distribution on $[-\frac{1}{2}, \frac{1}{2}]$. On the average no information will be

lost to the wall, but the variance of the solution will be increased. Better strategies can be devised, but require thought in each special case. If the walls are at rest, V = 0, one can proceed as follows: impose the boundary condition on the right at time nk and a point $i_1 h$, and on the left at time $(n+\frac{1}{2})k$ at a point $(i_2+\frac{1}{2})h$, i_1, i_2 integers. One can see that if θ_1, θ_2 are so chosen that $\theta_1 \leq 0$ at time nk, and $\theta_2 \geq 0$ at time $(n+\frac{1}{2})k$, then θ_1 and θ_2 can be used at the boundary as well as in interior without loss of resolution.

Detonations and Deflagrations in a One Dimensional Ideal Gas

Our goal in this section is to present a quick summary of the elementary theory of one dimensional detonation and deflagration waves, (for more detail, see, e.g., [4] and [10], and then derive some relations between the hydrodynamical variables on the two sides of such waves for later use.

The equations of gas dynamics are

$$\rho_t + (\rho v)_x = 0 , \tag{4a}$$

$$(\rho v)_t + (\rho v^2 + p)_x = 0 , \tag{4b}$$

$$e_t + ((e+p)v)_x = 0 , \tag{4c}$$

where the subscripts denote differentiation, ρ is the density of the gas, v is the velocity, ρv is the momentum, e is the energy per unit volume and p is the pressure. We have

(4d) $$e = \rho\varepsilon + \frac{1}{2}\rho v^2 ,$$

where $\varepsilon = \varepsilon_i + q$, ε_i is the internal energy per unit mass,

(4e) $$\varepsilon_i = \frac{1}{\gamma-1}\frac{p}{\rho}$$

where γ is a constant, $\gamma > 1$, and q is the energy of formation which can be released through chemical reaction (see [4]). In the present section it will be assumed that part of q is released instantaneously in an infinitely thin reaction zone. Let the subscript 0 refer to unburned gas (i.e., gas which has not yet undergone the chemical reaction) and let the subscript 1 refer to burned gas. The unburned gas is on the right. We have

$$\varepsilon_1 = \frac{1}{\gamma_1-1}\frac{p_1}{\rho_1} + q_1$$

$$\varepsilon_0 = \frac{1}{\gamma_0-1}\frac{p_0}{\rho_0} + q_0 .$$

For the sake of simplicity, we shall make here the unrealistic assumption $\gamma_1 = \gamma_0 = \gamma$. (The case $\gamma_1 \neq \gamma_0$ is more difficult only because of additional algebra.) When $\gamma_1 = \gamma_0 = \gamma$ the reaction can be exothermic (i.e., release energy) only if $q_1 > q_0$.

Let U be the velocity of the reaction zone. Let

$$w_1 = v_1 - U$$

$$w_0 = v_0 - U .$$

Conservation of mass and momentum is expressed by

(5) $$\rho_1 w_1 = \rho_0 w_0 = -M$$

(6) $$\rho_0 w_0^2 + p_0 = \rho_1 w_1^2 + p_1$$

(see [4]). From these relations one readily deduces

$$M^2 = -\frac{p_0-p_1}{\tau_0-\tau_1}, \text{ where } \tau = 1/\rho .$$

Define the function H by

$$H = \varepsilon_1-\varepsilon_0 + \frac{(\tau_1-\tau_0)}{2}(p_1+p_0) .$$

Conservation of energy is expressed by

$$H = H(\tau_1, p_1, \tau_0, p_0) = 0 .$$

Define $\Delta = q_0-q_1$, ($\Delta \leq 0$ for an exothermic process), and $\mu^2 = \frac{\gamma-1}{\gamma+1}$; we find

(7)
$$\begin{aligned} 2\mu^2 H = 0 &= (1-\mu^2)\tau_1 p_1 - (1-\mu^2)\tau_0 p_0 - 2\mu^2\Delta + \mu^2(\tau_1-\tau_0)(p_1+p_0) \\ &= -p_0(\tau_0-\mu^2\tau_1) + p_1(\tau_1-\mu^2\tau_0) - 2\mu^2\Delta . \end{aligned}$$

In the (τ_1, p_1) plane the locus of points which can be connected to (τ_0, p_0) by an infinitely thin combustion wave is a curve which reduces to a hyperbola when Δ is independent of p and τ. (See Figure 1.) The lines through (τ_0, p_0) tangent to H = 0 are called the Rayleigh lines. Their points of tangency, S_1 and S_2, are called the Chapman-Jouguet (CJ) points. The portion, $p_1 > p_0$ and $\tau_1 > \tau_0$, of the curve is omitted because it corresponds to

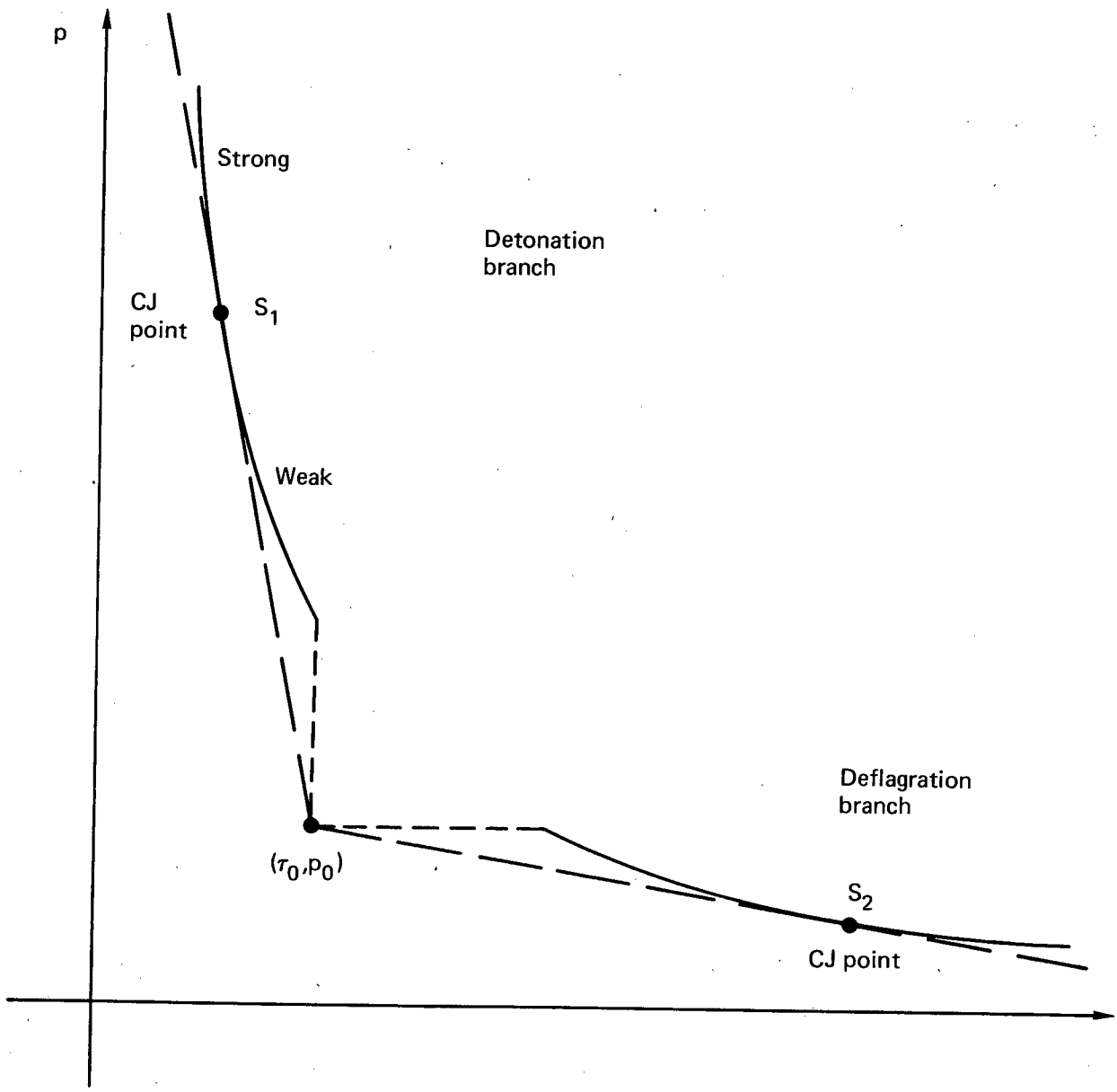

Figure 1. The Hugoniot curve for exothermic gas flow.

unphysical events in which $M^2 < 0$. The upper portion of the curve corresponds to detonations; the portion above S_1 to strong detonations and the portion below to weak detonations. The lower part of the curve corresponds to deflagrations.

The velocity and strength of a strong detonation are entirely determined by the state of the unburned gas in front of the detonation and one quantity behind the detonation, just as in the case with shocks. Let p_0, ρ_0, τ_0, ε_0 and v_0 be given, as well as p_1, and assume the unburned gas lies to the right of the detonation. We have from (7)

$$\tau_1 = \tau_0\left(\frac{p_0+\mu^2 p_1}{\mu^2 p_0+p_1}\right) + \frac{2\mu^2\Delta}{\mu^2 p_0+p_1} \tag{8}$$

and thus

$$M^2 = -\frac{p_0-p_1}{\tau_0-\tau_1} = \frac{p_0-p_1}{\tau_0\left(\frac{p_0+\mu^2 p_1}{p_1+\mu^2 p_0} + \frac{2\mu^2\Delta\rho_0}{\mu^2 p_0+p_1} - 1\right)} .$$

Let $[p] = p_1-p_0$; some algebra yields

$$M^2 = p_0\rho_0\left(\frac{\gamma-1}{2} + \frac{\gamma+1}{2}\left(\frac{p_1}{p_0}\right)\right)/\left(1 - (\gamma-1)\rho_0\Delta/[p]\right) . \tag{9}$$

If $\Delta = 0$ this formula reduces to the expression for M in a shock, as given in [2] or [9]. M is real if $[p] - (\gamma-1)\rho_0\Delta \geq 0$; this can be readily seen to hold in a strong detonation.

The states on the curve $H = 0$ located between the CJ point S_1 and the line $\tau = \tau_0$ correspond to weak detonations. As described in [4], the state behind a weak detonation is entirely determined by the velocity U of the detonation and the state in front of it.

In fact, a weak detonation cannot occur and what does happen is a CJ detonation followed by a rarefaction wave. Our next objective is to derive an explicit criterion for determining whether a detonation will be a strong detonation or a CJ detonation.

It is shown in [4] that at S_1, $|w_1| = c_1$ where $c_1 = \sqrt{\gamma p_1/\rho_1}$ is the sound speed, i.e., a CJ detonation moves with respect to the burned gas with a velocity equal to the velocity of sound in the burned gas. We now use this fact to determine the density ρ_{CJ}, velocity v_{CJ} and pressure p_{CJ} behind a CJ detonation.

From equations (4) and (5) one finds

$$\frac{p_1-p_0}{\tau_1-\tau_0} = -\rho_1^2 w_1^2 = -\rho_0^2 w_0^2 = -M^2 ,$$

and thus in a CJ detonation

$$\frac{p_1-p_0}{\tau_1-\tau_0} = -\rho_1^2 \frac{\gamma p_1}{\rho_1} = -\gamma p_1/\tau_1 , \quad \tau_1 = 1/\rho_1 ,$$

or

$$\tau_1(p_1(1+\gamma)-p_0) = \gamma\tau_0 p_1 . \tag{10}$$

Equating τ_1 obtained from (8) to τ_1 in (10), we find

$$\tau_0\left(\frac{\mu^2 p_1+p_0}{p_1+\mu^2 p_0}\right) + \frac{2\mu^2\Delta}{(p_1+\mu^2 p_0)} = \frac{\gamma\tau_0 p_1}{p_1(1+\gamma)-p_0} .$$

Some algebra reduces this equation to

$$p_1^2 + 2p_1 b + c = 0 ,$$

where

(11a) $$b = -p_0 - \Delta(\gamma-1)\rho_0$$

(11b) $$c = p_0^2 + 2\mu^2 p_0 \rho_0 \Delta \quad ;$$

a trivial calculation shows that $b^2-c \geq 0$ if $\gamma \geq 1$ and $\Delta \leq 0$. Thus

(11c) $$p_{CJ} = p_1 = -b + \sqrt{b^2-c}$$

where the + sign is mandatory since a detonation is compressive. Given $p_{CJ} = p_1$, $\rho_{CJ} = \rho_1 = \tau_1^{-1}$ can be obtained from equation (10). Since $M = -\rho_1 w_1$, and $w_1 = -c_1$, we find

$$M = \sqrt{\gamma p_1 \rho_1} = \sqrt{\gamma p_{CJ} \rho_{CJ}} \cdot$$

The velocity U_{CJ} of the detonation is found from

$$\rho_0(v_0 - U_{CJ}) = -M$$

which yields $U_{CJ} = (\rho_0 v_0 + \sqrt{\gamma p_{CJ} \rho_{CJ}})/\rho_{CJ}$, and then

(12) $$v_{CJ} = U_{CJ} - c_{CJ} \cdot$$

v_{CJ} depends only on the state of the unburned gas.

Suppose v_1, the velocity of the burned gas, is given. If $v_1 \leq v_{CJ}$ a CJ detonation will appear, followed by a rarefaction wave. If $v_1 = v_{CJ}$ a CJ detonation will appear alone, and if $v_1 > v_{CJ}$ a strong detonation will take place.

If the unburned gas lies to the left of the burned gas analogous relations are found; the only difference lies in the signs of v, in particular,

$$M = +\rho_1(v_1-U) = +\rho_0(v_0-U) \ .$$

The velocity of a possible deflagration cannot be determined within the context of a theory which assumes the gas to be nonconducting; this point will be further discussed below. It will turn out that for a nonconducting gas the only possible deflagration is a constant pressure deflagration, $p_1 = p_0$, which moves with zero velocity with respect to the gas; i.e., it is indistinguishable from a slip line.

Application of the Method to Reacting Gas Flow

One interesting feature of our method is its applicability to the analysis of gas flow in which exothermic chemical reactions are taking place and producing substantial dynamical effects. A Riemann problem is solved at each time step and at each point in time; this solution is then sampled. The advantage of this procedure is that the interaction of the flow and the chemical reaction can be taken into account when the Riemann problem is solved, even when the time scales of the chemistry and the fluid flow are very different. As a result, the basic conservation laws are satisfied at the end of each time step. It can be readily seen that if the chemical reactions and the gas flow were to be taken into account in separate fractional steps, the basic conservation laws may be violated at the end of each hydrodynamical step, thus either inducing unwanted oscillations and waves, or requiring time steps small enough for all changes to be very gradual — usually a costly remedy. It is interesting to note that the Riemann solu-

tions with energy deposition in the flow field are equivalent to the exothermic centers introduced by Oppenheim [3] and serve the same purpose of accounting for the dynamical effects of the exothermic reactions. These discrete exothermic centers correspond to a physical reality whose origin can be ascribed to the fluctuations to the levels of chemical species [1].

We consider here the simplest possible description of a reacting gas (see e.g. [9]):

$$\rho_t + (\rho v)_x = 0 \tag{13a}$$

$$(\rho v)_t + (\rho v^2 + p)_x = 0 \tag{13b}$$

$$e_t + ((e+p)v)_x - \lambda T_{xx} = 0 \tag{13c}$$

where, as before, ρ is the density, v is the velocity, e the energy per unit volume,

$$e = \rho\varepsilon + \frac{1}{2}\rho v^2 , \tag{13d}$$

ε is the internal energy. In this section,

$$\varepsilon = \frac{1}{\gamma-1}\frac{p}{\rho} + Zq \tag{13e}$$

where γ is a constant, $\gamma > 1$, q is the total available bonding energy ($q \leq 0$), and Z is a progress parameter for the reaction. $T = p/\rho$ is the temperature, and λ is the coefficient of heat conduction. Z is assumed to satisfy the rate equation

$$\frac{dZ}{dt} = -KZ , \quad Z(0) = 1 \tag{13f}$$

where

$$K = 0 \quad \text{if} \quad T = p/\rho \leq T_0 \,,$$

(13g)

$$K = K_0 \quad \text{if} \quad T = p/\rho > T_0 \,.$$

T_0 is the ignition temperature and K_0 is the reaction rate. The equations of the preceding section are recovered if we set $\lambda = 0$, $q = \Delta$, and $K = \infty$. Equation (13f) is a reasonable prototype of the vastly more complex equations which describe real chemical kinetics. Viscous effects have been omitted here; their inclusion in the present context has little effect and presents little difficulty. (Thus, we assume here a zero Prandtl number.)

The approximation of the dissipation term will be relegated to a separate fractional step, where it is to be handled by straightforward finite differences. In view of (13e), and the perfect gas law $T = p/\rho$ (in appropriate units), this fractional step requires merely the approximation of

$$\partial_t T = (\gamma-1)T_{xx} \,. \tag{14}$$

The differencing of a heat conduction term alone introduces negligible numerical dissipation. Several more sophisticated approximation methods were tried, but did not seem to be worth pursuing.

All that remains to be done is to describe the solution of the Riemann problem for equations (13) with $\lambda = 0$. This will be done with the following simplifying assumption: whatever energy may be released during the time $k/2$ in a portion of the fluid is released instantaneously. This approximation is well in the spirit

of our method (since it approximates Z by a piecewise constant function); it also has some physical justification [1].

Solution of a Riemann Problem With Chemistry

Our goal is to solve equations (13) and the following data:

$$S_\ell(\rho = \rho_\ell,\ p = p_\ell,\ v = v_\ell,\ Z = Z_\ell) \quad \text{for} \quad x \leq 0$$

and

$$S_r(\rho = \rho_r,\ p = p_r,\ v = v_r,\ Z = Z_r) \quad \text{for} \quad x > 0$$

with $\lambda = 0$. We begin by a partial review of the case $K_0 = 0$ (no chemistry; see [2], [6], [9]). The solution consists of a right state S_r, a left state S_ℓ, a middle state $S_*(p = p_*,\ v = v_*)$, separated by waves which are either rarefactions or shocks. S_* is divided by the slip line $\frac{dx}{dt} = v_*$ into two parts with possibly differing values of ρ, ρ_{*r} to the right of the slip line and $\rho_{*\ell}$ to its left. To determine v_* and p_* we proceed as follows: define the quantity

$$M_r = \frac{p_r - p_*}{v_r - v_*} \,. \tag{15}$$

If the right wave is a shock,

$$M_r = -\rho_r(v_r - U_r) = -\rho_{*r}(v_* - U_r) \tag{16}$$

where U_r is the velocity of the right shock. From the Rankine-Hugoniot conditions one obtains

$$M_r = \sqrt{p_r \rho_r}\,\phi(p^*/p_r) \,, \quad p_*/p_r \geq 1 \,, \tag{17a}$$

where

(17b) $$\phi_1(\alpha) = \sqrt{\frac{\gamma+1}{2}\alpha + \frac{\gamma-1}{2}} \ .$$

If the right wave is a rarefaction, we find

(18a) $$M_r = \sqrt{p_r\rho_r}\ \phi_2(p_*/p_r) \ , \quad p_*/p_r \leq 1 \ ,$$

where

(18b) $$\phi_2(\alpha) = \frac{\gamma-1}{2\sqrt{\gamma}} \frac{1-\alpha}{1-\alpha^{\gamma-1/2\gamma}} \ .$$

(18b) is derived through the use of the isentropic law $p\rho^{-\gamma} =$ constant and the constancy of the right Riemann invariant $\Gamma_r = 2\sqrt{\gamma p/\rho}/(\gamma-1) - v$. The function

(19) $$\phi = \begin{cases} \phi_1(\alpha) \ , & \alpha \geq 1 \ , \\ \phi_2(\alpha) \ , & \alpha \leq 1 \ , \end{cases}$$

is continuous at $\alpha = 1$, with $\phi(1) = \phi_1(1) = \phi_2(1) = \sqrt{\gamma}$. Similarly, we define

(20) $$M_\ell = \frac{p_\ell - p_*}{v_\ell - v_*} \ ;$$

if the left wave is a shock,

(21) $$M_\ell = \rho_\ell(v_\ell - U_\ell) = \rho_{*\ell}(v_* - U_\ell) \ ,$$

where U_ℓ is the velocity of the left shock. As on the right, $M_\ell = \sqrt{p_\ell\rho_\ell}\ \phi(p_*/p_\ell)$, where $\phi(\alpha)$ is defined as in equations (17) and (18). From (15) and (20),

(22) $$p_* = (u_\ell - u_r + p_r/M_r + p_\ell/M_\ell)/((1/M_r) + (1/M_\ell)) \ .$$

These considerations lead to the following iteration procedure:

Pick a starting value p_*^0 (or values M_r^0, M_ℓ^0), and then compute $p_*^{\nu+1}$, $M_r^{\nu+1}$, $M_\ell^{\nu+1}$, $q \geq 0$ using

$$\tilde{p}^{\nu} = (u_\ell - u_r + p_r/M_r^\nu + p_\ell/M_\ell^\nu)/((1/M_r^\nu) + (1/M_\ell^\nu)) , \tag{23a}$$

$$p_*^{\nu+1} = \max\,(\varepsilon, \tilde{p}^{\nu}) , \tag{23b}$$

$$M_r^{\nu+1} = \sqrt{p_r \rho_r}\ \phi(p_*^{\nu+1}/p_r) , \tag{23c}$$

$$M_\ell^{\nu+1} = \sqrt{p_\ell \rho_\ell}\ \phi(p_*^{\nu+1}/p_\ell) . \tag{23d}$$

Equation (23b) is needed because there is no guarantee that in the course of iteration $\tilde{p}$ remains ≥ 0. We usually set $\varepsilon_1 = 10^{-6}$. The iteration is stopped when

$$\max\,(|M_r^{\nu+1} - M_r^\nu|, |M_\ell^{\nu+1} - M_\ell^\nu|) \leq \varepsilon_2 ,$$

(we usually picked $\varepsilon_2 = 10^{-6}$); one then sets $M_r = M_r^{\nu+1}$, $M_\ell = M_\ell^{\nu+1}$, and $p_* = p_*^{\nu+1}$.

To start this procedure one needs initial values of either M_r and M_ℓ (or p_*). The starting procedure suggested by Godunov appears to be ineffective, and better results were obtained by setting

$$p_*^0 = (p_r + p_\ell)/2 .$$

We also ensured that the iteration was carried out at least twice, to avoid spurious convergence when $p_r = p_\ell$.

As noted by Godunov, the iteration may fail to converge in the presence of a strong rarefaction. This problem can be overcome

by the following variant of Godunov's procedure: If the iteration has not converged after L iterations (we usually set L = 20), equation (23b) is replaced by

$$(23b)' \qquad p_*^{\nu+1} = \alpha \max(\varepsilon_1, \tilde{p}^{\nu}) + (1-\alpha)p_*^{\nu}$$

with $\alpha = \alpha_1 = \frac{1}{2}$. If further L iterations occur without convergence, we reset $\alpha_2 = \alpha_1/2$. More generally, the program was written in such a way that if the iteration fails to converge after ℓL iterations (ℓ integer), α is reset to

$$\alpha = \alpha_\ell = \alpha_{\ell-1}/2 \ .$$

In practice, the cases $\ell > 2$ were never encountered. The number of iterations required oscillated between 2 and 10, except at a very few points.

Once p_*, M_r, M_ℓ are known, we have

$$(24) \qquad v_* = (p_\ell - p_r + M_r U_r + M_\ell U_\ell)/(M_r + M_\ell)$$

from the definitions of M_r and M_ℓ.

Consider now the case $K_0 \neq 0$, ($\lambda = 0$); the right and left waves may now be CJ or strong detonations as well as shocks and rarefactions. The task at hand is to incorporate these possibilities into the solution of the Riemann problem.

The state S_r will remain a constant state; v_r and ρ_r are fixed. The energy in S_r must change at constant volume (and thus can do no work). The change δZ_r in Z_r can be found by integrating equations (13f), (13g), with $Z(0) = Z_r$ and $Z(k/2) = Z_r + \delta Z_r$, $\delta Z_r \leq 0$. The new pressure is

(25) $$p_r + \delta p_r = p_r + (\gamma-1)\delta Z\ q\rho_r$$

(see equation (7)). We write $p_r^{new} = p_r + \delta p_r$, and drop the superscript new. (We shall need the old Z_r again and thus refrain from renaming $Z_r + \delta Z_r$.) Similarly, Z_ℓ changes to $Z_\ell + \delta Z_\ell$, and a new p_ℓ is found using the obvious analogue of equation (25).

In S_* the values of Z differ from the values $Z_r + \delta Z_r$, $Z_\ell + \delta Z_\ell$. Let $Z_{*\ell}$ be the value of Z to the left of the slip line and let Z_{*r} be the value of Z to the right of the slip line. The difference in energy of formation across the right wave is $\Delta_r = (Z_{*r} - (Z_r + \delta Z_r))q$, and across the left wave it is $\Delta_\ell = (Z_{*\ell} - (Z_\ell + \delta Z_\ell))q$. We shall iterate on the values $Z_{*\ell}$, Z_{*r}, Δ_r, Δ_ℓ. In the first iteration, we set $Z_{*r} = Z_r + \delta Z_r$, $Z_{*\ell} = Z_\ell + \delta Z_\ell$, and thus $\Delta_r = \Delta_\ell = 0$, and carry out the iterations (23). When (23) has converged, a new pressure p^* is given, and new densities ρ_{*r}, $\rho_{*\ell}$ can be found from equations (16), (21) or the isentropic law. New temperatures $T_{*r} = p_*/\rho_{*r}$, $T_{*\ell} = p_*/\rho_{*\ell}$ are evaluated, equations (13f), (13g) are solved, and new values Z_{*r}, $Z_{*\ell}$, Δ_r, Δ_ℓ are found. If $\Delta_r \leq 0$ the right wave is either a shock or a rarefaction, and if $\Delta_r > 0$ the right wave is either a CJ detonation followed by a rarefaction or a strong detonation.

Let v_* be the velocity in S_*. Given Δ_r, Δ_ℓ, we can find the velocities v_{CJr}, $v_{CJ\ell}$ behind possible CJ detonations on the right and left (equation (12)). If $v_* \leq v_{CJr}$ the right wave is a CJ detonation followed by rarefaction, and if $v_* \geq v_{CJr}$ the right wave is a strong detonation. The CJ state is unaffected by S_* (since it depends only on S_r) and as far as the Riemann solution is concerned it is a fixed state. If the right wave is a CJ detonation, we redefine M_r.

$$M_r = \frac{p_{CJ}-p_*}{v_{CJ}-v_*} ,$$

(p_{CJ} from equation (11c)). Then

(26) $$M_r = \sqrt{\rho_{CJ}p_{CJ}}\ \phi_2(p_*/p_{CJ}) , \quad p_*/p_{CJ} \leq 1 ,$$

If the right wave is a strong detonation, we find from (9)

$$M_r = \sqrt{p_r\rho_r}\ \phi_3(\rho_r\Delta_r, p_r, p_*) ,$$

where

$$(\phi_3(\alpha_1,\alpha_2,\alpha_3))^2 = \frac{\frac{\gamma-1}{2} + \frac{\gamma+1}{2}\frac{\alpha_3}{\alpha_2}}{1 - \frac{(\gamma-1)\ \alpha_1}{\alpha_3-\alpha_2}} .$$

Similar expressions occur on the left. The iteration starts with M_r, M_ℓ from the previous iteration, and written out in full, appears as follows:

$$\tilde{p}^\nu = (\tilde{v}_\ell - \tilde{v}_r + \tilde{p}_r/M_r^\nu + \tilde{p}_\ell/M_\ell^\nu)/(1/M_r^\nu + 1/M_\ell^\nu) , \quad \nu \geq 0 ,$$

$$p_*^{\nu+1} = \max\ (\varepsilon, \tilde{p}^\nu) ,$$

$$v_*^\nu = (\tilde{p}_\ell - \tilde{p}_r + M_r^\nu\tilde{v}_r + M_\ell^\nu\tilde{v}_\ell)/(M_r^\nu + M_\nu^\nu) ,$$

where

$$(\tilde{\rho}_r, \tilde{p}_r, \tilde{v}_r) = \begin{cases} (\rho_{CJr}, p_{CJr}, v_{CJr}) & \text{if right wave = CJ detonation,} \\ (\rho_r, p_r, v_\ell) & \text{otherwise,} \end{cases}$$

$$(\tilde{\rho}_\ell, \tilde{p}_\ell, \tilde{v}_\ell) = \begin{cases} (\rho_{CJ\ell}, p_{CJ\ell}, v_{CJ\ell}) & \text{if left wave = CJ detonation,} \\ (\rho_\ell, p_\ell, v_\ell) & \text{otherwise,} \end{cases}$$

$$M_r^{\nu+1} = \begin{cases} \sqrt{p_r \rho_r}\ \phi_3(\rho_r \Delta_r, p_r, p_*^{\nu+1}) & \text{if right wave = strong detonation,} \\ \sqrt{\tilde{p}_r \tilde{\rho}_r}\ \phi(p_*^{\nu+1}/\tilde{p}_r) & \text{otherwise,} \end{cases}$$

$$M_\ell^{\nu+1} = \begin{cases} \sqrt{p_\ell \rho_\ell}\ \phi_3(\rho_\ell \Delta_\ell, p_\ell, p_*^{\nu+1}) & \text{if left wave = strong detonation,} \\ \sqrt{\tilde{p}_\ell \tilde{\rho}_\ell}\ \phi(p_*^{\nu+1}/\tilde{p}_\ell) & \text{otherwise.} \end{cases}$$

The complexity of this iteration is more apparent than real. It is stopped when it has converged, as before. New values of Z_{*r}, $Z_{*\ell}$ Δ_r, Δ_ℓ are evaluated, and the iteration is repeated; this process is stopped when Δ_r, Δ_ℓ change by less than some predetermined ε_3 over two successive iterations. It can be readily seen that with the present expression for the energy of formation, at most four iterations on Δ_r, Δ_ℓ are ever needed.

Once S_* has been determined, the solution must be sampled. Let $P = (\theta h, k/2)$ be the sample point, and $\tilde{\rho} = \rho(P)$, $\tilde{p} = p(P)$, etc. Four basic cases are to be considered:

A) P lies to the right of the slip line and the right wave is either a shock or a strong detonation;

B) P lies to the right of the slip line and the right wave is either a rarefaction or a CJ detonation followed by a rarefaction;

C) P lies to the left of the slip line and the left wave is either a shock or a strong detonation, and

D) P lies to the left of the slip line and the left wave is either a rarefaction or a CJ detonation followed by a rarefaction.

Case A. The velocity U_r of the shock or the strong detonation can be found from the relationship

$$M_r = -\rho_r(v_r - U_r) \ ;$$

if P lies to the right of $\frac{dx}{dt} = U_r$ we have the sampled values $\tilde{\rho} = \rho_r$, $\tilde{p} = p_r$, $\tilde{v} = v_r$, $\tilde{Z} = Z_r + \delta Z_r$. If P lies to the left of $\frac{dx}{dt} = U_r$, we have $\tilde{\rho} = \rho_{*r}$, $\tilde{p} = p_*$, $\tilde{v} = v_*$, $\tilde{Z} = Z_{*r}$.

Case B. Consider first the case of a rarefaction wave. The rarefaction is bounded on the right by the line $\frac{dx}{dt} = v_r + c_r$, $c_r = \sqrt{\gamma p_r/\rho_r}$, and on the left by $\frac{dx}{dt} = v_* + c_{*r}$, where c_* can be found by using the constancy of the Riemann invariant

$$\Gamma_r = 2c^*(\gamma-1)^{-1} - v_* = 2c_r(\gamma-1)^{-1} - v_r \ .$$

If P lies to the right of the rarefaction, $\tilde{\rho} = \rho_r$, $\tilde{p} = p_r$, $\tilde{v} = v_r$, $\tilde{Z} = Z_r + \delta Z_r$. If P lies to the left of the rarefaction, $\tilde{\rho} = \rho_{*r}$, $\tilde{p} = p_*$, $\tilde{v} = v_*$, $\tilde{Z} = Z_r + dZ_r$. If P lies inside the rarefaction, we equate the slope of the characteristic $\frac{dx}{dt} = v + c$ to the slope of the line through the origin and P, obtaining

$$\tilde{v} + \tilde{c} = 2\theta h/k \ ;$$

the constancy of Γ_r, the isentropic law $p\rho^{-\gamma}$ = constant and the definition $c = \sqrt{\gamma p/\rho}$ yield $\tilde{\rho}$, $\tilde{v}$, and $\tilde{p}$. $\tilde{Z} = Z_r + \delta Z_r$. If the wave is a CJ detonation, (ρ_r, p_r, v_r) are replaced everywhere by $(\rho_{CJr}, p_{CJ}, v_{CJ})$, and $\tilde{Z}$ inside the fan and to left of its equals Z_{*r}.

The cases C and D are mirror images of A and B, and will not be described in full.

Numerical Results

We begin by presenting some results for detonation waves with very large K_0 ($K_0 = 1000$). These results verify the accuracy of the programming rather than the general validity of the method, since the solutions of the corresponding problems are an intrinsic part of the Riemann problem solution routine.

To obtain Table I, I started with a gas at rest, $\rho = 1$, $v = 0$, $p = 1$, and at $t = 0$ imposed impulsively on the left boundary condition $v = V = 1$. I used $h = 1/7$, $k/h = .2$, $K_0 = 1000$, $T_0 = 1.1$, $q = 1$ and $\gamma = 1.4$. The result is a perfect strong detonation.

In Table II a Chapman-Jouguet detonation is exhibited. $h = 1/9$, $k/h = 2$, $K_0 = 1000$, $T_0 = 1.1$, $q = 12$ and $\gamma = 1.4$. $m = 11$. The solution is exhibited at $t = 2$, $n = t/k = 9$, i.e. n is not a multiple of m and the solution is not at its most accurate. This can be seen from the presence of a fake constant state (for $x = 6/9$ and $7/9$), which was discussed in the section about errors, and which is most likely to appear when n is not a multiple of m. The last column presents the right Riemann invariant Γ_r which is of course constant behind the CJ front. The chemical time scale is not resolved on the grid, and one should notice the small number of mesh points required to display sharp variations in all quantities.

Table I

Strong Detonation

$h = 1/7$, $k/h = .2$, $t = nk = .314$, $n = 11$, $K_0 = 1000$, $T_0 = 1.1$, $V = 1$, $q = 1$, $\gamma = 1.4$.

x	v	ρ	p	T	Z
0	1.	1.814	3.228	1.779	.000
1/7	1.	1.816	3.228	1.779	.000
2/7	1.	1.816	3.228	1.779	.000
3/7	1.	1.816	3.228	1.779	.000
4/7	0.	1.000	1.000	1.000	1.000
5/7	0.	1.000	1.000	1.000	1.000
6/7	0.	1.000	1.000	1.000	1.000
1	0.	1.000	1.000	1.000	1.000

Table II

Chapman-Jouguet Detonation

$h = 1/9$, $k/h = .2$, $t = nk = .2$, $n = 9$, $K_0 = 1000$, $T_0 = 1.1$, $V = 1$, $q = 12$, $\gamma = 1.4$.

x	v	ρ	p	T	Z	Γ_r
0	1.000	1.179	6.965	5.907	0.000	13.379
1/9	1.000	1.179	6.965	5.907	0.	13.379
2/9	1.000	1.179	6.965	5.907	0.	13.379
3/9	1.000	1.179	6.965	5.907	0.	13.379
4/9	1.186	1.257	7.621	6.061	0.	13.379
5/9	1.251	1.287	7.862	6.115	0.	13.379
6/9	1.524	1.410	8.952	6.346	0.	13.379
7/9	1.524	1.410	8.952	6.346	0.	13.379
8/9	1.623	1.457	9.373	6.430	0.	13.379
1	0.	1.000	1.000	1.000	1.000	5.916

We now present some results for a problem whose solution is not programmed into the solution algorithm — a deflagration wave with finite reaction rate. For $t < 0$ a gas at rest lies in $x \geq 0$, with $\rho = 1$, $p = 1$, $(v = 0)$, and $Z = 1$; the left boundary is maintained at zero velocity, $V = 0$. At $t = 0$ the gas in the first cell to the left is raised to a temperature $T = 2$, (i.e. the pressure is increased to $p = 2$). The resulting deflagration wave is observed. It is known that the velocity of the wave is asymptotically proportional to $\sqrt{\lambda K_0}$ (see e.g. [10], p. 99); thus, the wave does not propagate unless $\lambda \neq 0$, as one can readily verify on the computer. This last justifies an earlier assertion to the effect that when $\lambda = 0$ the wave is indistinguishable from a slip line. The results in Table III were obtained with $h = 1/11$, $k/h = .35$, $T_0 = 1.6$, $K_0 = 1$, $q = 10$, $\gamma = 1.4$ and $m = 11$. They are presented at $t = nk = .273$, $(n = q)$. One can clearly see the precursor shock, and the deflagration zone (characterized by $Z < 1$) in which the density and pressure decrease. The small number of mesh points should again be noticed.

Table III

A Deflagration With Finite Conduction and Reaction Rate

$h = 1/11$, $k/h = .35$, $t = nk = .273$, $n = 9$, $K_0 = 1$, $T_0 = 1.6$, $V = 0$, $q = 10$, $\gamma = 1.4$.

x	v	ρ	p	T	Z
0	0.	.567	1.667	2.937	.334
1/11	0.139	.650	1.781	2.739	.614
2/11	0.261	.547	1.315	2.402	.614
3/11	.385	1.074	1.726	1.607	1.000
4/11	.575	1.550	1.998	1.288	1.
5/11	.544	1.519	1.800	1.185	1.
6/11	.023	1.016	1.058	1.041	1.
7/11	.002	1.001	1.003	1.002	1.
8/11	.000	1.000	1.000	1.000	1.
9/11	0.	1.	1.	1.	1.
10/11	0.	1.	1.	1.	1.
1	0.	1.	1.	1.	1.

Conclusions

We have presented a numerical method capable of describing a complex gas flow with chemical reactions. The relative complexity of the method is balanced by economy in the representation of the solution. Generalization of the method to problems in more space dimensions is a straightforward application of the fractional step method presented in [2], and the inclusion of a more realistic chemical process presents no difficulties other than the standard difficulties of finding a plausible kinetic scheme and acceptable numerical values for the corresponding coefficients. The interesting and major difficulties in multidimensional problems arise when one attempts to take into account boundary layers and turbulence effects. In a forthcoming paper we shall show that boundary layer effects at least can be incorporated into our method in a natural and efficient way; once this has been explained, multidimensional results will be presented.

Bibliography

[1] A. A. Borisov, Acta Astronautica, 1, 909 (1974).

[2] A. J. Chorin, J. Comp. Phys., 22, 517 (1976).

[3] L. M. Cohen, J. M. Short and A. K. Oppenheim, Combustion and Flame, 24, 319 (1975).

[4] R. Courant and K. O. Friedrichs, Supersonic Flow and Shock Waves, Interscience (1948).

[5] J. Glimm, Comm. Pure Appl. Math., 18, 697 (1965).

[6] S. K. Godunov, Mat. Sbornik, 47, 271 (1959).

[7] P. D. Lax, SIAM Review, 11, 7 (1969).

[8] A. Majda and S. Osher, Comm. Pure Appl. Math., 30, 671 (1977).

[9] R. D. Richtmyer and K. W. Morton, Finite Difference Methods for Initial Value Problems, Interscience (1967).

[10] F. A. Williams, Combustion Theory, Addison-Wesley (1965).

A NUMERICAL STUDY OF CYLINDRICAL IMPLOSION

Gary A. Sod

Courant Institute of Mathematical Sciences
New York University
New York, New York 10012

Abstract

A numerical procedure is introduced to solve the one-dimensional equations of gas dynamics for a cylindrically or spherically symmetric flow. The method consists of a judicious combination of Glimm's method and operator splitting. The method is applied to the problem of a converging cylindrical shock.

Introduction

The one-dimensional equations for an inviscid, non-heat conducting, radially symmetric flow can be written in the form

$$\underline{U}_t + \underline{U}(\underline{U})_r = -\underline{W}(\underline{U}) \,, \tag{1}$$

where

$$\underline{U} = \begin{pmatrix} \rho \\ m \\ e \end{pmatrix}, \quad \underline{F}(\underline{U}) = \begin{pmatrix} m \\ m^2/\rho + p \\ m(e+p)/\rho \end{pmatrix}, \text{ and } \underline{W}(\underline{U}) = (\alpha-1) \begin{pmatrix} m/r \\ m^2/\rho r \\ m(e+p)/\rho r \end{pmatrix} \tag{2}$$

where ρ is the density, u is the velocity, $m = \rho u$ is the momentum, p is the pressure, e is the energy per unit volume, t is time, r is the space coordinate of symmetry, α is a constant which is 2 for cylindrical symmetry and 3 for spherical symmetry, and the subscripts refer to differentiation. We may write

$$e = \frac{p}{\gamma-1} + \frac{1}{2}\rho u^2 \tag{3}$$

where γ is the ratio of specific heats (a constant greater than 1).

There are two major problems involved in solving the system (1) directly. The first is the singular nature near the axis ($r = 0$), that is, there are singular terms proportional to $1/r$. The second problem is that the momentum equation (the second component equation of (1)) cannot be put in conservation form.

These problems cause major difficulties near the axis. These are usually overcome by some ad hoc method such as extrapolation (Payne 1956). Another approach has been to treat this as a problem in Cartesian coordinates in two space dimensions (Lapidus 1971).

In the method described below both of these problems have been completely eliminated. Thus there is not need to resort to any trickery in order to solve the system (1).

Outline of the Method

The first step in the problem is to use the method known as operator splitting to remove the inhomogeneous terms $-\underline{W}(\underline{U})$ from the system (1). Thus we solve the system

$$\underline{U}_t + \underline{F}(\underline{U})_r = 0 \tag{4}$$

which represents the one-dimensional equations of gas dynamics in Cartesian coordinates.

The method used to solve system (4) is the random choice method introduced by Glimm (1965) and developed for hydrodynamics by Chorin (1976). Details of this method will be given in the next section, for completeness.

Once system (4) is solved, the system of ordinary differential equations

$$\underline{U}_t = -\underline{W}(\underline{U}) \tag{5}$$

is solved, where the solution of system (4) is used to determine the inhomogeneous term -W in (5). There are several reasons for this approach, which will be discussed in later sections.

Glimm's Method

Consider the nonlinear system of equations (4). Divide time into intervals of length Δt and let Δr be the spatial increment. The solution is to evaluated at times $n\Delta t$ where n is a nonnegative integer at the spatial points $i\Delta r$, where $i = 0, \pm 1, \pm 2, \ldots$ and at time $(n+\frac{1}{2})\Delta t$ at $(i+\frac{1}{2})\Delta r$.

The method is a two step method. Let $\underset{\sim}{u}_i^n$ approximate $\underline{U}(i\Delta r, n\Delta t)$ and $\underset{\sim}{u}_{i+1/2}^{n+1/2}$ approximate $\underline{U}((i+\frac{1}{2})\Delta r, (n+\frac{1}{2})\Delta t)$ in (4). To find the solution $\underset{\sim}{u}_{i+1/2}^{n+1/2}$, consider the system (4) along with the piecewise constant initial data

$$\underline{U}(r, n\Delta t) = \begin{cases} \underline{u}_{i+1}^n, & r > (i+\frac{1}{2})\Delta r, \\ \underline{u}_i^n, & r < (i+\frac{1}{2})\Delta r. \end{cases} \tag{6}$$

This gives a sequence of Riemann problems. If $\Delta t < \frac{\Delta r}{2(|u|+c)}$ where c is the local sound speed, the waves generated by the different Riemann problems will not interact. Hence the solution $\underline{v}(r,t)$ to the Riemann problem can be combined into a single exact solution.

See Figure 1. Let ξ_n be an equidistributed random variable which is given by the Lebesgue measure on the interval $[-\frac{1}{2}, \frac{1}{2}]$. Define

$$\underset{\sim}{u}_{i+1/2}^{n+1/2} = \underline{v}((i+\xi_n)\Delta r, (n+\tfrac{1}{2})\Delta t) \quad . \tag{7}$$

See Figure 2.

At each time step, the solution is approximated by a piecewise constant function. The solution is then advanced in time exactly and the new values are sampled. The method depends on solving the Riemann problem exactly and inexpensively.

Chorin (1976) (see also Sod (1976) and (1978a)) modified an iterative method due to Godunov (1959) which will now be described.

Consider the system (4) with the initial data

$$\underline{U}(r,0) = \begin{cases} S_\ell = (\rho_\ell, u_\ell, p_\ell) \ , & r < 0 \ , \\ S_r = (\rho_r, u_r, p_r) \ , & r \geq 0 \ . \end{cases} \tag{8}$$

The solution at later times looks like Figure 3, where S_1 and S_2 are either a shock or centered rarefaction wave. The region S_* is a steady state. The lines ℓ_1 and ℓ_2 are separating the states. The contact surface $\frac{dr}{dt} = u_*$ separates the region into two parts with possibly different values of ρ_*, but equal values of u_* and p_*.

Using this iterative method we first evaluate p_* in the state S_*. Define the quantity

$$M_\ell = \frac{p_\ell - p_*}{u_\ell - u_*} \ . \tag{9}$$

If the left wave is a shock, using the jump condition $U_\ell[\rho] = [\rho u]$, we obtain

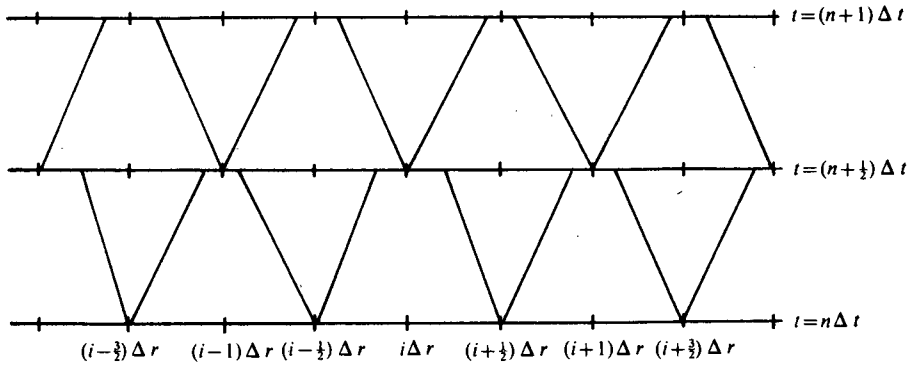

Figure 1. Sequence of Riemann problems on grid.

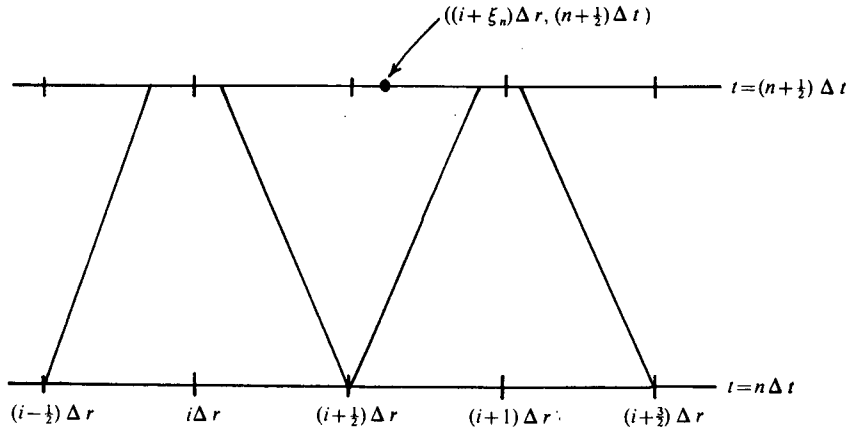

Figure 2. Sampling procedure for Glimm's scheme.

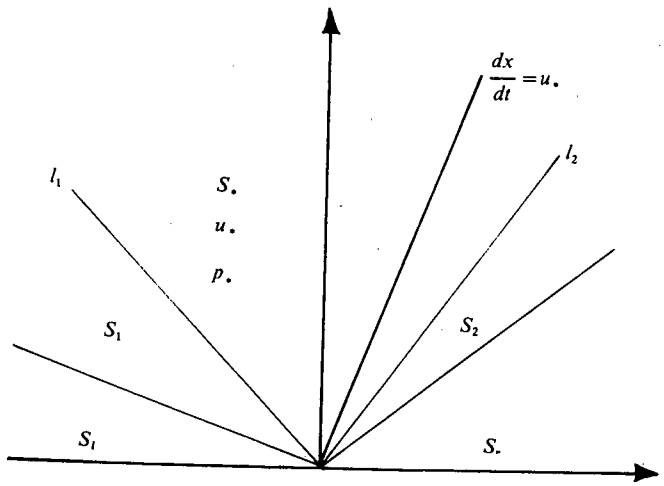

Figure 3. Solution of Riemann problem.

(10) $$M_\ell = \rho_\ell(u_\ell - U_\ell) = \rho_*(u_* - U_\ell) ,$$

where U_ℓ is the velocity of the left shock and ρ_* is the density in the portion of S_* adjoining the left shock. Similarly, define the quantity

(11) $$M_r = \frac{p_r - p_*}{u_r - u_*} .$$

If the right wave is a shock, using the jump condition $U_r[\rho] = [\rho u]$, we obtain

(12) $$M_r = -\rho_r(u_r - U_r) = -\rho_*(u_* - U_r) ,$$

where U_r is the velocity of the right shock and ρ_* is the density in the portion of S_* adjoining the right shock.

In either case ((9) or (10) for M_ℓ and (11) or (12) for M_r) we obtain

(13) $$M_\ell = \sqrt{\rho_\ell p_\ell}\ \phi(p_*/p_\ell) ,$$

(14) $$M_r = \sqrt{\rho_r p_r}\ \phi(p_*/p_\ell) ,$$

where

(15) $$\phi(x) = \begin{cases} \sqrt{\frac{\gamma+1}{2}\,x + \frac{\gamma-1}{2}} , & x \geq 1 , \\ \frac{\gamma-1}{2\sqrt{\gamma}}\,\frac{1-x}{1-x^{\gamma-1/2\gamma}} , & x \leq 1 . \end{cases}$$

Upon elimination of u_* from (9) and (11) we obtain

$$p_* = \frac{u_\ell - u_r + \frac{p_\ell}{M_\ell} + \frac{p_r}{M_r}}{\frac{1}{M_\ell} + \frac{1}{M_r}} . \tag{16}$$

Equations (13), (14), and (16) represent three equations in three unknowns for which there exists a real solution. Upon choosing a starting value p_*^0 (or M_ℓ^0 and M_r^0), we iterate using these three equations. We chose $p_*^0 = \frac{1}{2}(p_\ell + p_r)$ (for details see Chorin (1976) or Sod (1976)).

After p_*, M_ℓ, and M_r have been determined we may obtain u_* by eliminating p_* from equations (9) and (10),

$$u_* = \frac{p_\ell - p_r + M_\ell u_\ell + M_r u_r}{M_\ell + M_r} . \tag{17}$$

For a discussion of the method of choosing the random numbers most efficiently see Chorin (1976).

Solution of the Ordinary Differential Equations

Once the solution of (4) $\underline{\tilde{u}}_i^{n+1}$ is obtained, we have to solve a system of ordinary differential equations (5). We approximate (5) by

$$\frac{\underline{u}_i^{n+1} - \underline{u}_i^n}{\Delta t} = -\underline{W}(\underline{\tilde{u}}_i^{n+1}) ,$$

or

$$\underline{u}_i^{n+1} = \underline{u}_i^n - \Delta t \underline{W}(\underline{\tilde{u}}_i^{n+1}) . \tag{18}$$

This approximation (18) is the basic Cauchy-Euler scheme which is just first order accurate. However, the Glimm scheme is at most

first order accurate so there is no reason for using a high order method for solving the system of ordinary differential equations.

Since this system (5) is solved only at interior points and the scheme (18) does not require values at $r = 0$, the singularity at the axis is eliminated.

Boundary Conditions

Boundary conditions need only be applied to the system (4) since the system of ordinary differential equations (5) use only interior points. So that with the procedure described by Chorin (1976) the boundary condition at the axis ($r = 0$) is readily handled. The boundary condition is imposed on the grid point closest to $r = 0$, say $i_0\Delta r$. A fake left state is created at $(i_0 - \frac{1}{2})\Delta r$ by setting

$$\tilde{\rho}_{i_0-1/2} = \tilde{\rho}_{i_0+1/2} ,$$

$$\tilde{u}_{i_0-1/2} = -\tilde{u}_{i_0+1/2} ,$$

$$\tilde{p}_{i_0-1/2} = \tilde{p}_{i_0+1/2} .$$

In this way the shock or rarefaction wave will reflect which on the average is exact.

Application to a Converging Cylindrical Shock

Initially, a cylindrical diaphragm of radius r_0 separates two uniform regions of gas at rest as in a shock tube with the outer

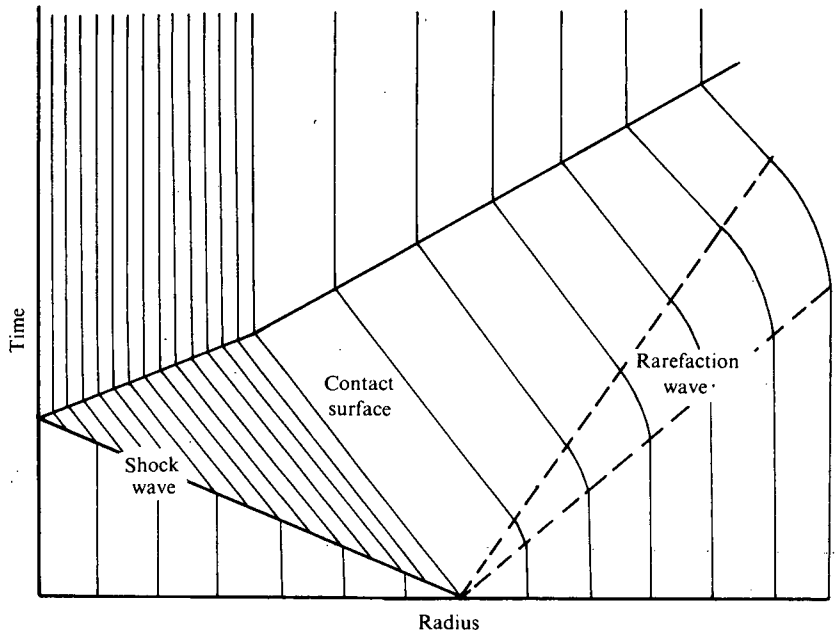

Figure 4. Flow pattern for converging cylindrical shock.

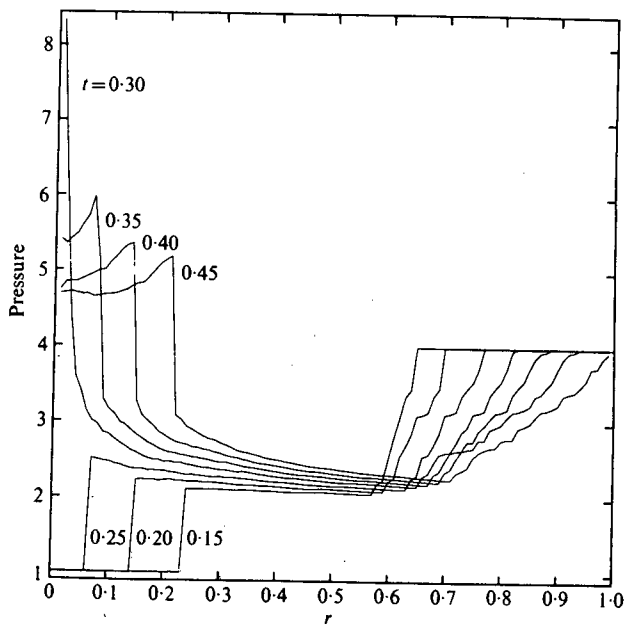

Figure 5. Pressure profiles at time intervals of 0.05.

pressure and density being larger than the inner ones. After the diaphragm is ruptured ($t > 0$), a shock wave is created and travels into the low pressure region followed by a contact discontinuity. A rarefaction wave travels into the high pressure region. See Figure 4.

It is known that a cylindrical shock wave in a compressible fluid increases in strength as it converges toward the axis. This can be seen experimentally in Perry and Kantrowitz (1951).

In the example given below the pressure and the density in the inner region were set equal to 1.0 and the pressure and density in the outer region were set equal to 4.0. This will produce a shock with initial strength of 1.93, a contact discontinuity and a rarefaction wave. We took $\Delta r = 0.01$. The time step Δt is chosen so that the Courant-Friedrichs-Lewy condition is satisfied, i.e.

$$\max\ (|u| + c)\frac{\Delta t}{\Delta r} \leq 1\ ,$$

where c is the local sound speed.

In Figure 5 the pressure distribution is displayed at time intervals of 0.05. The shock appears as a rapid variation in p which is completely sharp, i.e. the number of zones over which this variation takes place is zero. As time increases the shock propagates toward the axis. It is observed that the strength of the shock increases with time. After the passage of the shock, the pressure behind the shock increases. When the shock arrives at the axis it is reflected and rises to a large but finite value and a diverging shock appears. It is also observed that the pressure at a given point behind the reflected shock decreases with time.

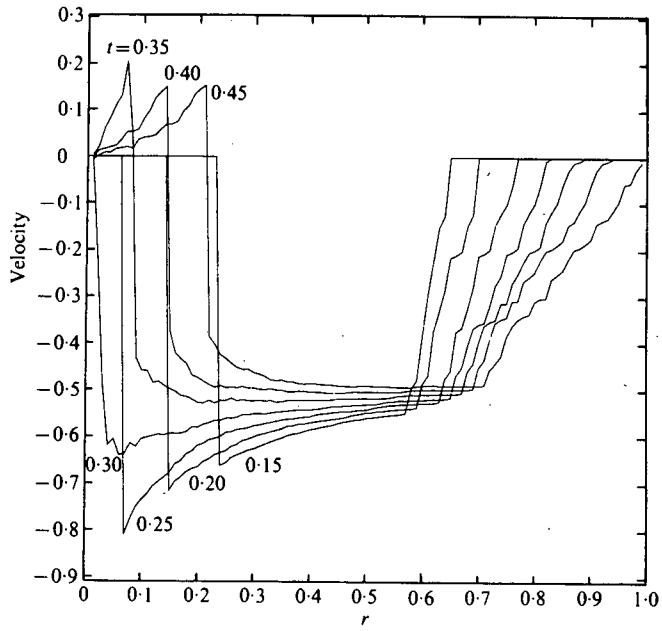

Figure 6. Velocity profiles at time intervals of 0.05.

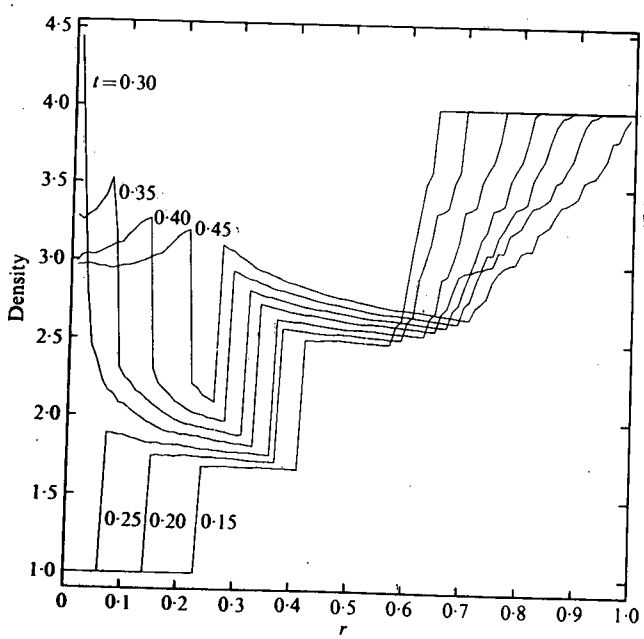

Figure 7. Density profiles at time intervals of 0.05.

In Figure 6 the velocity of the gas is displayed. The behavior is similar to that of the pressure except that the converging shock decreases the velocity from zero to a negative value. When the shock is reflected from the axis, the diverging shock has the effect of producing a small positive (outward) velocity. As in the case of the pressure profile, at a given point behind the converging shock the velocity increases with time and behind a diverging shock the velocity decreases with time.

The density and energy profiles are displayed in Figures 7 and 8 respectively. The basic properties of the shock are similar to those of the pressure distribution, except that the rise in density across the shock is smaller due to a temperature increase. In the density and energy profiles a contact discontinuity appears. It is a result of using Glimm's scheme that the contact discontinuity (as well as the shock wave) is completely sharp. The contact discontinuity propagates toward the axis behind the converging shock and is traversed by the reflected (outgoing) shock.

In Figure 9 the density profile where the contact discontinuity and the reflected shock wave have crossed. For a polytropic gas with the same values of γ, higher sound speeds correspond to higher densities (Courant and Friedrichs, 1948). The interaction of a diverging shock wave and a contact discontinuity propagating toward the axis results in a reflected (converging) shock (represented by Ⓐ), a contact discontinuity propagating toward the axis (represented by Ⓑ), and a transmitted (diverging) shock (represented by Ⓒ).

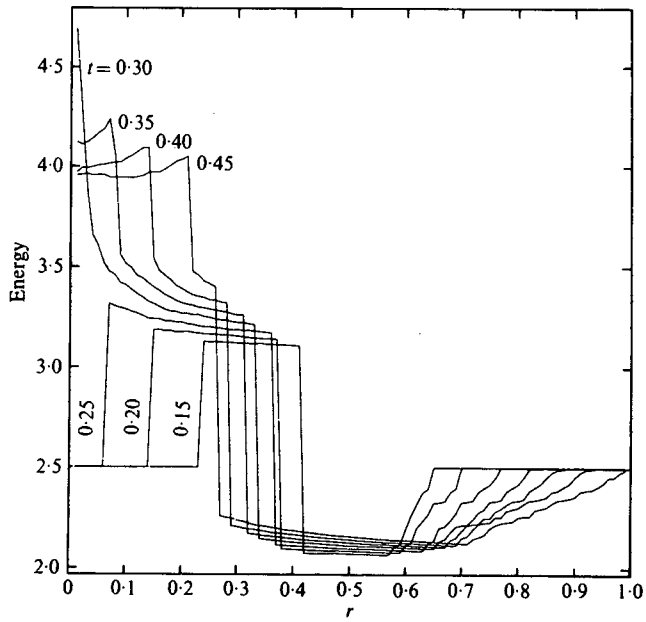

Figure 8. Energy profiles at time intervals of 0.05.

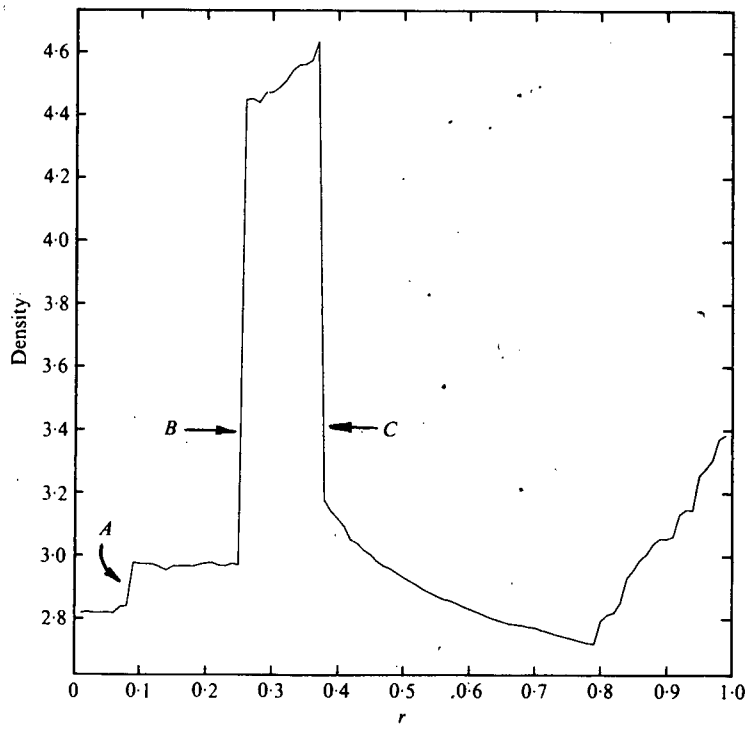

Figure 9. Density profile after interaction of diverging shock and contact discontinuity at time t = 0.6.

In general the overall trend of the results agree with those of Abarbanel and Goldberg (1972), Lapidus (1971), and Payne (1956). There is, however, one major difference, the time at which the shock reaches the axis. Our method is in agreement with the method of Abarbanel and Goldberg. However, with the methods of Lapidus and Payne, the shock reaches the axis sooner.

It should be noted that as a result of the randomness of Glimm's method, at a given time, the position of the shock or contact discontinuity may not be exact. Yet on the average their positions are exact.

With the three other methods used in this comparison, the shock and contact discontinuity are smeared. The smearing of the shock is less dramatic. The contact discontinuity obtained by Payne's method is almost immediately smeared to such a degree that it is barely visible. However, our technique produces perfectly sharp shocks and contact discontinuities.

As discussed above, the interaction of the reflected shock and the contact discontinuity will produce a contact discontinuity, a transmittal shock and reflected shock. The reflected shock is produced by our technique (see Figure 9). However, the reflected shock is not produced by the methods of Abarnael and Goldberg, Lapidus and Payne.

Conclusions

This method reduces the problem of solving the one-dimensional equations of gas dynamics for a cylindrically or spherically

symmetric flow to solving the one-dimensional equations of gas dynamics in Cartesian coordinates and a single system of ordinary differential equations, by using operator splitting.

The equations of gas dynamics are solved using Glimm's method which keeps the shock waves and contact discontinuities perfectly sharp. The ordinary differential equations are solved using the Cauchy-Euler scheme at the interior points only and for one time step. Thus, the singular nature of the original system near the axis is eliminated. Since the equations of gas dynamics are solved in Cartesian coordinates the momentum equation can be written in conservation form.

It should be noted that the roughness in the rarefaction wave is a result of the randomness of the Glimm scheme.

In all our calculations there were 100 spatial grid points, and it takes about 10.3 seconds on a CDC 7600 to complete 300 time steps.

This method can be generalized to treat a two-dimensional axially symmetric flow. This is being developed to study the flow in a motored engine chamber in two dimensions with a single intake/exhaust valve along the axis. It is planned that boundary layer effects be included also. See Sod (1978b).

Further it is planned that this method be coupled with chemistry as in a modified version of Chorin (1977) or Sod (1978c). It is hoped that this will represent a reliable model of a cylinder of an axially symmetric internal combustion engine. This method will not be directly applicable to three-dimensional engine

flow. However, this can yield important information concerning the relative effects on the flow field of valve size, swirl rates, piston and head geometry, and engine speeds.

This work was supported in part by the National Science Foundation, Grant MCS76-07039 and the U.S. Energy Research and Development Administration under Contract W-7405-Eng-48.

References

Abarbanel, S., and Goldberg, M., 1972, "Numerical Solution of Quasi-Conservative Hyperbolic Systems — the Cylindrical Shock Problem", J. Comp. Phys. 10, 1.

Chorin, A. J., 1976, "Random Choice Solution of Hyperbolic Systems", J. Comp. Phys. 22, 517.

_____, 1977, "Random Choice Methods with Applications to Reacting Gas Flow", J. Comp. Phys. 25, 253.

Courant, R., and Friedrichs, K. O., 1948, Supersonic Flow and Shock Waves, Interscience, New York.

Glimm, J., 1965, "Solutions in the Large for Nonlinear Hyperbolic Systems of Equations", Comm. Pure Appl. Math. 18, 697.

Godunov, S. K., 1959, "Finite Difference Methods for Numerical Computation of Discontinuous Solutions of the Equations of Fluid Dynamics", Mat. Sbornik, 47, 271.

Lapidus, A., 1971, "Computation of Radially Symmetric Shocked Flows", J. Comp. Phys. 8, 106.

Payne, R. B., 1956, "A Numerical Method for Converging Cylindrical Shock", J. Fluid Mech. 2, 185.

Perry, R. W., and Kantrowitz, A., 1951, "The Production and Stability of Converging Shock Waves", J. Appl. Phys. 22, 878.

Sod, G. A., 1976, "The Computer Implementation of Glimm's Method", Lawrence Livermore Laboratory Report UCID-17252.

_____, 1978a, "A Survey of Several Finite Difference Methods for Systems of Nonlinear Hyperbolic Conservation Laws", J. Comp. Phys., 27, 1.

_____, 1978b, "A Numerical Method for Axisymmetric Flows with Application to Internal Combustion Engines", J. Comp. Phys., to appear.

_____, 1978c, "A Numerical Model of Unsteady Combustion Phenomena, to appear.

COMBUSTION INSTABILITY

Samuel Burstein

Courant Institute of Mathematical Sciences
New York University
New York, New York 10012

1. THERMALLY INDUCED VIBRATIONS

It has been known for well over one hundred years that there is, under suitable conditions, a strong interaction between sound waves and flames. Rayleigh describes a simple experiment by which a high frequency sound, when applied to the point of efflux of a pressurized gas jetting into a quiescent environment, causes the combustion process to increase in intensity. The flame roars and the total distance required for complete burning to take place is substantially reduced so that the efflux region, also called a "preheat" zone, is where diffusion of heat and molecules of the intermediate products of reaction take place and dominate all other processes.

From this simple observation (and also from jet engine design) it is strongly suspected that a similar, although more complex, process occurs in the internal combustion mechanism of a liquid propellant rocket motor. In such a motor liquid jets of fuel and oxidizer are discharged from an injector head at the base of a combustion chamber. The location of the region of intense combustion depends not only on the design parameters of the injection system, including fuel and oxidizer properties, but upon the complex liquid and gas phase mixing processes occurring in the

region near the injector head. The natural presence of combustion noise in the combustion chamber leads to pressure waves traveling from the combustion zone towards the injection region. This is the sensitive "preheat" zone of the entire combustion process so that pressure fluctuations in this flow zone can lead to disruptions in the physicochemical processes. Thus, a mechanism is available for the presence of a driving force which can cause an oscillatory combustion instability similar to an organ pipe type of resonance. Such observed high frequency oscillations in the combustion chamber, called "screaming," are characterized by finite amplitude pressure waves which cause large fluid motions which, in turn, lead to extreme heat transfer rates to the walls of the combustion chamber. The result is usually a catastrophic burnout of the motor.

In this paper, we will consider nonlinear vibrations in a combustion chamber which can support resonance and which simulates some of the basic flow characteristics present in a liquid propellant rocket motor. To achieve a reasonable representation of combustion, the equations of compressible fluid dynamics, written as a quasilinear system of equations, i.e.,

$$\sum_i A_i \frac{\partial w}{\partial x_i} + b = 0 , \tag{1}$$

is modified by replacing the right hand side by a vector source term S which is assumed to be given. In this model S is a function of the gas variables w and droplet variables w^*. Thus, S is prescribed by computing the interaction of the gas field with the

droplet field, the former of which is generated from the burning of the fuel droplet field. The droplets are produced by breakup of the sprays of liquid fuel and oxidizer jets; the droplet burning mechanism is assumed to be described by an evaporation rate controlling process which is slower than the chemical kinetic process by a significant time scale.

In addition to liquid propellant rocket motors, the method described in this paper can be used as a basis for the analysis of direct fuel injected engines, i.e., diesel or stratified charge engines.

2. FORMULATION OF THERMAL FORCING FUNCTION

Let the properties of the droplet be denoted by w^*

$$w^* = \begin{pmatrix} m^* \\ u^* \\ v^* \\ e^* \end{pmatrix} \tag{2}$$

The droplet velocity in the x_2, x_3 direction is u^* and v^* and the liquid mass, m^*. The fuel droplet is then completely specified if e^*, the internal energy is known; $e^* = c_v^* T^*$, c_v^* is the specific heat at constant volume of the droplet. The conservation laws for the fuel droplet can be written in the convenient form

$$\frac{dw^*}{dt} + S(w^*, w) = 0 \tag{3}$$

subject to the initial condition

$$w^*(0, \theta, t) = w_o^* \,. \tag{3'}$$

Here we use a Lagrangian representation so that for an annular coordinate system $(x_1, x_2, x_3) = (t, \theta, z)$, and the particle derivative is

$$\frac{d}{dt} = \frac{\partial}{\partial t} + \frac{u^*}{r^*} \frac{\partial}{\partial \theta} + v^* \frac{\partial}{\partial z} .$$

The value of r^* is the radius of the annular domain; it is taken as a constant and for convenience $r^* = 1$. The inhomogeneous term $S(w^*, w)$, having dependence on droplet and product gas properties, is given by

$$S = \frac{1}{\rho^*} \begin{pmatrix} -\frac{3}{4\pi} \dot{m}^* \\ f^\theta \\ f^z \end{pmatrix} \tag{4}$$

The rate of evaporation of the droplet is $\dot{m}^*$ while the aerodynamic drag forces acting on the droplet in the θ and z directions are f^θ and f^z respectively.

The internal droplet temperature, T^*, is computed from the integrated Clausius-Clapeyron equation

$$T^{*-1} = \hat{T}^{*-1} + \alpha \, \mathrm{Ln} \frac{p}{\hat{p}^*} . \tag{5}$$

Here $\hat{p}^*$ and $\hat{T}^*$ correspond to the pressure and temperature of the droplet at the critical point while the gas pressure $p = \rho(\gamma-1)e$ is taken to be a function of the combustion gas density ρ and internal energy e; the constant α is the negative reciprocal of the vapor pressure equilibrium curve when the natural logarithm of the vapor pressure is plotted against the reciprocal of the vapor temperature.

The drag forces are assumed to be described by Stokes drag laws so that f^θ and f^z are proportional to the square of the relative velocity difference between the combustion gas and liquid droplet,

$$\begin{pmatrix} f^\theta \\ f^z \end{pmatrix} = \frac{3}{8} C_D \frac{\rho}{a\rho^*} \begin{pmatrix} (u-u^*)\,|u-u^*| \\ (v-v^*)\,|v-v^*| \end{pmatrix}. \tag{6}$$

The proportionality factor is the coefficient of drag C_D and $a = a(t)$ is the droplet radius which can be given in terms of the droplet mass $m^* = (4/3)\pi a^3 \rho^*$. The drag coefficient depends on the droplet Reynolds number Re^* through

$$C_D = 27/(Re^*)^{.84}. \tag{7}$$

In order to compute the time rate of change of m^*, $\dot{m}^*$ is specified through an evaporation law given by

$$\dot{m}^* = \frac{4\pi k a}{C_p} \left(\frac{p}{p^0}\right)^\tau \left(1 + \ell \sqrt{Re^*}\, \sqrt[3]{Pr}\right) \tag{8}$$

with the combustion gas Prandtl number defined by $Pr = C_p\mu/k$. The diffusion of the fuel vapor from the spherical droplet is reflected by the specific heat at constant pressure, C_p, of vapor and thermal conductivity, k, of fuel vapor. The local Reynolds number is defined in terms of the difference of the magnitudes q of the local gas and droplet velocities, i.e. $Re^* = 2\rho a|q-q^*|/\mu$. The constant ℓ, obtained empirically, is 0.276 and p^0 is the initial uniform pressure of undisturbed flow.

If the local fuel oxidizer ratio is F, the number density of the droplet spray is N, the heat of reaction of the combustion process is ΔH_R, and the latent heats of the fuel and oxidizer is L_F and L_O then the source term S for the conservation laws describing the motion of the combustion gas is

$$S = \dot{M}^* \begin{pmatrix} 1 + F^{-1} \\ 0 \\ 0 \\ \Delta H_R - (L_F + F^{-1} L_O) \end{pmatrix} \tag{9}$$

where drag forces on the gas have been neglected. It is clear that $S = S(\theta, z, t)$ through the arbitrary trajectories of the moving droplets in the combustion gas.

In general the number density of droplets, N, in a spray is not a constant but is described by a distribution function that has initial value

$$N_O = N(t, \theta, 0, a, \underline{u}^*) = Ka^2 \exp - \left\{ \omega a + \left(\frac{u^* - u_O^*}{K_u} \right)^2 + \left(\frac{v^* - v_O^*}{K_v} \right)^2 \right\},$$

defined at the injector face $z = 0$. The constants K, ω, K_u and K_v in the above relation depend upon the injector characteristics. The distribution function is subject to the evolutionary equation

$$\frac{\partial N}{\partial t} + \frac{\partial N\dot{a}}{\partial a} + \nabla_{\underline{x}} \cdot (N\underline{u}^*) + \nabla_{\underline{u}^*} \cdot (N\underline{f}) = 0 .$$

The vectors $\underline{u}^*$ and $\underline{f}$ are the velocity and acceleration (Eq. 6) of the drops while $\dot{a} = da/dt$ is the rate of change of the droplet radius.

Here we have set the source term to zero under the simplifying assumptions that the droplets will not collide with each other (dilute spray) nor with the chamber wall. It is also assumed that the drops will not be created by breaking through aerodynamic shear forces nor be created by nucleation processes.

Then $\dot{M}^*$ is given by

$$\dot{M}^* = 4\pi\rho^* \int_{\underline{u}^*} \int_a a^2 \dot{N} da d\underline{u}^* \ .$$

3. DIFFERENTIAL EQUATIONS FOR COMBUSTION GASES

Before we can write down the final form of our conservation law we must describe how to produce a supersonic outflow condition which simulates the state of affairs in a converging-diverging nozzle attached to the tail end of the combustion chamber. Although this is not the usual procedure, it turns out to be convenient. We assume that there is a converging-diverging duct placed immediately after the uniform annular chamber. In this duct we assume that the rate of change of fluid properties normal to the streamline direction is small compared to the rate of change of fluid properties along streamlines. If, in the duct, we allow for a variable cross-sectional area A which depends only on the axial distance z, then we would expect small errors in computing stream properties if d Ln A/dz is small compared with unity.

We prescribe the schedule of area variation in the axial direction through

$$\frac{A}{A_0} = 1 + \alpha_1 (z - z_0) + \alpha_2 (z - z_0)^2 \ ,$$

where z_0 is the terminal axial position of the combustion chamber with radius $r^* = 1$ and area A_0. The constants α_1 and α_2 are chosen so that

$$\frac{dA}{dz} \leq 0 , \quad z_0 < z \leq z_t ; \quad \frac{dA}{dz} > 0 , \quad z_t < z \leq z_L .$$

The total length of the simulated nozzle is z_L and z_t is the position of minimum area, the throat, of the nozzle. The only condition imposed on the choice of $A(z)$ is the requirement that the prescribed steady state flow, (design flow) be shock-free.

This is achieved by allowing the local Mach number, M, at $z = z_t$ to be unity for the asymptotically steady problem. The other condition fixing the two coefficients specifying the area variation is determined by providing for a large enough area ratio between the throat and the point $z = z_L$ so that

$$M(z_L, \theta, t) > 1 . \tag{10}$$

This is the boundary condition required so that characteristic surfaces are pointing into the boundary from the interior of the flow. Hence, in the z direction the three characteristics v+c, v-c are all positive.

The differential system, Eq. (1), can now be written in divergence form

$$w_t + G_\theta + H_z + B = 0 , \tag{11}$$

with the vector B given by

$$B = \frac{d \text{ Ln } A}{dz} \begin{pmatrix} \rho v \\ \rho v^2 \\ \rho vu \\ Ev \end{pmatrix} - S(w, w^*) , \tag{12}$$

The vector of unknowns w, axial flux H, and the tangential flux G, is given by

$$w = \begin{pmatrix} \rho \\ \rho u \\ \rho v \\ E \end{pmatrix} , \quad H = \begin{pmatrix} \rho v \\ \rho u^2 + p \\ \rho vu \\ (E+p)v \end{pmatrix} , \quad G = \begin{pmatrix} \rho u \\ \rho vu \\ \rho v^2 + p \\ (E+p)u \end{pmatrix} .$$

In Eq. (12) we emphasize the dependence of the energy and mass sources S on the interaction of the combustion gas with properties w and droplet field with properties w^*.

Equation (10) is equivalent to our prescription of extrapolating from the interior to the boundary $z = z_L$ the conservation variables w via the forward difference approximation

$$D_+ w = 0 . \tag{13}$$

The necessity for introducing a nozzle into the calculation, even though only a study of processes in the neighborhood of the injector face of the combustion chamber is desired, stems from the inability to describe the correct nonlinear time dependent downstream pressure level in the combustion chamber. Physically this pressure is determined by flow being choked in the neighborhood of the minimum area, where the Mach number is unity; the flow then accelerates to a supersonic state downstream of the throat. At the

throat, or point of minimum area, the flow is sonic at steady state. However, when time dependent perturbations exist in the combustor, the sonic point can oscillate in some neighborhood of $z = z_t$.

At the injector boundary, $z = 0$, the reflection rules

$$\rho_- = \rho_+ , \quad p_- = p_+ , \quad u_- = u_+ , \quad v = -v_+ , \tag{14}$$

are used across the injector; here we denote $\rho_\mp = (0, \mp \Delta z, t)$, etc.

4. COMPUTATIONAL PROCEDURE

We apply the following procedure for computing a solution to the coupled set of partial differential equations, Eq. (11), and ordinary differential equations, Eq. (3):

A steady state is achieved by first assuming a smooth distribution for $w(\theta,z,0)$ and $w^*(\theta,z,0)$. Then generate $w(t+\Delta t)$ by solving Eq. (11) using a two step difference scheme given w^*. The first step is analogous to a predictor equation since the solution is first order accurate while the second step is analogous to a corrector equation and is second order accurate. The approximation to $w(\theta,z,t)$ is represented by $V(\theta_i, z_j, t_n) = V^n_{i,j}$. The two steps are given by

Step 1

$$\begin{aligned} \tilde{V}^{n+1}_{i+\frac{1}{2}, j+\frac{1}{2}} &= \frac{1}{4}(V^n_{i+1,j} + V^n_{i,j+1} + V^n_{i+1,j+1} + V^n_{i,j}) - \frac{\Delta t}{2\Delta\theta}\,(G^n_{i+1,j} - G^n_{i,j} \\ &\quad + G^n_{i+1,j+1} - G^n_{i,j+1}) - \frac{\Delta t}{2\Delta z}\,(H^n_{i+1,j+1} - H^n_{i+1,j} + H^n_{i,j+1} - H^n_{i,j}) \\ &\quad - \frac{\Delta t}{4}\,(B^n_{i+1,j} + B^n_{i,j+1} + B^n_{i+1,j+1} + B^n_{i,j}) \,. \end{aligned} \tag{15}$$

Step 2

$$V^{n+1}_{i,j} = V^{n}_{i,j} - \frac{\Delta t}{4\Delta\theta}\left(G^{n}_{i+1,j} - G^{n}_{i-1,j} + \tilde{G}^{n+1}_{i+\frac{1}{2},j+\frac{1}{2}} - \tilde{G}^{n+1}_{i-\frac{1}{2},j+\frac{1}{2}}\right.$$

$$\left. + \tilde{G}^{n+1}_{i+\frac{1}{2},j-\frac{1}{2}} - \tilde{G}^{n+1}_{i-\frac{1}{2},j-\frac{1}{2}}\right) - \frac{\Delta t}{4\Delta z}\left(H^{n}_{i,j+1} - H^{n}_{i,j-1}\right.$$

$$\left. + \tilde{H}^{n+1}_{i+\frac{1}{2},j+\frac{1}{2}} - \tilde{H}^{n+1}_{i+\frac{1}{2},j-\frac{1}{2}} + \tilde{H}^{n+1}_{i-\frac{1}{2},j+\frac{1}{2}} - \tilde{H}^{n+1}_{i-\frac{1}{2},j-\frac{1}{2}}\right)$$

$$- \frac{\Delta t}{2}\left[\frac{1}{4}\left(\tilde{B}^{n+1}_{i+\frac{1}{2},j+\frac{1}{2}} + \tilde{B}^{n+1}_{i+\frac{1}{2},j-\frac{1}{2}} + \tilde{B}^{n+1}_{i-\frac{1}{2},j+\frac{1}{2}}\right.\right.$$

$$\left.\left. + \tilde{B}^{n+1}_{i-\frac{1}{2},j-\frac{1}{2}}\right) + \frac{1}{2}\left(B^{n}_{i+1,j} + B^{n}_{i-1,j}\right)\right] , \qquad (15')$$

where

$$H(V^{n}_{i,j}) = H^{n}_{i,j} , \quad H(\tilde{V}^{n+1}_{i+\frac{1}{2},j+\frac{1}{2}}) = \tilde{H}^{n+1}_{i+\frac{1}{2},j+\frac{1}{2}} , \text{ etc.}$$

Obtain the first iterate to w^*, i.e., $w^*(\theta, z, t+\Delta t)$, by solving Eq. (3) using the analogue of system (15) and (15'), the modified Euler method. The second iterate to w is now computed using (15) and (15'). This process is continued until convergence of w and w^* is achieved. The asymptotic limit of $n\Delta t$, thinking of time as an iteration counter, defines the self-consistent steady state:

$$\lim_{n\Delta t\to\infty}\begin{pmatrix} w(n\Delta t) \\ w^*(n\Delta t) \end{pmatrix} = \begin{pmatrix} w_0 \\ w^*_0 \end{pmatrix} .$$

To compute the evaporation and combustion process, at any point (θ, z, t) in the combustion chamber, one needs to keep track of the previous history of the droplet. Since a Lagrangian

representation of the droplet field has been adopted, each drop is tracked from its point of injection into the combustor $(\theta_0, 0, t_0)$ to the point (θ^*, z^*, t^*); the elapsed time of flight of the droplet is t^*-t_0, t_0 the time of droplet injection.

We have assumed a dilute spray approximation which means that droplets do not interact. Also, as a result of this approximation $w^*(\theta^*, z^*, n\Delta t^*)$ can be evaluated at Eulerian mesh points $(\theta_i, z_j, n\Delta t)$, of the system (15) and (15'), by interpolation from the Lagrangian mesh upon which $w^*(\theta^*, z^*, n\Delta t^*)$ is defined. The tracking process ceases if

$$a(t^*-t_0) < .1\ a(t_0)$$

since the mass associated with the drop would be less than one-thousandth the original droplet mass; for these calculations the initial mean droplet radius was $a(t_0) = 50$ microns.

With the steady state established, the flow field is perturbed to observe the modes of resonance established and maintained in the annular combustion chamber. Let p_0 be the steady state pressure; then the perturbed pressure p' is

$$p' = p_0 + p_1 = p_0(1 + A \sin \Theta \sin Z) \tag{16}$$

where we scale θ and z by the functions

$$\Theta(\theta) = \beta_1\theta + \beta_2\ , \quad \theta_1 \leq \theta \leq \theta_2$$

$$Z(z) = \beta_3 z + \beta_4\ , \quad z_1 \leq z \leq z_2$$

so that the perturbation can be placed at an arbitrary position in

the annular chamber. However, just as Rayleigh described the importance of the placement of the sound source near the efflux point of the gas jet, so do we observe that the perturbation must be placed in some neighborhood of the point of injection of the drops, $z = 0$, to have an appreciable effect on the flow field. The amplitude of the perturbation, A, is taken to be proportional to the total energy of the combustion gas in the annular chamber, usually a few percent of the steady state chamber energy. For these calculations, a value of A is chosen so that the total perturbed energy in the rectangle $\Delta\theta$, Δz centered about $((\theta_1+\theta_2)/2, (z_1+z_2)/2)$ is equal to four percent of the energy of the combustion gas.

We found that the transients obtained by this disturbance were so severe that strong shock waves were generated. The difference scheme Eqs. (15) and (15') did not remain stable in the presence of these steep gradients so that a smoothing operator was required. A two step operator was used. Let D_- denote the backward difference operator

$$D_- w_{m+1} = w_{m+1} - w_m$$

then

$$\hat{w}_m = w_m + k\left(\frac{\Delta t}{\Delta m}\right) D_-\left(|D_- u_{m+1}| D_- w_{m+1}\right) \tag{17}$$

where u is the velocity in the m-th direction, m is the step size in that direction and k is a constant. Equation (17) is first applied to the solution w in m-coordinate direction to obtain a temporary value $\hat{w}$; replacing w with $\hat{w}$, Eq. (17) is then applied once more to yield the final solution. It was also found that Eq.

(17) need not be applied each time cycle; as few as one application every five time steps was sufficient once the initial strong transient dissipated after about 100 time steps.

5. RESULTS

We show below, in Figure 1(a), a typical nonlinear periodic pressure trace of the pressure history near the injector face $z \sim 0.15\ z_0$. For a value of $\tau = 0.9$ in Eq. (8), Figure 1(b) shows the local energy release rate as a function of angular position θ and axial distance z downstream from the injector. The nonuniform energy release distribution is a result of the local variation of w so that the greatest value of energy release coincides with the peak pressure of the spinning wave being traced in Figure 1(a).

An additional computation was carried out using a modified model of the combustion chamber; a set of acoustic baffles are placed at various angular positions in the annular chamber. The baffles have arbitrary length z_b such that $0 < z_b \leq z_0$. The baffles are placed in the chamber to act as diffractors of the spinning waves in the region of maximum energy release — in the neighborhood of the injector face. Figure 2 shows a typical nonlinear acoustic pressure trace when two baffles, at essentially equal angular spacing, are placed in the chamber; here $z_0 \sim .25\ z_0$. The energy release rate, after the initial transient, is uniform; at each value of θ the energy release looks similar to $\theta = 0$ at Figure 1(b).

REFERENCES

1. Burstein, S., Nonlinear Time Dependent Problems in Fluid Dynamics, AGARD Lecture Series No. 64 on Advance in Numerical Fluid Dynamics.

2. Williams, F.A., Combustion Theory, Addison-Wesley, 1965.

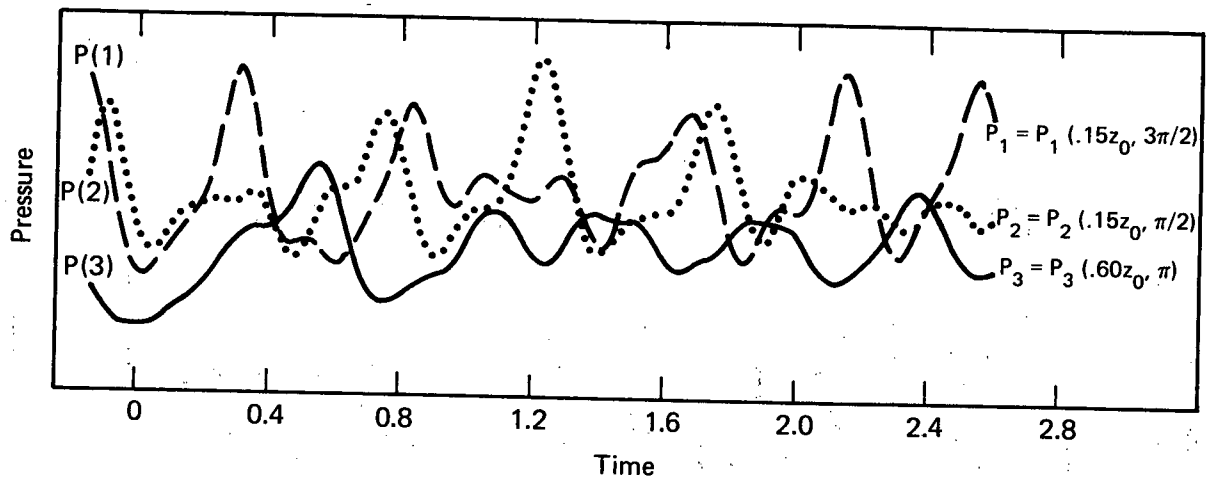

Figure 1(a). Pressure history at three positions in an annular resonant cavity for a spinning wave.

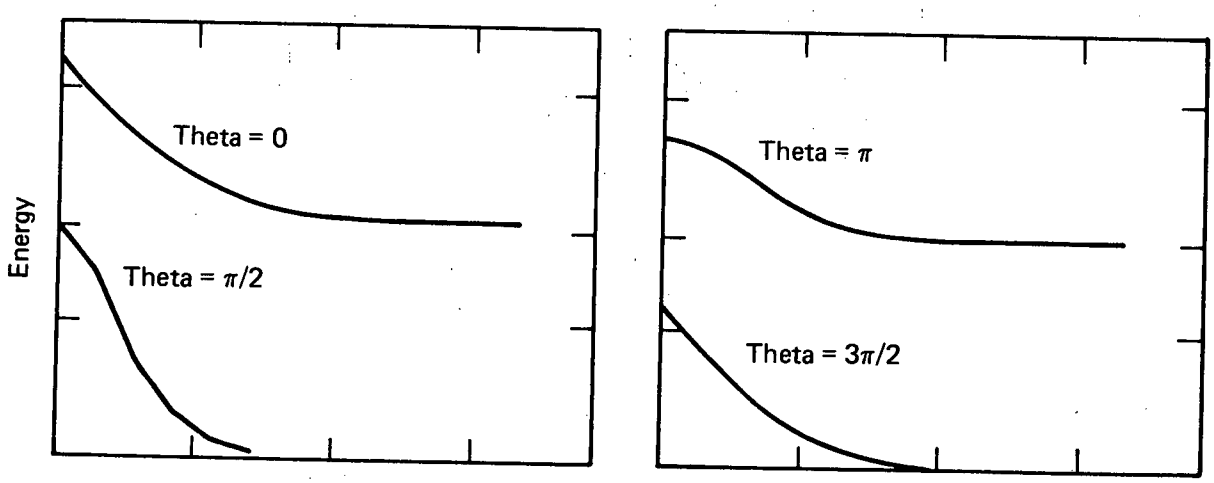

Figure 1(b). Driving energy source distribution at t = 3.

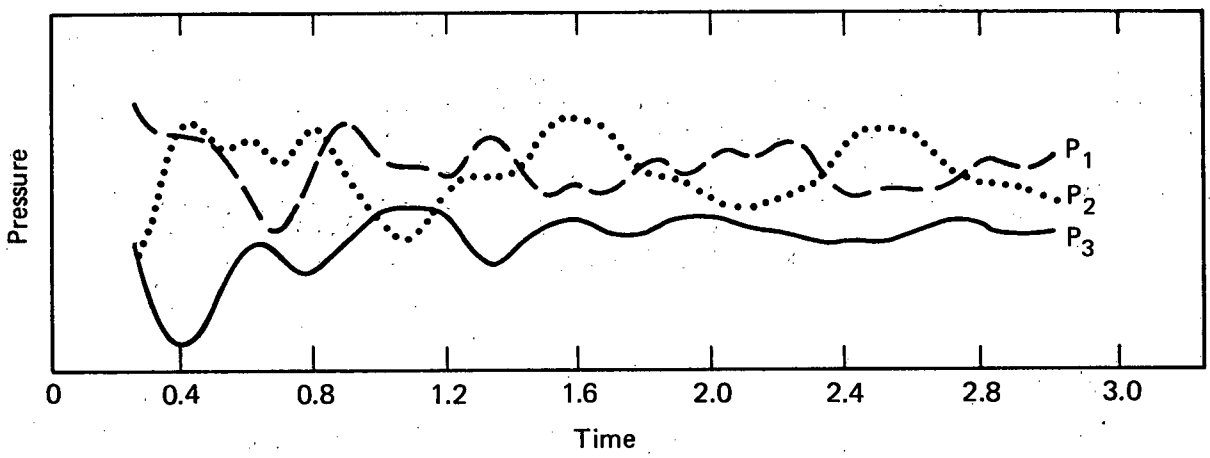

Figure 2. Attenuated pressure history at the same three positions as in Fig. 1(a) in an annular resonant cavity but with two equally spaced baffles inserted near the injector.

THEORY OF FLAME SPREAD ABOVE SOLIDS

W. A. Sirignano

Guggenheim Laboratories
Princeton University
Princeton, New Jersey

Abstract:

A theory for flame spread above a solid fuel is presented. The special case is considered whereby the oxidation is an exothermic surface reaction. The spreading rate is predicted as a function of the thermochemical properties, fuel-bed thickness, and convective velocity. Also, the theory predicts temperature, mass fraction, and heat flux as a function of position.

Introduction:

The understanding of the method by which a flame propagates above a solid fuel is necessary in order to solve the fire safety problem. In particular, we wish to know the most significant mechanism (or mechanisms) by which energy is transferred ahead of the flame; gas-phase conduction, solid-phase conduction, and radiation each play some role. Of course, this transfer of energy ahead of the flame front is necessary for flame propagation. The solid phase fuel must be heated and gasified in order for reaction to occur in the flame front.

A physical description of the general phenomenon of flame spread above condensed phase fuels and a review of existing theories has already been presented by this author.[1] In this presentation, we shall continue along the general direction suggested in that paper. The case of horizontal or vertically-downward flame spread is considered; that is, the fire plume does not move ahead of the propagating flame front and cause convective

heating of the solid fuel. However, natural or forced convection is allowed in a direction opposite to that of flame propagation.

Typically, the fuel might be a polymer. This polymer will be assumed to gasify directly; that is, no molten layer exists.

The special case will be considered in this lecture whereby the oxidation is an exothermic surface reaction. Most polymers, of course, would not burn in this manner but rather in the gas phase. However, this assumption reduces the mathematical complexity in two ways: (1) the number of governing partial differential equations is reduced since the fuel species no longer exists in the vapor phase and (2), as we shall later see, the two-dimensional problem may be reduced to a one-dimensional problem.

The case of steady propagation will be considered where the spreading rate is to be determined as a function of ambient temperature, pressure, and oxidizer concentration, transport properties, and thermochemical properties. The velocity of the incoming flow due to forced or natural convection shall be assumed to be known.

The method of solution to be proposed here is original in that it is the only one which allows for consideration of the nonlinearity due to chemical kinetics. Other approaches have either taken an empirical value of the spreading rate as known and calculated temperature fields[2,3] or have determined the spreading rate as a function of some heuristic parameter which is not readily related to other fundamental properites[4]. One exception is the study by Tarifa, et al[5] but there radiation is the only mechanism by which energy is allowed to be transferred ahead of the flame.

The originality of the method caused the author to be cautious and to attempt, in the first instance, to solve the case of surface reactions rather than the more physically interesting case of gas-phase reactions.

Theoretical Analysis:

The frame of reference will be fixed to the moving flame front so that a steady-state problem is obtained. The ambient pressure is uniform and no pressure gradients exist throughout the heat-up and reaction zones at the low Mach numbers involved. Due to the temperature increases and density decreases associated with the reaction, the streamlines will diverge somewhat. However, this effect is neglected in the governing equations and the Oseen approximation is made with the convective terms. Radiation is neglected in this model since it is not expected to be important for small-scale fires, at least. The flow in the flame-front region is considered to be laminar. Also, the Prandtl number is assumed to be negligible compared to unity so that the viscous layer is much thinner than the thermal layer. Then the momentum equation may be considered trivial and the gas phase equations may be written as:

Species:

$$\rho V \frac{\partial Y_O}{\partial x} = \nabla \cdot (\rho D \nabla Y_O) \qquad (1)$$

Energy:

$$\rho V c_p \frac{\partial T}{\partial x} = \nabla \cdot (\lambda \nabla T) \qquad (2)$$

where ρ is the gas density, c_p is the specific heat which is

assumed identical for all species, V is the velocity of the air relative to the flame front, Y_O is the mass fraction for the oxidizer, T is the temperature, D is the mass diffusivity, λ is the thermal conductivity, x is the coordinate parallel to the direction of flame propagation and y is the coordinate normal to the flame propagation direction.

In the solid phase, the energy equation is written as

$$\rho_s V_F c_s \frac{\partial T_s}{\partial x} = \nabla \cdot (\lambda_s \nabla T_s) \tag{3}$$

where the subscript s implies solid phase. V_F is the flame spreading rate relative to the solid. Note that in the absence of natural or forced convection $V = V_F$. $y = 0$ is taken as the solid gas surface and the ratio of surface regression rate to spreading rate is neglected. λ_s = constant may be assumed.

Certain matching conditions will be applied at the solid-gas interface. First of all, the combined flux of oxidizer due to diffusion and convection at the interface must balance the oxidation rate at the surface; i.e.,

$$\rho D \frac{\partial Y_O}{\partial y} = \dot{m}(Y_O + \frac{1}{\nu}) \tag{4}$$

where $\dot{m}$ is the mass flux emitted from the surface and ν is the stoichiometric mass ratio of fuel-to-oxidizer. The gasification rate is given by a kinetic law which assumes a first order dependence upon local oxidizer concentration and an Arrhenius dependence upon temperature.

$$\dot{m} = A\rho Y_O e^{-E/R(T-T_\infty)} \tag{5}$$

where A, E, and R are constants and T_∞ is the ambient temperature. The mass flux is conveniently taken to be zero at the ambient temperature.

The energy balance at the surface is given by

$$\lambda \frac{\partial T}{\partial y} + \dot{m}\left[Q - \int_{T_\infty}^{T} (c_p - c_s)dT'\right] = \lambda_s \frac{\partial T}{\partial y_s} \tag{6}$$

where Q is the energy released per unit mass of fuel in surface oxidation.

Furthermore, the ambient temperature and concentrations are known providing the boundary conditions at infinity.

Note that the transformations $\xi = \rho\lambda x/c_p$ and $\eta = \int \rho dy$ (where $\rho\lambda$ and c_p are assumed to be constant throughout the gas phase) result in a simplification of Equations (1) and (2). The above assumptions together with the assumption that an average transport property may be employed for diffusion in the x-direction, reduce the above set of differentials equations, (1)-(4) and (6), to a set of differential equations with constant coefficients.

After scaling the independent variables we find the specie and energy equations satisfy:

$$V \frac{\partial Y_O}{\partial \xi} = \frac{\partial^2 Y_O}{\partial \eta^2} + \frac{\overline{\lambda}^2}{c_p^2} \frac{\partial^2 Y_O}{\partial \xi^2}, \tag{7}$$

$$V \frac{\partial T}{\partial \xi} = \frac{\partial^2 T}{\partial \eta^2} + \frac{\overline{\lambda}^2}{c_p^2} \frac{\partial^2 T}{\partial \xi^2} . \tag{8}$$

In the above equations, unitary Lewis number is assumed; however, that assumption can be relaxed with some increase of complexity in the calculations.

The following nondimensional variables are employed:

$$s = \left(\frac{c_p}{\bar{\lambda}}\right)^2 V\xi = x/L$$

$$z = \frac{Vc_p\eta}{\bar{\lambda}} = \frac{\rho_\infty Vc_p}{\bar{\lambda}} \int \frac{dy}{\theta} = \int \frac{1}{\theta}\,\frac{dy}{L}$$

and

$$\theta = T/T_\infty$$

where $L = \lambda/\rho_\infty c_p V$ is a characteristic thermal length. These lead to the equations governing the gas phase

$$\frac{\partial\theta}{\partial s} = \frac{\partial^2\theta}{\partial z^2} + \frac{\partial^2\theta}{\partial s^2} \tag{9}$$

and

$$\frac{\partial Y_O}{\partial s} = \frac{\partial^2 Y_O}{\partial z^2} + \frac{\partial^2 Y_O}{\partial s^2} \quad . \tag{10}$$

For the solid phase, we define the nondimensional variables and parameter

$$\theta_s = T_s/T_\infty \quad ,$$

$$y_s = -\,y/L \quad ,$$

$$a = \frac{\bar{\lambda}\rho_s c_s V_F}{\lambda_s \rho_\infty c_p V} \quad .$$

This results in the following form of the energy equation for the solid phase

$$a \frac{\partial \theta_s}{\partial s} = \frac{\partial^2 \theta_s}{\partial y_s^2} + \frac{\partial^2 \theta_s}{\partial s^2} \quad . \tag{11}$$

The boundary conditions at infinity are that:

$$\theta \to 1 \ , \quad Y_0 \to 1 \quad \text{as} \quad z \to \infty \quad \text{or} \quad s \to -\infty$$

$$\theta_s \to 1 \quad \text{as} \quad y_s \to \infty \quad \text{or} \quad s \to -\infty \tag{12}$$

The boundary conditions (4), (5), and (6) may be combined and transformed to

$$\frac{\partial Y_0}{\partial z} = \left(\frac{A}{V}\right) \frac{Y_0}{\theta} \, e^{-\theta_c/\theta - 1} \left(Y_0 + \frac{1}{\nu}\right) \tag{13}$$

and

$$\frac{\partial \theta}{\partial z} + \left(\frac{A}{V}\right) \frac{Y_0}{\theta} \, e^{-\theta_c/\theta - 1} \left[\frac{Q}{h_\infty} - \left(1 - \frac{c_s}{c_p}\right)(\theta - 1)\right] = -\left(\frac{\lambda_s}{\lambda_\infty}\right) \frac{\partial \theta_s}{\partial y_s} \quad . \tag{14}$$

The system of equations (9), (10), and (11) together with the boundary conditions may be solved with the aid of the Green's function which is developed in the Appendix. A system of nonlinear integral equations with one independent variable are obtained as follows:

$$\theta(s) = 1 + \Lambda \int_{-\infty}^{s^*} \left[e^{\frac{s-\xi}{2}} K_0\left(\frac{|s-\xi|}{2}\right)\right] \left\{\frac{Q}{h_\infty} - (\theta - 1)\left(1 - \frac{c_s}{c_p}\right)\right\} \frac{Y}{\theta} \, e^{-\theta_c/(\theta-1)} \, d\xi$$

$$- \frac{1}{\pi} \frac{\lambda_s}{\lambda_\infty} \int_{-\infty}^{\infty} \left[e^{\frac{s-\xi}{2}} K_0\left(\frac{|s-\xi|}{2}\right)\right] u\theta \, d\xi \quad , \tag{15}$$

$$Y_0 = Y_{0_\infty} - \Lambda \int_{-\infty}^{s^*} \left[e^{\frac{s-\xi}{2}} K_0\left(\frac{|s-\xi|}{2}\right)\right] \left(Y_0 + \frac{1}{\nu}\right) \frac{Y_0}{\theta} \, e^{-\theta_c/(\theta-1)} \, d\xi \tag{16}$$

and

$$\theta = 1 + \frac{1}{\pi} \int_{-\infty}^{\infty} \left[2^{\frac{a}{2}(s-\xi)} K_0\left(\frac{a}{2} |s-\xi|\right) \right] u d\xi \qquad (17)$$

where the definitions have been made that

$$\Lambda = \frac{A}{\pi V} ,$$

$$u = - \frac{\partial \theta}{\partial y_s} (s,0)$$

and s^* is the position beyond which the surface oxidation no longer occurs. For an infinitely thick fuel-bed, $s^* \rightarrow \infty$.

Realize that the fuel is gasifying so that the surface is regressing as the flame moves along it. When the fuel-bed is very thick, the position of fuel-bed burn-out is so far downstream of the flame front that the exact position of burn-out or the exact thickness of the bed is not important. That is, above a certain fuel-bed thickness, the spreading rate and the field solution in the flame front region do not depend upon the fuel-bed thickness τ. In this range of τ, the results are independent of s^*. For a thin fuel-bed, on the other hand, our equations are accurate if we consider the following situation. Assume a fuel, of thickness τ, is coated upon an inert substrate of thickness δ^*. Furthermore, $\tau << \delta^*$ so that the total thickness $\tau + \delta^* \simeq \delta^*$. Also, the substrate and the fuel have identical thermal diffusivities.

The spreading velocity V_F (and therefore V) is still unknown and must be considered as an eigenvalue. This implies that Λ is an eigenvalue of the problem. Since (15), (16), and (17) form a system of three equations for the temperature θ, oxidizer concentration Y_0, and heat flux u at the surface. However, since Λ

is still unknown, we require another equation in order to obtain a solution to the system. This equation is developed by consideration of the conservation of mass in the solid phase.

Let τ be the thickness of the unburned fuel-bed. It follows that

$$\rho_s V_F \tau = \int_{-\infty}^{\infty} \dot{m}\, dx$$

since the mass flux of solid fuel into the flame zone must equal the total gasification rate at the surface. Defining

$$B = \frac{\rho_s V_s \tau c_p}{\pi \lambda_\infty}$$

and using (5) and previous notation, we obtain

$$\Lambda = B\left[\int_{-\infty}^{s^*} \frac{Y_O}{\theta} e^{-\theta_c/(\theta-1)}\, d\xi\right]^{-1} . \qquad (18)$$

Now (18) may be solved together with (15), (16), and (17) to obtain θ, Y_O, and u along the surface together with Λ. Actually, since the spreading rate not only appears in Λ but also appears in a and B it is more convenient to consider the pre-exponential chemical kinetic constant A as the eigenvalue since it appears only through Λ. In that case the spreading rate V_F is taken as known while the constant A is taken as unknown. Once the results are obtained A versus V may be plotted and the appropriate inversion can be readily made.

The advantages of formulating the problem as a system of integral equations rather than partial differential equations are:

(1) there is only one independent variable instead of two variables and (2) the nonlinear system is readily solved by the method of successive substitutions. If, in addition to the spreading rate and the surface values, one wishes to determine the solution through the gas and solid fields, they may be constructed from the surface values through the use of Equation (A-4) in the Appendix.

Special cases:

The system of three integral equations may be reduced under special circumstances. In one special case, all of the energy is conducted through the gas phase and none is conducted through the solid phase. In this case the heat flux in the solid phase need not be determined in a coupled fashion. Therefore, Equations (15), (16) and (18) are solved together neglecting Equation (17) and setting $u = 0$ in Equation (15).

This limit could be obtained by letting $\delta \rightarrow 0$ in which case the kernel in Equation (17) becomes infinite yielding the solution $u = 0$. Physically, this implies that as the fuel-bed becomes very thin no energy is conducted through it. In this limit, we are left with the following equation

$$\theta = 1 + \Lambda \int_{-\infty}^{s^*} e^{\frac{s-\xi}{2}} K_0\left(\frac{|s-\xi|}{2}\right)\left\{\frac{Q}{h_\infty} - (\theta-1)\left(1 - \frac{c_s}{c_p}\right)\right\} \frac{Y_0}{\theta} e^{-\theta_c/(\theta-1)} d\xi \qquad (19)$$

which is the limiting form of (15) and must be solved together with Equations (16) and (18) for θ, Y_0, and Λ.

A further special subcase occurs when $c_p = c_s$ and $\nu << 1$ with $u = 0$. Then Equations (16) and (19) yield

$$\frac{\theta-1}{Q/h_\infty} = \Lambda \int e^{\frac{s-\xi}{2}} K_0\left(\frac{|s-\xi|}{2}\right) \frac{Y_0}{\theta} e^{-\theta_c/(\theta-1)} d\xi \approx \frac{Y_{0_\infty} - Y_0}{1/\nu} \qquad (20)$$

or

$$Y_0 \approx Y_{0_\infty} + \frac{h_\infty}{\nu Q}(1-\theta) \qquad (21)$$

which may be substituted into the integrals in (18) and (20) to obtain

$$\theta \approx 1 + \frac{\Lambda}{\nu} \int_{-\infty}^{s^*} \left[e^{\frac{s-\xi}{2}} K_0\left(\frac{|s-\xi|}{2}\right) \right] \frac{e^{-\theta_c/(\theta-1)}}{\theta} (q-\theta) d\xi \qquad (22)$$

and

$$\Lambda \approx B \left[\int_{-\infty}^{s^*} \frac{Y_{0_\infty} + (h_\infty/\nu Q)(1-\theta)}{\theta} e^{-\theta_c/(\theta-1)} d\xi \right]^{-1} \qquad (23)$$

where the definition has been made that

$$q = 1 + \frac{\nu Q}{h_\infty} Y_{0_\infty} .$$

Here (22) and (23) may be solved together for θ and Λ. Afterward, Y_0 may be determined from (21).

Numerical Methods:

The nonlinear integral equations are solved by the method of successive substitutions. A guess is made at the solution and substituted into the integrals on the right-hand sides of the equations. The left-hand sides of the equations as calculated become the next guess and are substituted into the integrals for the next step in the iterative process. This continues until convergence occurs.

This technique has been successfully employed in the above-mentioned special subcase where Equations (22) and (23) have been solved simultaneously. The technique has also been employed in the special case where (16), (18), and (19) are solved together.

A modified form of this technique has been employed in the solution of the general case where (15), (16), (17) and (18) are solved together. Some difficulty occurs because the unknown heat flux appears only in the integrands of (15) and (17); therefore, the next value for u in the iteration procedure is not immediately calculated. However, the linearity of Equation (17) may be used to advantage since it is possible to invert that equation and obtain u as a function of θ. This function may then be used to substitute for u in (15). Then, with u eliminated, the method of successive substitutions may be employed. The particular method of inversion of (17) involved approximating the integral as a finite summation over the discretized range of ξ. For each discrete value of s a different linear algebraic equation applied. This linear algebraic system was inverted.

Results and Discussion:

Calculated results were first obtained for the special subcase where $\nu << 1$ and $u = 0$. In Figure 1, the surface temperature profile determined from the solution of (22) and (23) is given. Also, given are the results obtained from the solution of Equations (15), (16) and (18) with $\nu = .1$. It is seen that as long as $\nu << 1$, the results of the two methods are in good agreement. We see that the temperature increases through the flame front, reaching a maximum, and then decreases. The increase occurs due

to the exothermic reaction while the decrease occurs when the reaction is completed and just diffusion of energy away from the surface occurs. Actually, the temperature begins to decrease just before the point where the reaction is completed $s^* = 5$. This decrease occurs because some diffusion of energy in the positive x-direction occurs.

In Figure 2, the oxidizer mass fraction at the surface is plotted versus position. One curve is the result of the solution of (22) and (23) followed by the use of (21) while the other curve is the result of the solution of (15), (16), and (18). Again the two methods have results which are in excellent agreement. The oxidizer mass fraction decreases as the reaction occurs and then increases after the reaction ceases at $s^* = 5$ due to mass diffusion.

It is seen therefore that in the case $u = 0$, the approximation given by Equations (20) and (23) is reasonable when $\nu << 1$. It may be used in lieu of the more exact set of equations which are larger. This approximation will be employed henceforth wherever $u = 0$.

In Figure 3, we see the effect of increasing the energy release on the surface temperature profiles. The larger the value of Q/h_∞, the higher is peak value of temperature and the faster is the temperature rise (or the more narrow is the reaction zone front region). Since the independent variable s depends upon a characteristic thermal length which varies, we shall see later that the front regions are even more narrow than indicated.

As the fuel-bed thickness increases the overall length of the reaction zone will increase. However, above a certain thickness (or above a certain value of B) the temperature profile in the front region is essentially independent of B. This is clearly seen in Figure 4, where the calculated temperature results are superimposed for three different fuel-bed thicknesses. The front region thickness is of the order of a few thermal lengths and disturbances far downstream do not propagate upstream.

Nondimensional spreading rate versus energy release is shown in Figure 5 and a nearly linear increasing dependence is seen. Also spreading rate will increase with the nondimensional thickness B up to a certain value of B beyond which Λ is independent of B. It is also seen that an increase in the nondimensional activation energy results in a decrease in the spreading rate.

In Figure 6, we see temperature results for the case with solid phase heat transfer (u = 0). The same characteristics exist as did for the no-solid-phase-heat-transfer case except that the temperature values are significantly reduced by the cooling effect of the solid. For the values of a = 1.0 and λ_s/λ_∞ = 0.1 as given, the main effect of the solid phase is to cool the reaction zone thereby decreasing the spreading rate; Λ = 3.7 here versus Λ = 1.6 with no solid phase heat transfer. Realize, of course, that with lower values of a (hight solid thermal diffusivity or greater values of V/V_s) the solid phase will begin to play a more important role in transferring energy ahead of the flame which would tend to enhance the spreading rate.

The results shown in Figure 7 would indicate at first sight that solid phase heat transfer makes only slight differences in the results for oxidizer mass fraction. The difference would be made through the temperature which modifies the reaction rate. Realize that again the independent variable s is based on a characteristic thermal length which depends upon the spreading rate. Therefore, since the spreading rate depends significantly upon solid phase heat transfer even the oxidizer mass fractions are affected. This discussion also relates to Figure 3.

In Figure 8, we see the surface heat flux plotted versus position along the surface. The heat flux has its maximum in the flame front region with another local maximum occurring just before the burnout position $s^* = 5.0$. This last maximum coincides with region of surface temperature decrease as would be expected.

The calculations are preliminary in the sense that no extensive parameter survey has yet been performed. However, it is felt that the feasibility of using this integral technique for such nonlinear calculations has been demonstrated.

Acknowledgements:

The author wishes to acknowledge the support of the National Aeronautics and Space Administration and the National Science Foundation for their support of this effort under Contract NAS2-6705 and Grant GI 3255 4X1.

References

(1) Sirignano, W.A., "A Critical Discussion of Theories of Flame Spread across Solid and Liquid Fuels", Combustion Science and Technology 6 (1972) pp. 95-105.

(2) Lastrina, F.A., Magee, R.S. and McAlevy, R.F., "Flame Spread Over Fuel Beds: Solid Phase Energy Considerations", Thirteenth Symposium (International) on Combustion (1971) Combustion Institute, Pittsburgh, p. 935.

(3) Fernandez-Pello, A., Kindelan, M., and Williams, F.A., "Surface Temperature Histories During Downward Propagation of Flames on PMMA Sheets", preprinted for 1973 Spring Meeting of Western States Section/The Combustion Institute, April 16-17, 1973.

(4) de Ris, J., "The Spread of a Laminar Diffusion Flame", Twelfth Symposium (International) on Combustion 1969) Combustion Institute, Pittsburgh, p. 241.

(5) Tarifa, C.S., del Notario, P.P., and Torralbo, A.M., "On the Process of Flame Spreading Over the Surface of Plastic Fuels in an Oxidizing Atmosphere", Twelfth Symposium (International) on Combustion, Combustion Institute, Pittsburgh, p. 229.

APPENDIX

Consider the partial differential equation

$$L(u) \equiv \Delta u - ku_x = f(x,y) \qquad \text{(A-1)}$$

where $\Delta \equiv \nabla \cdot \nabla$ (the Laplacian operator) and u is any unknown while k is constant and f is known. Realize that Equations (9), (10) and (11) are of this form where $u = \theta - 1$, $Y_O - Y_{O_\infty}$, or $\theta_s - 1$. In those cases $f = 0$ identically. The more general case with gas phase reactions would have a non-zero f. The boundary conditions are that: $u \to 0$ as $y \to \infty$ or as $x \to -\infty$ and $\frac{\partial u}{\partial y}(x,0) = g(x)$ a known function.

The adjoint operator is

$$M(v) \equiv \Delta v + kv_x \qquad \text{(A-2)}$$

so that application of Green's theorem yields

$$\iint [vL(u) - uM(v)]dxdy = -\int_{\substack{\text{along} \\ y=0}} [v\frac{\partial u}{\partial y} - u\frac{\partial v}{\partial y}]dx \ . \qquad \text{(A-3)}$$

Let Q be a source point (ξ, η) and P be some other point (x,y). We wish that $v = G(P,Q)$ be the Green's function whereby:

(1) $M(G) = 0$ if $P \neq Q$,

(2) $G \to \frac{1}{2\pi} \log r$ as $r \to 0$,

(3) $\frac{\partial G}{\partial y} = 0$ along $y = 0$.

Note that r is the distance between P and Q so that

$$r = \sqrt{(x-\xi)^2 + (y-\eta)^2} \ .$$

Then we have from (A-3)

$$u(\xi,\eta) = \int_0^\infty \int_{-\infty}^{\infty} G(x,y;\xi,\eta) f(x,y)\,dx\,dy + \int_{-\infty}^{\infty} G(x,0;\xi,\eta) g(x)\,dx \ . \tag{A-4}$$

Now it only remains to determine the G which satisfies the above three conditions.

Consider the adjoint equation (A-2) and let

$$\mu(x,y) \equiv v(x,y) e^{(k/2)x} \ .$$

Then

$$\Delta v + k v_x = e^{-(k/2)} [\Delta\mu - \frac{k^2}{4} \mu] = 0$$

so that

$$\Delta\mu - \frac{k^2}{4} \mu = 0 \ .$$

Considering the cylindrically symmetric solution for μ we would obtain

$$\frac{d^2\mu}{dr^2} + \frac{1}{r} \frac{d\mu}{dr} - \frac{k^2}{4} \mu = 0$$

which is a modified Bessel's equation of zero order. One solution is the modified Bessel function of zero order and second kind $K_0(\frac{kr}{2})$ where

$$K_0(z) = - \sum_{\ell=0}^{\infty} \frac{(\frac{1}{2}z)^{2\ell}}{(\ell!)^2} \left\{ \log \frac{1}{2} z + \gamma - \sum_{m=1}^{\ell} \frac{1}{m} \right\} \ .$$

Note that γ is Euler's constant .5772157... .

Asymptotically we have

$$K_0(z) \sim - \log z \quad \text{as} \quad z \to 0$$

and

$$K_0(z) \sim \left(\frac{\pi}{2z}\right)^{1/2} e^{-z} \quad \text{as} \quad z \to \infty \ .$$

Now $v = e^{-(k/2)x} K_0(\frac{k}{2} r)$ is a fundamental solution to the adjoint equation so that condition (1) is satisfied. It remains to satisfy conditions (2) and (3). Condition (3) is satisfied by the symmetric reflection about the line $y = 0$. Defining $r' = \sqrt{(x-\xi)^2 + (y+\eta)^2}$, we have

$$v = e^{-(k/2)x}[K_0(\tfrac{k}{2}r) + K_0(\tfrac{k}{2}r')]$$

which satisfies the boundary condition that $\frac{\partial v}{\partial y}(x,0) = 0$ as well as satisfying the partial differential equation (A-2).

Condition (2) is satisfied by multiplying by the constant $-\frac{1}{2\pi} e^{(k/2)\xi}$ so that finally

$$v = G(x,y;\xi,\eta) = -\frac{1}{2\pi} e^{(k/2)(x-\xi)}[K_0(\tfrac{k}{2}r) + K_0(\tfrac{k}{2}r')] \ . \quad \text{(A-5)}$$

In particular

$$G(x,0;\xi,0) = -\frac{1}{\pi} e^{(k/2)(x-\xi)} K_0(|x-\xi|) \ . \quad \text{(A-6)}$$

The difference between "upstream" and "downstream" influence may be readily seen. Consider the region where $|x-\xi| >> |y|$ and $x-\xi >> |\eta|$. Then

$$G \approx -\frac{1}{\pi} e^{-(k/2)(x-\xi)} K_0\left(\frac{k}{2}|x-\xi|\right)$$

$$\sim -\frac{1}{\pi} e^{-(k/2)(x-\xi)} \left(\frac{\pi}{k|x-\xi|}\right)^{1/2} e^{-(k/2)|x-\xi|}$$

so that if $x > \xi$, we have

$$G \sim -\left(\frac{1}{\pi k|x-\xi|}\right)^{1/2} e^{-k|x-\xi|}$$

and for $x < \xi$, we have

$$G \sim -\left(\frac{1}{\pi k|x-\xi|}\right)^{1/2} .$$

The solution at the position x has some influence on the solution at the point ξ and the Green's function G is a measure of that influence. When ξ is upstream of x (or $x > \xi$), the influence is relatively weak since there is an exponential decay as $|x-\xi|$ increases. However, when ξ is downstream of x (or $x < \xi$), the influence is somewhat stronger since the decay goes as $|x-\xi|^{-1/2}$. On account of the convection, a disturbance to the field at the position x would be felt more strongly in the downstream direction than in the upstream direction.

Suppose we were considering a solid fuel with a thickness δ^* that is not very much larger than a characteristic thermal thickness. Then the boundary condition given by (12) is modified so that $\frac{\partial \theta_s}{\partial y_s} = 0$ at $\delta = \delta^*/L$. In the nomenclature of this appendix, we must impose a fourth condition on our Green's function; namely $\frac{\partial G}{\partial y}(x,\delta;\xi,\eta) = 0$. By the method of images the Green's function is found to be

$$G(x,y;\xi,\eta) = -\frac{1}{2\pi} e^{(k/2)(x-\xi)}\Big[K_0(\tfrac{k}{2} r) + K_0(\tfrac{k}{2} r') + \sum_{n=1}^{\infty}\Big\{K_0(\tfrac{k}{2}[(x-\xi)^2 + (2n\delta - y - \eta)^2]^{1/2}) + K_0(\tfrac{k}{2}[(x-\xi)^2 + (2n\delta + y - \eta)^2]^{1/2}) + K_0(\tfrac{k}{2}[(x-\xi)^2 + (y - 2n\delta - \eta)^2]^{1/2}) + K_0(\tfrac{k}{2}[(x-\xi)^2 + (-y - 2n\delta - \eta)^2]^{1/2})\Big\}\Big] . \quad \text{(A-7)}$$

Therefore, we have that

$$G(x,0;\xi,0) = -\frac{1}{\pi} e^{(k/2)(x-\xi)}\Big[K_0(k/2\ |x-\xi|) + 2\sum_{n=1}^{\infty} K_0(\tfrac{k}{2}[(x-\xi)^2 + (2n\delta)^2]^{1/2})\Big] . \quad \text{(A-8)}$$

Note that as $\delta \to \infty$, the modified Bessel functions in the summation series above will tend towards zero so that (A-7) and (A-8) become identical with (A-5) and (A-6).

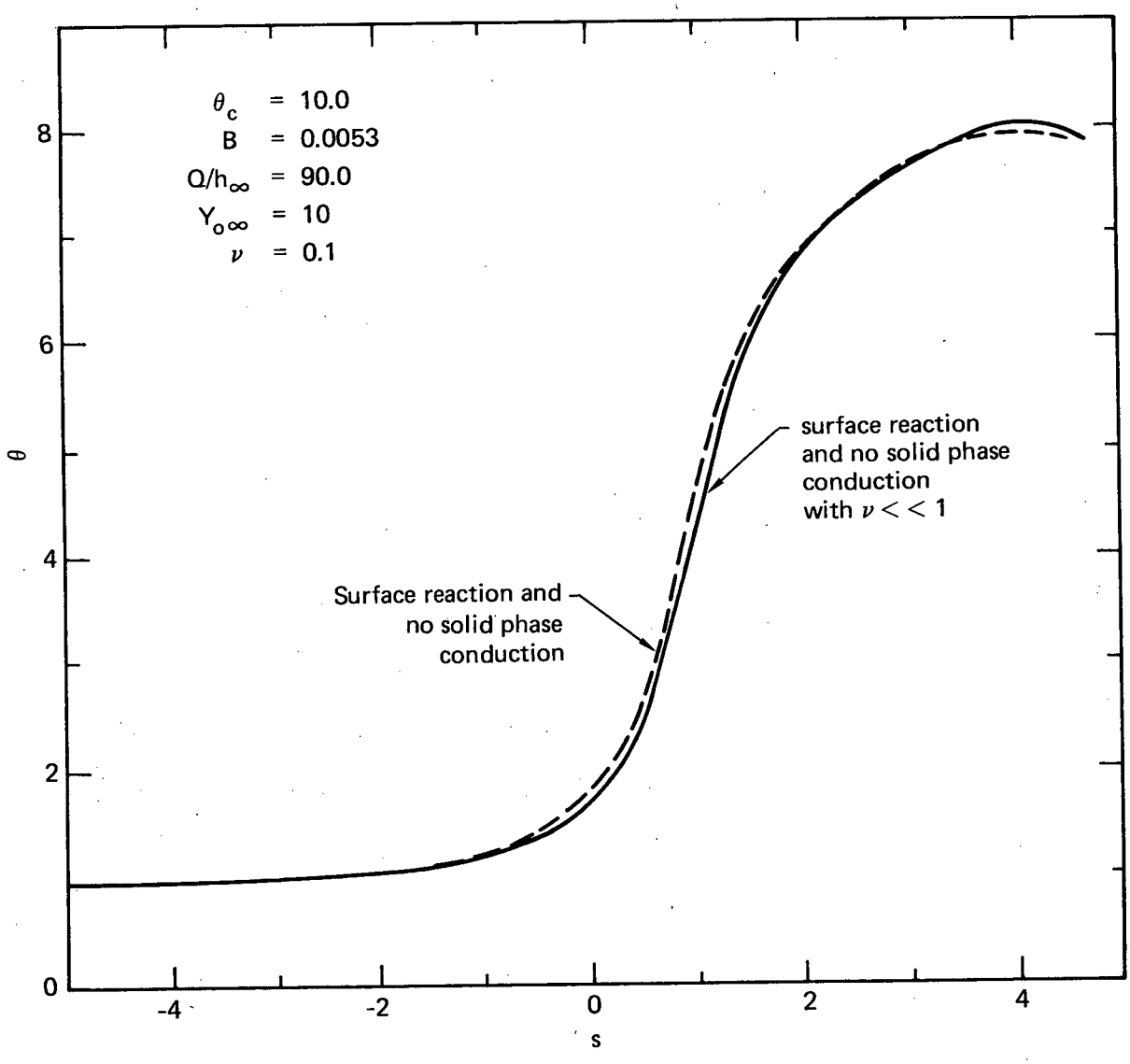
θ_c = 10.0
B = 0.0053
Q/h_∞ = 90.0
$Y_{o\infty}$ = 10
ν = 0.1
surface reaction and no solid phase conduction with $\nu << 1$
Surface reaction and no solid phase conduction
θ
s
0
2
4
6
8
-4
-2
0
2
4

Figure 1

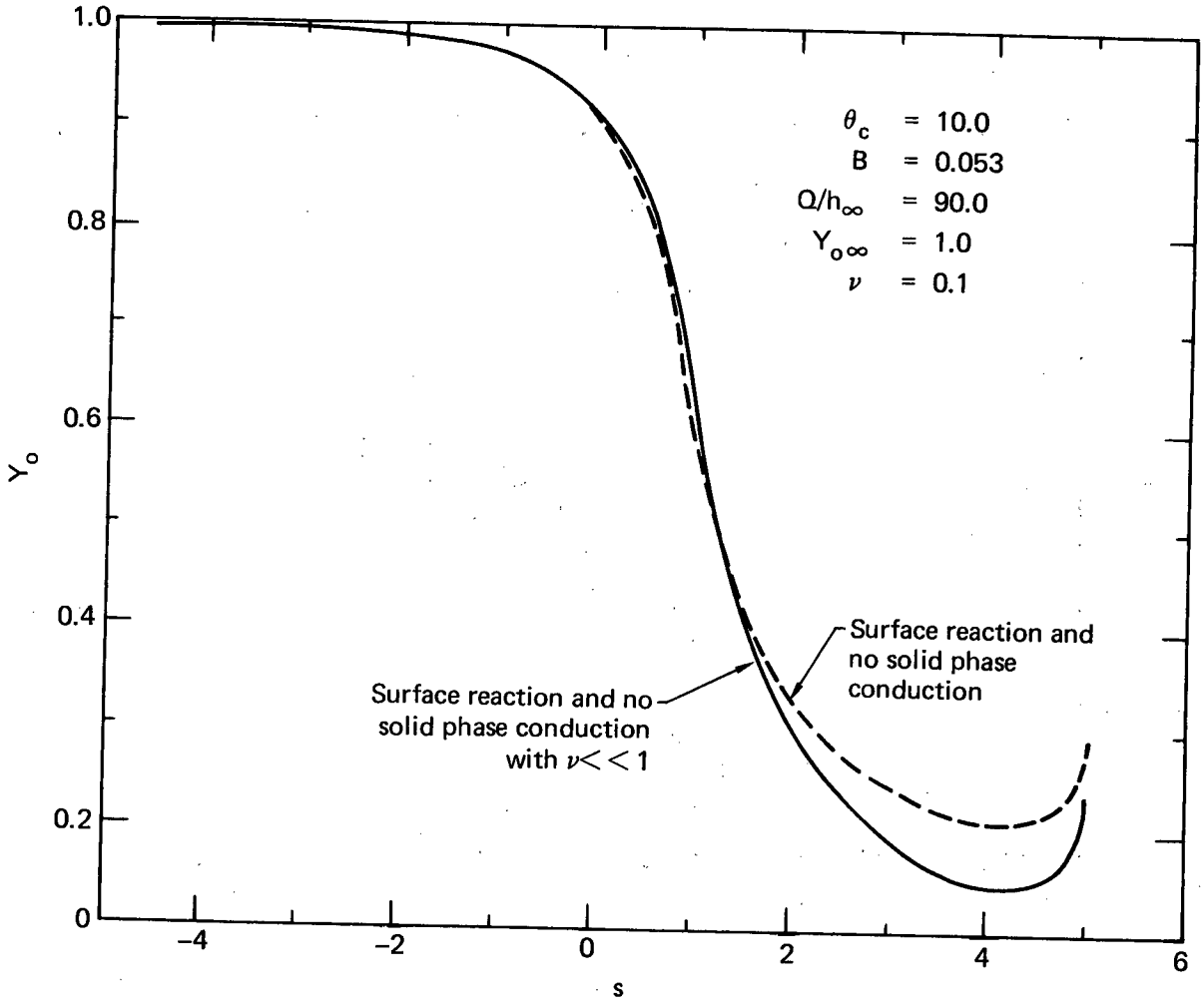
1.0
0.8
0.6
0.4
0.2
0
Y_o
-4
-2
0
2
4
6
s
θ_c = 10.0
B = 0.053
Q/h_∞ = 90.0
$Y_{o\infty}$ = 1.0
ν = 0.1
Surface reaction and no solid phase conduction with $\nu << 1$
Surface reaction and no solid phase conduction

Figure 2

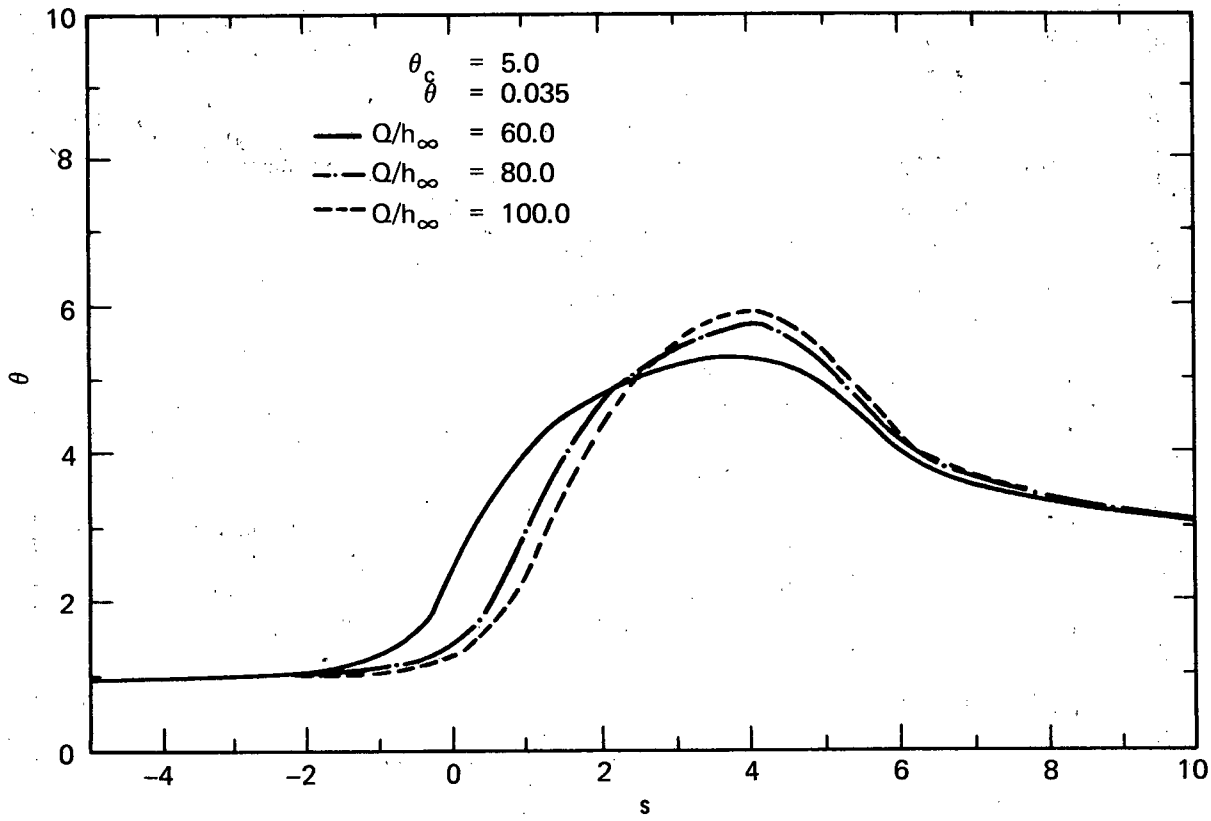
θ_c = 5.0
θ = 0.035
Q/h_∞ = 60.0
Q/h_∞ = 80.0
Q/h_∞ = 100.0
10
8
6
4
2
0
θ
-4
-2
0
2
4
6
8
10
s

Figure 3

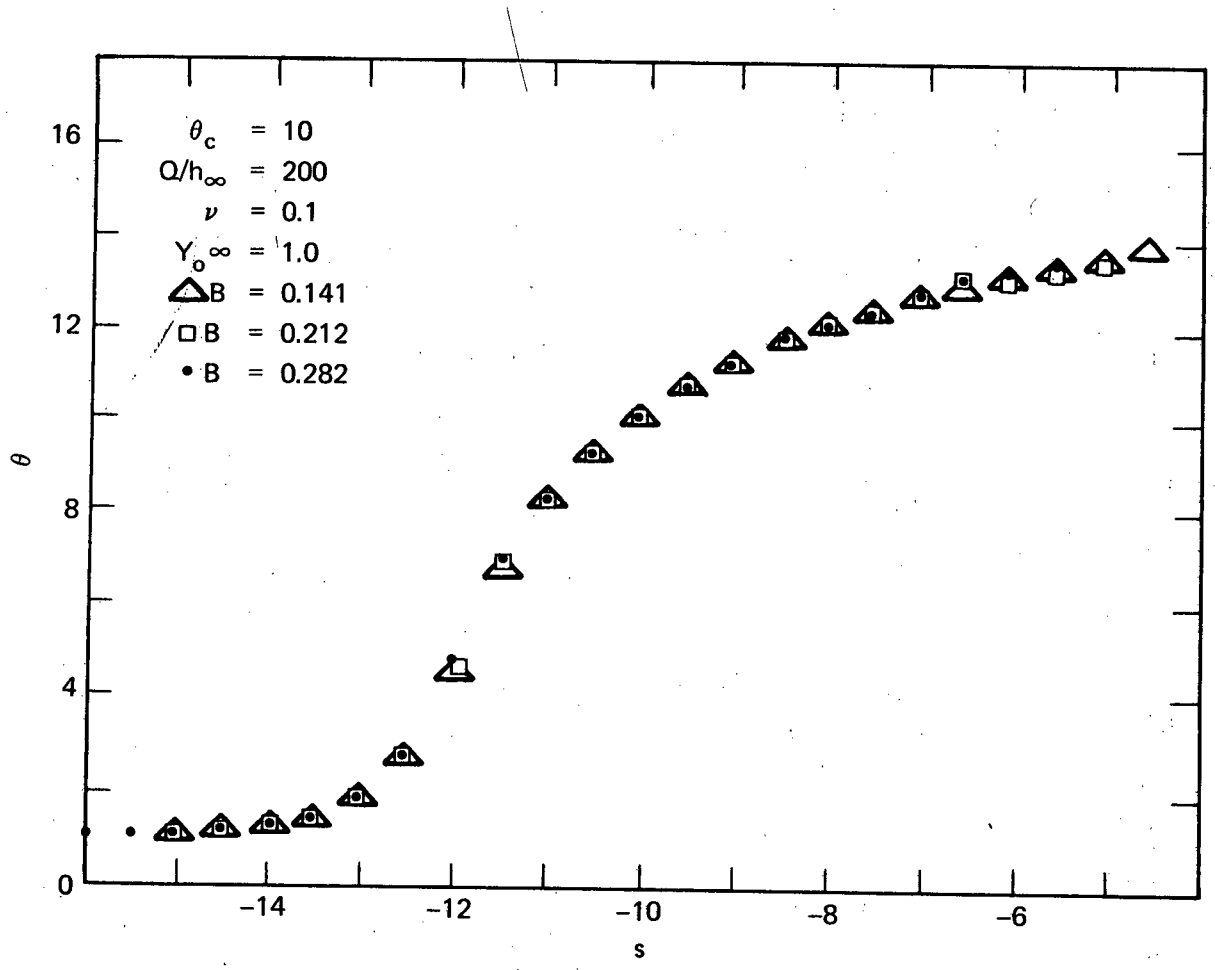
θ_c = 10
Q/h_∞ = 200
ν = 0.1
$Y_{o\infty}$ = 1.0
△ B = 0.141
□ B = 0.212
• B = 0.282
16
12
8
4
0
θ
−14
−12
−10
−8
−6
s

Figure 4

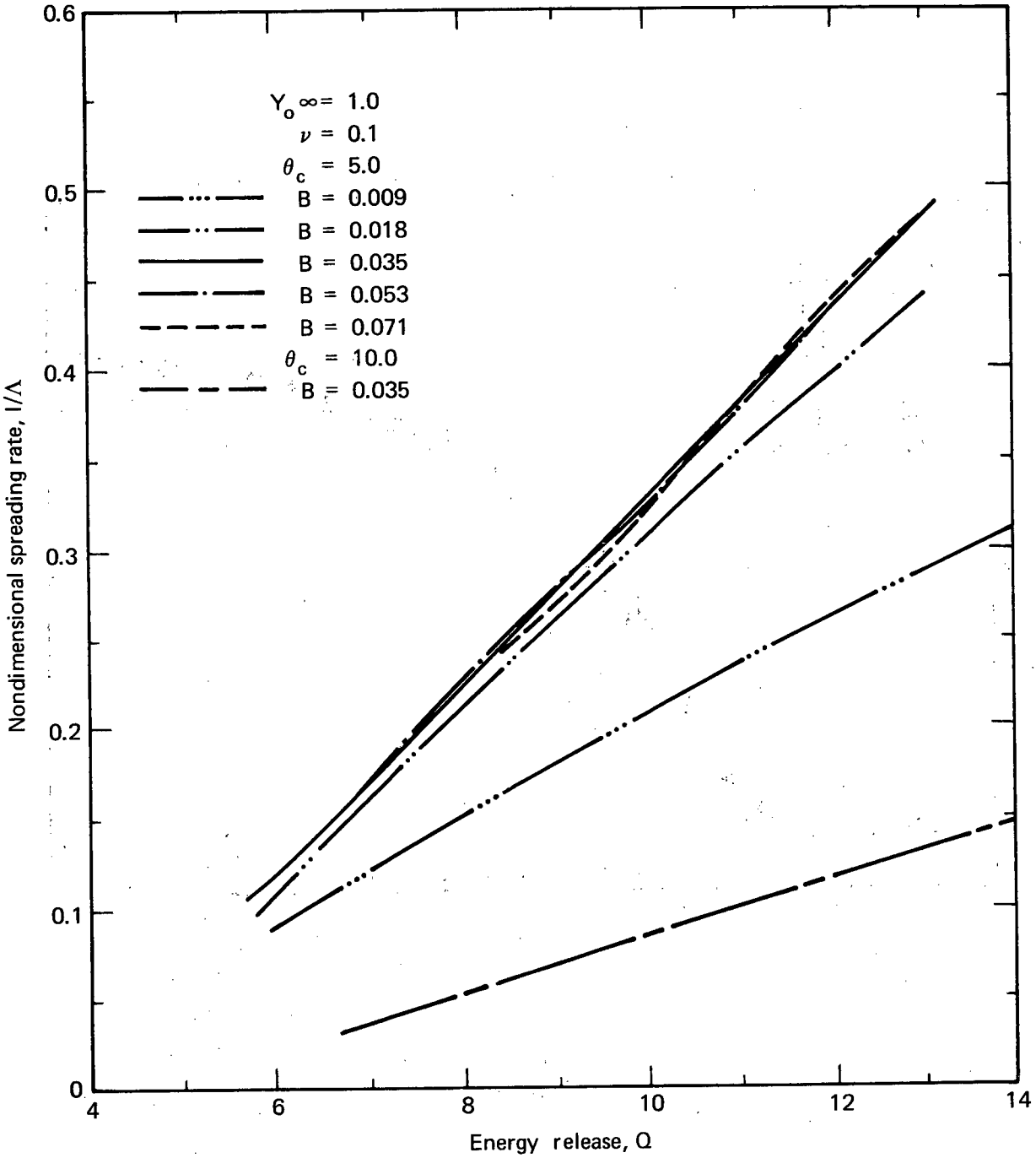
$Y_{o\infty}$ = 1.0
ν = 0.1
θ_c = 5.0
B = 0.009
B = 0.018
B = 0.035
B = 0.053
B = 0.071
θ_c = 10.0
B = 0.035
Nondimensional spreading rate, l/Λ
Energy release, Q
0
0.1
0.2
0.3
0.4
0.5
0.6
4
6
8
10
12
14

Figure 5

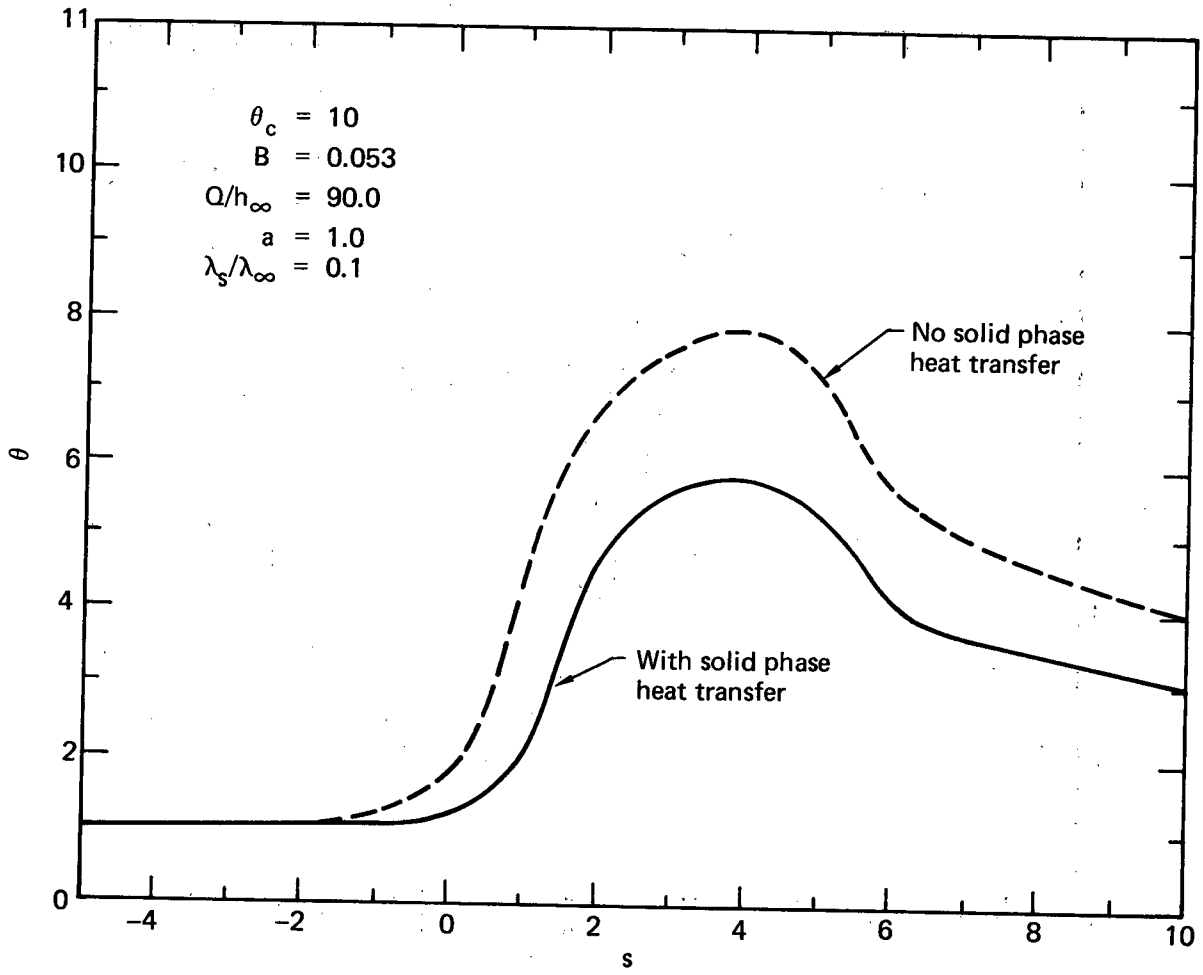
θ_c = 10
B = 0.053
Q/h_∞ = 90.0
a = 1.0
λ_s/λ_∞ = 0.1
No solid phase heat transfer
With solid phase heat transfer
θ
s
11
10
8
6
4
2
0
-4
-2
0
2
4
6
8
10

Figure 6

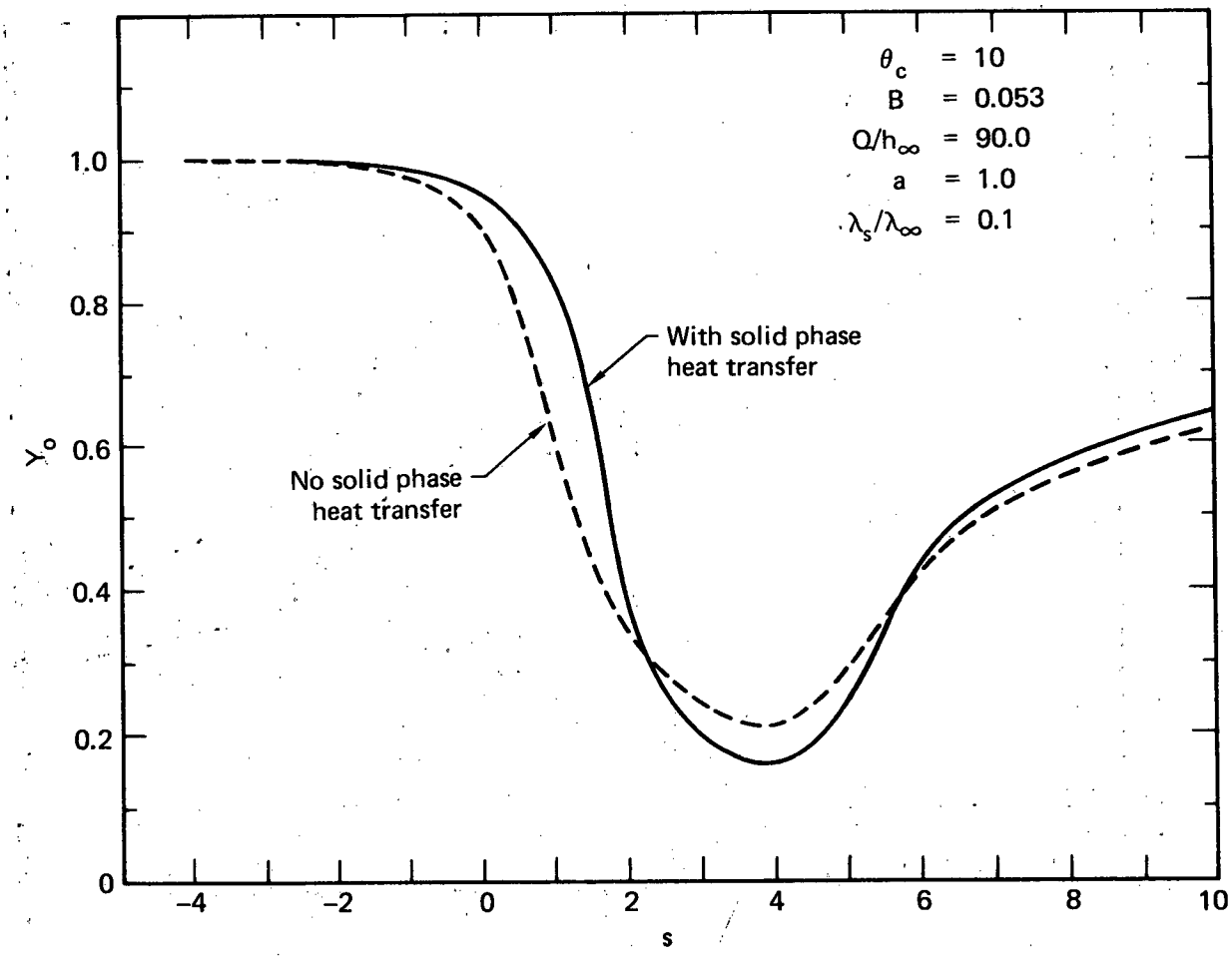
θ_c = 10
B = 0.053
Q/h_∞ = 90.0
a = 1.0
λ_s/λ_∞ = 0.1
With solid phase heat transfer
No solid phase heat transfer
Y_o
1.0
0.8
0.6
0.4
0.2
0
−4
−2
0
2
4
6
8
10
s

Figure 7

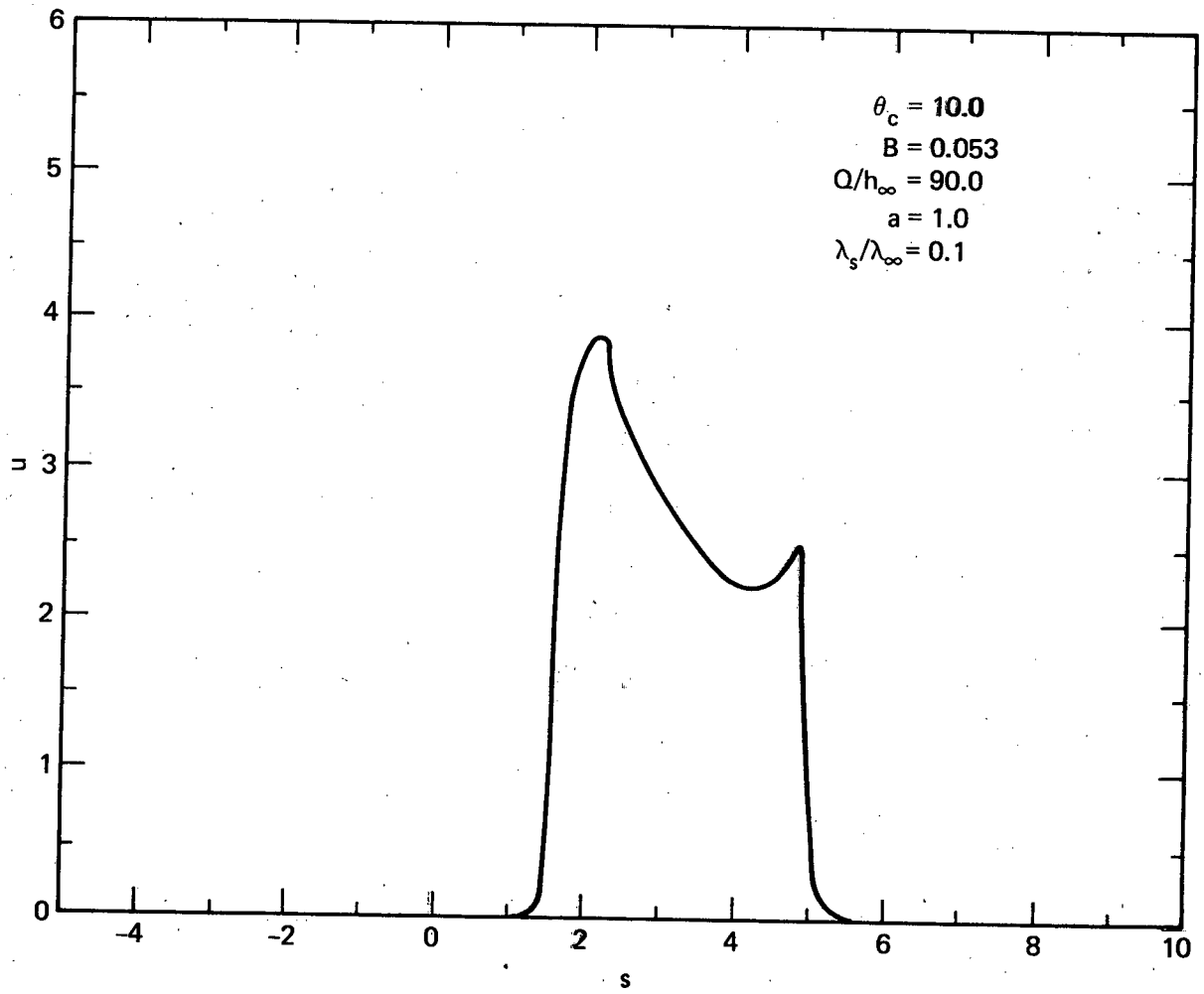
θ_c = 10.0
B = 0.053
Q/h_∞ = 90.0
a = 1.0
λ_s/λ_∞ = 0.1
Π
s
0
1
2
3
4
5
6
-4
-2
0
2
4
6
8
10

Figure 8

One-Dimensional Analysis of Combustion in a Spark-Ignition Engine

W. A. Sirignano

Guggenheim Laboratories
Princeton University

Abstract

A theory based upon a concept of turbulent flame propagation has developed and has resulted in the calculation of pressure versus crank angle and temperature versus both crank angle and chamber position as a function of various design parameters. Ultimately, the theory would result in the calculation of NO concentration. Turbulent mixing occurs to a significant extent throughout the chamber especially for larger turbulent eddy sizes. After burning is completed, the mixing tends to uniformize the temperature distribution somewhat.

The calculation of the concentration of emissions of a spark ignition (Otto) engine requires a knowledge of the pressure and temperature dependence upon space and time in the combustion chamber. The reason for this is that such species, such as NO, are formed in a nonequilibrium manner and their exhaust concentrations cannot be calculated solely from a knowledge of the exhaust temperature distribution and pressure. In order to determine pressure and temperature histories by mathematical analysis, it is necessary to understand the mechanism of flame propagation in such an engine. The flame propagation rate determines the rate of energy release in the combustion cylinder. Together with the rate of compression (or expansion) by the piston motion, the energy release rate determines the pressure and temperature variations in the chamber which in turn govern the NO kinetics.

The interesting work of Lavoie, Heywood, and Keck (1970) avoids the question of the mechanism of flame propagation. Emperical pressure results are employed to calculate temperatures and unburnt mass fraction as functions of space and time from certain thermodynamic considerations. This use of empiricism made a specific statement about the mechanism of flame propagation unnecessary or redundant. From their analysis, the flame propagation speed and the temperature variation could be calculated. No details concerning the propagation mechanism were deduced. As a consequence of their simplification, however, they could not predict the complete dependencies of the NO concentrations upon parameters which would enter through the description of the mechanism of flame propagation. Such parameters include the rpm, mixture ratio, spark advance, compression ratio, and displacement since these parameters affect the pressure profile which is taken empirically in that work.

It would be most useful, therefore, to have an analysis which models the flame propagation mechanism and can predict the complete dependencies of the NO concentration upon these critical parameters. This paper discusses such a model. It is argued in this model that the flame propagation involves, in an essential manner, the turbulent transfer of heat ahead of the flame. A calculation of the Reynolds number (based upon bore and maximum piston velocity) for a typical situation gives $O(10^4)$ which justifies the employment of a turbulent model. A Reynolds number based upon the intake flow is also high.

MODEL OF THE TURBULENT DIFFUSIVITIES

An analysis of the combustion process in an Otto engine has been performed based upon the argument that a turbulent flame propagates through the gaseous combustible mixture at a speed which is controlled by the rate at which the turbulent motion transfers heat ahead of the flame. This heat-up process continually brings the gas immediately before the flame to the ignition point and progressive combustion (or flame propagation) results. The turbulent intensity associated with these eddies is related to both the piston velocity and the velocity of the unburned gases through the intake valve. Obviously, the turbulent intensity increases with rpm. One expects, therefore, that flame speed would increase with rpm in this model. This trend, of course, has been experimentally determined. The length scale of the turbulence is related to the cylinder bore and stroke dimensions and the valve opening size.

It is assumed that spatially homogeneous, but time-varying turbulence exists in the combustion cylinder. In particular, an eddy diffusivity (assumed identical for both mass and heat transfer) is taken to be the sum of two diffusivities, one due to piston-motion-generated turbulence and the other due to intake-flow-generated turbulence. By dimensional analysis, it can be concluded that each diffusivity is the product of a characteristic length and a characteristic velocity. With one diffusivity, the characteristic velocity equals the (absolute value of) piston velocity at each instant, and, with the second diffusivity, the characterisitic velocity is proportional to the average intake gas

velocity and decays with time after the closing of the intake valve. The decay process is assumed to follow an exponential law and, by dimensional analysis, the characteristic time for eddy break-up is the ratio of the characteristic length to the intake gas velocity.

In particular, we have for the eddy diffusivity

$$\alpha(t) = L_1 u_p(t) + L_2 u_I \exp\left\{-\frac{u_I}{L_2}(t-t_I)\right\} \tag{1}$$

where t is time, u_p is the piston velocity, L_1 is a characteristic dimension for turbulent eddies produced due to shear of the gas flowing over the cylinder walls and head and the piston, L_2 is a characteristic dimension for turbulent eddies produced by the flow of intake gases, u_I is the average intake gas velocity, and t_I is the time at which the intake valve is shut. This relationship is clearly over-simplified; for example, one would expect spatial variation of the diffusivity, a dependence upon the history of the piston velocity not merely the instantaneous value, and some break-up of the eddies resulting in a distribution of the characteristic length. It is felt, however, that (1) contains much of the essential physics which governs the turbulent transfer of heat and mass and is an appropriate first representation of the eddy diffusivity.

EQUATIONS OF FLUID MOTION AND THERMODYNAMICS

The equations governing the fluid motion may now be written. The momentum equation may be replaced by the condition of uniform

but time-varying pressure. It is convenient in the first analysis to consider a one-dimensional unsteady problem. Figure 1 indicates two interesting models for flame propagation. On the left-hand side of the figure we see a planar wave propagating from the cylinder head (where the spark ignition occurs) towards the piston. That is, variations across the circular cross-section of the cylinder are neglected in comparison to variations in the axial direction. This is strictly valid only in the case where the bore-to-stroke ratio is much less than unity and the primary direction of flame propagation is the axial direction. Although, this is not realistic with regard to practical automotive design, the essential physics of the problem remain intact under this idealization and basic trends should be noteworthy. On the right-hand side, we model a cylindrical flame propagating from the center of the chamber (where ignition occurs) towards the cylinder walls. Here gradients in the vertical direction are neglected. This is perhaps a somewhat more realistic model than the planar flame case but slightly more complex mathematically. The planar model was chosen as the first model in what is hoped to become an improving succession of models. The primary intent here is to show the feasibility of calculating the field properties in a combustion chamber with turbulent flame propagation. Once this feasibility is demonstrated more realistic and more complex models may be studied. In future analyses, one could treat the two or three-dimensional problem where the bore-to-stroke ratio could be a more realistic value.

The continuity equation is given as

$$\frac{\partial \rho}{\partial t} + \frac{\partial}{\partial x}(\rho u) = 0 \tag{2}$$

and the energy equation is given as

$$\frac{\partial}{\partial t} h + u \frac{\partial}{\partial x} h - \frac{1}{\rho} \frac{d}{dt} p = \frac{1}{\rho} \frac{\partial}{\partial x} (\alpha \rho c_p \frac{\partial}{\partial x} T) + \dot{Q} \tag{3}$$

where ρ is the density, u is the gas velocity, x is the axial dimension, p is the pressure, h is the enthalpy, T is the temperature, c_p is the specific heat at constant pressure, and $\dot{Q}$ is the energy released per unit time by the combustion process.

After the intake valve closes, the amount of mass m in the cylinder is fixed.* The fixed mass, moving boundary problem is most conveniently handled in a Lagrangian frame of reference. The transformation

$$\psi = \int_0^x \rho dx'$$

is made where $x = 0$ and $\psi = 0$ are at the cylinder head while ψ = total gas mass divided by cylinder cross-sectional area occurs at the piston face. This transformation essentially replaces the continuity equation and leads to the following form of the energy equation

$$\frac{\partial}{\partial t} T - \frac{1}{\rho c_p} \frac{d}{dt} p = \frac{\partial}{\partial \psi} (\rho^2 \alpha \frac{\partial}{\partial \psi} T) + \frac{\dot{Q}}{c_p} \tag{4}$$

where c_p has been considered as constant. Furthermore, assuming the perfect gas relationship and realizing α and p are functions

* This mass m is generally a weak function of rpm according to empirical results given by Lichty (1939).

of time only, we can rewrite Eq. (4) as

$$\frac{\partial T}{\partial t} - \frac{\gamma-1}{\gamma} T\left(\frac{1}{p}\frac{dp}{dt}\right) = \left(\frac{p}{R}\right)^2 \alpha \frac{\partial}{\partial \psi}\left[\left(\frac{1}{T}\right)^2 \frac{\partial T}{\partial \psi}\right] + \frac{\dot{Q}}{c_p} \tag{5}$$

where γ is the ratio of the specific heats and R is the gas constant.

The first term on the right-hand side of Eq. (5) represents the turbulent transfer of energy while the second term represents the energy release. If both of these terms were zero, no entropy is produced and the temperature and pressure follow the isentropic relationship. (Indeed, it is seen that setting the left-hand side of the equation to zero and integrating yields that $p^{1-\gamma/\gamma}$ T is a constant.)

The boundary conditions on Eq. (5) are that negligible energy is transferred through the piston face and cylinder head, namely

$$\frac{\partial T}{\partial \psi}(t,0) = 0 \tag{6}$$

and

$$\frac{\partial T}{\partial \psi}(t,m/A) = 0 \ . \tag{7}$$

Furthermore, the initial temperature distribution is specified; some temperature exists in the neighborhood of the spark plug just after ignition with lower temperatures away from the spark plug.

The pressure can be related to the integral of the temperature distribution. In particular, from the perfect gas law we have

$$p = \rho RT = \frac{\partial \psi}{\partial x} RT$$

or, integrating over the total gas volume, we obtain

$$(8) \qquad \int \rho dx = p \int dx = \rho x_p = \rho V/A = R \int_0^{m/A} T d\psi$$

where x_p is the piston face position, V is the instantaneous gas volume, m is the total mass of gas in the cylinder and $A = \pi B^2/4$ is the cross-sectional area of the cylinder. Substitution of Eq. (8) into Eq. (5) implies that an integro-differential equation for temperature exists.

It is convenient at this point to nondimensionalize Eq. (5) through Eq. (8). We define

$$\theta = T/T_o$$
$$P = p/p_o$$
$$v = V/V_o$$
$$\eta = \psi A/m$$
$$\zeta = \omega t$$

where ω is the angular frequency of the crankshaft and the zero subscript implies conditions just prior to ignition. It is also convenient to define $K = \theta P^{1-\gamma/\gamma}$.

Now Eq. (5) through Eq. (8) may be replaced by

$$(5a) \qquad \frac{\partial K}{\partial \zeta} = \left(\frac{A}{V_o}\right)^2 \frac{\alpha}{\omega} P^{2/\gamma} \frac{\partial}{\partial \eta} \left(\frac{1}{K^2} \frac{\partial K}{\partial \eta}\right) + \frac{\dot{Q} P^{1-\gamma/\gamma}}{\omega c_p T_o}$$

with the boundary conditions

$$(6a) \qquad \frac{\partial K}{\partial \eta} (\zeta, 0) = 0$$

and

$$(7a) \qquad \frac{\partial K}{\partial \eta} (\zeta, 1) = 0$$

and the subsidiary condition

(8a) $$Pv = \int_0^1 \theta d\eta \ .$$

Of course, now the initial condition on Eq. (5a) amounts to the specification of K just following ignition.

Note that Eq. (5a) now has the effect of the rate of change of pressure concealed within the definition of K. The variation of K from unity occurs due to the nonisentropic processes of turbulent diffusion of energy and chemical energy release.

It is realized that the energy release $\dot{Q}$ depends upon both the temperature and concentration. Assuming a second order reaction, we can show that with a stoichiometric mixture*

(9) $$\dot{Q} = a\rho\varepsilon^2 e^{-E/RT}$$

where E is the activation energy, ε is the mass fraction of unburnt gases, and a is a pre-exponential constant (which could be assumed dependent upon temperature if desired). Of course, it is possible to use some other relationship for $\dot{Q}$ instead of Eq. (9) if so desired.

SPECIES EQUATION

It is clear from Eq. (5a) and Eq. (9) that the mass fraction of unburnt species must be determined as a function of space and time. The governing equation is

* Equation (9) could be easily modified to account for off-stoichiometric cases or could be replaced by a system of equations to describe detailed kinetics.

$$\frac{\partial \varepsilon}{\partial t} = \frac{\partial}{\partial \psi} \left(\rho^2 \alpha \frac{\partial \varepsilon}{\partial \psi} \right) - \frac{\dot{Q}}{Q} \tag{10}$$

where Q is the chemical energy per unit mass of unburnt gas. The first term on the right-hand side represents the turbulent diffusion of the unburnt species while the second term represents the depletion of the species due to combustion. Note that the turbulent diffusivity for mass transfer has been assumed equal to the diffusivity for energy transfer.

Using the perfect gas law and transforming to the non-dimensional variables, Eq. (10) may be rewritten as

$$\frac{\partial \varepsilon}{\partial \zeta} = \left(\frac{A}{v_o} \right)^2 \frac{\alpha}{\omega} p^2 \frac{\partial}{\partial \eta} \left[\left(\frac{1}{\theta} \right)^2 \frac{\partial \varepsilon}{\partial \eta} \right] - \frac{\dot{Q}}{\omega Q} \, . \tag{11}$$

The boundary conditions are

$$\frac{\partial \varepsilon}{\partial \eta} (\zeta, 0) = 0 \tag{12}$$

and

$$\frac{\partial \varepsilon}{\partial \eta} (\zeta, 1) = 0 \tag{13}$$

which imply that no mass diffuses through the cylinder head or piston face. The initial condition is given as $\varepsilon = 1$ everywhere throughout the combustion chamber when the value of ζ is ζ_o except for a small region near the spark plug where ignition occurs.

Rather than integrating Eq. (5a) and Eq. (11) simultaneously, it is convenient to define

$$\beta = K + \frac{Q}{c_p T_o} \varepsilon \, . \tag{14}$$

Then combination of Eqs. (5a), (6a), and (7a) with Eqs. (11), (12), and (13) leads to the following equation:

$$(15) \qquad \frac{\partial \beta}{\partial \zeta} = \left(\frac{A}{V_o}\right)^2 \frac{\alpha}{\omega} P^{2/\gamma} \frac{\partial}{\partial \eta}\left[\frac{\lambda}{K^2} \frac{\partial \beta}{\partial \eta}\right] + \frac{\dot{Q}}{\omega c_p T_o}\left[P^{1-\gamma/\gamma} - 1\right]$$

with the boundary conditions

$$(16) \qquad \frac{\partial \beta}{\partial \eta}(\zeta, 0) = 0$$

and

$$(17) \qquad \frac{\partial \beta}{\partial \eta}(\zeta, 1) = 0 \ .$$

The initial condition for β is readily determined given the initial conditions for ε and K.

In a constant pressure process it would follow that the Eq. (15) and the boundary conditions Eqs. (16) and (17) are satisfied by the solution β = constant. With varying pressure, however, some variation in β occurs. The variation in β is substantially less than the variation in ε and, for this reason, numerical errors are minimized when Eqs. (15), (16), and (17) are employed in lieu of Eqs. (11), (12), and (13). Therefore, the system of partial differential equations which are to be solved numerically are Eqs. (5a) and (15) subject to the definitions Eqs. (9) and (14), to the boundary conditions Eqs. (6a), (7a), (16), and (17), and to the appropriate initial conditions.

NUMERICAL INTEGRATION OF THE EQUATIONS

Since the coefficients of the second derivative terms in Eqs. (5a) and (15) are strong functions of time or crank angle ζ, the step-size $\Delta\zeta$ required for accuracy could vary substantially with ζ. In order to proceed with constant step-size, it is convenient to make a certain transformation; i.e.,

$$z = \left(\frac{A}{V_o}\right)^2 \frac{1}{\omega} \int_{\zeta_o}^{\zeta} \alpha P^{2/\gamma} d\zeta' \quad . \tag{18}$$

Now Eqs. (5a) and (15) are transformed to

$$\frac{\partial K}{\partial z} = \frac{\partial}{\partial \eta}\left(\frac{1}{K^2}\frac{\partial K}{\partial \eta}\right) + \frac{\lambda \varepsilon^2}{\Omega K P} e^{-\theta_c/\theta} \tag{19}$$

and

$$\frac{\partial \beta}{\partial z} = \frac{\partial}{\partial \eta}\left(\frac{1}{K^2}\frac{\partial \beta}{\partial \eta}\right) + \frac{\lambda \varepsilon^2}{\Omega K} e^{-\theta_c/\theta}\left[\frac{1}{P} - \frac{1}{P^{1/\gamma}}\right] \tag{20}$$

subject to the definitions*

$$\Omega = \left(\frac{A}{V_o}\right)^2 \frac{\alpha}{\omega} = C_3 |\sin \zeta| + C_1 e^{-C_2(\zeta - \zeta_3)} \quad ,$$

$$\theta_c = E/RT_o; \quad \varepsilon = \frac{c_p T_o}{Q}(\beta - K); \quad \theta = K P^{\frac{\gamma-1}{\gamma}} \quad ,$$

$$\lambda = Q_m/(\omega c_p T_o V_o) \quad ,$$

(21)

$$C_1 = C_2(AL_2/V_o)^2 = 4\delta_3 \chi/[\pi(\gamma-1)\delta_1 \frac{B}{L_2} \delta_2 \zeta_\gamma (\frac{1+\chi}{\chi-1} - \cos \zeta_o)^2] \quad ,$$

$$C_2 = u_I/L_2\omega = \delta_1 \frac{B}{L_2} \delta_3 \chi/[\delta_2 \delta_4 \pi(\chi-1)] \quad ,$$

$$C_3 = \frac{AL_1}{V_o} \frac{\chi-1}{2} \frac{V_{min}}{V_o} = 2/[\delta_1 \frac{B}{L_1}(\frac{1+\chi}{\chi-1} - \cos \zeta_o)^2] \quad ,$$

---

* Note that the absolute value of the piston velocity is used to determine the diffusivity. Also, χ is defined as the compression ratio, B is the bore, V_{min} is the chamber volume with the piston at top dead center, δ_1, is the stroke to bore ratio, δ_2 is intake valve area to piston area ratio, δ_3 is the volumetric efficiency of the cylinder, and δ_4 is the duration of time during which the intake valve is open divided by the time for piston traverse between top dead center and bottom dead center.

and the conditions

$$\frac{\partial K}{\partial \eta}(\zeta,0) = \frac{\partial K}{\partial \eta}(\zeta,1) = \frac{\partial \beta}{\partial \eta}(\zeta,0) = \frac{\partial \beta}{\partial \eta}(\zeta,1) = 0 \,, \tag{22}$$

$$K(0,\eta) \quad \text{and} \quad \beta(0,\eta) \quad \text{specified} \,, \tag{23}$$

$$P = (1/V)\int_0^1 \theta d\eta = \left[(1/V)\int_0^1 K d\eta\right]^{\gamma} \,. \tag{24}$$

Equations (19) and (20) have been placed into a finite difference form by means of the method of quasi-linearization (3,4,5). A three-point formula is employed for the difference representation of the first derivatives with respect to z. This allows second-order accuracy in Δz. n and j are integers such that we have the relations $z = n\Delta z$ and $\eta = j\Delta\eta$. ℓ is an integer denoting the step in the iterative scheme to be described. The difference equations obtained are:

$$A^{\ell}_{n,j} K^{\ell+1}_{n,j+1} + B^{\ell}_{n,j} K^{\ell+1}_{n,j} + C^{\ell}_{n,j} K^{\ell+1}_{n,j-1} = D^{\ell}_{n,j} \tag{25}$$

and

$$F^{\ell}_{n,j} \beta^{\ell+1}_{n,j+1} + G^{\ell}_{n,j} \beta^{\ell+1}_{n,j} + H^{\ell}_{n,j} \beta^{\ell+1}_{n,j-1} = K^{\ell}_{n,j} \tag{26}$$

where the definitions have been made that

$$A_{n,j} = -\frac{1}{(K^2)^{\ell}_{n,j+1}} \,; \qquad C^{\ell}_{n,j} = \frac{1}{(K^2)^{\ell}_{n,j-1}} \,,$$

$$B^{\ell}_{n,j} = \lambda\left(\frac{c_p T_o}{Q}\right)^2(\Delta\eta)^2\left[\frac{(\beta-K)^2 e^{-\theta_c/KP^{(\gamma-1)/\gamma}}}{\Omega KP}\right]^{\ell}_{n,j}\left\{\frac{1}{K^{\ell}_{n,j}} + \frac{2}{(\beta-K)^{\ell}_{n,j}}\right.$$

$$\left. - \frac{\theta_c}{(K^2)^{\ell}_{n,j}(P^{\gamma-1/\gamma})^{\ell}_{n}}\right\} + \frac{2}{(K^2)^{\ell}_{n,j}} + \frac{3}{2}\frac{(\Delta\eta)^2}{\Delta z} ,$$

$$D^{\ell}_{n,j} = 2\left[\frac{2}{K^2_{n,j}} - \frac{1}{K^2_{n,j+1}} - \frac{1}{K^2_{n,j-1}}\right]$$

$$+ \lambda\left(\frac{c_p T_o}{Q}\right)^2(\Delta\eta)^2\left[\frac{(\beta-K)^2 e^{-\theta_c/KP^{(\gamma-1)/\gamma}}}{\Omega KP}\right]^{\ell}_{n,j}\left\{2 + 2\frac{K^{\ell}_{n,j}}{(\beta-K)^{\ell}_{n,j}}\right.$$

$$\left. - \frac{\theta_c}{(P^{\gamma-1/\gamma})^{\ell}_{n} K^{\ell}_{n,j}}\right\} + (4K_{n-1,j} - K_{n-2,j})\frac{(\Delta\eta)^2}{\Delta z} ,$$

$$F^{\ell}_{n,j} = -\frac{1}{(K^2)^{\ell+1}_{n,j}} - \frac{K^{\ell+1}_{n,j-1} - K^{\ell+1}_{n,j+1}}{(K^2)^{\ell+1}_{n,j}} ,$$

$$H^{\ell}_{n,j} = -\frac{1}{(K^2)^{\ell+1}_{n,j}} + \frac{K^{\ell+1}_{n,j-1} - K^{\ell+1}_{n,j+1}}{(K^3)^{\ell+1}_{n,j}} ,$$

$$G^{\ell}_{n,j} = 2\lambda\left(\frac{c_p T_o}{Q}\right)^2(\Delta\eta)^2\left\{\frac{[1 - P^{(\gamma-1)/\gamma}]e^{-\theta_c/KP^{(\gamma-1)/\gamma}}}{\Omega KP}\right\}^{\ell-1}_{n,j}$$

$$\cdot (K^{\ell+1}_{n,j} - \beta^{\ell+1}_{n,j}) + \frac{2}{(K^2)^{\ell+1}_{n,j}} + \frac{3}{2}\frac{(\Delta\eta)^2}{\Delta z} ,$$

$$K^{\ell}_{n,j} = \lambda\left(\frac{c_p T_o}{Q}\right)^2 (\Delta\eta)^2 \left\{ \frac{[1 - P^{(\gamma-1)/\gamma}]e^{-\theta_c/KP^{(\gamma-1)/\gamma}}}{\Omega KP} \right\}^{\ell+1}_{n,j}$$

$$\cdot [(\beta^{\ell}_{n,j} - K^{\ell+1}_{n,j})^2 - 2(\beta^{\ell}_{n,j} - K^{\ell+1}_{n,j})\beta^{\ell}_{n,j}]$$

$$+ (4\beta_{n-1,j} - \beta_{n-2,j})(\Delta\eta)^2/2\Delta z \ .$$

Note that when n = 1 the last terms in $D^{\ell}_{n,j}$ and $K^{\ell}_{n,j}$ are replaced by $K_{o,j}(\Delta\eta)^2/\Delta z$ and $\beta_{o,j}(\Delta\eta)^2/\Delta z$. Also when n = 1 the last term in each of $B^{\ell}_{n,j}$ and $G^{\ell}_{n,j}$ is replaced by $(\Delta\eta)^2/\Delta z$. The boundary conditions Eq. (22) are replaced by

$$K^{\ell+1}_{n,-1} = K^{\ell+1}_{n,1} \ ; \quad K^{\ell+1}_{n,j+1} = K^{\ell+1}_{n,j-1}$$

(27)

$$\beta^{\ell+1}_{n,-1} = \beta^{\ell+1}_{n,1} \ ; \quad \beta^{\ell+1}_{n,j+1} = \beta^{\ell+1}_{n,j-1}$$

with the initial conditions $K_{o,j}$ and $\beta_{o,j}$ given for all j of interest. Equation (24) is represented by

$$P^{\ell+1}_{n} = \left[(1/V_n)\Delta\eta\left(\frac{1}{2}\left(K^{\ell}_{n,o} + K^{o}_{n,j}\right) + \sum_{j=1}^{J-1} K^{\ell}_{n,j}\right)\right]^{\gamma} . \tag{28}$$

The method of quasi-linearization is a technique for improving the accuracy of the coefficients in Eqs. (25) and (26) in an iterative manner. At each value of n, the solutions for all j are obtained in each step of the iteration until satisfactory convergence occurs. Then, the solution for the next value of n is determined. The iteration begins by choosing $(\quad)^{\ell+1}_{n,j} = (\quad)_{n-1,j}$ which is the final value from the previous iteration. The coefficients in Eqs. (25) and (26) have been defined such that,

for each value of n and each value of $\ell+1$, the tridiagonal matrix Eq. (25) is solved. Then $F^{\ell}_{n,j}$, $G^{\ell}_{n,j}$, $H^{\ell}_{n,j}$, and $K^{\ell}_{n,j}$ are calculated and the other tridiagonal matrix Eq. (26) is solved. Now the index ℓ is increased by unity and the coefficients in Eq. (25) may be calculated for the next step in the iteration and so forth.

The initial conditions were chosen such that, at $\zeta = \zeta_o$, K had a Gaussian distribution near $\eta = 0$ but $K = 1$ for larger η. ε also had a Gaussian distribution chosen in such a way as to relate thermal energy to chemical energy. This procedure was intended to simulate spark ignition.

The calculations were performed on the IBM 360/91 computer.*

RESULTS OF THE CALCULATIONS AND DISCUSSION

The calculations have been performed in a limited number of cases and results for profiles of nondimensional pressure, nondimensional temperature and mass fraction of unburnt species have been obtained. Note that the pressure and temperature are nondimensionalized with respect to the pressure and chamber temperature just prior to ignition. These reference conditions may be determined from the known conditions at the end of intake by assuming an isentropic compression up to the point of ignition. Thus, knowledge of the volumetric efficiency and maximum volume of the chamber leads to the determination of the dimensional pressure and dimensional temperature profiles.

* The author wishes to acknowledge Mr. T.O. Williams for the programming of this finite difference scheme.

The parameters in the basic case (Case I) were chosen as follows:

$$\theta_c = 20.0\,, \qquad \lambda = 1.28 \times 10^5\,, \qquad \delta_1 \frac{\beta}{L_1} = 40.0\,,$$

$$\zeta_o = -20^o\,, \qquad \chi = 10.0\,, \qquad \delta_2 = 0.1\,,$$

$$\delta_3 = 0.7\,, \qquad \delta_4 = 1.0\,, \qquad \delta_1 = -180^o\,,$$

$$\gamma = 1.3\,, \qquad \frac{Q}{c_p T_o} = 4.0\,, \qquad L_1 = L_2\,.$$

Note that λ is directly proportional to the pre-exponential constant in the chemical kinetic law and inversely proportional to the rpm value. The given value of λ represents a constant of the order of 10^{13} $cm^3/(mole\text{-}sec)$ and an rpm value of 2000. The value of θ_c implies a value of the activation energy which is about 20 $\frac{kcal}{mole}$.

The results for the unburnt mass fraction versus chamber position for various crank angles are presented in Figure 2. They indicate that burning begins near the spark plug and propagates towards the piston. The flame has a certain thickness and reaction and turbulent mass diffusion are significant throughout some portion of the chamber at each instant.

In Figure 3, K versus chamber position is plotted versus various crank angles. Again, the propagation of a flame structure is indicated. At the end of burning, K has a nearly uniform value between 4.0 and 5.0 due to mixing effects. This implies that temperature gradients tend to be eliminated by the mixing. Effects of wall quenching and heat transfer are not included in this

analysis, however. The nearly uniform and nearly time-independent value of K after the completion of burning at $\zeta = 0^{\circ}$ implies that an isentropic expansion is occurring.

Temperature versus chamber position for various crank angles is plotted in Figure 4. The previously-mentioned trends are also demonstrated there but it is also indicated that after combustion is completed the temperature decreases uniformly during the expansion process.

Now, a study may be performed of the effects of changing various parameters. A listing of the parameter survey is given in Table 1.

Table 1 - Summary of the Parameter Survey

Case	λ	θ_c	$\delta_1 \frac{\beta}{L_1}$	χ	ζ_o
I	1.28×10^5	20.0	40.0	10.0	-20°
II	1.28×10^5	20.0	50.0	10.0	-20°
III	1.60×10^5	20.0	40.0	10.0	-20°
IV	6.40×10^5	25.0	40.0	10.0	-20°
V	1.28×10^5	20.0	40.0	9.0	-20°
VI	1.28×10^5	20.0	40.0	10.0	-15°

The effects of changes in the ratio of stroke-to-eddy size (Case II) are demonstrated in Figures 5 and 6. It is seen that an increase (decrease) in the eddy size implies a decrease (an increase) in the burning angle. This indicates that design modifications which can change eddy size should have a profound effect upon burning angle. The effect upon peak pressures and temperatures would not be as profound but significant. Another

interpretation is that a decrease in the stroke (or maximum chamber length) implies a shorter travel distance for the flame and therefore a smaller burning angle. Realize that in these calculations, the compression ratio was held constant as the stroke was varied. Again peak temperatures were not too sensitive to the parameter change.

Figure 7 (Case III) shows the effect of increasing λ to the value of 1.60×10^5. This case can be viewed either as an increase in the pre-exponential kinetic constant or a decrease in the rpm value. Although the results indicate some decrease in the burning angle, it is not as large as would occur if the combustion process were constant in duration. The results indicate that as the rpm increases, the rate of turbulent mixing increases due to increases in the piston velocity and in the velocity of the mixture during intake (if the mass of the charge were only weakly dependent upon rpm). The burning angle is much less sensitive to the value of λ than to the value of θ_c. Peak temperatures are not too sensitive to the value of λ or the value of θ_c.

In Figure 8, we see the effect of increasing the nondimensional activation energy θ_c to a value of 25.0 and increasing λ to 6.40×10^5 (Case IV). Both parameters must be changed simultaneously if the burning angle is to remain at a realistic value. Increasing θ_c tends to slow down flame propagation while increasing λ results in a faster flame propagation.

Note that in Figure 9, the results for Case V are plotted. Here, the effect of decreasing the compression ratio χ to the value of 9.0 is considered. The decrease in the compression ratio

results in an increase in the burning angle. It is found, however, that the change in peak temperatures is not very significant.

In Figure 10, the effect of spark advance is demonstrated. In this Case VI, $\zeta_o = -15^o$ and, as expected, burning occurs later relative to top dead center. Interestingly enough, the burning angle is found to decrease as the spark is advanced. Apparently, this results from the larger value of the eddy diffusivity during the burning period. The larger diffusivity and more rapid mixing occur since the piston velocity during burning is larger when the burning occurs significantly away from top dead center.

The effects of the parameters upon the pressure results are indicated in Figure 11. It is seen that changes in the pre-exponential chemical kinetic constants, or in the rpm value, can produce somewhat significant variation in the pressure traces but changes in the activation energy can produce large changes. A modification in the eddy size is noticed; larger pressures are obtained sooner due to the decrease in burning angle as eddy size increases. The peak pressure, however, is only slightly higher. Also, it is noticed that the increased compression ratio results in an increase in the peak pressure. The spark advance modification results in a relatively more significant increase in the peak pressure.

The results of the calculations indicate that the primary factor in the eddy diffusivity given by (1) is the term due to piston motion. The term due to the intake is negligible in comparison. It should be noted, however, that interaction may exist in reality; the turbulence generated during intake may provide the

necessary initial conditions for the intensification of the turbulence by the piston motion.

The interesting results obtained are that the final value of K and the peak value of temperature θ were insensitive to parameter changes. Realize that K as defined before Eq. (5a) can be directly related to the entropy, so that the implication is that the final entropy is insensitive to parameter changes. This is not surprising since the combustion process is very nearly a constant volume process. That is, during combustion, the piston is near top dead center and moving slowly so that very little work is done by (or on) the piston. Therefore, with the chemical energy to be released given, it is found that the chemical kinetic constants, the rpm value, eddy-size, etc. have little effect upon temperature and entropy at the end of the combustion process. The peak temperature and the temperature at the end of the combustion process were very similar in the cases calculated here.

At this point, it is possible to use these pressure and temperature results to calculate the concentration of NO as a function of crank angle and chamber position. In particular, the concentration in the emissions could be calculated. These calculations are intended for the near future.

There is an earlier version of this paper (Sirignano (1971)) which comes to somewhat different conclusions. In the calculations presented there, larger eddies and slower chemical kinetics were employed. This resulted in "thick" flames. The present

calculations which result in thinner flames are now felt to be more realistic.*

The model could be extended in the future by considering the effects of heat transfer, dependence of the specific heat upon temperature and concentration, and more realistic geometries for flame propagation. An interesting application of a similar model of flame propagation to the Wankel combustion process is discussed in another paper by Bracco and Sirignano (1973). There, in fact, the combustion chamber is more reasonably modelled in a one-dimensional manner than in the reciprocating engine case.

* Discussions with Drs. J. Heywood and F. Bracco on this point were most useful.

REFERENCES

Bracco, F.V., and Sirignano, W.A., "Theoretical Analysis of Wankel Engine Combustion", Combustion Science and Technology.

Fay, J.A., and Kaye, H., "A Finite Difference Solution of Similar Non-Equilibrium Boundary Layers", AIAA Journal 5, pp. 1949-1954.

Lavoie, G.A., Heywood, J.B., and Keck, J.C., "Experimental and Theoretical Study of Nitric Oxide Formation in Internal Combustion Engines", Combustion Science and Technology 1, Feb. 1970, pp. 313-326.

Libby, P.A. and Chen, K.K., "Remarks on Quasilinearization Applied in Boundary-Layer Calculations", AIAA Journal 4, 1966, pp. 937-939.

Lichty, L.C., Internal Combustion Engines, 1939, pp. 456-457, McGraw-Hill.

Sirignano, W.A., "One-Dimensional Analysis of Combustion in a Spark Ignition Engine", Proceedings of 1971 Intersociety Energy Conversion Engineering Conference, Boston, Mass., August 3-5, 1971.

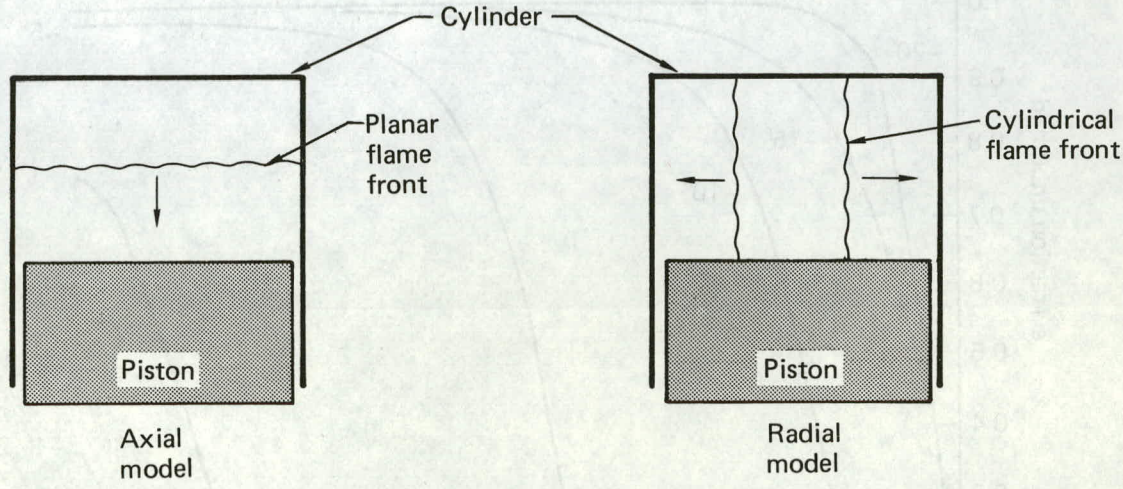
Cylinder
Planar
flame
front
Piston
Axial
model
Cylindrical
flame front
Piston
Radial
model

Figure 1

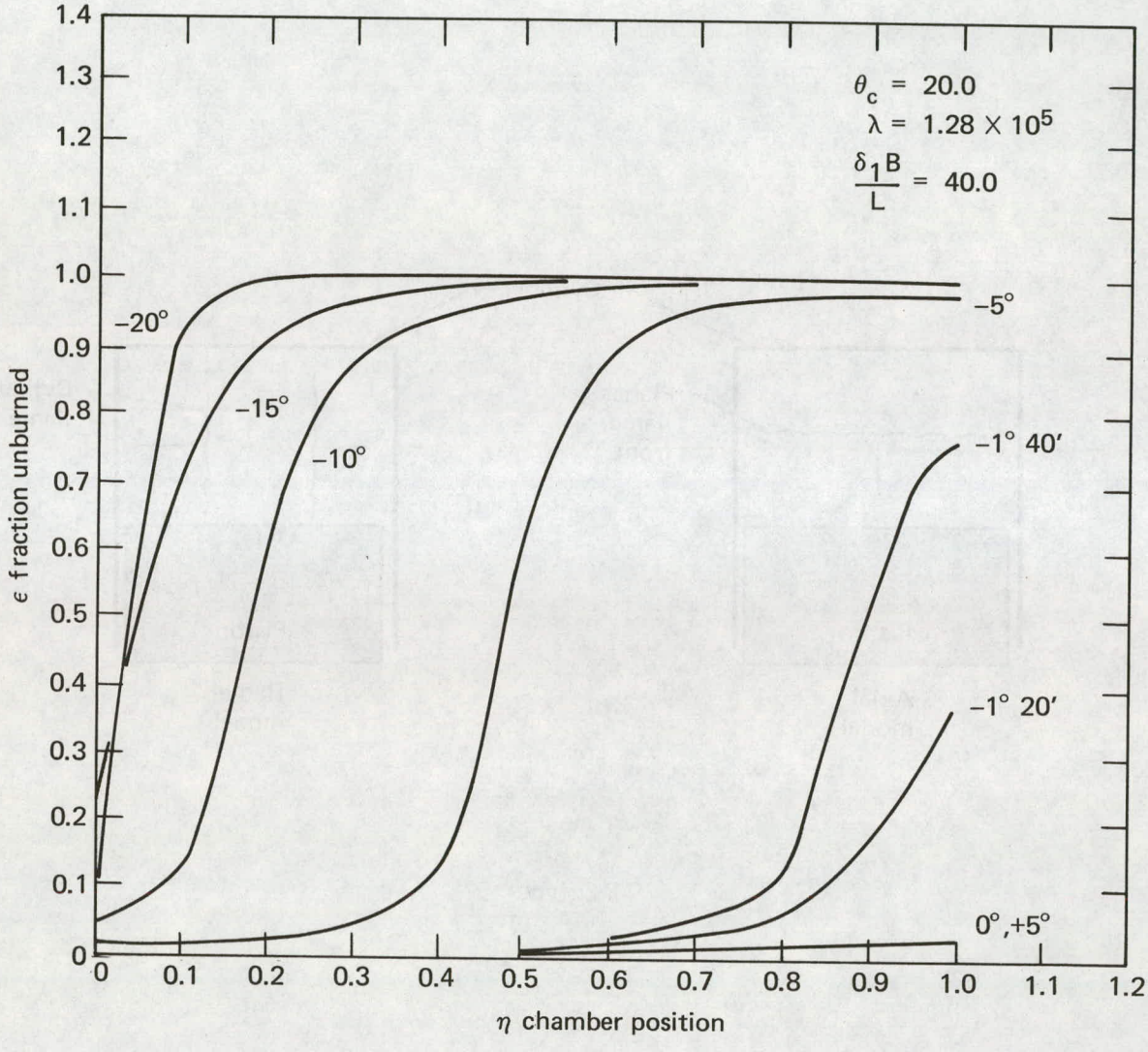
θ_c = 20.0
λ = 1.28 × 10^5
$\frac{\delta_1 B}{L}$ = 40.0
−20°
−15°
−10°
−5°
−1° 40′
−1° 20′
0°,+5°
ϵ fraction unburned
η chamber position
0
0.1
0.2
0.3
0.4
0.5
0.6
0.7
0.8
0.9
1.0
1.1
1.2
1.3
1.4

Figure 2

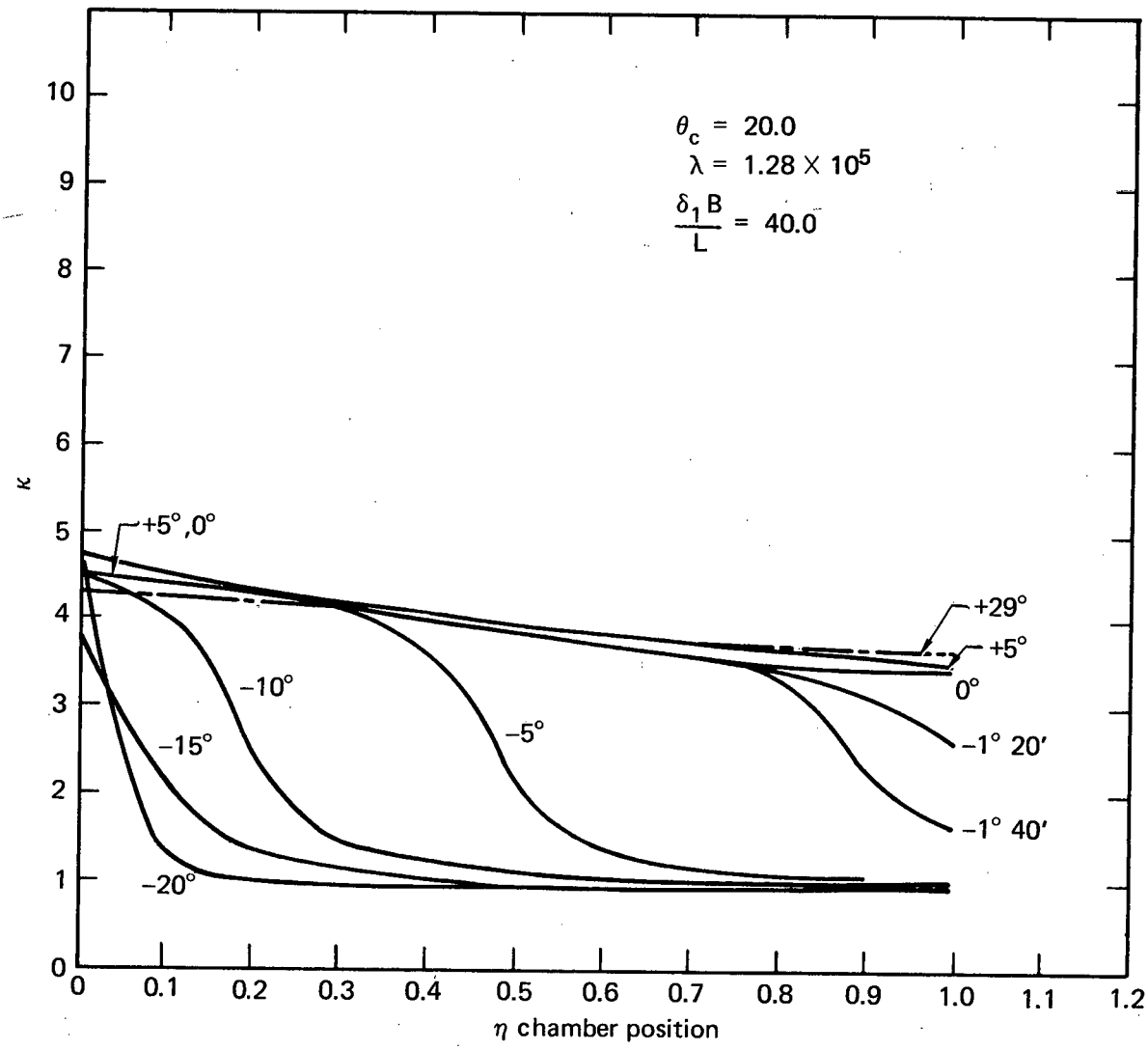
θ_c = 20.0
λ = 1.28 X 10^5
$\frac{\delta_1 B}{L}$ = 40.0
κ
η chamber position
+5°,0°
+29°
+5°
0°
−1° 20′
−1° 40′
−10°
−5°
−15°
−20°
0
0.1
0.2
0.3
0.4
0.5
0.6
0.7
0.8
0.9
1.0
1.1
1.2
1
2
3
4
5
6
7
8
9
10

Figure 3

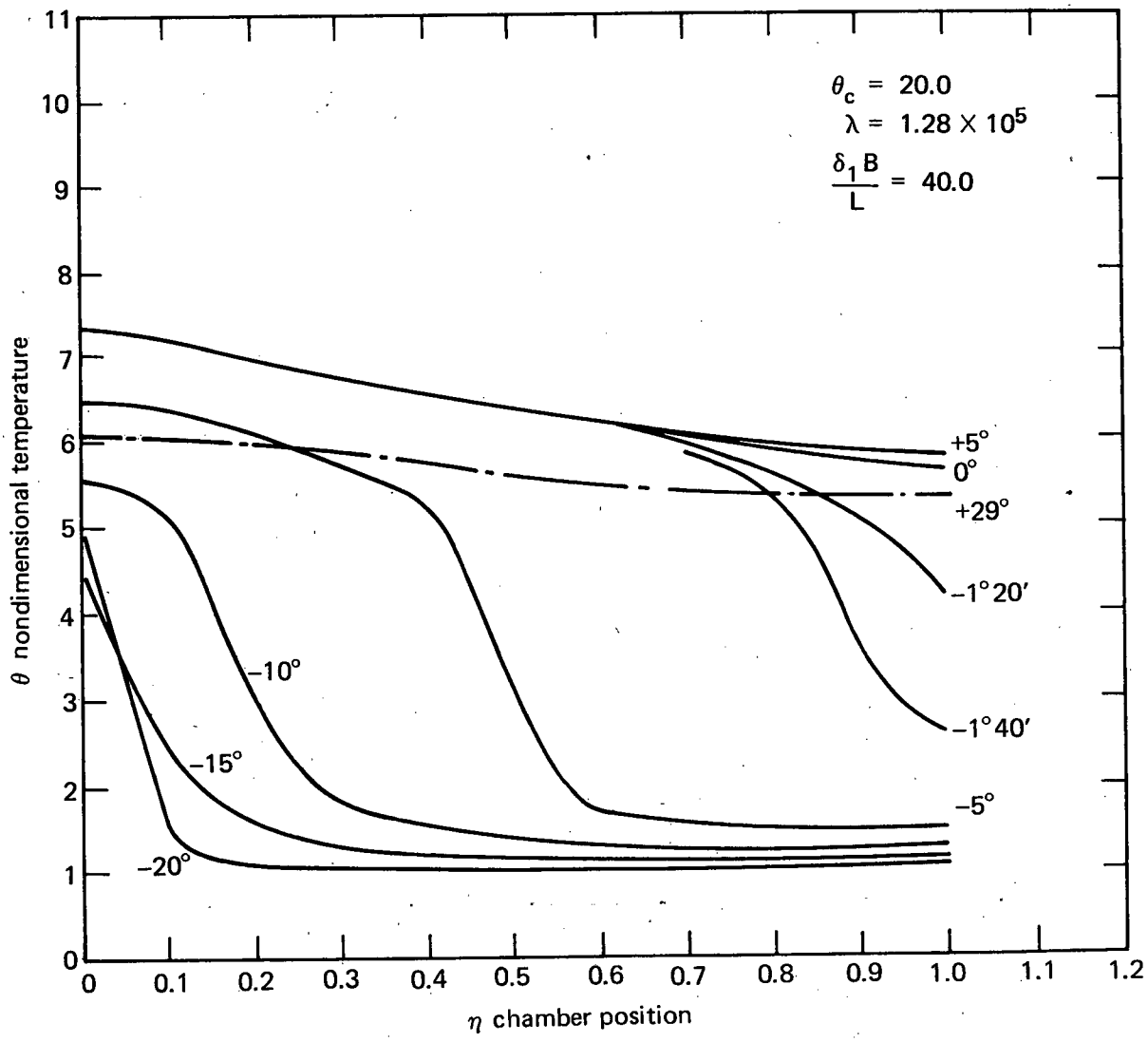
θ_c = 20.0
λ = 1.28 X 10^5
$\frac{\delta_1 B}{L}$ = 40.0
+5°
0°
+29°
−1°20′
−1°40′
−5°
−10°
−15°
−20°
θ nondimensional temperature
η chamber position
0
1
2
3
4
5
6
7
8
9
10
11
0
0.1
0.2
0.3
0.4
0.5
0.6
0.7
0.8
0.9
1.0
1.1
1.2

Figure 4

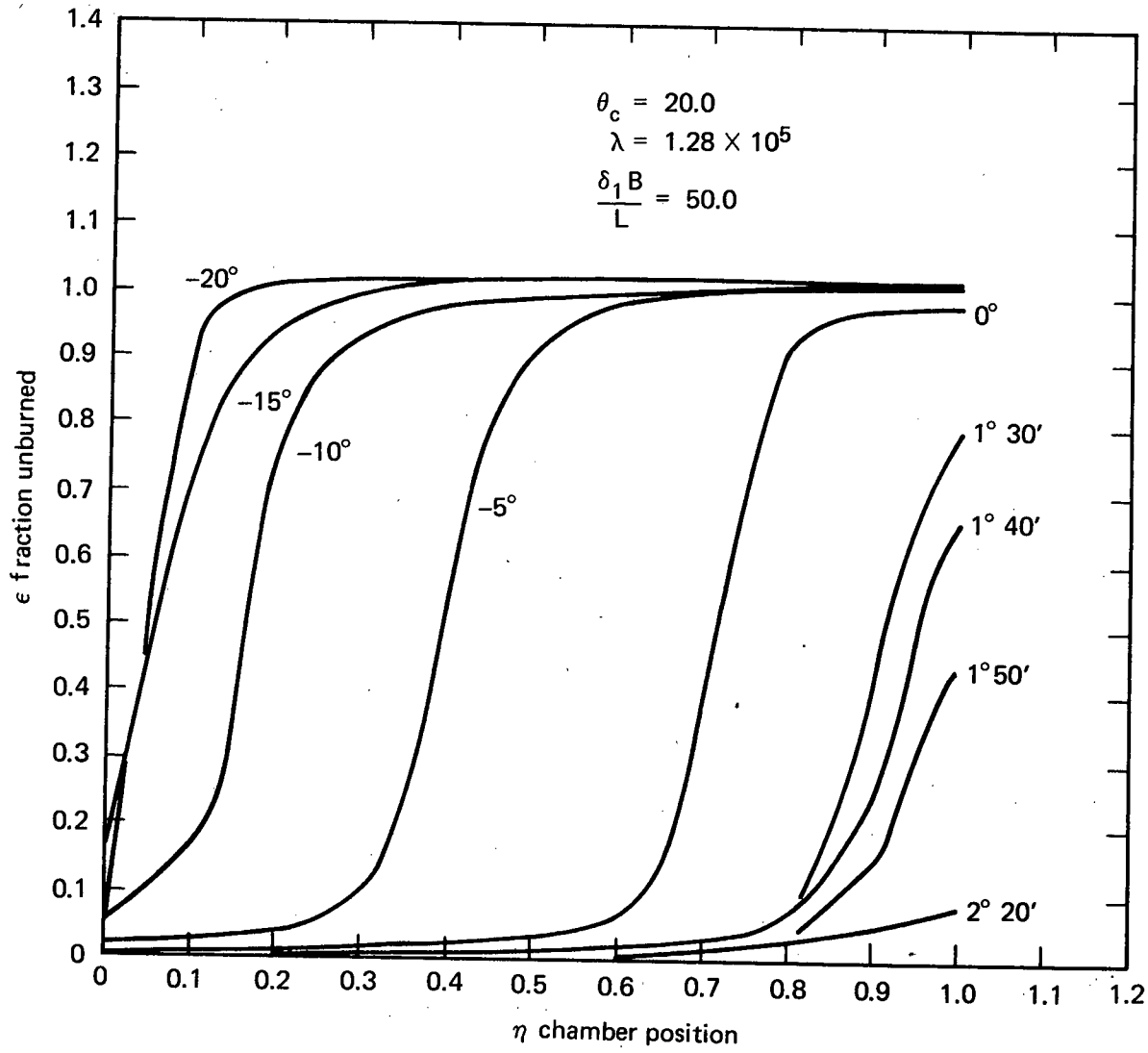
θ_c = 20.0
λ = 1.28 × 10^5
$\frac{\delta_1 B}{L}$ = 50.0
−20°
−15°
−10°
−5°
0°
1° 30′
1° 40′
1°50′
2° 20′
ϵ fraction unburned
η chamber position
0
0.1
0.2
0.3
0.4
0.5
0.6
0.7
0.8
0.9
1.0
1.1
1.2
1.3
1.4

Figure 5

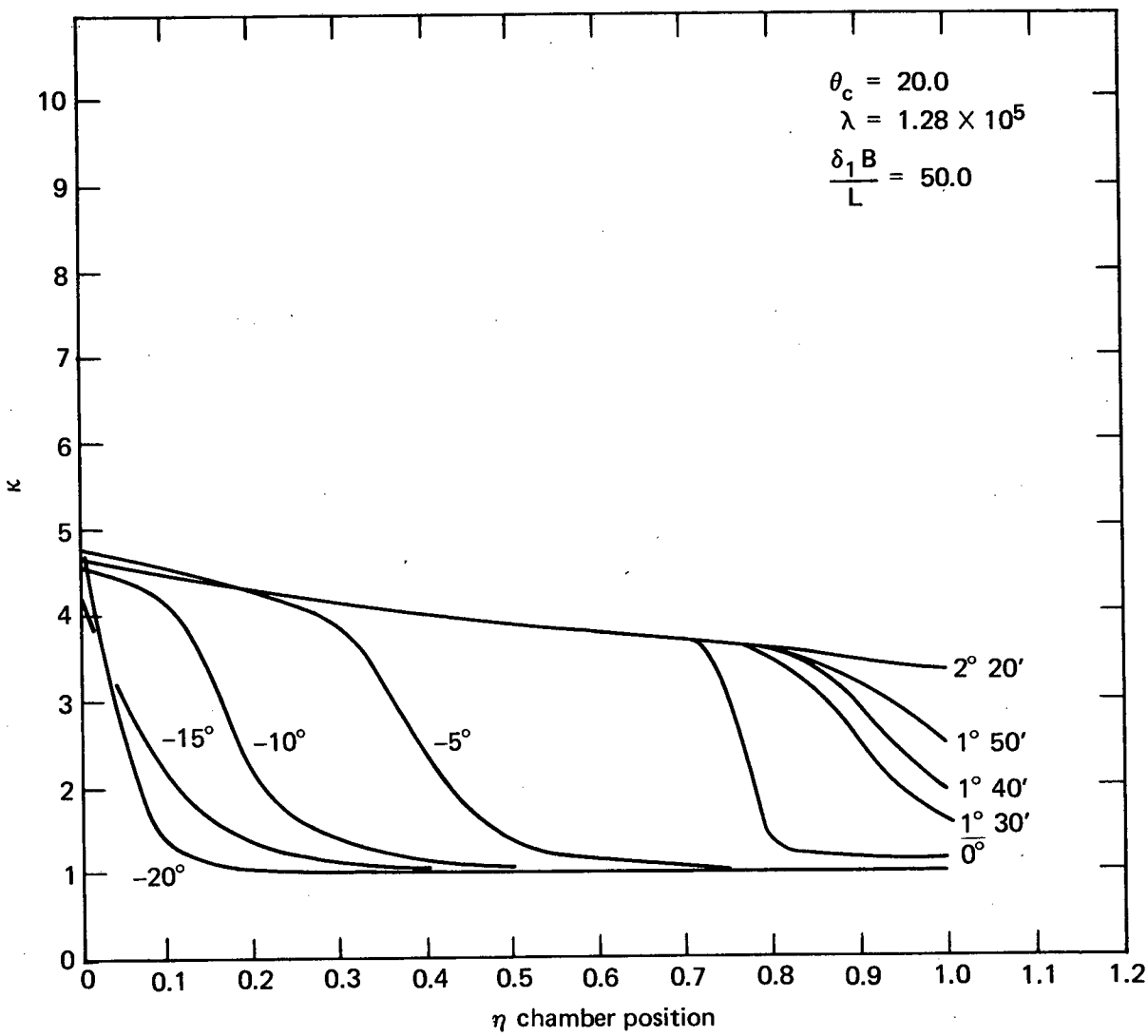
θ_c = 20.0
λ = 1.28 × 10^5
$\frac{\delta_1 B}{L}$ = 50.0
κ
η chamber position
2° 20′
1° 50′
1° 40′
1° 30′
0°
−5°
−10°
−15°
−20°
0
0.1
0.2
0.3
0.4
0.5
0.6
0.7
0.8
0.9
1.0
1.1
1.2
1
2
3
4
5
6
7
8
9
10

Figure 6

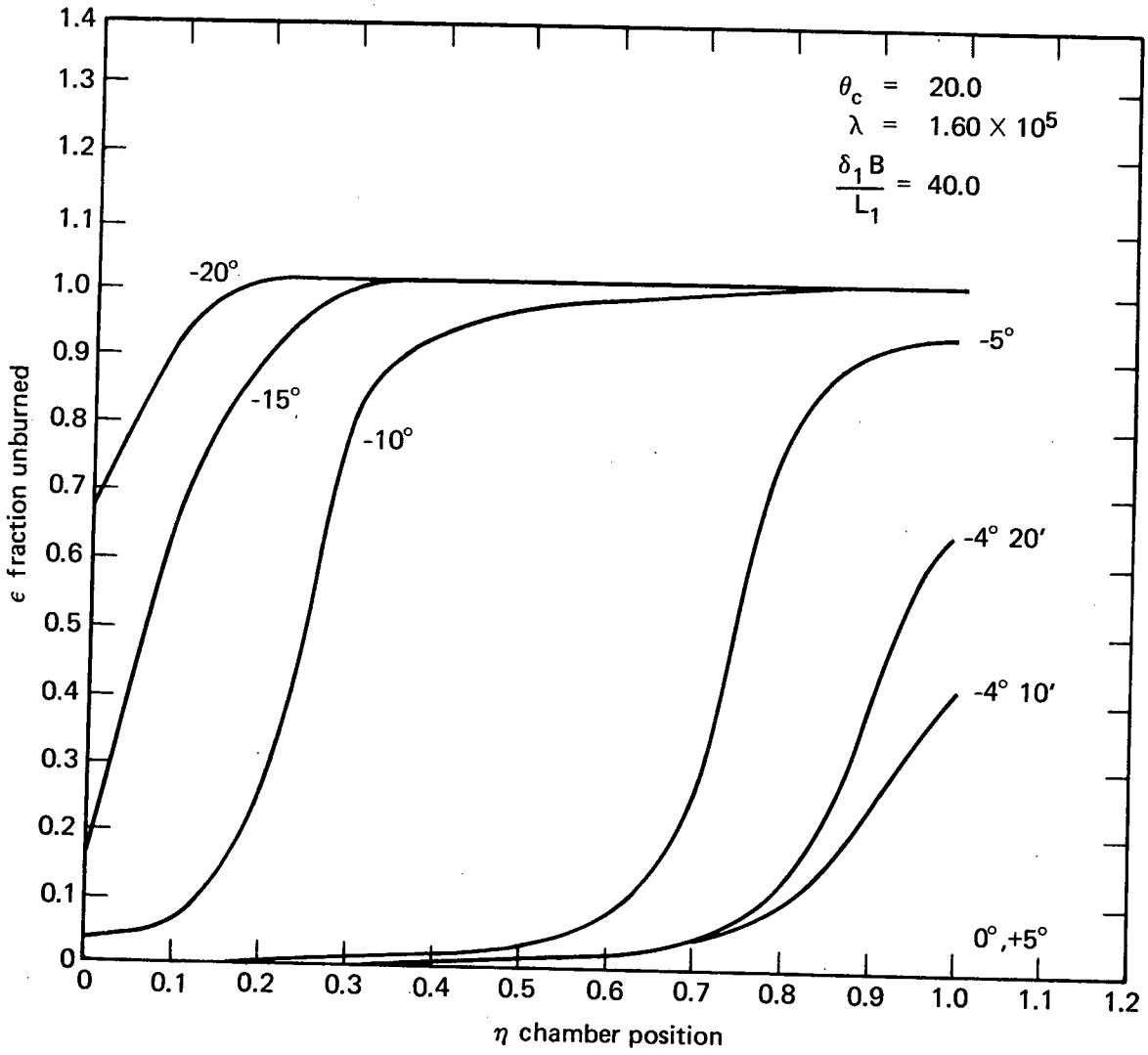
θ_c = 20.0
λ = 1.60 X 10^5
$\frac{\delta_1 B}{L_1}$ = 40.0
-20°
-15°
-10°
-5°
-4° 20′
-4° 10′
0°,+5°
ϵ fraction unburned
η chamber position
0
0.1
0.2
0.3
0.4
0.5
0.6
0.7
0.8
0.9
1.0
1.1
1.2
1.3
1.4

Figure 7

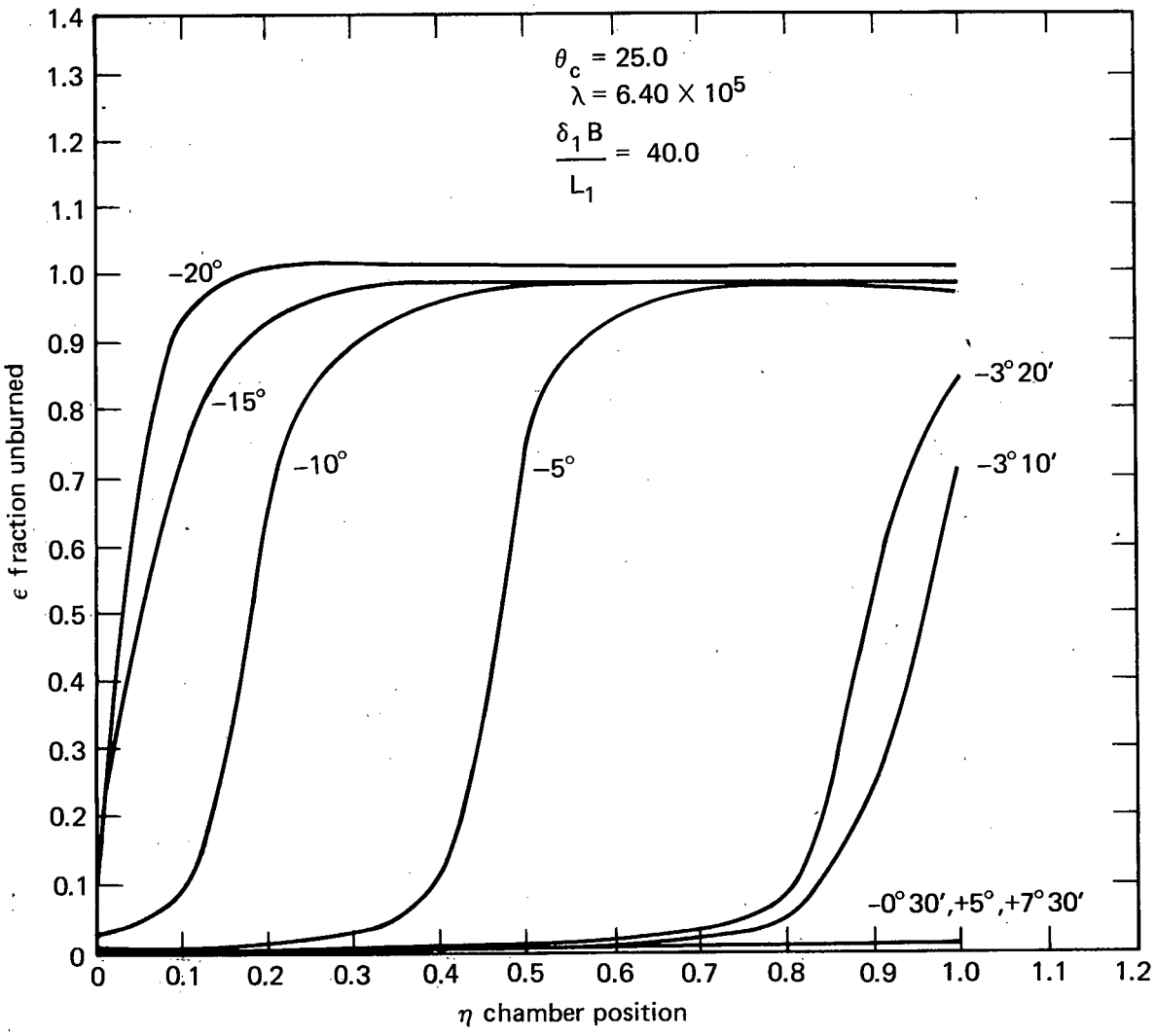
θ_c = 25.0
λ = 6.40 X 10^5
$\frac{\delta_1 B}{L_1}$ = 40.0
-20°
-15°
-10°
-5°
-3° 20′
-3° 10′
-0° 30′,+5°,+7° 30′
ϵ fraction unburned
η chamber position
0
0.1
0.2
0.3
0.4
0.5
0.6
0.7
0.8
0.9
1.0
1.1
1.2
1.3
1.4

Figure 8

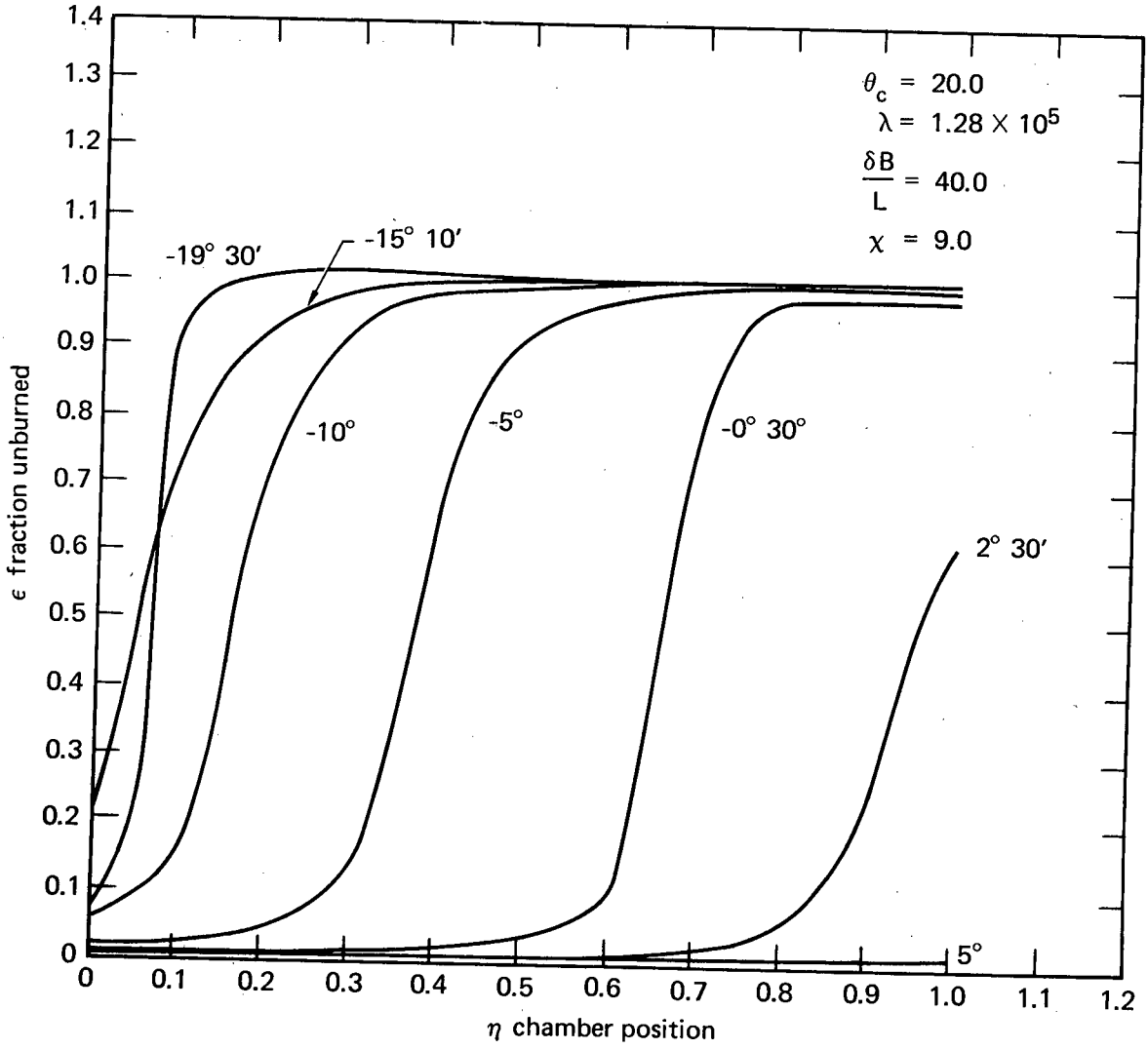
θ_c = 20.0
λ = 1.28 X 10^5
$\frac{\delta B}{L}$ = 40.0
χ = 9.0
-19° 30′
-15° 10′
-10°
-5°
-0° 30°
2° 30′
5°
ϵ fraction unburned
η chamber position
0
0.1
0.2
0.3
0.4
0.5
0.6
0.7
0.8
0.9
1.0
1.1
1.2
1.3
1.4

Figure 9

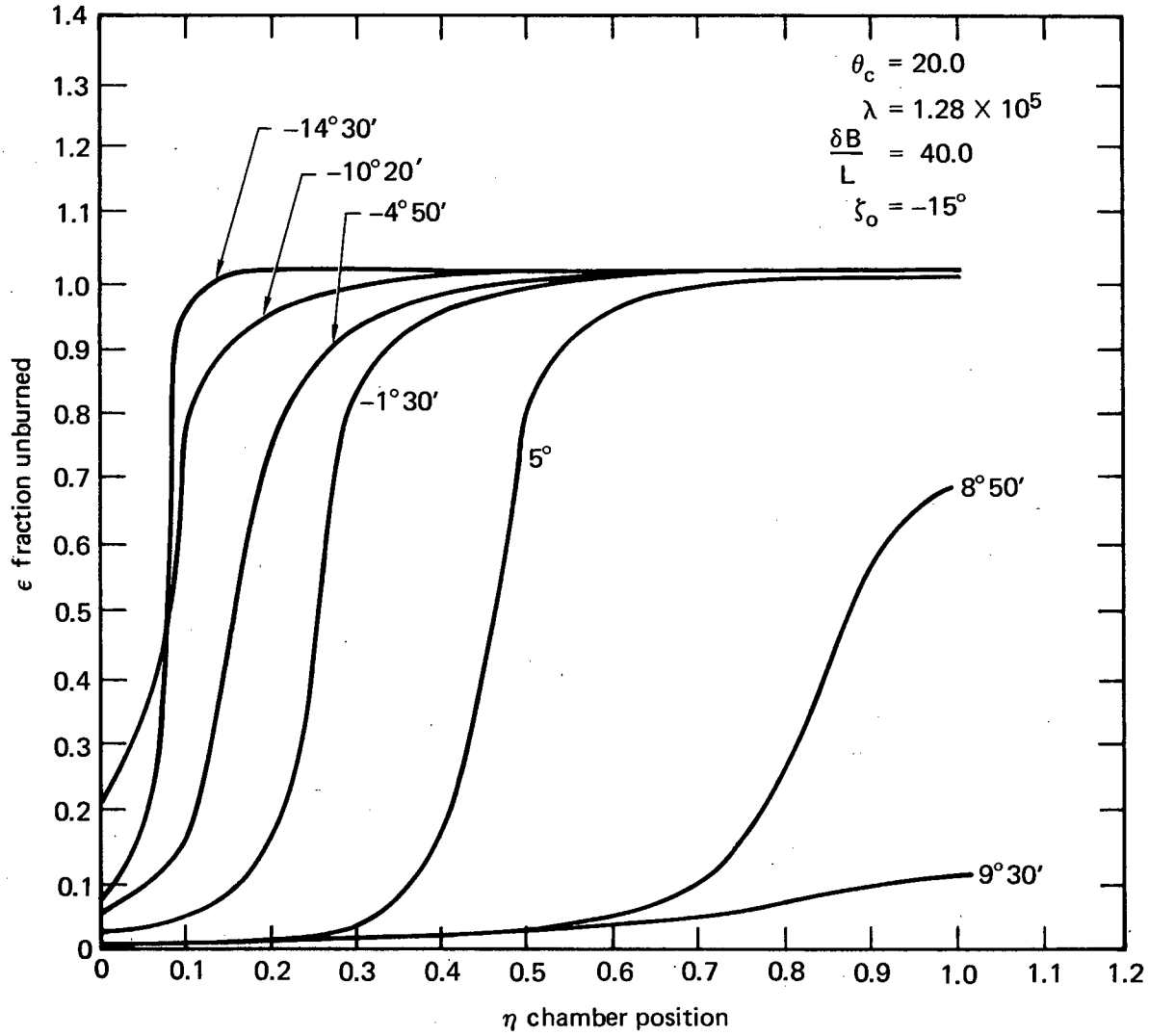
θ_c = 20.0
λ = 1.28 X 10^5
$\frac{\delta B}{L}$ = 40.0
ζ_o = −15°
−14°30′
−10°20′
−4°50′
−1°30′
5°
8°50′
9°30′
ϵ fraction unburned
η chamber position
0
0.1
0.2
0.3
0.4
0.5
0.6
0.7
0.8
0.9
1.0
1.1
1.2
1.3
1.4

Figure 10

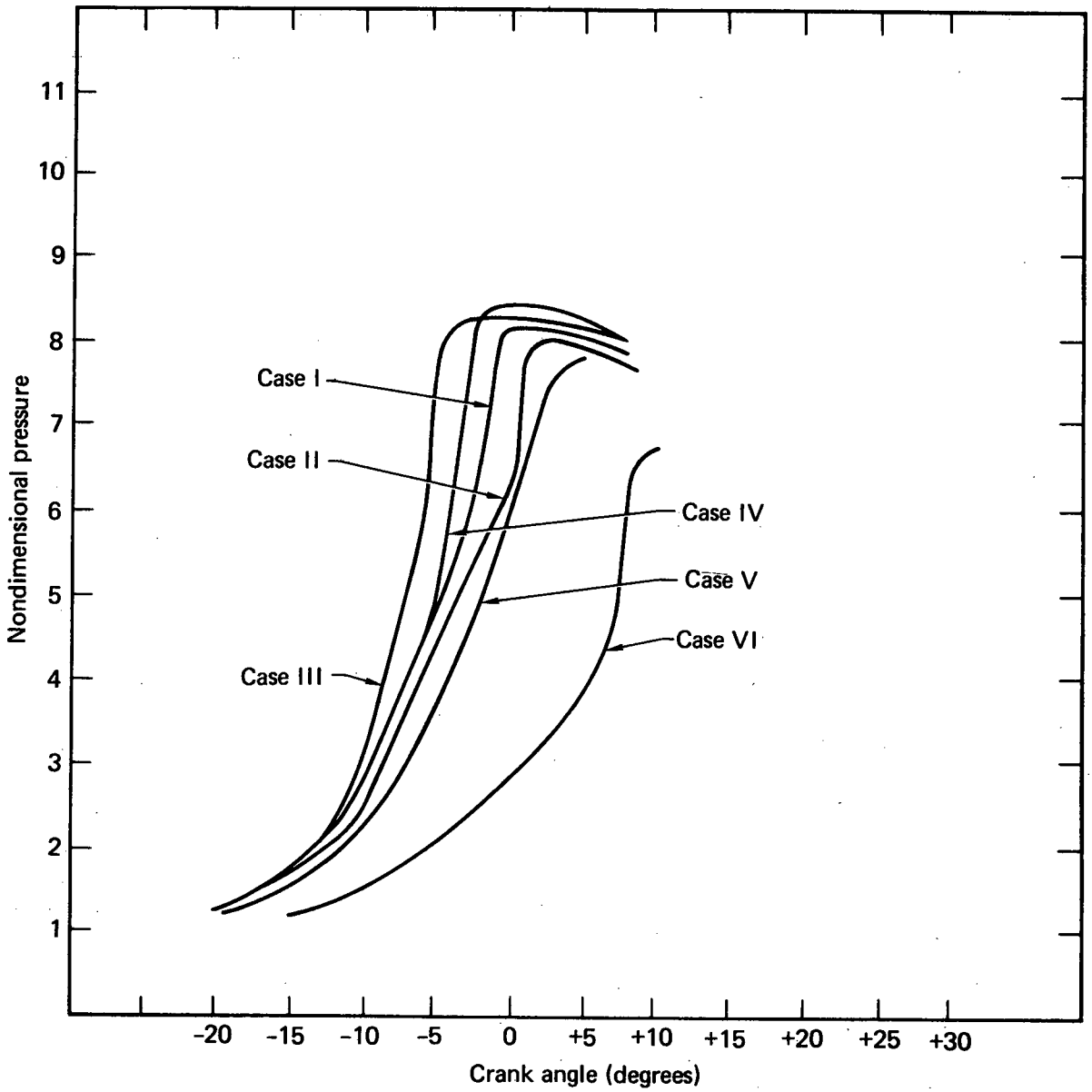
Nondimensional pressure
11
10
9
8
7
6
5
4
3
2
1
Case I
Case II
Case III
Case IV
Case V
Case VI
-20
-15
-10
-5
0
+5
+10
+15
+20
+25
+30
Crank angle (degrees)

Figure 11

The Mass Burning Rate of Single Coal Particles

Irvin Glassman

Department of Aerospace and Mechanical Sciences
Princeton University
Princeton, N. J. 08540

Abstract

The burning rate of coal particles are examined under two different sets of ideal conditions – (1) an ash-free material undergoing quasi-steady burning in which the kinetics of oxidation on the surface are fast with respect to the diffusional time for oxidizing material to reach the surface and (2) an ash-forming coal in which diffusion through the ash controls. Simple modification of analyses already in the literature show that for the ash-free condition, the mass burning rate per unit area is proportional to the mass fraction of the free stream oxygen to the first power and for the integral ash condition the burning rate is proportional to the square root of oxygen mass fraction. The burning rate of an ash-free particle is also shown to be a function of the chemical transformation at the surface. If CO forms, the burning rate is twice the value that would be obtained if CO_2 formed.

I. Introduction

The renewed interest in coal combustion motivated this paper which is essentially a re-analysis of mass burning rate determinations for certain unique properties of coal. There are two conditions examined. The first concerns the burning of ash-free coal under the assumption that the hetergeneous oxidation at the coal surface is fast with respect to the rate at which the oxidizing material is brought to the surface. This assumption is valid for large particles at high temperatures – the most practical case of coal combustion. Mulcahy and Smith [1] have shown that for pulverized coal even at high temperatures, the surface oxidation

kinetics control. Nevertheless, as will be shown, the burning rate dependence on free stream oxygen mass fraction is the same. Although most coals contain a modest amount of volatiles, they burn rapidly and the coal burning rate is determined by the consumption time of the carbon char. The second condition examined is the case of an ash-forming coal.

II. Ash-Free Coal

As described in the Introduction, the burning rate of coal at high temperatures is determined by the burning of the carbon char. Carbon is essentially non-volatile at the temperatures that can be created in coal combustion and thus its oxidation must take place hetergeneously; i.e., on the char surface. If the coal is porous then, under these conditions, it is not likely that the pores will play a role since the oxidizing material will be removed rapidly on the exterior surface before it can diffuse into the pores. The problem then can be idealized into the surface burning of a spherical particle of carbon. The general problem of surface (heterogeneous) oxidation has been treated by Frank-Kamenetskii [2]. For surface oxidation, whether the chemical rate or diffusion is controlling, in the steady state rate which oxidizer is being consumed at the surface by chemical reaction must be equal to the rate at which oxygen diffuses to the surface. Thus Frank-Kamenetskii writes the expression

$$G_o = k_s C_{o,s} = h_D (C_{o,\infty} - C_{o,s}) \tag{1}$$

G_o is the mass consumption rate per unit area (g/sec cm^2). k_s is heterogeneous specific reaction rate constant which includes the surface area and thus has units of velocity (cm/sec), $k_s = (k/S)$ where k is the ordinary Arrhenius rate constant for a first order reaction (sec^{-1}) and S is the surface area to volume ratio for the solid particle (cm^2/cm^3). h_D is the mass diffusion coefficient and as defined must have the units of velocity (cm/sec). It is inherent from Equation (1) that surface kinetics are assumed first order with respect to the oxygen concentration. C_o is the oxygen concentration (g/cm^3). The further subscripts s and ∞ refer to the surface and free stream respectively. The stoichiometric relation between the oxidizer and fuel can be written as

$$G_o = G_f/i \tag{2}$$

where G_f is the fuel consumption rate per unit area and i is the mass stoichiometric index. Thus Equation (1) may be written as

$$i\,G_o = i\,k_s\,\rho\,m_{o,s} = i\,h_D\,\rho\,(m_{o,\infty} - m_{o,s}) = G_f \tag{3}$$

in which ρ is the total gaseous density and m_o the mass fraction of oxygen. It is, of course, desirable to express the mass consumption rate of the fuel in terms of the known free stream condition, $m_{o,\infty}$. This result can be obtained by solving the two middle terms in Equation (3) for $m_{o,s}$. The simple algebraic result is

$$m_{o,s} = [h_D/(k_s+h_D)]m_{o,\infty}\ . \tag{4}$$

Substituting Equation (4) into (3), one obtains

(5) $$G_f = i\,\rho\,[k_s h_D/(k_s+h_D)]m_{o,\infty} = i\,\rho\,[h_D/(1+(h_D/k_s))]m_o \ .$$

It should be noted that (h_D/k_s) is a Damkohler number. When the chemical rates are fast with respect to the diffusion rate, small Damkohler number,

$$k_s >> h_D$$

then Equation (5) becomes

(6) $$G_f = i\,\rho\,h_D\,m_{o,\infty}$$

or from Equation (4)

(7) $$m_{o,s} << m_{o,\infty}$$

and $m_{o,s}$ may be assumed close to zero. When the chemical rates are slow compared to the diffusion rates, large Damkohler number,

$$k_s << h_D \ ,$$

Equation (5) gives

(8) $$G_f = i\,k_s\,\rho\,m_{o,\infty}$$

and Equation (4) shows that

(9) $$m_{o,s} \approx m_{o,\infty} \ .$$

Thus for the chemical rate controlling the mass consumption rate is found to be first order with respect to the free stream oxygen mass fraction and is a direct consequence of the assumption of first order kinetics.

Indeed, it appears from Equation (6), for diffusion controlling, that the consumption rate is first order with respect to the free stream oxygen mass fraction as well. Although this indeed will turn out to be the case for carbon, it is not apparent because h_D must be more clearly evaluated since there is diffusion of a gaseous product from the surface to the free stream. However, for carbon oxidation it will now be shown that this flux from the surface is small enough not to alter heat or mass diffusion to or from the surface.

In order to elaborate on this point it is interesting to examine the burning rate of a volatile fuel droplet in a quiescent atmosphere as initially given by Spalding [3]. Spalding has shown that

$$G_f = (D\rho/r)\ln(1+B) \tag{10}$$

where D is the molecular diffusion coefficient (cm^2/sec), r the particle radius (cm), and B the transfer number. It is convenient to write B in a form first written by Blackshear [4] and reviewed by the author [5]:

$$B_{fo} = \frac{i\, m_{o,\infty} + m_{fs}}{1 - m_{fs}}, \tag{11}$$

$$B_{fg} = \frac{C_p\,(T_\infty - T_s) - m_{fs}H}{L_v + H(m_{fs} - 1)}, \tag{12}$$

$$B_{of} = \frac{C_p\,(T_\infty - T_s) + i\, m_{o,\infty}H}{L_v}, \tag{13}$$

where H is the heat of combustion of the fuel (cal/g) and L_v is the latent heat of evaporation (cal/g). These results evolve from

solving the diffusion equations including the rate terms for heat, oxidizer and fuel. The non-homogeneous rate term can be eliminated by combining any of the two equations and writing the combined equation in terms of a new variable b. The transfer number arises when the equations are integrated and b is evaluated at the surface and in the ambient,

$$B \equiv b_{\infty} - b_s \quad . \tag{14}$$

Since there are three equations, there are three different forms of B, but they are equal. It is assumed in these types of developments that heat and mass diffusivity are equal. The equations and boundary conditions account for the mass efflux from the fuel surface and its subsequent effects on hear and mass diffusion.

For the case of coal burning on the surface the most convenient form of B is that given by Equation (11). m_{fs} for surface oxidation must be equal to zero and thus

$$B = i\, m_{o,\infty} \tag{15}$$

and Equation (10) becomes

$$G_f = \frac{D\rho}{r} \ln (1 + i\, m_{o,\infty}) \quad . \tag{16}$$

The case for condensed phase burning in a convective stream has been solved for a flat plate fuel surface by Emmons [6]. Emmons found

$$G_f = \frac{\mu}{\rho} \frac{Re_x^{1/2}}{x\sqrt{2}} [-f(0)] \tag{17}$$

where μ is the viscosity, Re the Reynold's number, x the distance

from the leading edge of the flat plate, and [-f(0)] is a modified Blasius function which is also a function of B. The oxygen dependence is in [-f(0)] and will be discussed later.

The stagnant film case, which represents convective flow parallel to the mass evolving from the fuel surface, gives an expression similar to Equation (10); i.e.,

$$G_f = (D\rho/\delta)\ln(1+B) \tag{18}$$

where δ is the boundary layer thickness. Of course, for the quiescent case, as found in heat transfer, $\delta = r$. A definition of h_D could be

$$h_D \equiv D/\delta \ . \tag{19}$$

The approximation given by Equation (18) is in reality quite good because B is small.

To evaluate B from Equation (15) the value of i must be known. The model for carbon combustion at high temperatures elaborated upon by Coffin and Brokaw [7] has been generally accepted. The concept is that CO forms at the surface diffuses away and is oxidized to CO_2 in the gas phase. The CO_2 diffuses to the surface, is the essential oxidizing agent and is reduced to CO by the Boudouard reaction

$$C + CO_2 \rightarrow 2CO \ .$$

No oxygen essentially reaches the surface, it is consumed by the CO in the gas phase. In this case it has been shown explicitly [4,5] that the stoichiometric index is 12/16 or 0.75. This result

may be seen by applying the Law of Heat Summation to the reactions in the overall system, i.e.,

$$CO + \tfrac{1}{2}O_2 \rightarrow CO_2 \qquad \text{(gas phase)}$$

$$\underline{CO_2 + C \rightarrow 2CO} \qquad \text{(surface)}$$

$$C + \tfrac{1}{2}O_2 \rightarrow CO \qquad \text{(overall)}$$

If CO_2 forms heterogeneously at the surface then the stoichiometry is

$$CO + \tfrac{1}{2}O_2 \rightarrow CO_2 \ .$$

For pure carbon, it is most likely that only CO forms at the surface. However, impurities could heterogeneously catalyst some CO to CO_2. Thus, although it is recommended that i be chosen equal to 0.75 it must be realized that for practical coals its exact value may be somewhat lower.

From either of the above results it is very apparent that B is a number small compared to one for combustion with air. Since $m_{o,\infty} = 0.23$ for air then B = 0.086 to 0.172. Thus

(20) $$\ln (1+B) \approx B$$

and Equation (18) becomes

(21) $$G_f = (D\rho/\delta)\, B = (D\rho/\delta)\, i\, m_{o,\infty}$$

which with Equation (19) takes the form

(22) $$G_f = h_D\, i\, m_{o,\infty}\, \rho$$

the same result as given by Equation (6). The physical meaning of

small B is that the surface efflux does not have any effect on the diffusional processes.

For small B, Equation (17) also can be reduced to the same form as Equation (22). B appears in an analytical manner in the boundary condition for the Blasius function. Therefore, one may assume [-f(0)] as analytic in B and, further, for the small B case, directly proportional to B. Thus the mass burning rate has the same oxidizer dependency for the particle burning in a convective atmosphere as in a quiescent atmosphere.

From Equation (22), one observes that the burning rate is not only directly proportional to the oxygen mass fraction but also the stoichiometric index. Consequently whether CO or CO_2 forms on the surface or not is crucial because the burning rate changes by a factor of two. One could have intuitively predicted this result because to form CO_2 one must diffuse twice as much oxygen to the surface.

The result for the dependency with respect to oxygen has been obtained by much more sophisticated analyses [2,8,9]. Many investigators have carried out detailed mathematical analyses of the ablation of carbon and of heterogeneously catalyzed systems. The purpose here was to show that since the transfer number could be shown small compared to one, the simple analyses by Frank-Kamenetskii give the proper oxidizer mass fraction dependency.

III. Ash-Forming Coal

If a coal forms an ash while it is being oxidized, then it is the diffusion of the oxidizer through the ash which controls the burning. Diffusion of oxygen to the surface, whether in quiescent or convective atmospheres, will always be very much faster than the diffusion through the ash layer. Thus, following a procedure similar to Knorre, et al. [10], the consumption rate of oxygen at the fuel surface may be written as

$$G_o = D_A \rho \frac{dm_o}{dr} \tag{23}$$

where D_A is the diffusion parameter for flow through the ash. From Equation (2),

$$G_f = i\, D_A \rho \frac{dm_o}{dr} \,. \tag{24}$$

Since $m_o \approx m_{o,\infty}$ at the outer edge of the ash and $m_o \approx 0$ at the surface, an approximate form of Equation (24) is

$$G_f = i\, D_A \rho \frac{m_{o,\infty}}{x} \tag{25}$$

where x is the thickness of the ash at any instant. Equation (25) would hold well provided x is small compared to the particle radius. In practical cases the tendency of the ash to separate from the char probably does keep x small. This analysis, of course, holds when the ash breaks away from the particle. The rate of conversion of the coal particle can be written as

$$G_f = \rho_c \, (dx/dt) \tag{26}$$

where ρ_c is the density of the coal. Equating Equations (25) and (26), one obtains

$$\rho_c \, (dx/dt) = i \, D_A \rho \, \frac{m_{o,\infty}}{x} \, . \tag{27}$$

Integrating and solving for x, one obtains

$$x = (2 \, D_A \rho \, i \, m_{o,\infty} \, t/\rho_c)^{1/2} \tag{28}$$

since $x = 0$ at $t = 0$. Equation (28) is combined with Equation (25) to give

$$G_f = (D_A \rho \, \rho_c \, i \, m_{o,\infty}/2t)^{1/2} \, . \tag{29}$$

Thus in the case of an ash forming coal, the burning rate decreases with time and proportional to the oxygen mass fraction to the one-half power. Similarly, it is proportional to $i^{1/2}$.

IV. Conclusions

For the case of non-ash forming coal particles burning at high temperatures in either a quiescent or convective atmosphere, it has been shown in a simple manner that the burning rate is directly proportional to the oxygen mass fraction. For coal particles which form an ash, the burning rate is proportional to the square root of the oxygen mass fraction.

The surface reaction is important in determining the burning rate as well. If CO forms at the surface in the ash-free case, the burning rate is twice as fast as if CO_2 forms.

V. References

[1] Mulcahy, M.F.R. and I.W. Smith, Rev. Pure Appl. Chem. 19, 81 (1969).

[2] Frank-Kamenetskii, D.A., "Diffusion and Heat Exchange in Chemical Kinetics," Chap. II, Princeton University Press, Princeton, N. J. (1955).

[3] Spalding, D.B., "Some Fundamentals of Combustion," Chap. 4, Butterworth, London (1955).

[4] Blackshear, P.L., Jr., "An Introduction to Combustion," Chap. V, Dept. of Mech. Eng., Univ. of Minnesota, Minneapolis, Minn. (1960).

[5] Glassman, Irvin, "Combustion," Chaps. 6 and 9, Academic Press, New York (1977).

[6] Emmons, H.W., Z. Angew. Math. Mech. 36, 60 (1956).

[7] Coffin, K.P. and R.S. Brokaw, N.A.C.A. Tech. Note 3929 (1957).

[8] Chung, P.M., "Chemically Reacting Non-Equilibrium Boundary Layers," p. 138, in "Advances in Heat Transfer," edited by J.P. Hartnett and T.F. Irvine, Jr., Academic Press, New York (1965).

[9] Ubhayakar, S.K., Combustion and Flame 26, 23 (1976).

[10] Knorre, G.F., K.M. Aref'yev, and A.G. Blokh, "Theory of Combustion Processes," Chap. 24, Transl. FTD-HT-23-495-68 by Foreign Tech. Div., Wright-Patterson AFB, Ohio (1968).

Studies of Hydrocarbon Oxidation in a Flow Reactor*

I. Glassman, F. L. Dryer and R. Cohen

Guggenheim Laboratories
and
Center for Environmental Studies
Princeton University
Princeton, N. J. 08540

I. Introduction

Recent concerns about energy needs and the associated environmental problems has again focused attention on the rather startling fact that after burning hydrocarbons for about a century a thorough understanding of their high temperature oxidation characteristics still does not exist. The central thrust of a program at Princeton on the homogeneous gas phase reaction kinetics of hydrocarbons at high temperatures is to contribute to this understanding by use of a turbulent flow reactor. Earlier work on methane and carbon monoxide oxidation kinetics (Dryer, 1972; Dryer and Glassman, 1973; Dryer, Naegeli and Glassman, 1971) has been reported in the literature. All the experimental work had been performed on the Princeton adiabatic, high temperature, turbulent-flow reactor (Dryer, 1972). Some recent experimental work on this reactor, albeit preliminary, and some further understanding of what is necessary to model complex chemical kinetic systems are thought to be of great significance in further elucidating the hydrocarbon

* This research effort was supported by the National Science Division, Research Applied to National Needs, Division of Energy and Resources Research and Technology, under Grant No. AER 75-09538.

oxidation kinetic process. More specifically this work which is reported here deals with some preliminary thinking and new results with respect to the processes in paraffin hydrocarbon combustion.

II. Experimental Apparatus

Basically, the Princeton flow reactor technique utilizes a heated cylindrical quartz duct 10 cm in diameter through which a hot inert carrier gas flows at velocities which yield Reynolds numbers in excess of 3500 (Figure 1). The reactor assembly is constructed so that the reactor walls rapidly equilibrate to the local gas temperature. Rapid mixing of small amounts of pre-vaporized reactants with the carrier is provided by radial injection at the throat of a high velocity mixing inlet nozzle. Proper adjustment of carrier temperature flow velocity and reactant concentrations result in a steady, one-dimensional, adiabatic reaction zone extending over a length of approximately 85 cm. Simultaneous thermal and chemical data at discrete axial locations in the reaction zone are obtained by longitudinal extension of an instrumented probe. Temperature measurements are made with a silica coated Pt/Pt-Rh thermocouple, and gas samples are removed through a water-cooled/expansion quenched stainless steel sampling probe. Consistent with the long range objective of more complex hydrocarbon oxidation studies, a sophisticated gas chromotographic chemical analysis procedure which was developed in this laboratory (Colket et al. (1973)), permits measurements of all stable hydrocarbon species (including partially oxidized compounds) as well as H_2 and O_2 to 1% precision.

The unique advantages of this flow reactor approach should be emphasized. By restricting experiments to highly diluted mixtures of reactants, and extending the reactions over large distances, gradients are such that diffusion may be neglected relative to convective effects (Glassman and Eberstein, 1963); thus, the measured specie profiles are a direct result of chemical kinetics only. This type of spreading is in contrast to low pressure one dimensional burner studies where diffusion effects must be determined analytically before useful chemical kinetic data are obtained. While these flame procedures have progressed significantly in their refinement, estimation of diffusive corrections remains very difficult.

Furthermore, in the flow reactor, uniform turbulence results not only in rapid mixing of the initial reactants, but radially 1-dimensional flow characteristics. Thus real "time" is related to distance through the simple plug flow relations. However, the relation of a specific axial coordinate to real time is not well defined since the initial time coordinate occurs at some unknown location within the mixing region. One would suspect that initial mixing history could therefore alter reaction phenomenon occurring downstream. However, the existence of very fast elementary kinetics, which initiate chemical reaction before mixing is complete, permit rapid adjustment of the chemistry to local conditions as the flow approaches radial uniformity. Furthermore, the large dilution of the reactants and rapidity of the kinetics reduce the coupling of turbulence and chemistry to the point that local kinetics are functionally related to the local mean flow properties (Glassman and

Eberstein, 1963). This conclusion is also supported experimentally by excellent agreement of the derived chemical kinetic data with that obtained from shock tubes and static reaction systems at other temperatures. Agreement also substantiates that the reactor surfaces do not significantly effect the gas phase kinetics. Comparison of flow reactor data from reactor tubes of significantly different surface to volume ratio also corroborates this conclusion. Finally and most important, the turbulent flow reactor approach permits kinetics measurements in a temperature range (800-1400K) generally inaccessible to low temperature methods (fast flow Electron Spin Resonance, Kinetic Spectroscopy techniques, static reactors, etc.) and high temperature techniques (shock tubes, low pressure post flame experiments).

III. Combustion of Paraffin Hydrocarbons

Combustion of paraffins above methane has always been thought to be complicated by the greater instability of the higher alkyl radicals and by the great variety of secondary products which can form. The oxidation mechanism characteristically follows the Semenov type. Minkoff and Tipper (1962) have reported some oxidation mechanisms of specific hydrocarbons.

At higher temperatures most have accepted the primary reaction in the system to be between the hydroxyl radical and the fuel.

$$RH + OH \rightarrow R + H_2O$$

Recent work at Princeton (Dryer, 1972) has suggested that other

reactions in addition to this one were important; mamely, in fuel lean and rich combustion

$$RH + O \rightarrow \dot{R} + OH$$

and in fuel rich combustion

$$RH + H \rightarrow \dot{R} + H_2 \ .$$

It is interesting to review a general pattern for the oxidation of hydrocarbons in flames as given by Fristrom and Westenberg (1965). They suggest two essentially thermal zones: the primary zone in which the initial hydrocarbons are attacked and reduced to CO, H_2, H_2O, and the various radicals (H, O, OH) and the secondary zone in which the CO and H_2 are oxidized. The primary zone, of course, is that in which the intermediates occur. In oxygen-rich saturated hydrocarbon flames, they suggest further that initially hydrocarbons lower than the initial fuel form according to

$$OH + C_nH_{2n+2} \rightarrow H_2O + C_nH_{2n+1} \rightarrow C_{n-1}H_{2n-2} + CH_3 \ .$$

Because hydrocarbon radicals higher than ethyl are thought to be unstable, the initial radical C_nH_{2n+1} usually splits off CH_3 and forms the next olefinic compound as shown. With hydrocarbons higher than C_3H_8, it is thought there may be fission into an olefinic compound and a lower radical. The radical alternately splits off CH_3. The formaldehyde which forms in the oxidation of the fuel and fuel radicals is rapidly attacked in flames by O, H, and OH, so that formaldehyde is usually found as a trace substance.

In fuel-rich saturated hydrocarbon flames, Fristrom and Westenberg state the situation is more complex, although the

initial reaction is simply the H atom abstraction analogous to the preceding OH reaction: e.g.

$$H + C_nH_{2n+2} \rightarrow H_2 + C_nH_{2n+1} \cdot$$

Under these conditions the concentration of H and other radicals is large enough that their recombination becomes important and hydrocarbons higher than the original fuel are formed as intermediates.

The general features suggested by Fristrom and Westenberg have been confirmed in recent experiments. However, this new work permits more detailed understanding of the high temperature oxidation mechanism. As stated earlier this work shows that under oxygen-rich conditions initial attack by O atoms must be considered as well as the primary OH attack. More importantly however, it has been established that the paraffin reactants produce intermediate products which are primarily olefinic and the fuel is consumed to a major extent before significant energy release occurs. The higher the initial temperature the greater the energy release as the fuel is being converted. This observation leads one to conclude that the olefin oxidation rate simply increases more appreciably with temperature; i.e., the olefins are being oxidized while they are being formed from the fuel. These conclusions are based on recent experimental results as typified by Figures 2-6 which represent the data taken throughout the reaction zone of ethane, propane, butane, hexane and 2-methyl pentane.

A summary of the intermediates formed from the oxidation of these four paraffin hydrocarbons is most revealing and is represented by Table I.

Table I

Fuel	Relative Hydrocarbon Intermediate Concentrations
ethane	ethene >> methane
propane	ethene > propene >> methane > ethane
butane	ethene > propene >> methane > ethane
hexane	ethene > propene > butene > methane >> pentene > ethane
2-methyl pentane	propene > ethene > butene > methane >> pentene > ethane

It would appear that the results in Table I would contradict elements of Fristrom and Westenberg's suggestion that the initial hydrocarbon radical C_nH_{2n+1} usually splits off the methyl radical. If this type of splitting were to occur, one could expect to find larger concentrations of methane. The large concentrations of ethene and propene found in all cases would suggest that primarily the initial C_nH_{2n+1} radical cleaves one bond from the carbon atom from which the hydrogen was abstracted. The bond next to this carbon atom is less likely to break since this type of cleavage would require both an electron and hydrogen transfer to form the olefin. The abstraction of hydrogen from a second carbon atom requires about 1.5 kcal less from the other carbon atoms (a tertiary carbon atom requires about 2.5 less). In a straight chain hydrocarbon there are, of course, more hydrogens on the first carbon atoms. Estimating relative probability of removal based on number and ease of removal and considering the cleavage rule mentioned indicates the proper trends designated by Table I and

relatively large concentrations of ethene and propene. These results suggest that oxidation studies of ethene and propene should be particularly important.

Figures 2-6 show clearly that experimentally there appears to be an initial iso-energetic step in the overall process. Of course, this step is not exactly iso-energetic. The conversion process from paraffin to olefin is endothermic; however, some of the hydrogen formed during what is essentially a pyrolysis step does react and release energy. The two reactions are compensating energetically. Thus, it is believed that this evidence suggests that there are three distinct, but coupled zones, in hydrocarbon combustion.

1) Following ignition, primary fuel disappears with little or no energy release and produces unsaturated hydrocarbons and hydrogen. A little of the hydrogen is concurrently being oxidized to water.
2) Subsequently, the unsaturated compounds are further oxidized to carbon monoxide and hydrogen. Simultaneously the hydrogen present and formed is oxidized to water.
3) Lastly, the large amount of carbon monoxide formed is oxidized to carbon dioxide and most of the heat release from the primary field is obtained.

Each zone must have a different temperature-rate dependency and thus at different temperatures the importance of a given step above may change. Again on the basis of some very preliminary experimental evidence as given by Figure 7 it is possible to put forth some interesting speculations. The initial conditions of the

experiment whose results are depicted in Figure 7 were such that not only was the stoichiometry more fuel rich than the examples of Figures 2-6 but also the initial temperature was higher. Examination of Figure 7 reveals that the maximum concentration of ethene is found earlier in the system. Essentially this trend indicates that the exothermic ethene oxidation step has become faster. This conclusion is supported by the fact that the temperature profile in Figure 7 rises continually and does not appear flat (iso-energetic) throughout most of the process as found for the conditions given in Figures 2-6.

The flow reactor permits highly reproducible accurate runs and analyses to be obtained. All the data points presented in Figures 2-7 are actually points and not smoothed data. Although present sampling techniques permit only stable species to be measured, estimates of radical reaction rates and rate constants can be made. For example, sample data during methane (Dryer and Glassman, 1973) oxidation as depicted in Figure 8 shows the presence of ethane and the subsequent transformation of this ethane to ethene. The ethane indicates the presence of and gives the clue to the methyl radical reaction rates and concentrations. Further, it is interesting to note in fuel rich, pre-mixed ethane oxidation system (Figure 7) that acetylene (ethyne) can be identified readily.

These results permit the conclusion that the turbulent flow reactor is a particularly valuable tool to study hydrocarbon oxidation processes.

IV. References

Colket, M.B. III, Naegeli, D.W., Dryer, F.L., and Glassman, I., (1973), "Flame Ionization Detection of Carbon Oxides and Hydrocarbon Oxygenates," Environmental Science and Technology 8, 43.

Dryer, F.L., (1972), "High Temperature Oxidation of Carbon Monoxide and Methane in a Turbulent Flow Reactor," AFOSR Scientific Report TR-72-1109.

Dryer, F.L., and Glassman, I., (1973), "The High Temperature Oxidation of CO and CH_4," Fourteenth International Symposium on Combustion, The Combustion Institute, Pittsburgh, p. 987.

Dryer, F.L., Naegeli, D.W., and Glassman, I., (1971), "The Temperature Dependence of the Reaction $CO + OH = CO_2 + H$," Comb. and Flame 17, 270.

Fristrom, D.C. Jr., and Westenburg, A.A., (1965), Flame Structure, McGraw-Hill, New York.

Glassman, I., and Eberstein, I.J., (1963), "Turbulence Effects in Chemical Reaction Kinetics Measurements," AIAA Journal 1, 1424.

Minkoff, G.I., and Tipper, C.F.H., (1962), Chemistry of Combustion Reactions, Butterworth & Co., Ltd., London.

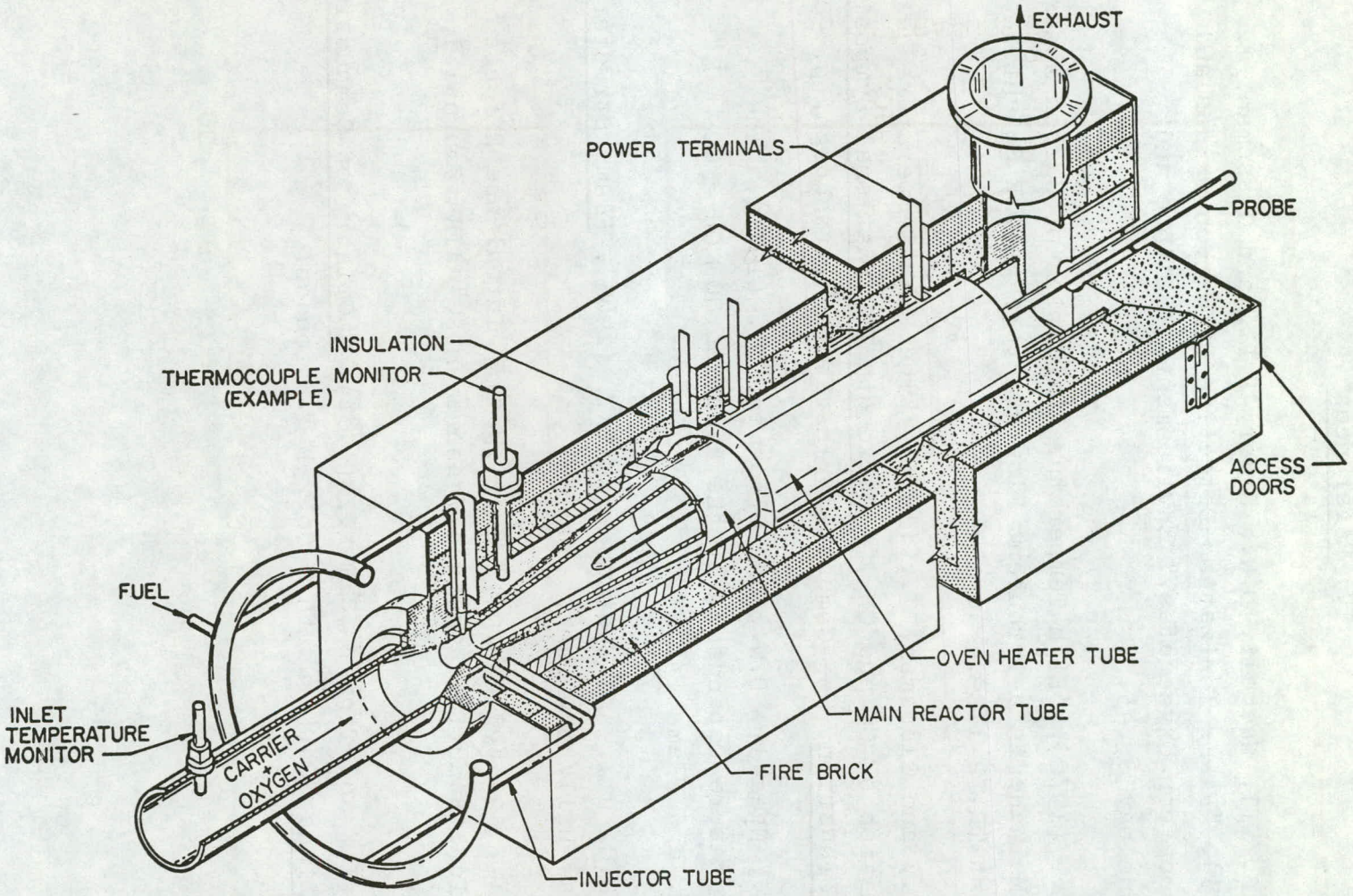

REACTOR ASSEMBLY

Figure 1

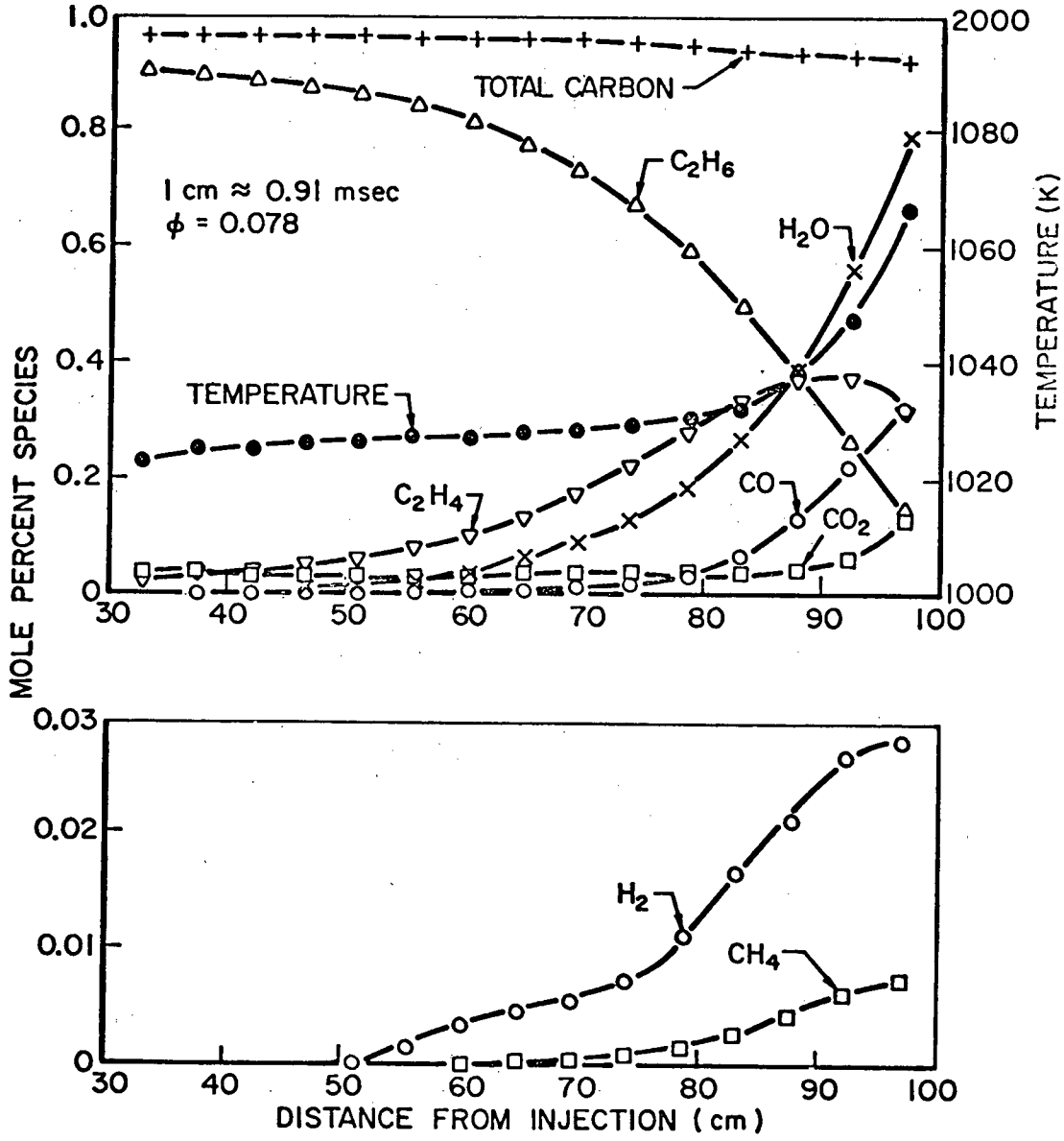

Figure 2

Chemical Composition of Spread Ethane-Air Reaction

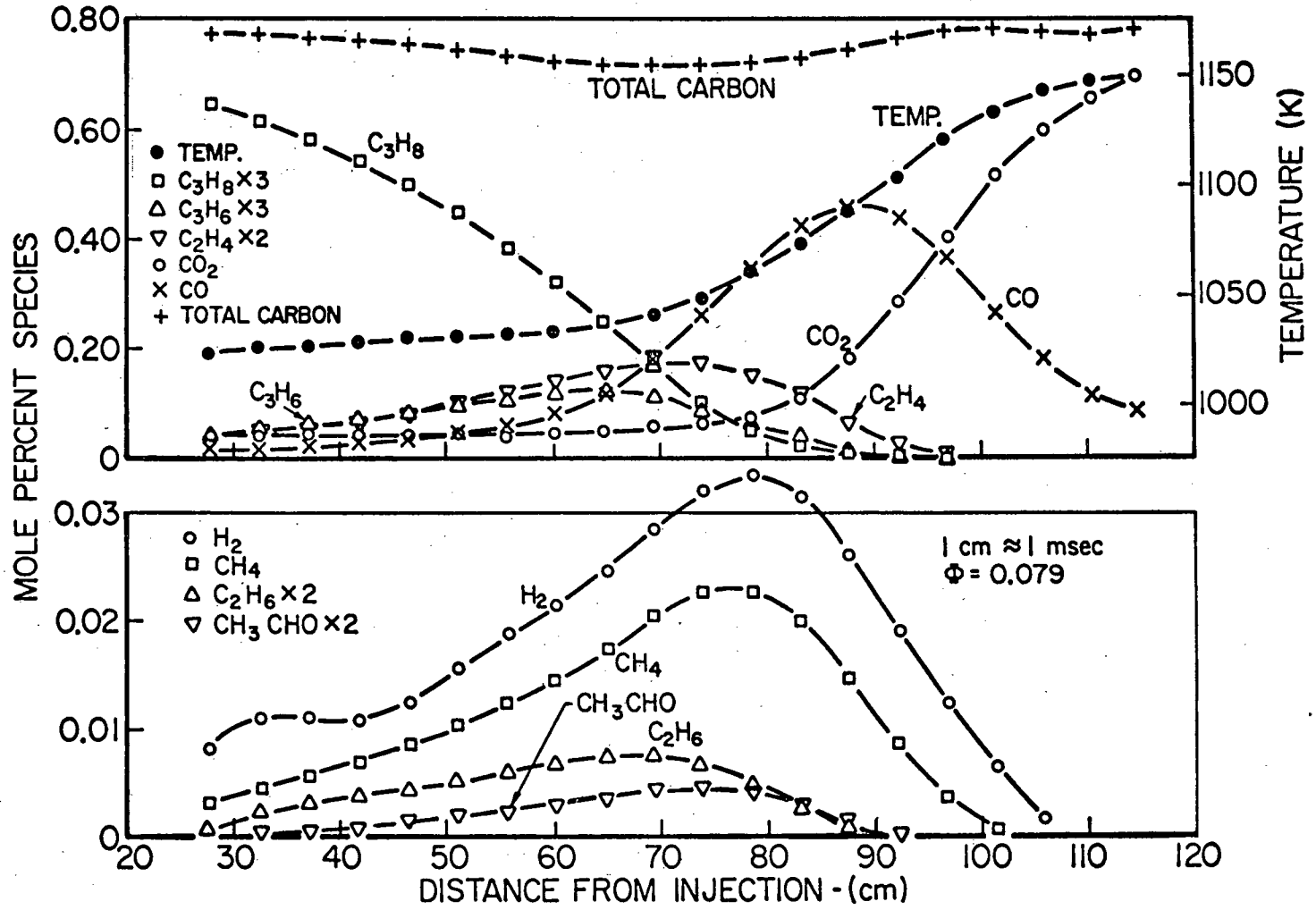

Figure 3

Chemical Composition of Spread Propane-Air Reaction

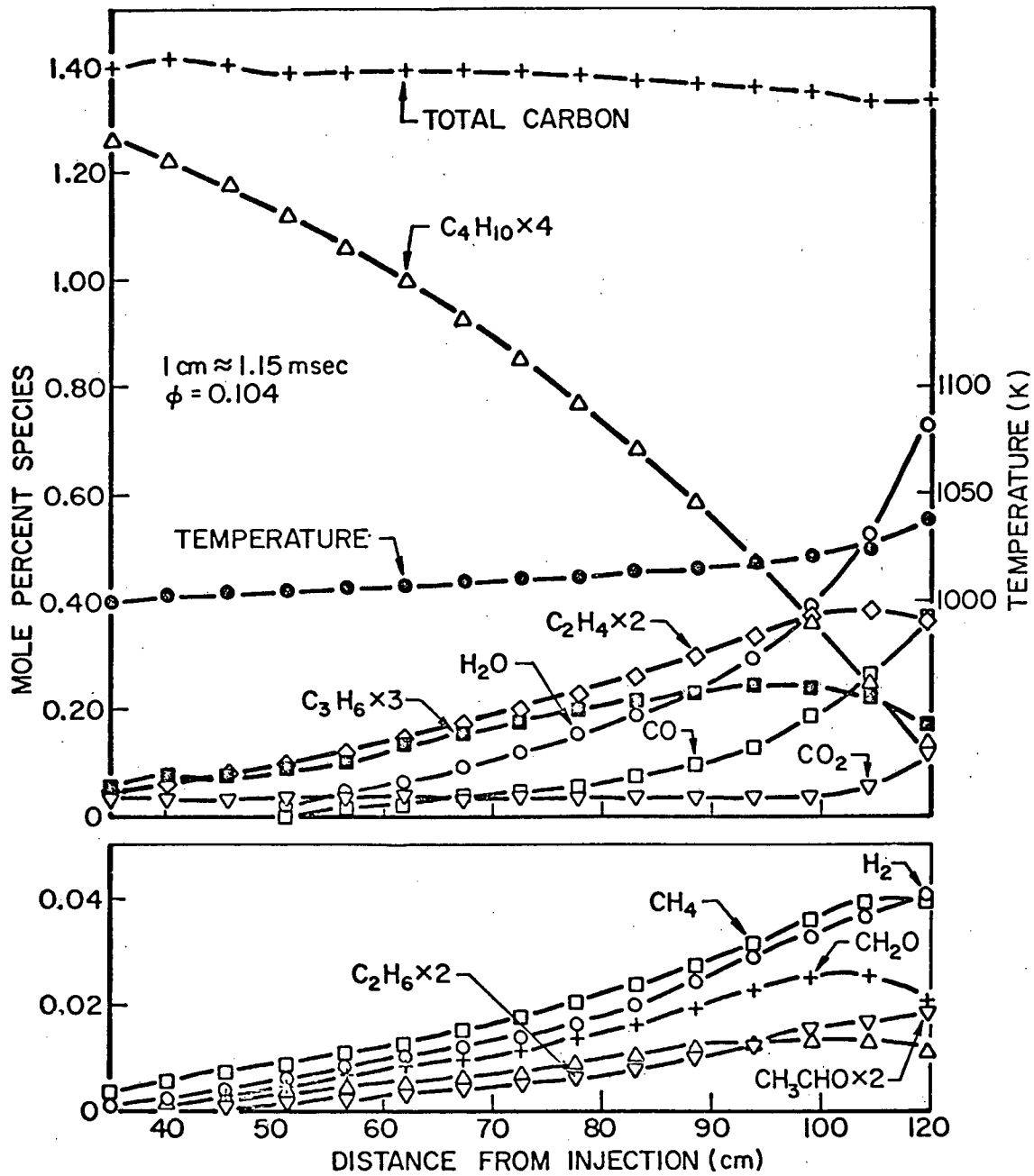

Figure 4

Chemical Composition of Spread Butane-Air Reaction

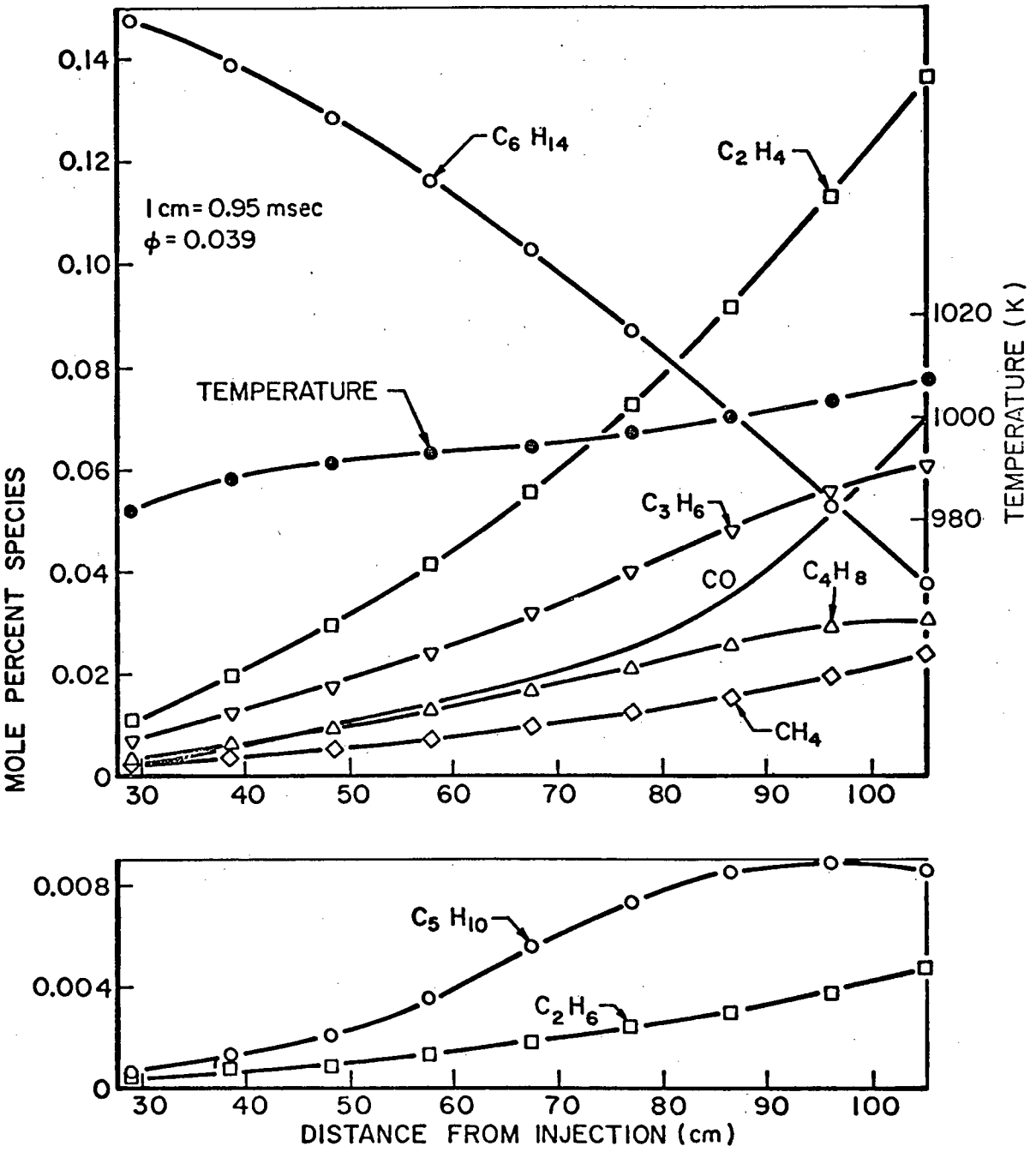

Figure 5

Chemical Composition of Spread Hexane/Air Reaction

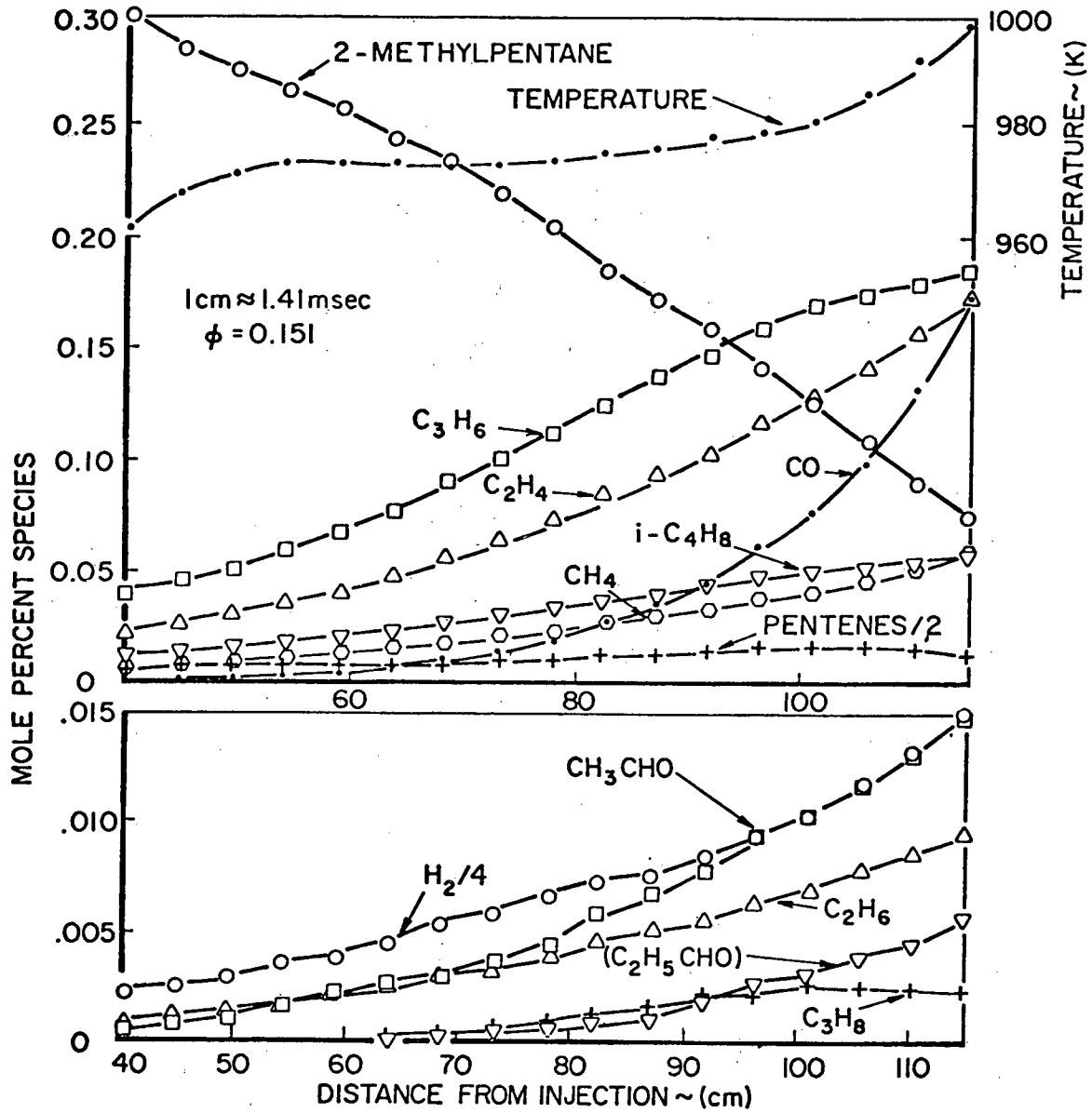

Figure 6

Chemical Composition of Spread 2-Methylpentane Air Reaction

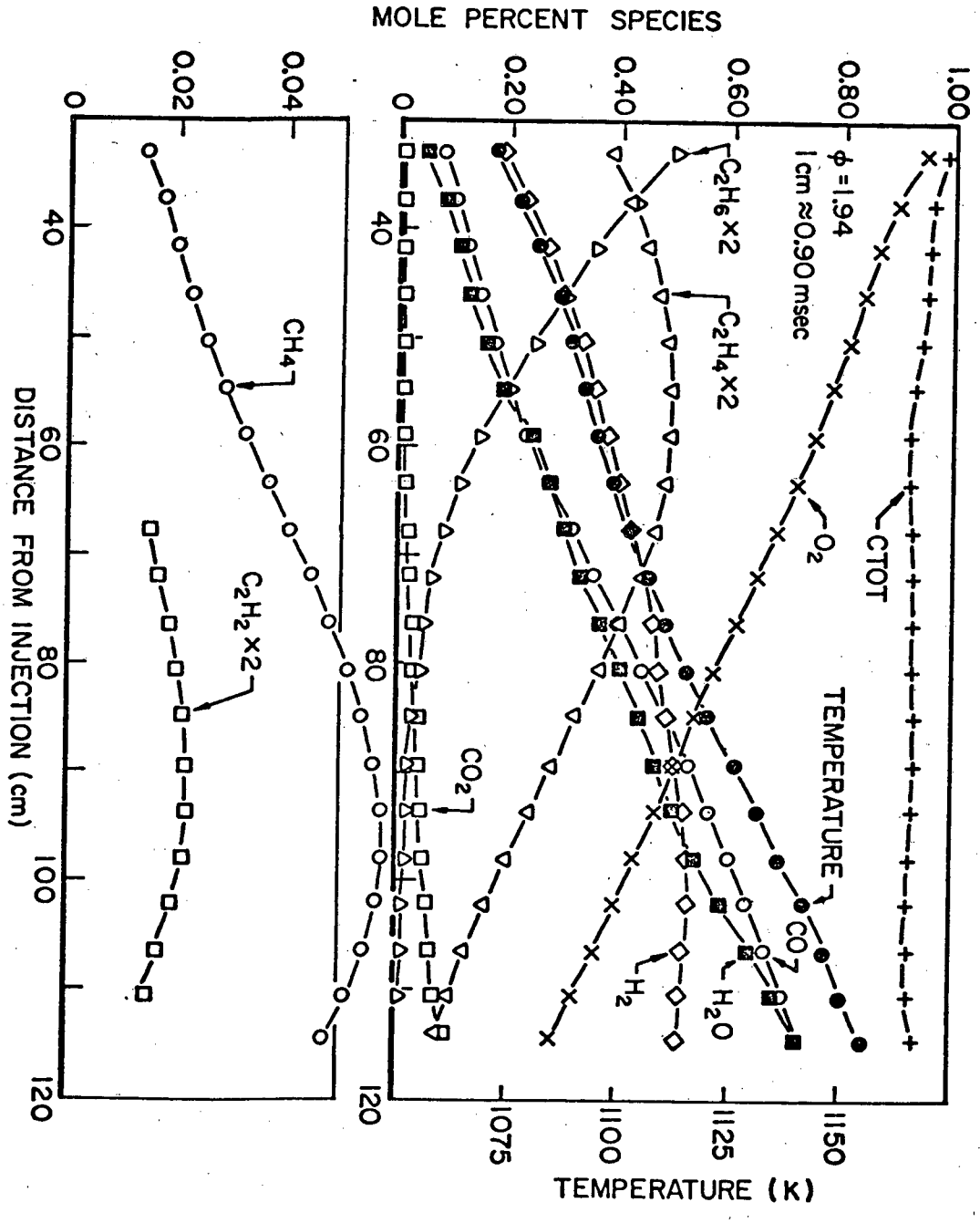

Figure 7

Chemical Composition of Spread Ethane-O_2 Reaction

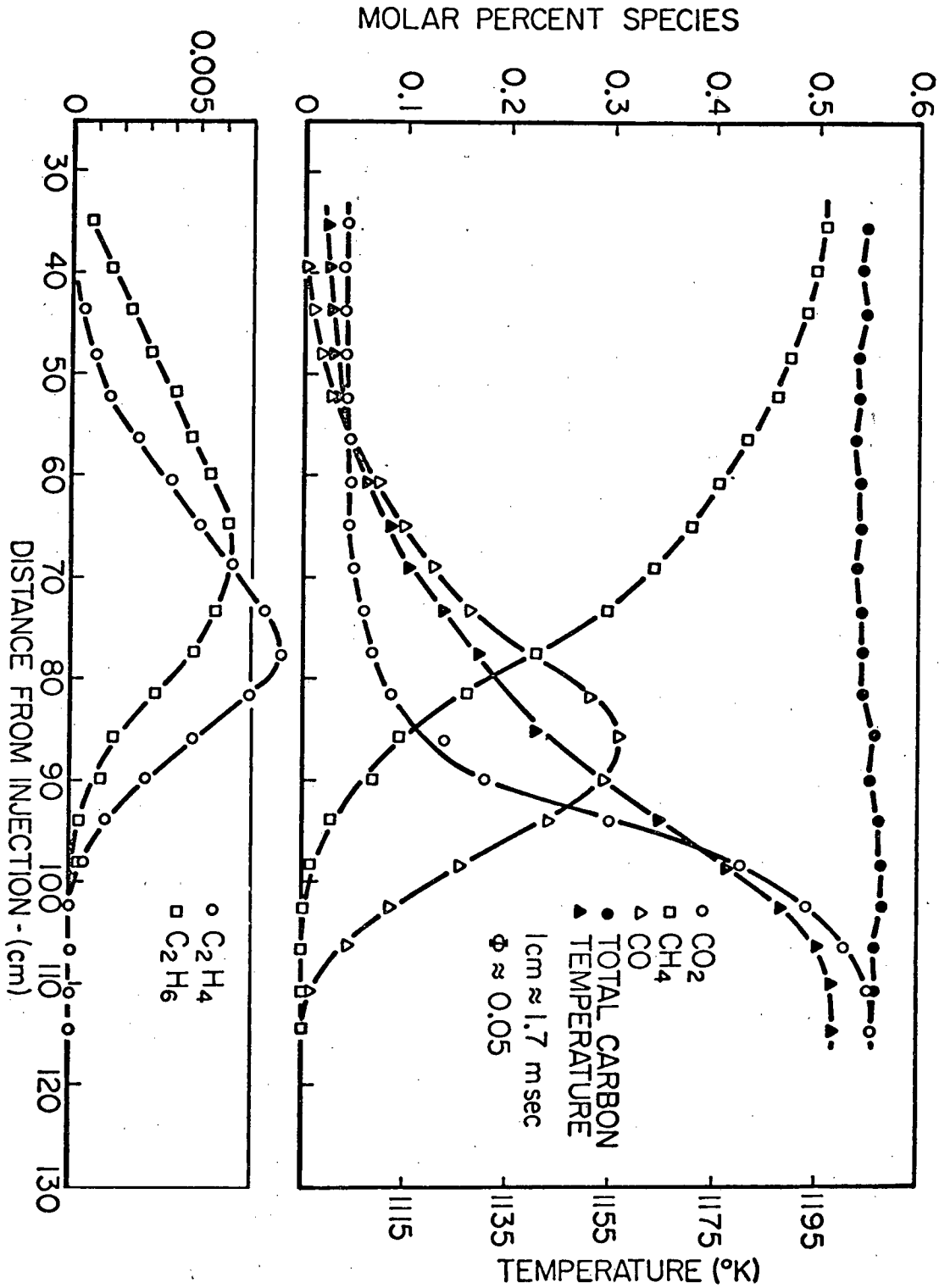

Figure 8

Chemical Composition of Spread Methane-Air Reaction

SOME PRECEPTIONS ON CONDENSED PHASE FLAME SPREADING AND MASS BURNING

I. Glassman

Department of Aerospace and Mechanical Sciences
Princeton University
Princeton, N. J. 08540

I. Introduction

Interest in problems associated with fire safety, particularly as related to the combustion characteristics of plastic materials, has arisen over the past years. Supposedly non-flammable plastic materials have been found not only to burn but also to emit relatively large quantities of toxic combustion products. Yet this result should not have been too surprising when one considers that flame spread was the primary test criterion for non-flammability. Materials with spreading rates so low that they are classified non-flammable will burn in fires supported by other combustibles. The phenomena which control rate of flame spread and rate of mass evolution are distinctly different. The purpose of this paper is to review certain fundamental concepts related to flame spreading and mass burning.

II. Flame Spreading

It is almost superfluous to review the field of flame spread after the recent publication of the excellent review by Williams (1976). In this most comprehensive conceptual review Williams treated almost every aspect of flame spreading — discrete and

continuous materials, orientation, phase change before combustion, etc. In this paper, only flame spreading across continuous media will be treated. By considering the spreading process only in the horizontal orientation, it is not necessary to distinguish between melting and non-melting material. Indeed because of the experience of the author, the subject of horizontal spreading across liquid fuels will be reviewed first and the insights gained from this work will be used to contribute to the understanding of flame spread across solid materials.

The approach is somewhat different than that used by Williams, but this subtle difference may help some in interpreting the disagreements which still exist in the field. The authors and their colleagues (Glassman, et al. 1976) recently reviewed the state of knowledge of flame spreading across liquid fuels. What follows are the basic physical concepts taken from this review with comparison to the case of flame propagation across solid materials.

The relationship between the flash point and bulk temperature of a liquid fuel determines the type and order of magnitude of the flame spread. The flash point temperature is indeed a relative concept, nevertheless it permits an important differentiation between two flame spread processes. When the bulk temperature of a liquid is above its flash point temperature, there exists above the liquid fuel a mixture of fuel vapor and air that lies with the flammability limits. It is generally assumed that equilibrium conditions prevail. In the actual open cup flash point test the height of the small flame ignition source above the liquid surface specifies that at that point when a flash is observed the fuel-air

mixture is just within the flammability limits. The temperature of the liquid when the flash occurs is the flash point temperature. It is obvious and it has recently been shown (Dryer and Neuman, 1976) that the flash point temperature varies with the ignition flame height over the liquid surface. The closer the source is to the fuel surface, the lower the flash point temperature. However a minimum must exist either because at some point the fuel surface exerts a quenching effect. Thus, in the flame spreading process a unique flash point temperature for the fuel cannot be specified, but the conceptual use is obvious.

In the case as mentioned above when the bulk liquid temperature is above the fire point, a flammable mixture exists everywhere above the surface. In the presence of an ignition source, a flame forms and spreads across the liquid surface. Under these temperature definitions the liquid does not contribute to the flame process. The flame that propagates is for all intents and purposes the same as a pre-mixed laminar flame. Its velocity is very large due to the stratification of air/fuel mixture above the surface (Feng, et al., 1975). The flame continually heats the cold unburned gases ahead of it until it begins to react (in Williams' context to an ignition temperature) and releases heat to continue the process.

When the bulk temperature is below the flash point, a flame will still propagate across the liquid fuel, but other mechanisms must control since a flammable mixture does not exist everywhere above the surface. Given that this fuel has been ignited and is burning, then there must exist some process which heats the liquid

ahead of the flame to a flash point condition ahead of the flame through the gas, or through the liquid. Or, there can be radiative heating from the flame.

In the context of Williams (1976) the burning fuel would have to heat ahead to the same ignition temperature, which in the terminology used here is the same as the flash point temperature. There is one important, subtle difference, however. In considering the flash point concept, we are essentially defining the flame spreading problem as a lean flammability limit problem for a gaseous fuel-air mixture. Following this reasoning there must be laminar gas phase flame propagation in all cases. Analyses dealing with the ignition temperature concept have the flame moving with the ignition temperature.

The lean limit flame propagation idea is important, because it says that if there is an opposing air flow so strong that the velocity near the surface were greater than the lean limit flame propagation velocity, then there could be no flame propagation. If one analytically follows the ignition temperature, then there can be no restriction.

In the case of high flash point liquids, the discovery was made (Mackinven, et al., 1970) that convection currents in the liquid were the dominant heat transfer mechanism. These currents were found to arise due to surface tension variations caused by the presence of the flame. The surface below the flame is obviously hotter than the liquid ahead of the flame. Since surface tension varies inversely with temperature, a surface tension gradient is established and draws hot liquid from behind the flame to a point

ahead. This liquid is obviously hotter than the flash point temperature.

For a viscous fluid, such as the fuel, under a surface tension gradient, it is well known that

$$\tau = \mu \left(\partial u/\partial y\right)_s = \sigma_x = \left(d\sigma/dT\right)\left(\partial T/\partial x\right)_s \tag{1}$$

where τ is the sheer stress, μ the viscosity, u the velocity parallel to the surface, y the direction normal to the surface, σ the surface tension, T the temperature and x the direction along the surface. $(d\sigma/dT)$ is a physical characteristic of the liquid. One can readily deduce the following proportionality for shallow pans:

$$u_s \sim \sigma x h/\mu \tag{2}$$

where u_s is the surface velocity and h is the depth of liquid in the pan. For deep pools and other analytical considerations with respect to the surface tension problem, one should refer to the review (Glassman, et al. 1976) mentioned earlier and the references therein.

From Equation (2), one would expect that the flame propagation velocity would also be proportional to pan depth and inversely proportional to the viscosity. Indeed these important trends were verified experimentally (MacKinven, et al., 1970). The experimental results show an almost linear variation of flame propagation with $1/\mu$ with slight thickening of the fuel by a chemical additive. However it is important to mention that as the liquid is made very viscous the linearity breaks down and the flame propagation

velocity asymptotically approaches a value of 0.3 cm/sec. For conventional kerosene, the propagation velocity is about 3 cm/sec. The asymptotic trend could indicate the onset of another type of controlling mechanism. Indeed, the propagation velocity of 0.3 cm/sec is similar to that obtained for many solid materials (Friedman, 1968).

Not only do the viscosity experiments validate the concept that convection currents in the liquid are the dominant heat transfer mode, but they also verify that heat transfer is the controlling mechanism. Indeed, the processes of fuel vaporizing, of the fuel vapor diffusing from the surface and mixing with the air, and of the flame propagating through this mixture must have characteristic rates faster than the heat transfer rate. In the case of flame propagation across solid materials, whether the dominant mode is heat conduction through the gas or solid, the rate must be slower than the convective rate in liquid. Thus if the convective rates are slower than the other steps in the lean limit propagation process, then indeed the conductive steps are. Even though the rate of evaporation of solid materials are kinetically controlled whereas liquids maintain evaporation equilibrium at their surfaces, the evaporation rate of solids are relatively fast, high temperature, high activation energy processes.

Williams (1976) deduces that for thermally thin solid material, conduction through the gas phase is the dominant heat transfer mechanism and that for thermally thick materials, conduction through the solid is the dominant heat transfer mechanism. In the spreading process across thick materials, the flame induces air

currents in the direction opposite to the propagation. The effect of these currents is still open to debate. For large fires radiation can play a dominant role in flame propagation across solids, however radiation is not nearly as important in liquids (Mackinven, et al., 1970). Considering flame propagation as a lean flammability process, permits one to explain the effects of flame retardants added to plastics. Indeed, one should again recall, that flame retardants limit flame spread, but retarded materials will burn. The three most common means of retarding flame propagation are to add chlorine (or other halogens), antimony or phosphorous compounds to the polymer structure. It is well known that halogens affect (narrow) flammibility limits. The presence of a halogen in the polymer would require the polymer to be heated to a high temperature before a flammable mixture could be created due to the presence of the chlorine atom. Antimony is found to be effective only when in halogenated compounds. Antimony chloride is a gaseous compound and it appears that the role of the antimony is to facilitate the presence of chlorine atoms in the gas phase. In contrast, phosphorous alters the surface characteristics of the polymer, causes a melt and effectively increases the heat of gasification.

Condensed phases must burn as diffusion flames and the flame must be essentially at the stoichiometric mixture ratio. Inhibitors such as halogens are only effective at the flammability limits where the radicals affecting the chain propagation are scarce. In stoichiometric flames, radicals are abundant and any removal by inhibition is ineffective in altering the mass burning process. Thus materials with flame retardants will alter the rate of flame

spread, but when they are involved in a massive fire, they burn and emit toxic compounds.

III. Mass Burning

The mass burning rate of plastic materials is inherently no different than the burning of a liquid or any other volatile solid material. Some materials under a high heat flux form a self-generated flame or due to external radiative source give off combustible gases and leave a char material. The gases burn quickly, however, the restrictions on the burning of the char are very similar to those associated with the burning of a porous carbon particle; that is, it is similar to coal combustion. Many small samples of plastics will not sustain their own combustion in air unless an external radiative source is applied. Since attempts are being made to develop tests to determine the mass burning rates of plastic materials in order to determine the so-called "burning intensity" of the plastic, it seems appropriate to review the parameters which control the mass burning rate of condensed phases. This topic is an old one, so the attempt here will be to deal with the subject with the test methods in mind.

The burning rate of the simple spherical droplet or volatile particle in a quiescent atmosphere will be considered first. Following Blackshear's (1960) adaptation of Spalding's approach (1955) as reported in detail recently by Kanury (1976) and Glassman (1977), one derives the following relation for the burning rate of the spherical particle:

$$(3) \qquad G_f = \dot{m}_f/4\pi r_s^2 = (D\rho/r_s)\ \ln(1+B) = (\lambda/C_p r)\ \ln(1+B)$$

$$= (\mu/r)\ \ln(1+B)$$

where G_f is the mass flux g/sec cm^2, $\dot{m}_f$ the mass burning rate g/sec, r_s the particle radius, B the transfer number, and D, λ, C_p, μ, and ρ the normal physical properties. Equation (3) is obtained under the assumptions that a quasi steady state exists and the particle is like a porous sphere fed with fuel at a rate equal to the consumption rate, Le = 1 and constant physical properties. The transfer number can take any of the following forms, all of which are equal:

$$(4) \qquad B = (im_{o\infty} + \dot{m}_{fs})/(1 - m_{fs})$$

$$(5) \qquad B = (C_p(T_\infty - T_s) - m_{fs}H)/L_v + H(m_{fs} - 1))$$

$$(6) \qquad B = (C_p(T_\infty - T_s) + im_{o\infty}H)/L_v$$

where m_o and m_f are the mass fraction of the oxidizer and fuel respectively; T, the temperature, H, the heating value of the fuel in cal/gm; L_v, the latent heat of evaporation; i, the mass stoichiometric index; and the subscript s and ∞ refer to the conditions at the surface and in the ambient atmosphere respectively.

Equation (3) may be interpreted in terms of an actual droplet burning, i.e.

$$(7) \qquad -\dot{m}_f = dm/dt = (d/dt)[(4/3)\pi\rho r^3]$$

$$(8) \qquad \dot{m}_f = -2\pi\rho r_s(dr^2/dt) \ .$$

Combining Equations (3) and (8), one obtains

$$dr^2/dt = - (2D\rho/\rho_l) \ln(1+B) . \quad (9)$$

The right hand side of the Equation (9) is constant and thus the rate of change of r^2 with time is constant. This result, of course, corresponds to the so-called d^2 (or r^2) law that is found experimentally.

It is interesting to note that the spherical particle burning in a quiescent atmosphere is the only mathematically tractable problem. The one dimensional burning of a strand of fuel or pool of liquid is not mathematically tractable unless one assumes that at a fixed distance, say δ, above the surface ambient conditions exist. In this case, referred to as the stagnant film case, it is readily shown that

$$G_f = (D\rho/\delta) \ln(1+B) . \quad (10)$$

A burning pool of liquid or a volatile solid will establish a stagnant film height due to the natural convection which ensues. From analogies to heat transfer without mass transfer, a first approximation to this liquid pool burning problem may be written

$$dG_f/\mu \ln(1+B) \sim Gr^a \quad (11)$$

where Gr is the Grashof number; d is the diameter of pool or strand, a equals 1/4 for laminar conditions and 1/3 for turbulent conditions. If air is forced concentrically around the pool or strand, very much like the Burke-Schumann gaseous fuel jet problem, then again, one can assume a stagnant film problem.

When the convective flow of air is normal or opposed to the mass evolving from the surface, the solution is more complex and

the stagnant film analysis does not hold. Emmons (1956) solved the problem of a burning longitudinal surface with forced convention. The fuel is essentially a flat plate with a leading edge. The problem is also described by Williams (1965) and is similar to the Blasius problem for the growth of a boundary layer over a flat plate. The Emmons result for Prandtl number equal to one takes the form

$$G_f = \mu(Re_x^{1/2}/x\sqrt{2})[-f(o)] \tag{12}$$

$$G_f x/\mu = Re_x^{1/2}\,[-f(o)]/\sqrt{2}$$

where Re_x is the Reynold's number based on the distance x from the leading edge of the longitudinal fuel surface and $[-f(o)]$ is a Blasius type variable which is a function of the transfer B. Williams (1965) gives the graphical relation between $[-f(o)]$ and Glassman (1977) has shown empirically that

$$[-f(o)] \approx \ln(1+B)/B^{.15} \tag{13}$$

over a large range of B values.

It would appear to follow that data for spherical particles burning in a convective atmosphere could correlate as

$$(G_f r/\mu)(B^{.15}/\ln(1+B)) = f(Re_r^{1/2}) \tag{14}$$

where Re_r is the Reynold's number based on the droplet. Even though a wake may exist in which very little burning occurs, Spalding (1955) has shown that Equation (14) without $B^{0.15}$ correlates data relatively well.

It is interesting to note that one may deduce from Equations (7) and (14) that in a constant velocity stream (or for constant relative velocity between stream and particle) that the particle will follow a $d^{3/2}$ ($r^{3/2}$) law rather than a d^2 law as found in the quiescent case.

If in the mass burning process there is flame radiation, or any other imposed radiation, as is frequently used in plastic mass burning tests, then a convenient expression for the burning rate can be obtained provided it is assumed that only the gasifying surface absorbs the radiation, i.e. there can be no absorption by the gaseous species present between the radiation source and the surface. In this case Fineman (1962) has shown that the stagnant film expression takes the form

$$G_f = (\lambda/C_p\delta)\ \ln[1+(B/(1-E))] \tag{15}$$

where

$$E \equiv Q_R/G_f\ L_v \tag{16}$$

and Q_R is the radiative flux. This simple form for the burning rate expression arises because the conservation equations are developed for conditions in the gas phase, and the mass burning rate enters explicitly in the boundary condition to the problem. Since the assumption is made that no radiation is absorbed by the gases, the radiation term appears only in the boundary condition to the problem.

Notice that as the radiant flux increases, E increases and the term [B/(1-E)] increases. When E = 1, the problem blows up

because the equation has developed in the framework of a diffusion analysis, and E = 1 means that the solid is gasified by the radiant flux alone.

As mentioned earlier, currently there are many investigators seeking to establish tests which determine the mass burning rate of plastics. One of the best of these procedures is that given by Tewarson and Pion (1976). In their experiment, an O_2/N_2 mixture passes around the burning plastic and the rate of flow is held constant. The gas flow is concentric with the circular cylinder sample and holder and is in the same direction as the mass evolution from the gasifying sample. The gas flow is contained within a quartz circular cylinder. Radiant heaters outside the quartz cylinder permit an external flux to be imposed on the sample. Tewarson and Pion report some excellent data and one of the interesting findings is that a linear relation exists between the mass burning rate of the plastic and the mass fraction of oxygen in the free stream, $m_{o\infty}$. The linearity breaks down at higher values of $m_{o\infty}$. Glassman (1977a) has attempted to explain these results by arguing that the order of B and [B/(1-E)] must be much less than one and that indeed the B values for most plastic material are smaller than previously estimated. For such small values

$$\ln(1 + B/(1-E)) \approx B/(1-E) \quad . \tag{17}$$

From Equation (15) then

$$\dot{m}_f \approx (\lambda/C_p\delta)(B/(1-E)) \quad . \tag{18}$$

Substituting Equation (16)

(19) $$\dot{m}_f = (\lambda/C_p\delta)B + Q_R/L_v \ .$$

Taking the form of B given by Equation (6)

(20) $$\dot{m}_f = (\lambda/C_p\delta)\, i\, Hm_{o\infty} + (C_p(T_\infty - T_s)/L_v) + (Q_R/L_v) \ .$$

Equation (20) shows the linearity with respect to $m_{o\infty}$. Since λ, C_p and δ probably do vary substantially for a fixed convective condition and various materials, it is possible to perform experiments with liquids of known values of B to determine $(k/C_p\delta)$ from a plot of m_f vs. B or more correctly m_f vs. $\ln(1+B)$. Then from a measured $\dot{m}_f$ of a plastic, its B value can be determined.

Tewarson (1977) has shown for plastics that the term $C_p(T - T_s)$ is a relatively large negative number and cannot be ignored in comparison to $im_{o\infty}H$ as it is often done for liquids. This fact and large values of L_v contribute to making B values of plastics small.

It is difficult to determine whether the non-linearity of Tewarson's $m_{o\infty}$ plots breaks down due to the fact that at higher $m_{o\infty}$ values B may not be small. Tewarson (1977) reports that for larger values of $m_{o\infty}$ black char formation on the surface of the PMMA was found. Such changes in pyrolysis mechanism could, of course, cause the observed trends.

In dealing with charring cellular plastics the mass evolution and burning process appears to be different. These materials are difficult to "burn" except under very large external radiant fluxes. Under such radiant fluxes, there is the initial evolution of relatively large amounts of combustible gases which will burn

when an ignition source is present. The rate of evolution of gases decreases with time as the pyrolysis gases must come from greater depths within the cellular plastic. It is these gases which contribute to room fires and are probably a factor in the so-called flashover problem.

The burning of the char certainly would not contribute in the early stages of fire, but the char will burn very much like a porous carbon (or coal) particle. In a major fire the surface temperature of char would be high enough so that the surface oxidation of the char was kinetically fast and controlled by the diffusion of oxygen to the surface. Under these circumstances it is again interesting to observe that

$$\dot{m}_f \sim \ln(1+B) \tag{21}$$

where $\dot{m}_f$ would be the mass burning rate of the char. If Equation (4) is used as the form of B, then a simple expression results since for this type of diffusion controlled heterogeneous surface burning $m_{fs} = 0$ and

$$B = im_\infty \ . \tag{22}$$

For burning in air $im_{o\infty}$ is small with respect to one, and again since $\ln(1+B) \approx B$ for small B, one has that

$$\dot{m}_f \approx m_{o\infty} \tag{23}$$

the same result that one obtains for the porous carbon (coal) particle as Glassman (1977) has recently discussed.

IV. Postscript

This paper has dealt with the problem of flame spreading and mass burning. The emphasis was placed on achieving greater understanding of how these processes occur with plastic materials. With respect to flame spreading, the review was limited compared to the recent work of Williams (1976), however it does suggest that flame spreading across condensed phases be considered a lean flammability limit problem. The mass burning considerations are in actuality a simple extension of the earlier work of Spalding (1955) and Emmons (1956). How the effects of flame and external radiation can be handled within the present simple analyses were given. In particulas the case of analyses in mass burning rate tests of plastics was explored.

V. References

Blackshear, P.L. Jr. (1960). "An Introduction to Combustion," Dept. of Mech. Eng., Univ. of Minnesota, Minn.

Dryer, F.L. and Neuman, (1976). "Flame Spread Over Liquid Fuels — The Mechanism of Flame Pulsation," presented at the Fall Meeting of the Western States Section of the Combustion Institute, La Jolla, Calif.

Emmons, H.W. (1956). Z. Angew. Math. Mech. 36, 6.

Feng, C.C., Lam, S.H. and Glassman, I, (1957). Comb. Sci. and Tech. 10, 59.

Fineman, S. (1962). "Some Analytical Considerations of the Hybrid Rocket Combustion Problem," Princeton Univ. Dept. of Aero. Eng. M.S.E. Thesis.

Friedman, R. (1968). Fire Res. Abst. Rev. 10, 1.

Glassman, I., Santoro, R.J. and Dryer, F.L. (1976). "A Review and Some Recent Results of the Princeton Program on Flame Spread Over Condensed Phase Combustibles," presented at the Fall Meeting of the Western States Section of the Combustion Institute, La Jolla, Calif. Paper No. WSCI-76-29.

Glassman, I. (1977). "Combustion," Academic Press, New York.

Glassman, I. (1977a). "Comment on 'Flammability of Plastics. I. Burning Intensity' by A. Tewarson and R.F. Pion," to appear in Combustion and Flame.

Kanury, A.M. (1976). "Introduction to Combustion Phenomena," Gordon and Breach, New York.

Mackinven, R., Hansel, J., and Glassman, I. (1970). Comb. Sci and Tech. 1, 293.

Spalding, D.B. (1955). "Some Fundamentals of Combustion," Butterworths, London.

Tewarson, A. (1977). "Reply to Comments on Our Paper," to appear in Combustion and Flame.

Tewarson, A. and Pion, R.F. (1976). Comb. and Flame 26, 85.

Williams, F.A. (1965). "Combustion Theory," Addison-Wesley, Reading, Mass.

Williams, F.A. (1976). "Mechanisms of Fire Spread," invited paper Sixteenth (Int'l) Symposium on Combustion, Cambridge, Mass.

This report was prepared as an account of Government sponsored work. Neither the United States, nor the Administration, nor any person acting on behalf of the Administration:

A. Makes any warranty or representation, express or implied, with respect to the accuracy, completeness, or usefulness of the information contained in this report, or that the use of any information, apparatus, method, or process disclosed in this report may not infringe privately owned rights; or

B. Assumes any liabilities with respect to the use of, or for damages resulting from the use of any information, apparatus, method, or process disclosed in this report.

As used in the above, "person acting on behalf of the Administration" includes any employee or contractor of the Administration, or employee of such contractor, to the extent that such employee or contractor of the Administration, or employee of such contractor prepares, disseminates, or provides access to, any information pursuant to his employment or contract with the Administration, or his employment with such contractor.